MECHANISMS AND NOVEL TREATMENTS OF PIGMENTARY DISORDERS AND SKIN REGENERATION

EDITED BY: Xing-Hua Gao, Bing Song, Hongxiang Chen and Rongya Yang

PUBLISHED IN: Frontiers in Medicine

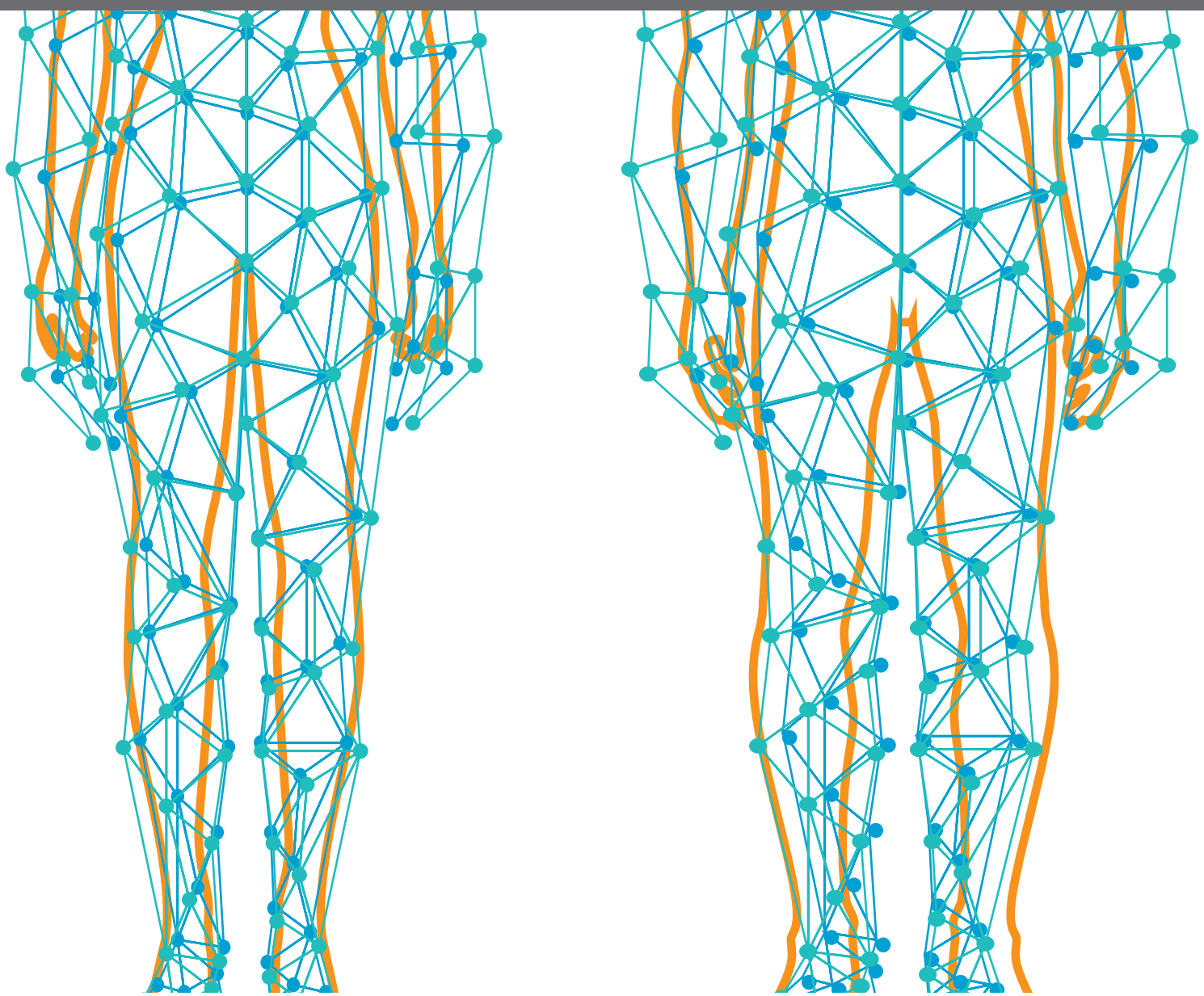

frontiers Research Topics

frontiers

ISSN 1664-8714
ISBN 978-2-83250-318-8
DOI 10.3389/978-2-83250-318-8

About Frontiers

Frontiers is more than just an open-access publisher of scholarly articles: it is a pioneering approach to the world of academia, radically improving the way scholarly research is managed. The grand vision of Frontiers is a world where all people have an equal opportunity to seek, share and generate knowledge. Frontiers provides immediate and permanent online open access to all its publications, but this alone is not enough to realize our grand goals.

Frontiers Journal Series

The Frontiers Journal Series is a multi-tier and interdisciplinary set of open-access, online journals, promising a paradigm shift from the current review, selection and dissemination processes in academic publishing. All Frontiers journals are driven by researchers for researchers; therefore, they constitute a service to the scholarly community. At the same time, the Frontiers Journal Series operates on a revolutionary invention, the tiered publishing system, initially addressing specific communities of scholars, and gradually climbing up to broader public understanding, thus serving the interests of the lay society, too.

Dedication to Quality

Each Frontiers article is a landmark of the highest quality, thanks to genuinely collaborative interactions between authors and review editors, who include some of the world's best academicians. Research must be certified by peers before entering a stream of knowledge that may eventually reach the public - and shape society; therefore, Frontiers only applies the most rigorous and unbiased reviews.
Frontiers revolutionizes research publishing by freely delivering the most outstanding research, evaluated with no bias from both the academic and social point of view. By applying the most advanced information technologies, Frontiers is catapulting scholarly publishing into a new generation.

What are Frontiers Research Topics?

Frontiers Research Topics are very popular trademarks of the Frontiers Journals Series: they are collections of at least ten articles, all centered on a particular subject. With their unique mix of varied contributions from Original Research to Review Articles, Frontiers Research Topics unify the most influential researchers, the latest key findings and historical advances in a hot research area! Find out more on how to host your own Frontiers Research Topic or contribute to one as an author by contacting the Frontiers Editorial Office: frontiersin.org/about/contact

MECHANISMS AND NOVEL TREATMENTS OF PIGMENTARY DISORDERS AND SKIN REGENERATION

Topic Editors:
Xing-Hua Gao, The First Affiliated Hospital of China Medical University, China
Bing Song, Cardiff University, United Kingdom
Hongxiang Chen, Huazhong University of Science and Technology, China
Rongya Yang, People's Liberation Army General Hospital, China

Citation: Gao, X.-H., Song, B., Chen, H., Yang, R., eds. (2022). Mechanisms and Novel Treatments of Pigmentary Disorders and Skin Regeneration. Lausanne: Frontiers Media SA. doi: 10.3389/978-2-83250-318-8

Table of Contents

frontiers | Frontiers in Medicine

TYPE Editorial
PUBLISHED 14 September 2022
DOI 10.3389/fmed.2022.1016741

OPEN ACCESS

EDITED AND REVIEWED BY
Robert Gniadecki,
University of Alberta, Canada

*CORRESPONDENCE
Xing-Hua Gao
gaobarry@hotmail.com

SPECIALTY SECTION
This article was submitted to Dermatology, a section of the journal Frontiers in Medicine

RECEIVED 11 August 2022
ACCEPTED 15 August 2022
PUBLISHED 14 September 2022

CITATION
Gao X-H (2022) Editorial: Mechanisms and novel treatments of pigmentary disorders and skin regeneration. *Front. Med.* 9:1016741. doi: 10.3389/fmed.2022.1016741

Editorial: Mechanisms and novel treatments of pigmentary disorders and skin regeneration

Xing-Hua Gao*

Department of Dermatology, The First Hospital of China Medical University, Shenyang, China

KEYWORDS

pigmentary abnormality, skin, regeneration, hypopigmentation, hyperpigmentation

Editorial on the Research Topic
Mechanisms and novel treatments of pigmentary disorders and skin regeneration

Pigmentary disorders, whether hyperpigmentary or hypopigmentary, are quite common dermatologic conditions (1). Depending on the extent and location of involvement, patients with pigmentary disorders may experience poor quality of life and psychosocial status owing to the disfiguring effect of these conditions and, occasionally, their systemic involvement.

The present issue collected two studies on rare genetic defects in pigmentary disorders from Chinese descendants. *KIT* is a proto-oncogene that is involved in the proliferation, survival, and regulation of melanocytes, among a couple of other cells. Yang et al. presented a case study of a three-generation Chinese family with progressive hyperpigmentation and generalized lentigines, inherited in an autosomal dominant pattern. A missense mutation of c. 2485G > C in the KIT gene was identified. Geno-pheno-correlation analysis was suggestive of cutaneous pigmentary changes without systemic involvement.

GS type 3 (GS3) is a very rare autosomal recessive disorder caused by mutations in the melanophilin (MLPH) gene, characterized by pigmentary dilution of skin and hair with no immunological or neurological manifestation. The MYO5A-MLPH-RAB27A ternary protein complex is required for anchoring mature melanosomes in the peripheral actin filaments of melanocytes for subsequent transfer to adjacent keratinocytes. Huang et al. identified a novel homozygous missense mutation (c.73G > C; p.D25H), residing in the conserved Slp homology domain of MLPH, in a Chinese GS3 patient who presented with hypopigmentation of the hair, eyebrows, and eyelashes.

Treatment of pigmentary disorders is challenging. Post-inflammatory hyperpigmentation (PIH) is a common acquired pigmentary disorder following skin inflammation and exaggerated by ultraviolet B (UVB) light. Zhao et al. demonstrated that a steroidal alkaloid glycoside, solamargine, exhibited an anti-inflammatory effect through the p38 MAPK/Nrf2/HO-1 signaling pathway and an inhibitory effect on UVB-induced melanin synthesis. It is tempting to test the *in vivo* effect of solamargine in PIH in future.

Melasma is a common acquired hyperpigmentation disorder characterized by hyperpigmented patchy skin in sun-exposed areas. Topical botanical products containing active ingredients have been increasingly applied as therapies for melasma. Wang et al. conducted a systemic review and meta-analysis of randomized controlled trials on agents with either herb-derived molecule, extracts of a single herb, or extracts of compound herbs. Of the 12 included studies, all showed superior effects in reducing the severity of melasma when compared with placebo, and better safety profiles compared to active controls. The authors assumed that the mechanisms of action are (1) direct or indirect inhibition of tyrosinase to suppress melanogenesis; (2) antioxidation to scavenge free radicals; (3) regulation of inflammatory mediators to inhibit inflammation; or (4) synergistic action of the above. Although these results are appealing, issues surrounding the characterization of specific molecules remain. Well-designed clinical trials are still needed, as well as observations on the long-term efficacies of these compounds.

Vitiligo is an autoimmune depigmentation disorder caused by the destruction of melanocytes, which is multifactorial in origin. Chang et al. conducted a combined therapy consisting of camouflage and psychotherapy on patients with vitiligo and demonstrated a significant improvement in their quality of life. Serum levels of neuropeptide-Y and melanin-concentrating hormone significantly decreased, and levels of adrenocorticotropic hormone increased, in treated patients but not in the control group. The serum levels of interferon-γ, CXC chemokine ligand 10, and interleukin-1β decreased in both the active and stable stages of the intervention group and only in the active stages of the control group. Non-randomized design and a lack of reporting on clinical improvement are the major limitations of this study.

Skin regeneration therapies aimed at the prevention and reversal of skin aging are greatly hoped for by the public. Mesenchymal stem cells (MSCs) are multipotent stem cells deriving from an array of sources such as bone marrow, adipose tissue, or umbilical cord blood. MSCs, as well as their derivatives, may promote cell proliferation and neovascularization in skin regeneration, decrease inflammation in injured skin, produce collagen and elastic fibers, inhibit metalloproteinase activation, and avoid UV-induced senescence (2). Wang et al. reviewed the mechanisms of action of extracellular vesicles secreted by adipose-derived MSCs on skin regeneration, skin barrier repair, and hair growth, specifically on their roles in inflammation, angiogenesis, cell proliferation, extracellular matrix remodeling, autophagy, and oxidative stress. Liang et al. conducted a randomized, controlled split-face study on volunteers with facial skin aging and demonstrated that the combination therapy of microneedling and conditioned media of human umbilical cord-derived MSCs was beneficial for skin rejuvenation. A major limitation of the study is that specific active molecules as well as potential hazardous molecules were not defined in the culture media.

A wound is defined as an injury or disorder in the normal skin structure, inducing discontinuous body tissue. Wound healing is an overlapping processes, and is divided into the stages of inflammation, blood clotting, cellular proliferation, and extracellular matrix remodeling (3). Xiong et al. constructed a rat scalp-expansion model and found that topical application of metformin enhanced the proliferative activity of skin-derived stem cells, as well as the regenerative capacity of mechanically stretched skin, as shown by increased epidermal thickness, collagen volume, and angiogenesis. Mao et al. reviewed the pivotal role of follicular stem cells in epithelial-mesenchymal interaction in the context of hair follicle regeneration and skin wound healing, emphasizing their control in the exchange of soluble molecules, modulation of key pathways, and signal transduction via the extracellular matrix.

To sum up, the current issue covers nine papers comprising original studies and reviews on pigmentary disorders and skin regeneration. These studies added new data on the genetics of a couple of rare pigmentary diseases and on the role of stem cells and their derivatives in skin regeneration. Several of these pioneering trials deserve attention and follow-up in the future.

Author contributions

The author confirms being the sole contributor of this work and has approved it for publication.

Acknowledgments

Thanks to Profs. Yan Wu and Yan Sun of the First Hospital of China Medical University for their critical reading.

Conflict of interest

The author declares that the research was conducted in the absence of any commercial or financial relationships that could be construed as a potential conflict of interest.

Publisher's note

References

1. Zubair R, Lyons AB, Vellaichamy G, Peacock A, Hamzavi I. What's new in pigmentary disorders. *Dermatol Clin.* (2019) 37:175–81. doi: 10.1016/j.det.2018.12.008

2. Jo H, Brito S, Kwak BM, Park S, Lee MG, Bin BH. Applications of mesenchymal stem cells in skin regeneration and rejuvenation. *Int J Mol Sci.* (2021) 22:2410. doi: 10.3390/ijms22052410

3. Takeo M, Lee W, Ito M. Wound healing and skin regeneration. *Cold Spring Harb Perspect Med.* (2015) 5:a023267. doi: 10.1101/cshperspect.a023267

frontiers in Medicine

SYSTEMATIC REVIEW
published: 24 January 2022
doi: 10.3389/fmed.2021.797890

Efficacy and Safety of Topical Therapy With Botanical Products for Melasma: A Systematic Review and Meta-Analysis of Randomized Controlled Trials

Tianyun Wang[1,2†], *Youmei Wang*[1,2†], *Jue Wang*[3], *Hongwei Chen*[4], *Biao Qu*[3*] and *Zheng Li*[5,6*]

[1] Department of Endocrinology, Huaian Hospital, Huaian, China, [2] Department of Pharmacy, Huaian Hospital, Huaian, China, [3] State Key Laboratory of Quality Research in Chinese Medicines, Macau University of Science and Technology, Macau, China, [4] School of Public Health, Sun Yat-sen University, Shenzhen, China, [5] Jiangsu Engineering Research Center of Cardiovascular Drugs Targeting Endothelial Cells, School of Life Sciences, College of Health Sciences, Jiangsu Normal University, Xuzhou, China, [6] State Key Laboratory of Natural and Biomimetic Drugs, Peking University, Beijing, China

OPEN ACCESS

Edited by:
Xing-Hua Gao,
The First Affiliated Hospital of China Medical University, China

Reviewed by:
Francesco Lacarrubba,
University of Catania, Italy
Mauro Picardo,
San Gallicano Hospital, Italy

***Correspondence:**
Zheng Li
lizhengcpu@163.com
Biao Qu
biaoqu2020@163.com

[†]These authors have contributed equally to this work

Specialty section:
This article was submitted to Dermatology, a section of the journal Frontiers in Medicine

Received: 19 October 2021
Accepted: 27 December 2021
Published: 24 January 2022

Citation:
Wang T, Wang Y, Wang J, Chen H, Qu B and Li Z (2022) Efficacy and Safety of Topical Therapy With Botanical Products for Melasma: A Systematic Review and Meta-Analysis of Randomized Controlled Trials. Front. Med. 8:797890. doi: 10.3389/fmed.2021.797890

Botanical products have been increasingly popular in topical therapies for melasma, as presumed safer and milder than fully synthetic products. Although the efficacy of different topical botanicals has recently been substantiated through randomized controlled trials (RCTs), there is a lack of sufficiently pooled evidence on their efficacy and safety for the treatment of melasma. Herein, a systematic review and meta-analysis was conducted on the efficacy and safety of topical botanical products for the treatment of melasma, following Preferred Reporting Items for Systematic Reviews and Meta-Analyses (PRISMA). All RCTs on the use of topical botanical products for the treatment of melasma in humans were included, except for trials enrolling pregnant patients. The primary outcome was Melasma Area and Severity Index (MASI) or its variation. The secondary outcomes included Mexameter® reading, melasma improvement evaluated by participants, and any reported adverse events (AEs). As a result, twelve eligible trials comprising 695 patients with melasma from 6 different countries were included. The topical botanical products contained active ingredients which varied among trials as follows: herb-derived molecule, extracts of a single herb, and extracts of compound herbs. Topical therapy with botanical products significantly improved melasma with a large effect on MASI reduction (SMD −0.79, 95% CI −1.14 to −0.44, $p < 0.00001$), and a moderate effect on Mexameter® reading reduction (SMD −0.52, 95% CI −0.81 to 0.23, $p = 0.0005$), when compared with placebo. It also showed a similar improvement of melasma with a better safety profile (RR 0.37, 95% CI 0.15–0.88, $p = 0.02$), when compared with active-comparators. Botanical products were well-tolerated across studies, with no serious AEs reported. Despite the limitations such as small sample size, short duration of follow up and varied botanical products, this work still represents the best level of evidence currently available on topical use of botanical products on melasma. Moreover, it should be noted that more well-designed studies are needed before recommending topical botanical products as a viable treatment option for melasma.

Systematic Review Registration: PROSPERO, identifier: CRD42021256328.

Keywords: botanical products, topical therapy, melasma, efficacy, safety, systematic review, meta-analysis

INTRODUCTION

Melasma is an acquired hyperpigmentation disorder characterized by the appearance of abnormal melanin deposits in different layers of skin, especially the face and neck (1). Although melasma can occur in both sexes and any skin type, it has a high prevalence in adult women with darker complexions, especially those living in areas with intense sun exposure (2–4). As classified according to the location of the pigment, three types of melasma exist, namely, epidermal, dermal, and mixed types (5). Although its pathogenesis has not yet been fully elucidated, genetic factors, chronic ultraviolet (UV) exposure, and hormones have been demonstrated to be implicated in the occurrence of it (6–8). Recent studies also suggested the role of inflammatory processes in the pathogenesis of melasma (2, 9).

The physiological and psychological effects of melasma have a considerable negative impact on the quality of life of affected individuals. This distressing condition is exacerbated by the therapeutic challenge due to its refractory and recurrent nature (3, 10). To date, various therapy modalities have been developed. Topical therapy with photoprotection and lightning products is still the mainstay for the treatment of melasma. Among these products, hydroquinone (HQ) has been used as the benchmark for decades, especially in epidermal melasma (3). It is a competitive inhibitor of tyrosinase which prevents the enzymatic oxidation of tyrosine to dopa, thus, preventing the synthesis of melanin. Unfortunately, safety concerns surrounding HQ are still controversial. The adverse events (AEs) were reported as exogenous ochronosis and permanent depigmentation (11). Other safety issues regarding its systemic absorption and drug-induced carcinogenesis have also been expressed (12, 13). Second-line treatment options include oral tranexamic acid, lasers, and chemical peels. However, no consensus has been reached on their robust efficacy for melasma, let alone the accompanied AEs, namely, postinflammatory dyspigmentation, scarring, and venous thromboembolism (14).

Botanical extracts have been used empirically in topical therapy for different diseases since ancient times. During past decades, many herbal extracts or isolated molecules have been reported to show the activities of inhibiting tyrosinase, scavenging free radicals, and suppressing inflammatory processes (15–17). Some of these have been used in topical drugs or cosmetic formulations for the treatment of melasma. These botanical products are increasingly popular as they are presumed safe, mild, and available over the counter (18). Only recently, though, the efficacy of some botanical products has been substantiated through clinical trials (3). In these trials, Melasma Area and Severity Index (MASI) is widely adopted as a standardized subjective method for evaluating efficacy (19). In addition, subjective methods are now often supplemented with objective methods, such as spectroscopic analysis using a Mexameter®. Although different topical botanical products have been evaluated for the treatment of melasma in many randomized controlled trials (RCTs), there is a lack of sufficiently pooled evidence on their efficacy and safety. In an attempt to address this uncertainty, we conducted a systematic review and meta-analysis of RCTs to investigate the efficacy and safety of topical botanical products in patients with melasma.

Abbreviations: MASI, Melasma Area Severity Index; EG, experimental group; CG, control group; mMASI, modified MASI; NR, not reported; HQ, hydroquinone.

MATERIALS AND METHODS

This systematic review and meta-analysis was prospectively registered at the International Prospective Register of Systematic Reviews (PROSPERO) (registration number. CRD42021256328) and conducted following the Preferred Reporting Items for Systematic Reviews and Meta-Analyses (PRISMA) guidelines (20).

Search Strategy

A systematic search was carried out using PubMed, Embase, the Cochrane Library, and Web of Science to collect relevant studies from inception to September 8, 2021. This search was conducted by two independent reviewers (BQ and HC), and the complete search strategies were reported in **Supplementary Table 1**. Reference lists of included studies and relevant systematic reviews were also reviewed manually to find additional eligible studies.

Study Selection

All identified studies were assessed to determine whether they met the following criteria: RCTs investigating the efficacy and safety of botanical products used in topical therapies for the treatment of melasma in humans. We excluded studies that included participants with pregnancy or breastfeeding. Moreover, participants included in trials should be healthy adults with melasma diagnosed by dermatological consultation and/or device examination. The first screening for potentially relevant records based on title and abstract, and following eligibility assessment based on full-text, were independently conducted by two reviewers (TW and YW). Any disagreement between investigators was resolved by discussion to reach a consensus.

Outcome Measures

The primary outcome was the improvement in melasma severity evaluated through the changes of MASI or its variation from baseline to follow-up. The secondary outcomes included melasma improvement evaluated through the changes of Mexameter® reading, improvement evaluated by participants, and any reported AE.

Data Extraction

Baseline characteristics and outcome data were extracted independently by two authors (TW and YW) using a standard data extraction form, with disagreements resolved by consensus. The following information from each study was extracted: the surname of the first author, publication year, country of origin, study period, study design, number of participants, percentage of female participants, mean ages of participants, description of interventions, and outcome measures. Data of multiple groups from one study were extracted using the recommendations from the Cochrane Handbook (21). For continuous outcomes, the

following were extracted: means, SD, and sample sizes at baseline and follow-up. For dichotomous outcomes, the number of cases and total sample sizes were extracted.

Quality Assessment

The risk of bias was assessed independently by two investigators (TW and YW) using the Cochrane Risk of Bias Tool (21) with disagreements resolved by discussion to reach a consensus. Based on the risk of bias, the included RCTs were graded as low, moderate, or high quality following the criteria (22): (1) RCT was considered low quality if either randomization or allocation concealment was considered at high risk; (2) RCT was considered high quality when both randomization and allocation concealment were considered at low risk, and all other items were considered at low or unclear risk; and (3) RCT was considered moderate quality if it met neither the criteria for high nor low quality.

Data Synthesis and Analysis

Data collected from RCTs were preprocessed in Microsoft Excel before meta-analyses were performed using RevMan (Ver. 5.4) using random effects. Pooled continuous data were expressed as standardized mean difference (SMD) and pooled dichotomous data were expressed as risk ratio (RR), with 95% CI. To facilitate the interpretation of estimated efficacy, we interpreted pooled SMD using rules of thumb as follow: <0.40 = small effect, 0.40–0.70 = moderate effect, >0.70 = large effect (21).

In this study, the meta-analyses compared: (1) efficacy of topical therapy with botanical products at each time point; (2) efficacy of topical therapy with botanical products compared with placebo; and (3) efficacy of topical therapy with botanical products compared with active-comparators. Therefore, subgroup analyses were conducted in these cases by intervention duration and comparator type (placebo/active-comparator). Heterogeneity was assessed through the I^2 statistic. For I^2 statistics, a value of <30, 30–60, and >60% represented low, moderate, or high heterogeneity, respectively. A $p < 0.05$ was considered significant for the test for the overall effect. Funnel plots were assessed to detect potential small-study effects as a signal of publication bias.

RESULTS

Search Results

The initial literature search yielded 839 unique records. A total of 817 records were excluded after the first screening, and two additional records were retrieved through a manual citation and reference search of relevant articles. The full-text of 24 studies were reviewed for inclusion, and finally, 12 eligible RCTs were included for meta-analysis (23–34). The detail of the study selection process are shown in **Figure 1**.

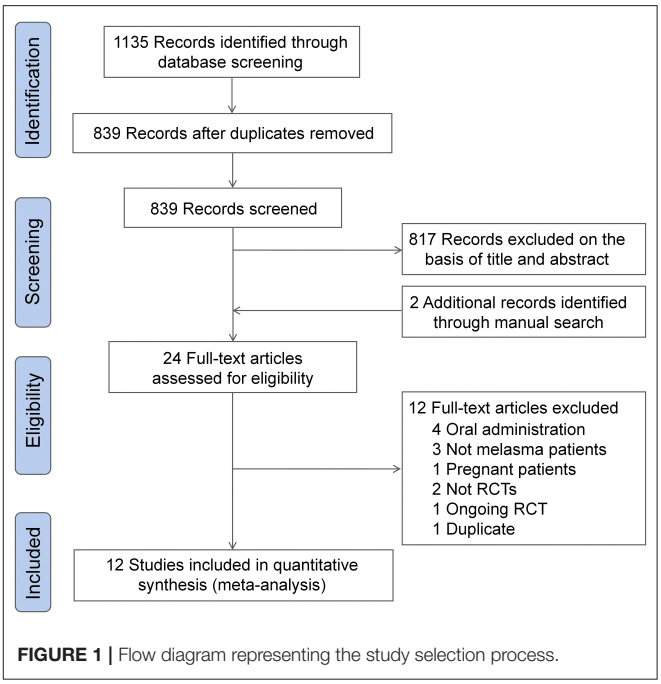

FIGURE 1 | Flow diagram representing the study selection process.

Study Characteristics

Characteristics of included RCTs were summarized in **Table 1**. These 12 studies included 695 patients with melasma from six different countries, in which female patients accounted for over 80%. Of 12 RCTs included, 2 studies included only epidermal melasma (29, 34), three studies included epidermal and mixed melasma (23, 25, 31), 1 study included only mixed melasma (26), 1 study included all types of melasma (24), and five studies did not specify the types (27, 28, 30, 32, 33). The active ingredients contained in botanical products varied among trials as follows: herb-derived molecules, extracts of a single herb, and extracts of compound herbs. The topical formulations of botanical products used for intervention included cream, oil, brewed, and solution. Six trials used placebo as a comparator (23, 24, 26–28, 32), four trials used actives as a comparator (25, 29, 30, 34), and two trials used both placebo and actives as a comparator (31, 33). The duration of intervention ranged from 4 to 12 weeks with a maximum follow-up duration of 16 weeks. A total of seven trials reported the incidence of AEs (23, 25, 29–31, 33, 34). Of 12 RCTs included, four declared sponsorship from non-profit organizations (24, 28–30), three from commercial industries (25, 27, 33), and five did not declare sponsorship (23, 26, 31, 32, 34).

Quality Assessment

Figure 2 shows the detailed assessment of the risk of bias. Of 12 RCTs included, 1 claimed unblinded (27), 2 claimed single-blind (23, 25), 8 claimed double-blind (24, 26, 28, 29, 31–34), and 1 claimed triple-blind (30). Five studies arose concern for risk of bias for the following reasons (23, 25, 27, 32, 33): (1) one study used an odd-even randomization method; (2) two studies had insufficient information about randomization method; (3) four studies had insufficient information on allocation concealment; (4) three studies did not use adequate blind method; and (5) three studies were funded by commercial industries. According to the declared criteria, seven studies were considered high quality (24, 26, 28–31, 34), four studies were considered moderate quality (23, 25, 27, 33), while one study was considered low quality

TABLE 1 | Characteristics of included studies.

Study	Country	Sample size (% female) and characteristics	Interventions	Duration (weeks)	Outcomes	Adverse events
Alvin et al. (23)	Philippines	Size: 50 (98%) Age: 44.5±7.5 (25–60) Melasma type: epidermal, mixed Melisma duration: 0–5 years	Oil (Mulberry) ***Vs.*** Placebo	8	MASI Mexameter reading Self-evaluation	**EG**: 16% 4 × mild itching **CG**: 48% 8 × mild pruritus 4 × mild erythema
Bavarsad et al. (24)	Iran	Size: 22 (100%) Age: 34.10 ± 8.99 Melasma type: epidermal, dermal, mixed Melisma duration: 210 ± 118 weeks	Cream (Lycopene and Wheat bran) ***Vs.*** Placebo	12	MASI Discoloration rate Area of melasma Self-evaluation	0%
Costa et al. (25)	Brazil	Size: 56 (100%) Age: 18–60 Melasma type: epidermal, mixed Melisma duration: NR	Cream (Emblica, Licorice and Belides) ***Vs.*** Cream (2% HQ)	12	Medical evaluation Self-evaluation UV spots Manchas UV	**EG**: 8.7% 2 × burning & increase of previous acne lesions **CG**: 26.9% 7 × erythema & burning & erythematous papules in the perioral region
Francisco-Diaz et al. (26)	Philippines	Size: 52 (84.6%) Age: 18–60 Melasma type: mixted Melisma duration: 3.75 years (mean)	Solution (Malva sylvestris, Mentha piperita, Primula veris, Alchemilia vulgaris, Achillea millefolium, Mellissa officinales) ***Vs.*** Placebo	12	mMASI Area of melasma Light reflectance	0%
He et al. (27)	China	Size: 70 (100%) Age: 24–52 Melasma type: NR Melisma duration: 0.5–20 years	Cream (herbal medicines) ***Vs.*** Placebo	8	MASI Medical evaluation	0%
Javedan et al. (28)	Iran	Size: 60 (81.6%) Age: 32.18 ± 8.69 (26–55) Melasma type: NR Melisma duration: NR	Cream (Dorema ammoniacum) ***Vs.*** Placebo	4	mMASI	0%
Khosravan et al. (29)	Iran	Size: 70 (100%) Age: 19–55 Melasma type: epidermal Melisma duration: NR	Parsley brewed ***Vs.*** Cream (4% HQ)	8	MASI	**EG**: 7.4% 2 × redness & itching **CG**: 7.4% 2 × redness & itching
Mahjour et al. (30)	Iran	Size: 40 (100%) Age: 18–59 Melasma type: NR Melisma duration: NR	Cream (C. Aritinum L. and C. melo var. inodorus H.Jacq) ***Vs.*** Cream (4% HQ)	12	MASI Self-evaluation	**EG**: 3.1% 1 × acne **CG**: 15.6% 3 × erythema 1 × ecne 1 × erythema & dryness & scaling
Mendoza et al. (31)	Philippines	Size: 45 (62.2%) Age: 29.04 ± 7.8 (18–50) Melasma type: epidermal, mixed Melisma duration: NR	Cream (Rumex occidentalis) ***Vs.*** 1. Cream (4% HQ) 2. Placebo	8	MASI Mexameter reading Medical evaluation Self-evaluation	**EG**: 6.7% 1 × mild peeling **CG1**: 0% **CG2**: 0%
Morag et al. (32)	Poland	Size: 50 (100%) Age: 37.67 ± 7.53 (26–55) Melasma type: NR Melisma duration: NR	Cream (Five-leaf serratula) ***Vs.*** Placebo	8	Mexameter reading	0%
Zhang et al. (33)	China	Size: 90 (NR) Age: 40.35 ± 6.02 (25–50) Melasma type: NR Melisma duration: 5.46 ± 3.72 years	Cream (China camellia, sanchi, Prinsepia utilis oil, and Portulaca oleracea) ***Vs.*** 1. Cream (arbutin) 2. Placebo	12	MASI Mexameter reading Inflammatory cells Self-evaluation	**EG**: 0% **CG1**: 6.7% 2 × slight erythema and pruritus **CG2**: 0%
Zubair et al. (34)	Pakistan	Size: 90 (96.7%) Age: 29.31 ± 6.47 (18–40) Melasma type: epidermal Melisma duration: 5.80 ± 3.93 years	Cream (4% Liquiritin) Cream (2% Liquiritin) ***Vs.*** Cream (4% HQ)	8	Medical evaluation	**EG**: 0% **CG**: 10% 2 × contact dermatitis 1 × hyperpigmentation

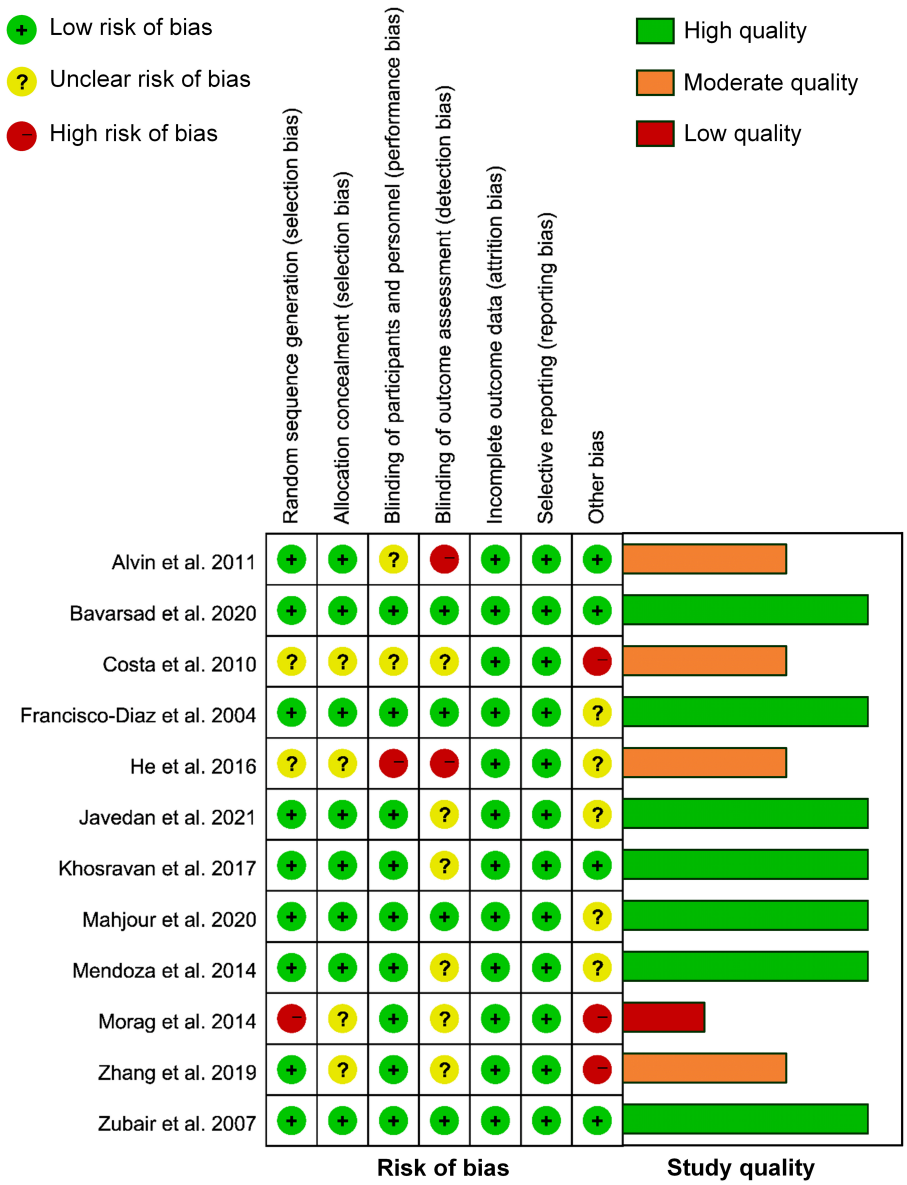

FIGURE 2 | Risk of bias and study quality assessment of included randomized controlled trials (RCTs).

(32). Overall, the major potential source of high bias was in the "other" bias domain which could be attributed to sponsorship from companies.

Primary Efficacy Outcomes

Ten RCTs with MASI outcomes included 299 and 299 participants in the botanical product and placebo groups, respectively. Pooled results showed that botanical products had a large effect on MASI reduction vs. placebo at 4 weeks (SMD −0.81, 95% CI −1.40– −0.22, $p = 0.007$; **Figure 3**). The effect size was larger when assessed at 8 weeks (SMD −0.94, 95% CI −1.64– −0.24, $p = 0.008$), compared with 4 weeks. However, the smallest effect was seen at 12 weeks (SMD −0.49, 95% CI −0.97– −0.05, $p = 0.03$). Therefore, the MASI reduction in patients receiving topical botanical products vs. placebo did not amplify with treatment time. Overall, botanical products improved melasma with a large effect vs. placebo (SMD −0.79, 95% CI −1.14– −0.44, $p < 0.00001$). In view of high heterogeneity across studies, we conducted a sensitivity analysis using fixed-effects, but the overall results were almost identical (SMD −0.69, 95% CI −0.86– −0.53, $p < 0.00001$). The funnel plot displayed a tolerably symmetrical funnel shape (**Figure 4A**), and the Egger test ($p = 0.2919$) also revealed the low risk of publication bias.

Eight RCTs included 228 and 228 participants in the botanical product and active-comparator groups, respectively. Pooled data showed that the SMD of MASI reduction in patients with

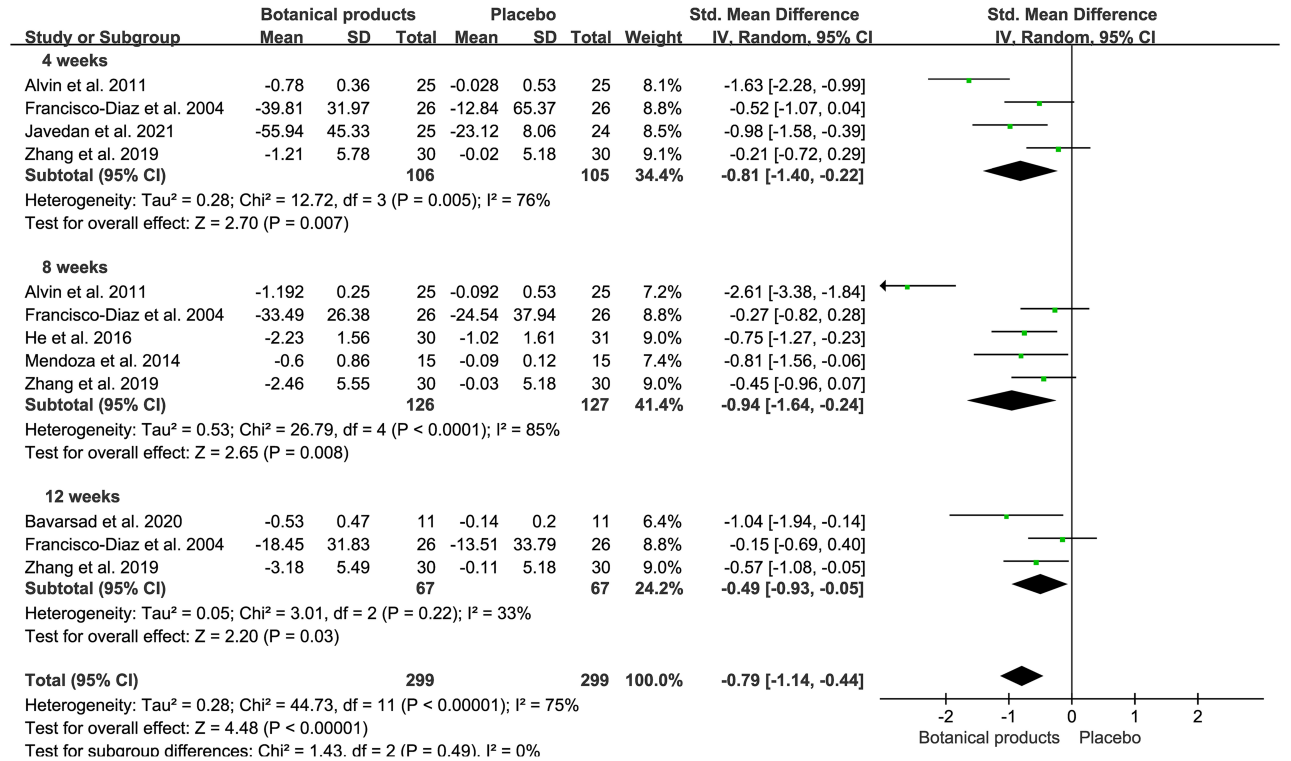

FIGURE 3 | Forest plots depicting the standardized mean difference (SMD) of Melasma Area and Severity Index (MASI) reduction in patients with melasma receiving botanical products in placebo-controlled trials. Subgroup analysis was stratified according to the duration of the intervention.

botanical products vs. actives was −0.00 (95% CI −0.36–0.35, $p = 0.98$) at 4 weeks, −0.10 (95% CI −0.37–0.17, $p = 0.48$) at 8 weeks, and −0.19 (95% CI −0.54–0.17, $p = 0.30$) at 12 weeks (**Figure 5**). The overall SMD was −0.10 (95% CI −0.28–0.09, $p = 0.30$), suggesting that botanical products had a similar effect to active-comparators. There was no remarkable asymmetry in the funnel plot (**Figure 4B**), and the Egger's test ($p = 0.9167$) also suggested the small potentiality of publication bias.

Secondary Efficacy Outcomes

Four placebo-controlled trials containing 190 participants, and active-controlled trials containing 90 participants, reported the efficacy of botanical products through measuring the changes of Mexameter® reading. Meta-analyses showed that botanical products had a moderate effect on the reduction of Mexameter® reading compared with placebo (SMD −0.52, 95% CI −0.81–0.23, $p = 0.0005$), but no significant difference when compared with active-comparators (SMD −1.31, 95% CI −2.72–0.10, $p = 0.07$; **Figure 6**). There was no heterogeneity between these placebo-controlled trials, but high heterogeneity between these active-controlled trials, and too few studies to assess for publication bias.

Improvement evaluated by patients was reported in 6 RCTs. For placebo-controlled trials, 36 (80.0%) of 45 patients allocated to botanical products reported improvement, compared with 12 (26.7%) of 45 patients receiving placebo, showing significant difference (RR 2.90, 95% CI 1.59–5.29, $p = 0.0005$; **Supplementary Figure 1**). For active-controlled trials, 86 (86.0%) of 100 patients allocated to botanical products achieved improvement, compared with 78 (75.7%) of 103 patients receiving placebo, but with no significant difference (RR 1.07, 95% CI 0.87–1.32, $p = 0.50$; **Supplementary Figure 1**).

Safety Outcome

Seven of 12 RCTs reported AEs, but no serious AEs. Common AEs included mild itching, erythema, and pruritus. For placebo-controlled trials, there were 5 (2.6%) of 192 patients receiving botanical products experienced AEs, compared with 12 (6.3%) of 192 patients receiving placebo. Pooled data showed that the incidence of AEs in patients taking botanical products was similar to those taking placebo (RR 0.60, 95% CI 0.09–4.08; $p = 0.60$; **Figure 6**). For active-controlled trials, there were only 6 (3.2%) of 187 patients receiving botanical products experienced AEs, compared with 20 (12.5%) of 160 patients receiving active-comparators. Pooled data also demonstrated a significant reduction in the incidence of AEs in patients receiving botanical products compared with active-comparators (RR 0.37, 95% CI 0.15–0.88, $p = 0.02$; **Figure 7**). Overall, topical therapy with botanical products was well-tolerated across studies. There was no remarkable asymmetry in the funnel plot (**Supplementary Figure 2**), and the Egger's test ($p = 0.2421$) also suggested the small potentiality of publication bias.

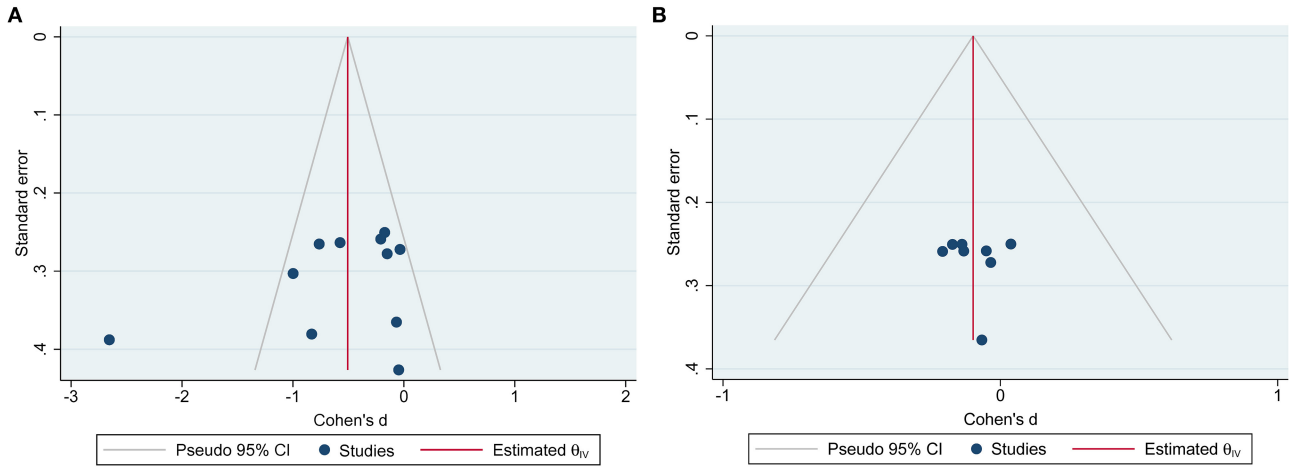

FIGURE 4 | Funnel plots for RCTs reported Melasma Area and Severity Index (MASI) outcome measures. **(A)** Funnel plot for placebo-controlled trials; **(B)** funnel plot for active-controlled trials.

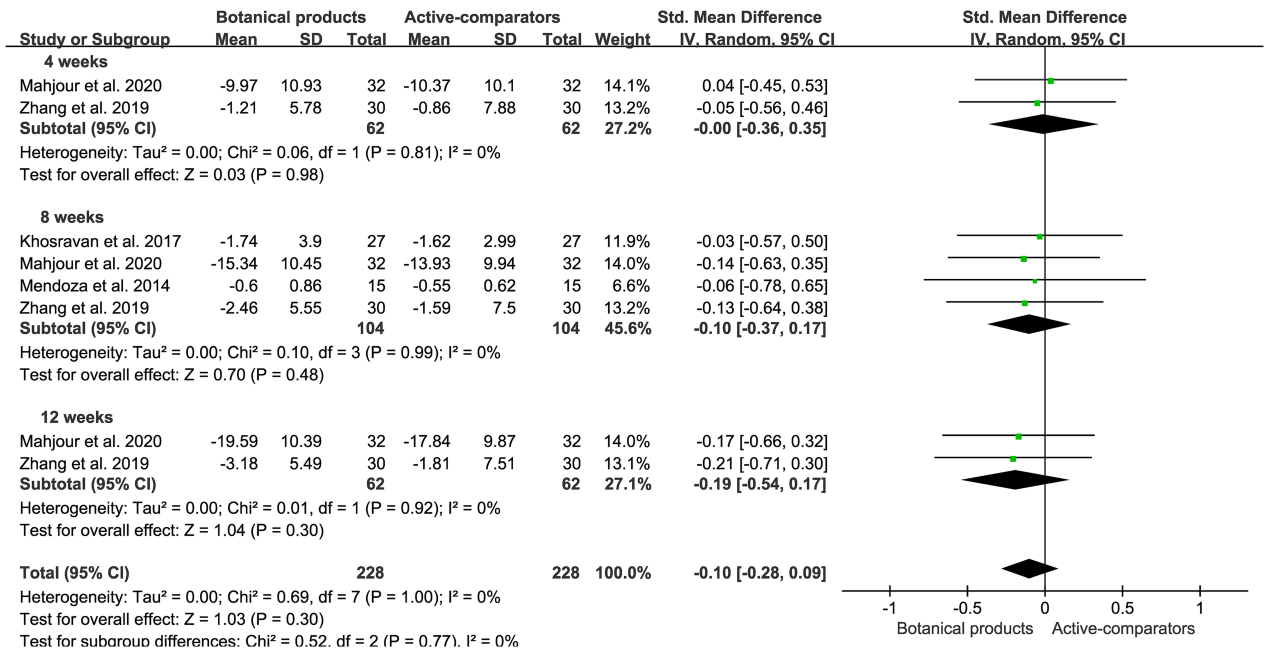

FIGURE 5 | Forest plots depicting the SMD of MASI reduction in patients with melasma receiving botanical products in active-controlled trials. Subgroup analysis was stratified according to the duration of the intervention.

DISCUSSION

To the best of our knowledge, this systematic review and meta-analysis could be the first to comprehensively assess the efficacy and safety of botanical products for the treatment of melasma. The pooled results suggested that botanical products significantly improved melasma compared to placebo and showed comparable efficacy to active-comparators. Currently, the most common subjective outcome is MASI, as confirmed by that 9 of 12 included RCTs adopted it. The effect sizes of botanical products for MASI outcomes were large compared with placebo. Objective outcome measures were used in some studies, such as Mexameter® reading, which was adopted in 4 of 12 included RCTs. Our meta-analysis demonstrated that there was significant benefit associated with the use of botanical products in Mexameter® reading when compared with placebo, and no difference when compared with active-comparators. These results were consistent with the findings from pooled MASI outcomes. In addition, our systematic review demonstrated that botanical products were well-tolerated, with only a small proportion of patients

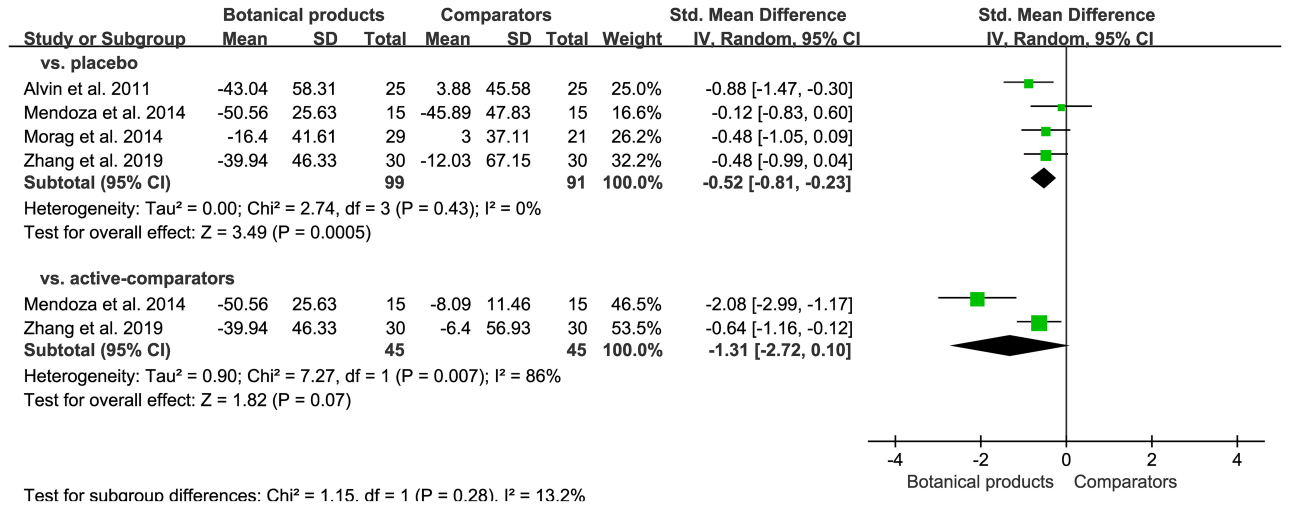

FIGURE 6 | Forest plot depicting the SMD of Mexameter® reading reduction in patients with melasma receiving botanical products in RCTs. Subgroup analysis was stratified according to comparators.

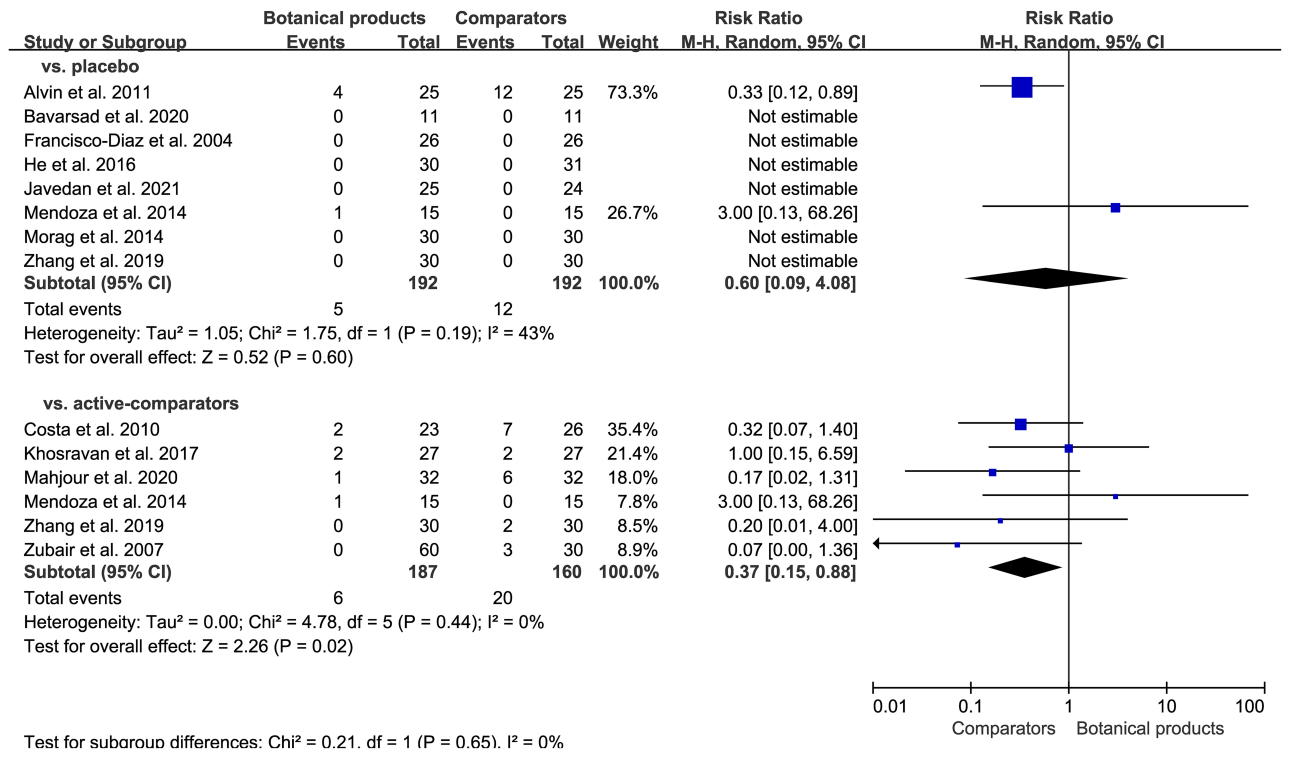

FIGURE 7 | Forest plot depicting the risk ratio (RR) for safety outcome in RCTs investigating the efficacy of botanical products. Subgroup analysis was stratified according to comparators.

experiencing mild AEs. Our meta-analysis also suggested that rates of AEs were lower for botanical products compared to active-comparators and were comparable to placebo.

Although topical phytotherapy produced a significant MASI reduction, we noted a decrease in effect size at the 12th week when compared with the 4th and 8th weeks. This condition was in agreement with the results from one trial where MASI reduction was reversed at the 12th week compared with the 8th week (26). These data suggested that the efficacy of topical botanical products might not amplify with treatment time, and

even there was a potential to fade. Therefore, their long-time efficacy still needs to be studied and validated in further trials. Moreover, melasma is known to have a high relapse rate which makes efficacy maintenance challenging (3). For instance, in a trial with 12 weeks follow-up, patients reported a melasma relapse with retrogressed MASI within 4 weeks of HQ cessation (35). By contrast, in one of the included trials, a cream containing lycopene and wheat bran caused a significant decrease in MASI during 12 weeks of treatment, with no recurrence within 4 weeks of phytotherapy cessation (24). This could provide a clue that botanical products might have an advantage over HQ in efficacy maintenance, but it still needs to be validated by better studies with a large sample size and longer follow-up.

Melanin is produced from the melanosomes and transferred from melanocytes to keratinocytes (36–38). Melanin synthesis is a tyrosinase-dependent process and requires several oxidative reactions, which consist of tyrosine hydrolysis to dopa, dopa oxidation to quinine, and quinine oxidation to melanin. Transfer of melanosomes to keratinocytes is controlled by keratinocyte protease-activated receptor-2 (PAR-2). The mechanisms of action supporting the efficacy of botanical products in the treatment of melasma vary with the contained active ingredients. Many botanical ingredients bind to the active site of tyrosinase and exert inhibitory activity, which is comparable to HQ (39–41). Moreover, recent studies demonstrate the indirect inhibitory effects of several botanicals on tyrosinase occurring at the transcriptional level through decreasing mRNA expression of tyrosinase-related protein 1 (TRP-1), TRP-2, and microphthalmia-associated transcription factor (MITF) (42, 43). Several botanicals suppress melanosome transfer through inhibition of the keratinocyte PAR-2 (44, 45). Since inflammatory mediators and radicals contribute to melanocyte pigment production, many botanicals inhibit melanin synthesis through anti-inflammatory and antioxidant effects (46, 47). Among the included RCTs, topical therapies with botanical products alleviated melasma through either (1) direct or indirect inhibition of tyrosinase to suppress melanogenesis (29–32); (2) antioxidation to scavenge free radicals (27); (3) regulating inflammatory mediators to inhibit inflammation (28); or (4) synergistic action of above several mechanisms (25, 33, 34).

This meta-analysis had some limitations that merit discussion. First, only a very few studies are RCTs with placebo or active-comparator among numerous published articles, thus the sample size and number of included studies for each meta-analysis were relatively small. Second, the treatment durations were relatively short within 12 weeks, which meant that the long-term efficacy and safety could not be evaluated. Furthermore, of all RCTs included, only one trial that was considered high quality based on the risk of bias assessment, reported the post-treatment assessment with a short follow-up (4 weeks) (24). However, given the recurrent nature of melasma, sufficient trials including a longer duration of posttreatment assessment are indispensable. The third limitation was the information absence on the types of melasma in many RCTs, making it fail to determine the inter-study variability in the type of melasma. A final limitation was the high heterogeneity observed in several meta-analyses, and it is to be expected due to the different botanicals across studies. This was also the uppermost limitation because different botanical products including different compounds and formulations could present different action mechanisms for the treatment of melasma, thus these heterogeneous medications could partly weaken the significance and reliability of obtained findings herein. Nevertheless, this work still represents the best level of evidence currently available on the topical use of botanical products in the management of melasma.

CONCLUSION

Botanical products have been increasingly popular in topical therapies for melasma, and many RCTs have been conducted to evaluate their efficacy. However, it still lacks sufficient pooled evidence on their efficacy and safety. Therefore, we conducted a systematic review and meta-analysis on the efficacy and safety of topical botanical products for the treatment of melasma. The pooled results suggested that topical therapy with botanical products produced significant improvement in melasma with beneficial effects on MASI reduction and Mexameter® reading reduction when compared with placebo. It also showed that botanical products produced comparable efficacy for melasma when compared with active-comparators. Moreover, these botanical products were well-tolerated across studies, with no serious AEs reported. This work could represent the best level of evidence currently available on the efficacy and safety of topical botanical products for the treatment of melasma. However, the limitations that existed in this work, namely, small sample size, a short period of treatment, lack of post-treatment follow-up, and importantly heterogeneous medications, could weaken the significance and reliability of these results to some extent. Therefore, it should be noted that more high-quality RCTs with longer intervention and follow-up duration are required before recommending topical botanical products as a viable clinical treatment option for melasma.

DATA AVAILABILITY STATEMENT

The original contributions presented in the study are included in the article/**Supplementary Material**, further inquiries can be directed to the corresponding authors.

AUTHOR CONTRIBUTIONS

ZL and BQ contributed to the conceptualization and supervision. ZL, TW, and YW contributed to the writing. JW and HC contributed to the software, methodology, and data curation. TW and YW contributed to the investigation and formal analysis. All authors contributed to the article and approved the submitted version of the manuscript.

FUNDING

This study was supported by the National Natural Science Foundation of China (Grant No. 82104525), the Natural Science

Foundation of the Jiangsu Higher Education Institutions of China (Grant No. 21KJB360009), Natural Science Foundation of Jiangsu Normal University (Grant No. 20XSRX002), and State Key Laboratory of Natural and Biomimetic Drugs (Grant No. K202114).

SUPPLEMENTARY MATERIAL

The Supplementary Material for this article can be found online at: https://www.frontiersin.org/articles/10.3389/fmed.2021.797890/full#supplementary-material

REFERENCES

1. Tamega AdA, Miot LDB, Bonfietti C, Gige TC, Marques MEA, Miot HA. Clinical patterns and epidemiological characteristics of facial melasma in Brazilian women. *J Eur Acad Dermatol.* (2013) 27:151–6. doi: 10.1111/j.1468-3083.2011.04430.x
2. Handel AC, Miot LDB, Miot HA. Melasma: a clinical and epidemiological review. *An Bras Dermatol.* (2014) 89:771–82. doi: 10.1590/abd1806-4841.20143063
3. Gupta AK, Gover MD, Nouri K, Taylor S. The treatment of melasma: a review of clinical trials. *J Am Acad Dermatol.* (2006) 55:1048–65. doi: 10.1016/j.jaad.2006.02.009
4. Taylor SC. Epidemiology of skin diseases in people of color. *Cutis.* (2003) 71:271–5. doi: 10.1034/j.1600-0536.2003.00091.x
5. Gilchrest BA, Fitzpatrick TB, Anderson RR, Parrish JA. Localization of malanin pigmentation in the skin with Wood's lamp. *Br J Dermatol.* (1977) 96:245–8. doi: 10.1111/j.1365-2133.1977.tb06132.x
6. Achar A, Rathi SK. Melasma: a clinico-epidemiological study of 312 cases. *Indian J Dermatol.* (2011) 56:380–2. doi: 10.4103/0019-5154.84722
7. Sheth VM, Pandya AG. Melasma: a comprehensive update: part I. *J Am Acad Dermatol.* (2011) 65:689–97. doi: 10.1016/j.jaad.2010.12.046
8. Ortonne JP, Arellano I, Berneburg M, Cestari T, Chan H, Grimes P, et al. A global survey of the role of ultraviolet radiation and hormonal influences in the development of melasma. *J Eur Acad Dermatol.* (2009) 23:1254–62. doi: 10.1111/j.1468-3083.2009.03295.x
9. Noh TK, Choi SJ, Chung BY, Kang JS, Lee JH, Lee MW, et al. Inflammatory features of melasma lesions in Asian skin. *J Dermatol.* (2014) 41:788–94. doi: 10.1111/1346-8138.12573
10. Arrowitz C, Schoelermann AM, Mann T, Jiang LI, Weber T, Kolbe L. Effective tyrosinase inhibition by thiamidol results in significant improvement of mild to moderate melasma. *J Investig Dermatol.* (2019) 139: 1691–8.e6. doi: 10.1016/j.jid.2019.02.013
11. Briganti S, Camera E, Picardo M. Chemical and instrumental approaches to treat hyperpigmentation. *Pigm Cell Res.* (2003) 16:101–10. doi: 10.1034/j.1600-0749.2003.00029.x
12. Mishra SN, Dhurat RS, Deshpande DJ, Nayak CS. Diagnostic utility of dermatoscopy in hydroquinone-induced exogenous ochronosis. *Int J Dermatol.* (2013) 52:413–7. doi: 10.1111/j.1365-4632.2011.05305.x
13. Westerhof W, Kooyers TJ. Hydroquinone and its analogues in dermatology - a potential health risk. *J Cosmet Dermatol.* (2005) 4:55–9. doi: 10.1111/j.1473-2165.2005.40202.x
14. McKesey J, Tovar-Garza A, Pandya AG. Melasma treatment: an evidence-based review. *Am J Clin Dermatol.* (2020) 21:173–225. doi: 10.1007/s40257-019-00488-w
15. Yokota T, Nishio H, Kubota Y, Mizoguchi M. The inhibitory effect of glabridin from licorice extracts on melanogenesis and inflammation. *Pigment Cell Res.* (1998) 11:355–61. doi: 10.1111/j.1600-0749.1998.tb00494.x
16. Zhu W, Gao J. The use of botanical extracts as topical skin-lightening agents for the improvement of skin pigmentation disorders. *J Investig Dermatol Symp Proc.* (2008) 13:20–4. doi: 10.1038/jidsymp.2008.8
17. Gunia-Krzyzak A, Popiol J, Marona H. Melanogenesis inhibitors: strategies for searching for and evaluation of active compounds. *Curr Med Chem.* (2016) 23:3548–74. doi: 10.2174/0929867323666160627094938
18. Levin J, Momin SB. How much do we really know about our favorite cosmeceutical ingredients? *J Clin Aesthet Dermatol.* (2010) 3:22–41.
19. Kimbrough-Green CK, Griffiths CE, Finkel LJ, Hamilton TA, Bulengo-Ransby SM, Ellis CN, et al. Topical retinoic acid (tretinoin) for melasma in black patients. A vehicle-controlled clinical trial. *Arch Dermatol.* (1994) 130:727–33. doi: 10.1001/archderm.1994.01690060057005
20. Moher D, Shamseer L, Clarke M, Ghersi D, Liberati A, Petticrew M, et al. Preferred reporting items for systematic review and meta-analysis protocols (PRISMA-P) 2015 statement. *Sys Rev.* (2015) 4:1. doi: 10.1186/2046-4053-4-1
21. Higgins J SGTCC. *Cochrane Handbook for Sytematic Reviews of Interventions*. version 5.1.0. New York, NY: John Wiley & Sons (2011).
22. Bai S, Guo W, Feng Y, Deng H, Li G, Nie H, et al. Efficacy and safety of anti-inflammatory agents for the treatment of major depressive disorder: a systematic review and meta-analysis of randomised controlled trials. *J Neurol Neurosurg Psychiatry.* (2020) 91:21–32. doi: 10.1136/jnnp-2019-320912
23. Alvin G, Catambay N, Vergara A, Jamora MJ. A comparative study of the safety and efficacy of 75% mulberry (Morus alba) extract oil versus placebo as a topical treatment for melasma: a randomized, single-blind, placebo-controlled trial. *J Drugs Dermatol.* (2011) 10:1025–31. doi: 10.1016/j.jdermsci.2011.05.004
24. Bavarsad N, Mapar MA, Safaezadeh M, Latifi SM. A double-blind, placebo-controlled randomized trial of skin-lightening cream containing lycopene and wheat bran extract on melasma. *J Cosmet Dermatol.* (2021) 20:1795–800. doi: 10.1111/jocd.13799
25. Costa A, Moisés TA, Cordero T, Alves CRT, Marmirori J. Association of emblica, licorice and belides as an alternative to hydroquinone in the clinical treatment of melasma. *An Bras Dermatol.* (2010) 85:613–20. doi: 10.1590/S0365-05962010000500003
26. Francisco-Diaz J, Cruz DD, Verallo-Rowell VM. A double-blind randomized placebo controlled trial on the efficacy and safety of botanical extract (Gigawhite 5% solution) in the treatment of melasma. *J Philipp Dermatolo Society*. (2004) 13:18–23.
27. He X, Xu B. Observation on the clinical efficacy of Yaokou Rose Jiaoyan cream in the treatment of melasma. *Asia-Pacific Traditional Medicine.* (2016) 12:147–8. doi: 10.11954/ytctyy.201615068
28. Javedan K, Hydarpur F, Mohammadi Pour P, Najafi F, Mirzaeei S, Rahimi R, et al. The formulation and efficacy of topical Dorema ammoniacum in treating melasma: a randomized double-blind, placebo-controlled trial. *J Complement Integr Med.* (2021). doi: 10.1515/jcim-2020-0191
29. Khosravan S, Alami A, Mohammadzadeh-Moghadam H, Ramezani V. The effect of topical use of petroselinum crispum (parsley) versus that of hydroquinone cream on reduction of epidermal melasma: a randomized clinical trial. *Holist Nurs Pract.* (2017) 31:16–20. doi: 10.1097/HNP.0000000000000186
30. Mahjour M, Banihashemi M, Rakhshandeh H, Vakili V, Khoushabi A, Kakhki MT, et al. triple-blind, randomized trial of a traditional compound as compared to 4% hydroquinone in melasma. *J Herb Med.* (2020) 19:100308. doi: 10.1016/j.hermed.2019.100308
31. Mendoza CG, Singzon IA, Handog EB. A randomized, double-blind, placebo-controlled clinical trial on the efficacy and safety of 3% Rumex occidentalis cream versus 4% hydroquinone cream in the treatment of melasma among Filipinos. *Int J Dermatol.* (2014) 53:1412–6. doi: 10.1111/ijd.12690
32. Morag M, Nawrot J, Siatkowski I, Adamski Z, Fedorowicz T, Dawid-Pac R, et al. A double-blind, placebo-controlled randomized trial of Serratulae quinquefoliae folium, a new source of β-arbutin, in selected skin hyperpigmentations. *J Cosmet Dermatol.* (2015) 14:185–90. doi: 10.1111/jocd.12147
33. Zhang Q, Tu Y, Gu H, Sun D, Wu W, Man MQ, et al. A cream of herbal mixture to improve melasma. *J Cosmet Dermatol.* (2019) 18:1721–8. doi: 10.1111/jocd.12938
34. Zubair S, Mujtaba G. Comparison of efficacy of topical 2% liquiritin, topical 4% liquiritin and topical 4% hydroquinone in the management of melasma. *J Pakistan Assoc Dermatologists.* (2009) 19:158–63.
35. Gheisari M, Dadkhahfar S, Olamaei E, Moghimi HR, Niknejad N, Najar Nobari N. The efficacy and safety of topical 5% methimazole vs 4%

hydroquinone in the treatment of melasma: A randomized controlled trial. *J Cosmet Dermatol.* (2020) 19:167–72. doi: 10.1111/jocd.12987
36. Yao C, Oh JH, Oh IG, Park CH, Chung JH. [6]-Shogaol inhibits melanogenesis in B16 mouse melanoma cells through activation of the ERK pathway. *Acta Pharmacol Sin.* (2013) 34:289–94. doi: 10.1038/aps.2012.134
37. Boissy RE. Melanosome transfer to and translocation in the keratinocyte. *Exp Dermatol.* (2003) 12(Suppl. 2):5–12. doi: 10.1034/j.1600-0625.12.s2.1.x
38. Smit N, Vicanova J, Pavel S. The hunt for natural skin whitening agents. *Int J Mol Sci.* (2009) 10:5326–49. doi: 10.3390/ijms10125326
39. Asl MN, Hosseinzadeh H. Review of pharmacological effects of Glycyrrhiza sp. and its bioactive compounds. *Phytother Res.* (2008) 22:709–24. doi: 10.1002/ptr.2362
40. Gillbro JM, Olsson MJ. The melanogenesis and mechanisms of skin-lightening agents–existing and new approaches. *Int J Cosmet Sci.* (2011) 33:210–21. doi: 10.1111/j.1468-2494.2010.00616.x
41. Maeda K, Fukuda M. Arbutin: mechanism of its depigmenting action in human melanocyte culture. *J Pharmacol Exp Ther.* (1996) 276:765–9.
42. Lee TH, Seo JO, Do MH, Ji E, Baek S-H, Kim SY. Resveratrol-enriched rice down-regulates melanin synthesis in uvb-induced guinea pigs epidermal skin tissue. *Biomol Ther.* (2014) 22:431–7. doi: 10.4062/biomolther.2014.098
43. Jun HJ, Lee JH, Cho BR, Seo WD, Kang HW, Kim DW, et al. Dual inhibition of γ-oryzanol on cellular melanogenesis: inhibition of tyrosinase activity and reduction of melanogenic gene expression by a protein kinase A-dependent mechanism. *J Nat Prod.* (2012) 75:1706–11. doi: 10.1021/np300250m
44. Seiberg M, Paine C, Sharlow E, Andrade-Gordon P, Costanzo M, Eisinger M, et al. The protease-activated receptor 2 regulates pigmentation via keratinocyte-melanocyte interactions. *Exp Cell Res.* (2000) 254:25–32. doi: 10.1006/excr.1999.4692
45. Paine C, Sharlow E, Liebel F, Eisinger M, Shapiro S, Seiberg M. An alternative approach to depigmentation by soybean extracts via inhibition of the PAR-2 pathway. *J Invest Dermatol.* (2001) 116:587–95. doi: 10.1046/j.1523-1747.2001.01291.x
46. Rizwan M, Rodriguez-Blanco I, Harbottle A, Birch-Machin MA, Watson REB, Rhodes LE. Tomato paste rich in lycopene protects against cutaneous photodamage in humans in vivo: a randomized controlled trial. *Brit J Dermatol.* (2011) 164:154–62. doi: 10.1111/j.1365-2133.2010.10057.x
47. Sun Z, Park SY, Hwang E, Zhang M, Seo SA, Lin P, et al. Thymus vulgaris alleviates UVB irradiation induced skin damage via inhibition of MAPK/AP-1 and activation of Nrf2-ARE antioxidant system. *J Cell Mol Med.* (2017) 21:336–48. doi: 10.1111/jcmm.12968

Conflict of Interest: The authors declare that the research was conducted in the absence of any commercial or financial relationships that could be construed as a potential conflict of interest.

Publisher's Note: All claims expressed in this article are solely those of the authors and do not necessarily represent those of their affiliated organizations, or those of the publisher, the editors and the reviewers. Any product that may be evaluated in this article, or claim that may be made by its manufacturer, is not guaranteed or endorsed by the publisher.

frontiers | Frontiers in Medicine

REVIEW
published: 14 April 2022
doi: 10.3389/fmed.2022.863786

Epithelial-Mesenchymal Interaction in Hair Regeneration and Skin Wound Healing

*Mei-Qi Mao†, Jing Jing†, Yu-Jie Miao and Zhong-Fa Lv**

Department of Dermatology, Second Affiliated Hospital, Zhejiang University School of Medicine, Hangzhou, China

Interactions between epithelial and mesenchymal cells influence hair follicles (HFs) during embryonic development and skin regeneration following injury. Exchanging soluble molecules, altering key pathways, and extracellular matrix signal transduction are all part of the interplay between epithelial and mesenchymal cells. In brief, the mesenchyme contains dermal papilla cells, while the hair matrix cells and outer root sheath represent the epithelial cells. This study summarizes typical epithelial–mesenchymal signaling molecules and extracellular components under the control of follicular stem cells, aiming to broaden our current understanding of epithelial–mesenchymal interaction mechanisms in HF regeneration and skin wound healing.

Keywords: skin, skin appendages, dermal papilla, epithelial-mesenchymal interactions, wound healing, hair follicle growth cycle

OPEN ACCESS

Edited by:
Xing-Hua Gao,
The First Affiliated Hospital of China Medical University, China

Reviewed by:
Ekaterina Vorotelyak,
Koltzov Institute of Developmental Biology (RAS), Russia
Takashi Hashimoto,
Osaka City University, Japan

***Correspondence:**
Zhong-Fa Lv
lzfskin@zju.edu.cn

†These authors have contributed equally to this work

Specialty section:
This article was submitted to Dermatology, a section of the journal Frontiers in Medicine

Received: *27 January 2022*
Accepted: *16 March 2022*
Published: *14 April 2022*

Citation:
Mao M-Q, Jing J, Miao Y-J and Lv Z-F (2022) Epithelial-Mesenchymal Interaction in Hair Regeneration and Skin Wound Healing. Front. Med. 9:863786. doi: 10.3389/fmed.2022.863786

INTRODUCTION

Hair follicles (HFs) consist of the infundibulum, isthmus, and hair bulb. The hair bulb is located in the thickened base of the hair root and consists of an epithelium-derived matrix wrapped around a mesenchymal cell-derived dermal papilla (DP), which contains DP cells, endothelial vascular cells, and extracellular matrix (ECM). Cell–cell contacts, cell–matrix interactions, and tissue–neural interplay are all controlled by epithelial–mesenchymal interactions (EMIs), which also incorporate morphogens, cell adhesion factors (proteoglycans, etc.), growth factors, ECM molecules, hormones, cytokines, enzymes, and specific pharmacologically relevant molecules (retinoid, etc.) and their receptors (1).

Sonic hedgehog (SHH), wingless (Wnt), bone morphogenetic protein (BMP), fibroblast growth factor (FGF), their receptors, and other pathways are linked to embryonic HF development, the hair cycle, and skin wound healing (2). Other underlying molecular families associated with HF morphogenesis are the transforming growth factor-beta (TGF-β) family and neurotrophic proteins (3, 4). In HFs, DPs can secrete components that act on the peripheral matrix, such as epidermal growth factor (EGF), FGF, hepatocyte growth factor (HGF), insulin-like growth factor-I (IGF-I), keratinocyte growth factor (KGF or FGF-7), TGF-β, basic FGF (bFGF or FGF-2), and interleukins (IL-1, etc.) (5). DP ensures and regulates the hair growth and hair cycle in order.

Through EMI between DPs and epithelial cells, HFs participate in postinjury skin wound healing. In patients with extensive skin burns, transplanting HF progenitor cells enhances angiogenesis, regulates the inflammatory response, speeds wound healing, and improves the physiological function of skin regeneration. HF progenitor cell transplantation is an innovative technique and could be a new therapeutic option for long-term unhealed wounds (6).

EMI IN HF MORPHOGENESIS AND CYCLIC REGENERATION

HF Morphogenesis

Hair follicle morphogenesis is the climax of a series of EMI through coordinated epidermal–mesenchymal signaling and gradual tissue remodeling, with stem cell populations evolving into a complete HF structure (7, 8). Due to the availability of mouse specimens, mouse models play a key role in EMI research during HF morphogenesis and cycle (9). Initially, the dermis emits the first dermal signal, which stimulates the production of epidermal placodes. The placode is the initial hair structure, a concavity of the epidermis descending into the dermis. Subsequently, the placode delivers epidermal impulses to the dermal cells beneath the epidermis, leading to the formation of dermal condensate (DC) (7, 8). Following the DC's second dermal signal, proliferative epithelial cells shape pegs and downwards (**Figure 1A**). HF stem cells (HFSCs) stimulate the subsequent downward expansion of hair pegs, eventually forming an integral HF.

HF Cyclic Regeneration

Bulge HFSCs and mesenchymal DPs act as progenitor cells for the HF epidermal and dermal layers, respectively (7). In the late telogen phase of humans and mice, DP activates bulge HFSCs, creating germ cells that continue to build the hair matrix, resulting in the production of the inner root sheath and the hair sheath (10).

Dermal papilla numbers are stable during HF cycles but drastically decrease in patients with androgenetic alopecia (11). Maintenance of the quantity and function of DP cells is required for healthy hair. In normal conditions, HF dermal stem cell (hfDSC) progeny supply lower DP cells and diverge toward the dermal sheath, but with injury, cell loss, senescence, and HF hypertrophy, they are transported to the upper DP, which initiates significant HF regeneration (12). During the anagen phase, hfDSCs replenish the DP and dermal sheath and exit the DP into the dermal cup during the catagen phase. Then, they enter a quiescent state or undergo apoptosis. Accordingly, to maintain the HF cycle, a balance between hfDSC reduction (differentiation and withdrawal from the hfDSC niche) and increase is critical (13).

The dermal papilla is dependent on EMI to induce HF regeneration, and the function of DP is inextricably tied to the progenitors of the epithelial matrix that surrounds it (14). The hair matrix is located in the proliferative zone of the hair bulb and consists of epithelial stem cells and transient amplifying cells. DP awakens the transient amplifying cells in anagen, enabling hair germs to migrate down with the DP, similar to how epithelial stem cells behave during embryonic HF development (**Figure 1C**) (8). In late anagen and catagen, DP loses contact with the hair matrix and ascends below the lower bulge as the hair sheath shortens. Moreover, the hair matrix transforms into secondary hair germs. In the next cycle, the secondary hair germ encloses the DP to form the newly generated hair matrix (15, 16).

EMI Signals Modulate HF Morphogenesis and Cycling

Wnt, SHH, and BMP Pathway

The epidermal NF-κB, Wnt/β-catenin, and SHH/patched pathways control HF development. In the mesenchyme, BMP signaling takes a predominant position, promotes HF regeneration, and preserves epithelial stem cell characteristics (17). Signal networks in the epithelium and mesenchyme regulate hair morphogenesis and cyclic regeneration. Due to the lack of a reliable model of human scalp HFs, most of the subsequent studies were completed using a mouse model. In cases not explicitly labeled, the laboratory specimens were mice in this part.

Wnt Pathway

Wingless proteins initiate HF development, preserve stem cell identities, and guarantee the formation of the hair sheath. The classic Wnt signaling pathway contributes to placode development and stimulates the differentiation of dermal progenitor cells into DCs (18). Specifically, the initial epithelial signal involved in DC development is Wnt10a/b, and Wnt5a is a secondary epithelial signal responsible for the descent of HF into the dermis (19, 20). Although the Wnt/β-catenin and EdaA1/NF-κB pathways both mediate placode formation, Wnt/β-catenin serves as the first and most critical signal related to HF morphogenesis (7). Interestingly, the absence of Lef1, a β-catenin-related molecule, results in structural and functional deficits in mutant mouse glands, teeth, and hair, revealing the central role of the Wnt pathway in skin appendages (21).

During the hair cycle, the hair matrix expresses Wnt3a and Wnt10b, and DP responds to Wnt pathway signals to activate HF epithelial cells (3, 20, 22). Matrix proliferation requires epithelial Wnt/β-catenin; inhibiting β-catenin or exogenously adding Dickkopf (Dkk) can inhibit matrix growth and anagen processing (23). Ectodysplasin A (Eda) indirectly inhibits the Wnt signaling pathway by targeting Dkk; Eda deficiency results in malformed hairs, whereas its overexpression impairs HF periodic renewal (7, 8, 23). Simultaneously, Wnt signaling controls the activity of hair sheath-specific signals, showing its function in HFSC-specific differentiation (24, 25). Furthermore, epithelial Wnt signaling is involved in DP-inducible properties, and experiments found that the addition of Wnt3a rebuilt the inducibility of DP that has been lost *in vitro* in both mice and human tissues (22, 26).

BMP Pathway

Bone morphogenic proteins (BMPs) are members of the TGF superfamily and are involved in organ morphogenesis. The human epidermis contains BMPR1A and BMP2, while DCs carry BMP4 and Noggin (8, 26). Inhibited BMP results in increased HF volume, and awl hair replaces zig-zag hair (7). Additionally, through a hybrid knockout test, the BMP signaling pathway was proved to be critical for stem cell rejuvenation: BMP/Wnt signaling maintains stem cell homeostasis by balancing the stem cell, EMI, and the HF–subcutaneous adipose tissue interaction (17, 27). By attenuating the inhibitory effect of BMP on the ectodysplasin A receptor (Edar), connective tissue growth factors

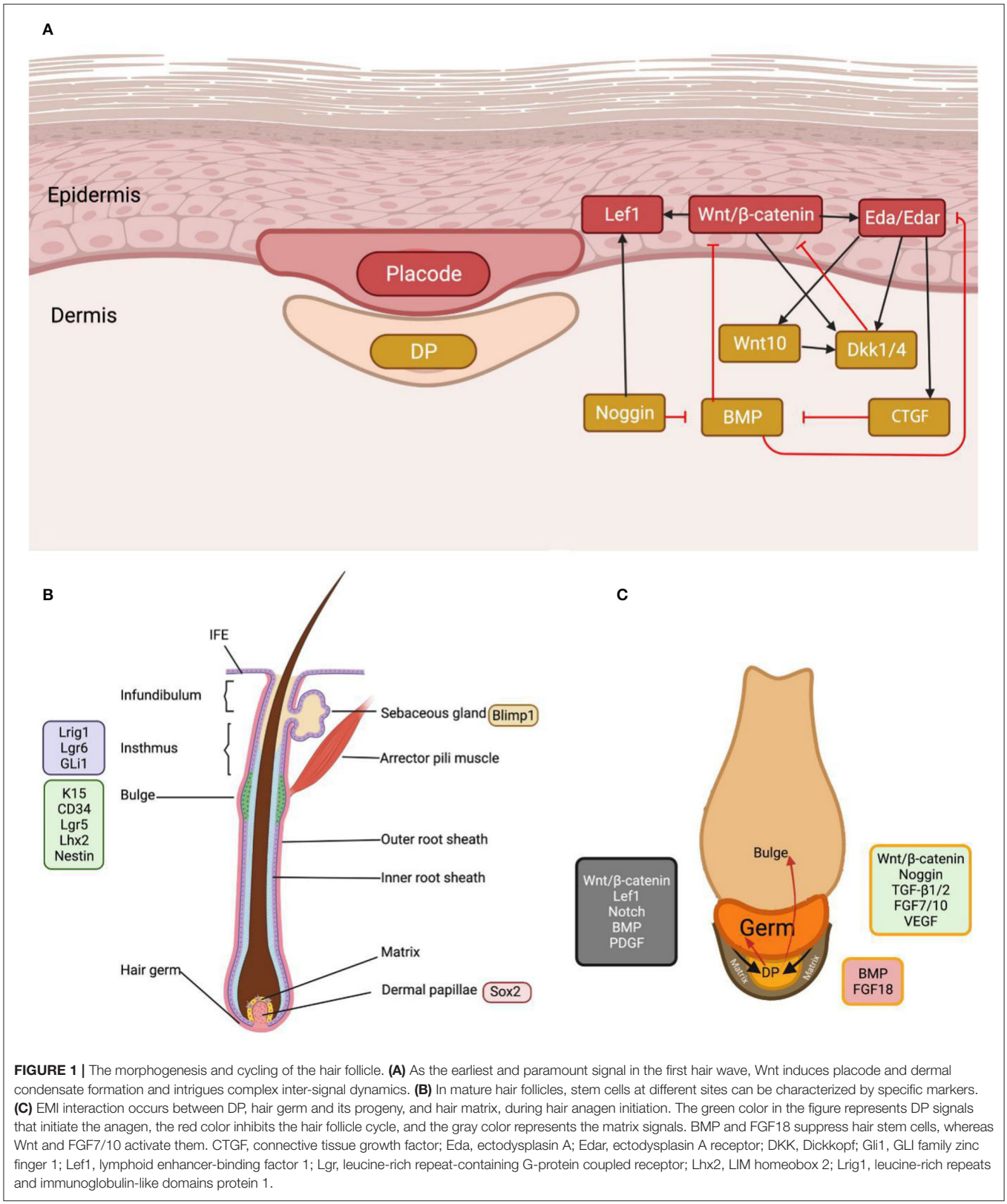

FIGURE 1 | The morphogenesis and cycling of the hair follicle. **(A)** As the earliest and paramount signal in the first hair wave, Wnt induces placode and dermal condensate formation and intrigues complex inter-signal dynamics. **(B)** In mature hair follicles, stem cells at different sites can be characterized by specific markers. **(C)** EMI interaction occurs between DP, hair germ and its progeny, and hair matrix, during hair anagen initiation. The green color in the figure represents DP signals that initiate the anagen, the red color inhibits the hair follicle cycle, and the gray color represents the matrix signals. BMP and FGF18 suppress hair stem cells, whereas Wnt and FGF7/10 activate them. CTGF, connective tissue growth factor; Eda, ectodysplasin A; Edar, ectodysplasin A receptor; DKK, Dickkopf; Gli1, GLI family zinc finger 1; Lef1, lymphoid enhancer-binding factor 1; Lgr, leucine-rich repeat-containing G-protein coupled receptor; Lhx2, LIM homeobox 2; Lrig1, leucine-rich repeats and immunoglobulin-like domains protein 1.

can form placodes at regular intervals in human hair regeneration (7). All studies validate the importance of BMP signaling in hair morphogenesis.

Bone morphogenic protein signaling is vital for maintaining DP inducibility and hair differentiation. BMP interacts with receptors in human DP and augments DP inducibility, with its

specific ablation leading to an inordinate DP feature (7, 26, 27). BMP–Smad signaling is required to maintain the hair sheath, and BMPR1A deficiency reveals an inclination toward severe hair loss and hair graying (8, 24, 28, 29). In addition, Noggin, a BMP2 ligand inhibitor, is involved in the formation of placodes, and it also prompts HFSC regeneration and HF expansion into the dermis in humans and mice (7, 28).

SHH Pathway

Sonic hedgehog is a second dermal signaling molecule in the placode and DP during HF morphogenesis (30). Additionally, SHH adjusts the HF polarity and angle of growth. In the hair cycle, the activated secondary hair germ produces SHH to reactivate the matrix, and HF will be blocked in anagen phase III with ablation of SHH (15, 31, 32). Moreover, the SHH downstream target genes and Gli and Ptch induce HFSC mitosis, with Gli2 activating Sox9 to affect the Wnt pathway (7, 33, 34). Collectively, as a typical morphogenetic signal, SHH is positively involved in HFSC proliferation and differentiation.

Growth Factors

Epidermal growth factor influences the lungs, mammary glands, small sweat glands, and skin, which is expressed in the HF outer root sheath and differentiated sebaceous glands (10). The EGF family impedes HF morphogenesis, generally manifesting as placode and DC deficits (7). The EGF family also controls hair sheath differentiation and morphology, with TGF-α mutations and deletions producing wavy hairs owing to distortions in the outer and inner root sheaths (2, 8).

The fibroblast growth factor is located in the epidermis and DC and is involved in placode formation in most circumstances. Similar to embryonic development, FGFR2b ablation results in abnormalities in the granular layer and skin appendages (2, 35, 36). In signal networks, FGF20 is secreted after Wnt signaling activation in epithelial placodes and promotes DC formation (37). Identifying the function of the FGF family is important due to the various mechanisms that they modulate in the hair cycle and related disorders. FGF5/18, as catagen-promoting factors, can inhibit stem cell growth, accelerating the anagen–catagen transition and adjusting the hair sheath length (3, 15, 38, 39). Similar to FGF7/10, more FGFs operate as transient amplifying cell-activating signals, catalyzing the telogen–anagen transition and HF renewal (8).

Transforming growth factor-beta has anti-proliferation potential for most epithelial cells, including follicular keratinocytes. When HF enters catagen, the epithelial TGF-β/activin signal induces apoptosis (3, 8, 38, 40). As a typical human hair disease-related gene, TGF-β deletion in HFSCs impairs the differentiation of adjacent pigmented stem cells in human follicular keratinocyte cells (41, 42).

Platelet-derived growth factor (PDGF) regulates cell growth and mesenchymal cell division, which remains the first epithelial signal in the placode (43). As a downstream target of SHH, PDGF is secreted by the epidermis, with receptors in the dermal sheath and DP, functioning in an adipose-stimulating manner to enhance HF regeneration (8). In addition, PDGF is secreted by the HF matrix during anagen and has a facilitative effect on the hair germ (8, 44).

Secreted by DP, vascular endothelial growth factor (VEGF) stimulates the expression of VEGFR-2 in human epidermal cells, hence promoting their proliferation, differentiation, and migration (45). Interestingly, VEGF can directly act on DP and promote human HF growth by stimulating local blood vessels during anagen, with bFGF promoting VEGF angiogenesis (8, 46, 47).

Cytokines and Chemokines

The TNF family member Eda modulates the induction, morphogenesis, and maintenance of skin appendages such as hair, teeth, and sweat glands (48). In HFs, Eda is present in the placode and the interfollicular epidermis throughout embryonic morphogenesis, and its mutation impairs the construction of guard hair in humans. The Eda cascade operates on the placode, and inadequate Eda results in aberrant appendages such as sparse hair, uneven teeth, and the absence of sweat glands (7).

Attention should be paid to the respective functions of IL family members because of their multifaceted regulatory mechanisms during the hair cycle, and the effect of the inflammatory responsiveness of the IL family in alopecia needs also to be studied. IL-36a aggregates HF rejuvenation, while IL-1β drives the anagen–catagen transition (8, 49). As an immunohistochemical biomarker, IL-1 expresses an HF morphogenesis-dependent localization during embryonic-like HF formation, and IL-1R^{+} keratin-forming cells are expressed in the hair germ and the outer root sheath (30), while the IL-2 receptor may be associated with hair regeneration (50). IL-6/10 is a downstream effector of the JAK–Stat pathway, and the JAK–Stat inhibitor ruxolitinib effectively relieved alopecia areata (12).

ECM-Specific Components

Human DP secretes a particular ECM, and epithelial cells selectively adhere to and grow on the surface of the basement membrane material, which jointly controls HF-related gene expression (51, 52). Extracellular collagen has a regulatory effect on maintaining DP growth and properties. Proteoglycans act as cell adhesion molecules, transmembrane signaling molecules, growth factor activators, and macromolecular transporters in the ECM. Persistently, low proteoglycan levels contribute to human pattern hair loss and telogen effluvium (53).

The macromolecular proteins in the ECM contribute to the stabilization of the HF microenvironment. Many specific ECM components can interact with small signaling molecules to maintain homeostasis. Specific proteoglycans in human ECM, such as aggrecan, biglycan, fibronectin, hyaluronic acid, and type I collagen, are pro-proliferative (14). Fibroblasts synthesize versican, which constitutes the ECM of human DP and modulates Wnt signaling in the anagen (44). Three secreted proteins, namely, apolipoprotein-A1, galectin-1, and lumican, are coenriched in the rat embryo dermis and induce HF *de novo* by stimulating IGF and Wnt (54). 6-phosphate chondroitin sulfate proteoglycan and cartilage oligomeric matrix protein are typically expressed in human HF connective tissue with HF

periodicity, interacting with BMP and various ECM proteins to stabilize the basement membrane. Overexpression of cartilage oligomeric matrix protein in humans induces connective tissue diseases, rheumatic diseases, and scleroderma, leading to hair graying and patchy hair loss (55). These findings demonstrate that ECM components are significant and irreplaceable for HF EMI and deserve further research.

EMI IN SKIN WOUND HEALING *VIA* HFSCS

Epidermal stem cells in HF can participate in wound re-epithelialization; for example, peri-wound melanocytes can migrate upwards to locate in the epidermis, and no pigment is present in new-born HF. After HF reconstruction, the interaction between bulge HFSCs or secondary hair germs and DPs proceeds the HF cycle, recovers melanocytes, and produces colored hairs (56). These findings inspired us to consider the association between the stem cell populations in HFs and cutaneous healing.

Overview of Wound Healing

In minor human skin wounds, myofibroblast contraction enables the formation of new skin without appendages; in more severe injuries, fibroblast contraction ceases, and scars appear before wound closure (56). At the human wound bed, early ECM forms to provide scaffolds for later cell attachment and development. On this basis, inflammatory cells, blood clots, and platelets are recruited, and damaged epithelial and endothelial cells secrete PDGF and chemokines. Then, inflammatory cells secrete the proinflammatory cytokines IL-1 and IL-6 and tumor necrosis factor-alpha (TNF-α) (**Figure 2**). Granulation tissue, mainly composed of myofibroblasts, keratinocytes, new capillaries, and type III collagen, drifts to the wound bed and initiates re-epithelialization in the lesion. After building a virgin epidermis, type I collagen gradually replaces type III collagen in the ECM, impairing stretching capacity and eventually resulting in scarred human skin devoid of skin appendages (57, 58).

HFSCs in Skin Wound Healing

HF Epidermal Stem Cells in Postinjury Epidermal Regeneration

The HF consists of the infundibulum, the isthmus, and the inferior part encompassing the bulge and DP (**Figure 1B**). The bulge and isthmus contain HF progenitor cell populations that assist in skin regeneration. Preclinical and clinical studies show that human wound rehabilitation is faster in locations with a high follicular density, such as the scalp, than in areas with a low follicular concentration, such as the palms of the hands and feet (10). Moreover, HFs can be used as autologous cell-derived grafts to offer a novel alternative treatment for long-term unhealed injuries by boosting re-epithelialization, revascularization, and skin restructuring (6, 10). HFs containing dermal fractions are comparable to split-thickness skin grafts concerning epithelialization rates, wound healing, and scar treatment, rendering HF transplantation clinically applicable to them (10).

The regenerated epidermis contains the basal lamina and HFSCs, which move to the damaged cutis and differentiate into epithelial cells, facilitating epidermal restoration by K15-labeled stem cells in the human HF bulge (56, 59, 60). After the injury, HFSCs upregulate cell migration-related genes and reduce bulge gene expression, eliciting epithelial-like characteristics (61). Additionally, as slow-periodic stem cells, bulge HFSCs can simultaneously produce transient amplifying cells, which migrate to specific sites along the basement membrane to repair emergency damage (62). All of the above studies confirm that HFSCs in the bulge region can undoubtedly contribute to re-epithelialization in the lesion.

Additionally, stem cells in the HF isthmus are pluripotent and self-renewing. Lgr6-positive cells are present in the wound neoplastic basal layer, where they bind to collagen to create a scaffold to support re-epithelialization, hair regrowth, and vascularization (10). Notably, in human skin reconstruction experiments, Lrig1-positive cells produce all epidermal cells that move to wounds and repair interfollicular epidermis (56). Gli1-positive cells are competent for long-term multiplication and differentiation after injury and are subject to external niche signaling (56). The stem cell population in the HF isthmus similarly possesses the potential to evolve into skin epidermal cells.

The outer root sheath serves as a reservoir for epithelial stem cells and gives rise to hair germ and matrix formation (15, 63, 64). Nestin-positive cells, presumably outer root sheath progenitor cells, are present in the bulge and upper outer root sheath during the mid-to-late anagen phase (7). Nestin-positive cells can differentiate into keratinocytes, melanocytes, neurons, glial cells, and smooth muscle cells under certain circumstances. A previous study has proved that the transplantation of nestin-positive cells into the severed sciatic nerve interstitial region stimulates neuronal regeneration and restores neurological function, suggesting their role in the skin appendages and neuronal stem cells (6).

Other epithelium-derived cells in the HF are also involved in skin tissue reconstruction after injury. As human sebaceous gland stem cells, Blimp1 protein-positive cells encourage keratinocyte and sebaceous gland differentiation and promote skin repair by sustaining sweat glands, ducts, and interappendage epithelium (6, 65). Under UV irradiation, melanocyte progenitor cells in the upper bulge migrate upwards to the interfollicular epidermis to become functional epidermal melanocytes, protecting the skin (66, 67).

HF Dermal Stem Cells in Skin Regeneration

Hair follicle dermal stem cells are fibroblast progenitors in the dermis. *In vitro*, clones of hfDSCs act as skin-derived precursors, healing the dermis following injury (13, 68). *In vivo*, hfDSCs are disposed to differentiate into dermal sheath and DP, smooth muscle cells, neurons, glial cells, and adipocytes, creating adipose and osteogenic tissue (6). DP is organized in the papillary dermis, hosts pluripotent neural crest stem cells, and is also ready to become neurons, glial cells, smooth muscle cells, and adipocytes (66). Therefore, both human hair dermis and mesenchymal stromal cells can be used for induced pluripotent stem cell therapy to rebuild the overall skin structure and improve skin function (37, 69). Moreover, DP promotes

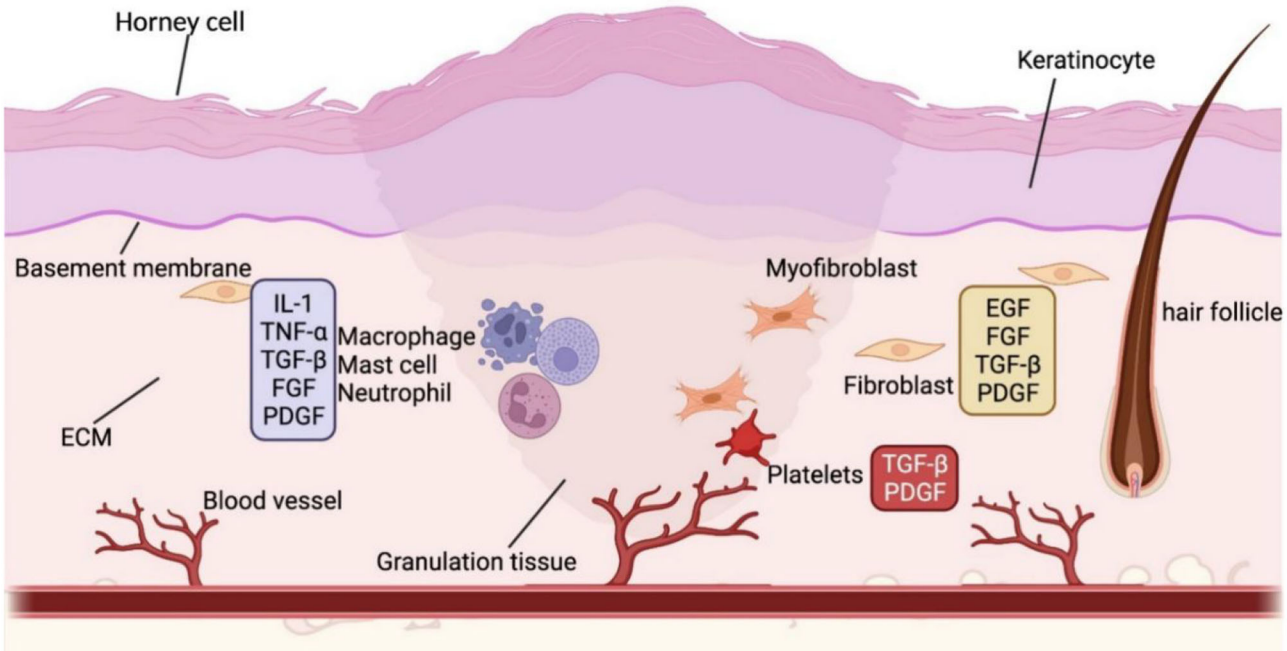

FIGURE 2 | The wound healing process. The various colors in the diagram frames indicate that the molecules in the frame are released by different cells. For example, blue represents inflammatory cells, yellow stands for fibroblasts, and red refers to platelets. Wound healing is a complex biological process. In the wound bed, inflammatory cells proliferate and recruit other required cells in the commence. As the inflammation subsides, endothelial cells in the wound bed increase, followed by the production of granulation tissue and wound site re-epithelialization. The wound contracts and ultimately forms a scar when the extracellular matrix is reconstructed with diminished cell counts. BMP, bone morphogenetic protein; DC, dermal condensate; DP, dermal papilla; Eda, ectodysplasin A; DKK, Dickkopf; EGF, epidermal growth factor; FGF, fibroblast growth factor; HF, hair follicle; HFSC, hair follicle stem cell; IL, interleukin; SHH, sonic hedgehog; PDGF, platelet-derived growth factor; TGF-β, transforming growth factor β; VEGF, vascular endothelial growth factor; Wnt, wingless/integrated.

keratinocyte differentiation and rebuilds the ECM during human wound healing while minimizing the risk of fibrosis and avoiding the harmful effects of the diabetic environment on cells, which suggests that DP may be utilized in diabetic foot healing instead of bone marrow and adipose mesenchymal cells (37).

EMI Signals Modulate Wound Healing

Wnt and SHH Signaling Pathways

Wnt signaling, a classical cell proliferation factor, also plays a role in cutaneous wound healing (70). Wnt7a upregulates collagen-I/III in the ECM (71), while increased β-catenin triggers matrix fibrosis and injury healing, as evidenced by fibroblast augmentation at the human wound site (37). Wnt signaling can also mediate melanocyte mobility (6, 72, 73). SHH is a typical epithelial signal, and its downstream signaling factor, Gli1, can respond to skin damage. Gli1-positive cells are triggered by injury to generate stem cells with the capability of long-term proliferation and differentiation, which are crucial for wound healing and skin reconstruction (56, 70, 74).

Growth Factors

The EGF family, including EGF and TGF-α, is involved in the control of development and cell renewal. Especially, in skin injury repair, EGF induces ECM composition, cell proliferation, and angiogenesis, as well as epithelium and mesenchyme regeneration (58, 70). Furthermore, increased expression of EGFR prompted the formation of an epidermal keratinized envelope (22).

Fibroblast growth factor advances wound healing by improving ECM composition, fibroblast proliferation, keratinocyte migration, and angiogenesis. The above properties qualify FGF as an indispensable signal for granulopoiesis, re-epithelialization, and tissue remodeling (58, 70). In many cases, FGF nourishes the wound area by suppressing collagen synthesis, lowering the density of connective tissue surrounding the DP, and increasing collagen vascular penetration (75). Before completing re-epithelialization in the lesion, T cells produce FGF9, demonstrating that immune cells and skin fibroblasts interact at the injury site to promote wound healing and HF regeneration (56, 57). Significantly, if there is a lack of FGF-9-expressing T cells in the dermis, HFs fail to form in human skin after scarring (60). Moreover, FGF7/10 triggers wound re-epithelialization and angiogenesis by activating keratinocyte mitogenic activity and VEGF secretion in endothelial cells, respectively (57). FGF7/10 deficiency impairs the proper interaction of T cells with keratinocytes, resulting in lower keratinocyte mobilization and limiting injury recovery (36).

In wound healing, TGF-β recruits neutrophils and macrophages, mediates ECM deposition, promotes angiogenesis, and enhances epithelial cell migration (70). TGF-β and PDGF

are released by platelets to facilitate fibroblast proliferation and migration and recruit immune cells to build granulation tissue (58, 70). The TGF-β family also regulates the degree of fibrosis in wounds, affecting scarring and the aesthetic properties of living tissue. In adult skin injuries, Wnt3 upregulates the profibrotic factor TGF-β1/2 *via* Smad2, but injecting recombinant human TGF-β3 into the embryo can minimize scarring (37, 57, 76). Fibromodulin-deficient mice show elevated TGF-β3 with reduced fibroblast mobility and delayed cut closure, indicating that TGF-β3 exhibits an anti-migratory effect in the early stages and an anti-fibrosis function in the late phase of wound healing (57).

As a representative epithelial signal, PDGF improves wound healing by recruiting neutrophils and macrophages, activating fibroblasts, recruiting vascular smooth muscle cells, and elevating IGF-1 to increase matrix metalloproteinase expression in the ECM (43, 57, 58, 70). For clinical application, human becaplermin/PDGF-BB, a wound healing factor, is the only FDA-approved profibrotic growth factor used to treat chronic healing failure (57, 68, 77).

Dermal papilla-secreted VEGF promotes epidermal cell migration and suppresses collagen production, making it a crucial growth factor for revascularization after tissue destruction (70, 75). VEGF is a significant growth factor that impacts revascularization and scarring. FGF-2 and VEGF accelerate wound healing in patients with neck dissection (78). A broad difference exists in ECM VEGF in embryonic and adult wounds, while VEGF expression is lower in adult wounds and more prone to forming scars (37, 57). In addition, VEGFR-2 influences the vascularization of keratinocytes in skin appendages such as HFs, sebaceous glands, and sweat glands (45).

Cytokines and Chemokines

The proinflammatory cytokines IL-1α, IL-1β, and IL-6 boost fibroblast and keratinocyte multiplication and recruit neutrophils, thus playing an essential role in forming granulation tissue (70). Nevertheless, in the late stages of inflammation, M2 macrophages generate the anti-inflammatory cytokine IL-10, which has antifibrotic properties and whose absence results in scarring, suggesting the potential function of ILs in skincare (57, 58).

ECM-Specific Components

Macromolecular components in the ECM play a significant role in human skin wound healing. For instance, high-molecular-weight hyaluronic acid is abundant in embryonic wounds and is beneficial for fibroblast migration, whereas its reduction leads to scarring (37, 79). During human skin damage, type III and type I collagen ratios are approximated to those in the embryo and are accompanied by increased hyaluronic acid. Theoretically, adding hyaluronic acid and collagen content at the wound site can proceed with embryonic wound healing and reduce fibrosis and scarring (9, 80). Decorin and lumican are rich in leucine and engage in collagen assembly, showing antifibrotic activity in adult human skin (37, 44, 57, 81). Fibromodulin is highly expressed in embryonic wounds, reduces fibrosis, and enhances fibroblast contraction by inhibiting TGF-β1. Elastin is responsible for the elasticity of connective tissue, and its deficiency influences the skin's nature (57). Moreover, the interaction of fibronectin and tenascin in sheep's wounds promotes ECM deposition, allowing cells to connect to and migrate within the matrix and advancing re-epithelialization (37). In summary, a collection of ECM components are involved in wound healing through their interactions and associations with adjacent cells (**Table 1**).

DISCUSSION

Epithelial–mesenchymal interaction is a wide-ranging biological activity involving hair, teeth, and mammary gland morphogenesis. In the past decade, significant progress has been made in the signaling involved in HF regeneration, hair cycle, and wound healing, making the HF an excellent model for investigating EMI. Communication of soluble factors, regulation of key pathways, and transduction of ECM signals all participate in HFSC-regulated EMI in HF tissue. Multiple signallings (Wnt, BMP, SHH, growth factors, etc.) regulate HFSC status and undergo periodic content fluctuations during the HF cycle. Moreover, HFSC can participate in both neo-epithelial tissue and neo-mesenchyme at the wound site, contributing to re-epithelialization. Current skin transplantation promotes cutaneous repair but fails to form intact and functional skin appendages, and common skin grafts are not desirable for healing large burns due to the increased risk of infection and donor region skin loss (10). Successful repair of injuries in the epidermal basal layer and skin appendages (HFs and glands) requires mesenchymal cells, including DP. Therefore, an improved understanding of the role of EMI and HFSC function in follicle regeneration and skin repair may provide a promising option for long-term unhealed wounds (82).

Since human organ culture models are time-consuming and the *in vitro* culture conditions are demanding, most of the studies on HF EMI are currently performed using murine follicular cycle models. However, the mouse model differs from human skin in terms of stem cell niche and skin contractility and is not entirely predictive of all clinical outcomes. Moreover, murine hair is densely distributed on the body surface, while HFs are sparsely distributed on human skin, suggesting that the beneficial effect of HFs on skin healing may be more evident in mouse wounds than in human wound healing. Thus, when replicating mouse experiments on human models, the translational study should be improved to focus on the dissemination differences of skin appendages, biomechanics, and transdermal absorption efficiency (83).

Hair follicle regeneration relies on HFSCs, thus understanding the signals in controlling survival, and death of HFSCs will update clinical guidelines for hair loss and other skin diseases. Notably, human HFs are the predilection sites of some basal cell carcinomas and pilomatrixoma, suggesting a link between human HF cells and skin cancers (84). Zhang found that stem cell damage in DP led to hair loss and tumor formation. In contrast, targeted destruction of Mx progenitors or precursors induced transient hair loss and HF

TABLE 1 | Signals in hair follicle regeneration and wound healing.

Signal factor	HF formation	HF cyclic regeneration	Wound healing	Research model	Reference
Wnt/β-catenin	Placode and DC formation	Facilitate HF growth and differentiation	Activate epithelial cell proliferation	Mouse and human	(18, 20, 24, 70)
BMP	Negative for placode formation; Noggin is involved in placode development	Enhancing DP induction and maintaining HFSC quiescence; Noggin promotes HFSC regeneration	Conversion of fibroblasts into adipocytes	Mouse and human	(7, 8, 17, 27, 89)
SHH	Placode growth and acts as the second epithelial signal to epithelial cell multiplication	Activate second hair germ to initiate HF periodic regeneration	Favorable to epidermal recovery and regeneration	Mouse	(7, 74)
EGF family	Delayed placode and absent DC	Hair sheath differentiation and morphology	Extracellular matrix composition and epithelial cornification	Mouse	(2, 7, 22, 70)
FGF family	Placode and DC development	Control the length of the telogen phase	Granulation tissue formation, re-epithelialization and tissue remodeling	Mouse and human	(8, 37, 70)
TGF-β	Inhibiting epithelial cell proliferation and placode formation	Induce catagen	Extracellular matrix deposition and epithelial cell migration	Mouse	(38, 65, 70)
PDGF	Acting as the first epithelial signal to shape DC	Enhance HF regeneration	Speed up wound healing	Mouse and human	(7, 8, 57)
VEGF	Epidermal cell multiplication and migration	Maintain the anagen	Angiogenesis and keratinocyte migration	Mouse and human	(8, 45)
IL family	IL-36 promotes HF development	IL-1b triggers catagen	Recruit immune cells and promote fibroblast and keratinocyte multiplication	Mouse	(8, 49, 70)
Eda/Edar	Placode generation	Induce anagen	Promote epithelial wound healing	Mouse and human	(8, 90, 91)
ECM specific components	Stable basement membrane	Some proteoglycans are pro-proliferative	Regulate pro-regenerative matrix and wound fibrillation	Mice, human and sheep	(14, 57, 81)

Epithelial–mesenchymal interaction is essential for HF neogenesis, HF cycle, and skin tissue regeneration. Wnt signaling in the epidermis initiates the placode, and the hierarchies and connections of known signals and pathways govern the development of placode and dermal cohesions, HF downstaging, and HF regeneration. While in the HF cycle, the initial signal arises in DP, and the normal functioning of hair growth is ensured by multiple positive and negative regulators between the matrix and the DP in an autocrine fashion to activate the HFSC or maintain its quiescent state. Each signal acts as a regulator involved in the fluctuation of the HFSC state and the expression of other pathways (Wnt, BMP, SHH, growth factors, etc.), forming a network in the HF cycle. Also, HFSC contributes to re-epithelialization at the wound site. Changes in cell type, growth factors, and extracellular matrix components exist within the injured tissue, accounting for matrix deposition, wound healing, and scar formation. BMP, bone morphogenetic protein; DC, dermal condensate; DP, dermal papilla; Eda, ectodysplasin A; DKK, Dickkopf; EGF, epidermal growth factor; FGF, fibroblast growth factor; HF, hair follicle; HFSC, hair follicle stem cell; IL, interleukin; PDGF, platelet-derived growth factor; SHH, sonic hedgehog; TGF-β, transforming growth factor β; VEGF, vascular endothelial growth factor; Wnt, wingless/integrated.

morphological damage without tumorigenesis (24). Growth factors provide further evidence in HF EMI that can exert tumor-suppressive effects in other organs. In direct support of this notion, FGFR2b is associated with tumorigenesis and prognosis in migratory cell carcinoma, salivary gland carcinoma, and prostate cancer, but no significant correlation was observed in skin models (85–87). FGF7/10 can also induce cancer by affecting inflammatory cell properties *via* inflammatory responsiveness (88). Therefore, a controlled dose or alteration of the nature of these tumor-related molecules is vital to ensure that they can induce follicle formation without producing harmful side effects.

Despite recent striking advances in HFSCs, the parallel comparison between HFs and other cell populations still needs further studies. Rendl found that discrepancies in molecular signatures between DP and matrix were similar to those during the separation of neural and non-neural ectoderm in vertebrates (42). Similarly, Taylor compared corneal stem cells and HFSCs and revealed commonalities in slow-cycling, proliferative potential, storage patterns, microenvironment, and tumor relevance (62). Thus, EMI similarities between HF and other organs may help us further probe the role of HFSC in skin regeneration and tumorigenesis.

Clinical trials have shown that HFs can be used as dermal grafts to treat chronic wounds and minor burns, but no clinical studies have used HF transplantation to treat large defects such as extensive burns. The scalp is an excellent donor site for skin grafts, with the advantage of faster growth and re-harvesting ability. Given the critical role of EMI in the majority of hair physiology, further studies are needed in alopecia treatments, and HF progenitor cell transplantation may bring us solutions

to some of the concerns about skin grafting to provide future therapeutic applications.

AUTHOR CONTRIBUTIONS

M-QM gathered the information and wrote the original draft. JJ is responsible for funding acquisition and modification. All authors contributed to the study, participated in resources, wrote the review, edited, and approved the submitted version.

FUNDING

This study was supported by the National Natural Science Foundation of China (Nos. 81972955 and 81972959).

REFERENCES

1. Holbrook KA, Smith LT, Kaplan ED, Minami SA, Hebert GP, Underwood RA. Expression of morphogens during human follicle development *in vivo* and a model for studying follicle morphogenesis *in vitro*. *J Invest Dermatol*. (1993) 101(1 Suppl):39–49s. doi: 10.1111/1523-1747.ep12362616
2. Choi BY. Hair-growth potential of ginseng and its major metabolites: a review on its molecular mechanisms. *Int J Mol Sci*. (2018) 19:2703. doi: 10.3390/ijms19092703
3. Rezza A, Wang Z, Sennett R, Qiao W, Wang D, Heitman N, et al. Signaling networks among stem cell precursors, transit-amplifying progenitors, and their niche in developing hair follicles. *Cell Rep*. (2016) 14:3001–18. doi: 10.1016/j.celrep.2016.02.078
4. Lei M, Gao X, Yang L, Yang T, Lian X. Gsdma3 gene is needed for the induction of apoptosis-driven catagen during mouse hair follicle cycle. *Histochem Cell Biol*. (2011) 136:335–43. doi: 10.1007/s00418-011-0845-8
5. Madaan A, Verma R, Singh AT, Jaggi M. Review of hair follicle dermal papilla cells as in vitro screening model for hair growth. *Int J Cosmet Sci*. (2018) 40:429–50. doi: 10.1111/ics.12489
6. Ojeh N, Pastar I, Tomic-Canic M, Stojadinovic O. Stem cells in skin regeneration, wound healing, and their clinical applications. *Int J Mol Sci*. (2015) 16:25476–501. doi: 10.3390/ijms161025476
7. Wang X, Tredget EE, Wu Y. Dynamic signals for hair follicle development and regeneration. *Stem Cells Dev*. (2012) 21:7–18. doi: 10.1089/scd.2011.0230
8. Sennett R, Rendl M. Mesenchymal-epithelial interactions during hair follicle morphogenesis and cycling. *Semin Cell Dev Biol*. (2012) 23:917–27. doi: 10.1016/j.semcdb.2012.08.011
9. du Cros DL, LeBaron RG, Couchman JR. Association of versican with dermal matrices and its potential role in hair follicle development and cycling. *J Invest Dermatol*. (1995) 105:426–31. doi: 10.1111/1523-1747.ep12321131
10. Nuutila K. Hair follicle transplantation for wound repair. *Adv Wound Care*. (2021) 10:153–63. doi: 10.1089/wound.2019.1139
11. Liu W, Li K, Wang G, Yang L, Qu Q, Fan Z, et al. Impairment of autophagy may be associated with follicular miniaturization in androgenetic alopecia by inducing premature catagen. *J Dermatol*. (2021) 48:289–300. doi: 10.1111/1346-8138.15672
12. Shin W, Rosin NL, Sparks H, Sinha S, Rahmani W, Sharma N, et al. dysfunction of hair follicle mesenchymal progenitors contributes to age-associated hair loss. *Dev Cell*. (2020) 53:185–98.e7. doi: 10.1016/j.devcel.2020.03.019
13. Rahmani W, Abbasi S, Hagner A, Raharjo E, Kumar R, Hotta A, et al. Hair follicle dermal stem cells regenerate the dermal sheath, repopulate the dermal papilla, and modulate hair type. *Dev Cell*. (2014) 31:543–58. doi: 10.1016/j.devcel.2014.10.022
14. Kalabusheva E, Terskikh V, Vorotelyak E. Hair germ model *in vitro* via human postnatal keratinocyte-dermal papilla interactions: impact of hyaluronic acid. *Stem Cells Int*. (2017) 2017:9271869. doi: 10.1155/2017/9271869
15. Panteleyev AA. Functional anatomy of the hair follicle: the secondary hair germ. *Exp Dermatol*. (2018) 27:701–20. doi: 10.1111/exd.13666
16. Deng Z, Lei X, Zhang X, Zhang H, Liu S, Chen Q, et al. mTOR signaling promotes stem cell activation via counterbalancing BMP-mediated suppression during hair regeneration. *J Mol Cell Biol*. (2015) 7:62–72. doi: 10.1093/jmcb/mjv005
17. Kandyba E, Leung Y, Chen YB, Widelitz R, Chuong CM, Kobielak K. Competitive balance of intrabulge BMP/Wnt signaling reveals a robust gene network ruling stem cell homeostasis and cyclic activation. *Proc Natl Acad Sci U S A*. (2013) 110:1351–6. doi: 10.1073/pnas.1121312110
18. Gupta K, Levinsohn J, Linderman G, Chen D, Sun TY, Dong D, et al. Single-cell analysis reveals a hair follicle dermal niche molecular differentiation trajectory that begins prior to morphogenesis. *Dev Cell*. (2019) 48:17–31.e6. doi: 10.1016/j.devcel.2018.11.032
19. Reddy S, Andl T, Bagasra A, Lu MM, Epstein DJ, Morrisey EE, et al. Characterization of Wnt gene expression in developing and postnatal hair follicles and identification of Wnt5a as a target of Sonic hedgehog in hair follicle morphogenesis. *Mech Dev*. (2001) 107:69–82. doi: 10.1016/S0925-4773(01)00452-X
20. Ouji Y, Yoshikawa M, Shiroi A, Ishizaka S. Wnt-10b secreted from lymphocytes promotes differentiation of skin epithelial cells. *Biochem Biophys Res Commun*. (2006) 342:1063–9. doi: 10.1016/j.bbrc.2006.02.028
21. Li N, Liu S, Zhang HS, Deng ZL, Zhao HS, Zhao Q, et al. Exogenous R-spondin1 induces precocious telogen-to-anagen transition in mouse hair follicles. *Int J Mol Sci*. (2016) 17:582. doi: 10.3390/ijms17040582
22. Hu XM, Li ZX, Zhang DY, Yang YC, Fu SA, Zhang ZQ, et al. A systematic summary of survival and death signalling during the life of hair follicle stem cells. *Stem Cell Res Ther*. (2021) 12:453. doi: 10.1186/s13287-021-02527-y
23. Choi YS, Zhang Y, Xu M, Yang Y, Ito M, Peng T, et al. Distinct functions for Wnt/β-catenin in hair follicle stem cell proliferation and survival and interfollicular epidermal homeostasis. *Cell Stem Cell*. (2013) 13:720–33. doi: 10.1016/j.stem.2013.10.003
24. Zhang J, He XC, Tong WG, Johnson T, Wiedemann LM, Mishina Y, et al. Bone morphogenetic protein signaling inhibits hair follicle anagen induction by restricting epithelial stem/progenitor cell activation and expansion. *Stem Cells*. (2006) 24:2826–39. doi: 10.1634/stemcells.2005-0544
25. Hsu YC, Pasolli HA, Fuchs E. Dynamics between stem cells, niche, and progeny in the hair follicle. *Cell*. (2011) 144:92–105. doi: 10.1016/j.cell.2010.11.049
26. Ohyama M, Kobayashi T, Sasaki T, Shimizu A, Amagai M. Restoration of the intrinsic properties of human dermal papilla *in vitro*. *J Cell Sci*. (2012) 125(Pt 17):4114–25. doi: 10.1242/jcs.105700
27. Rendl M, Polak L, Fuchs E, BMP. signaling in dermal papilla cells is required for their hair follicle-inductive properties. *Genes Dev*. (2008) 22:543–57. doi: 10.1101/gad.1614408
28. Kandyba E, Hazen VM, Kobielak A, Butler SJ, Kobielak K. Smad1 and 5 but not Smad8 establish stem cell quiescence which is critical to transform the premature hair follicle during morphogenesis toward the postnatal state. *Stem Cells*. (2014) 32:534–47. doi: 10.1002/stem.1548
29. Genander M, Cook PJ, Ramsköld D, Keyes BE, Mertz AF, Sandberg R, et al. BMP signaling and its pSMAD1/5 target genes differentially regulate hair follicle stem cell lineages. *Cell Stem Cell*. (2014) 15:619–33. doi: 10.1016/j.stem.2014.09.009
30. Müller-Röver S, Handjiski B, van der Veen C, Eichmüller S, Foitzik K, McKay IA, et al. A comprehensive guide for the accurate classification of murine hair follicles in distinct hair cycle stages. *J Invest Dermatol*. (2001) 117:3–15. doi: 10.1046/j.0022-202x.2001.01377.x
31. Ge W, Tan SJ, Wang SH, Li L, Sun XF, Shen W, et al. Single-cell transcriptome profiling reveals dermal and epithelial cell fate decisions during embryonic hair follicle development. *Theranostics*. (2020) 10:7581–98. doi: 10.7150/thno.44306
32. Noto M, Noguchi N, Ishimura A, Kiyonari H, Abe T, Suzuki T, et al. Sox13 is a novel early marker for hair follicle development. *Biochem Biophys Res Commun*. (2019) 509:862–8. doi: 10.1016/j.bbrc.2018.12.163

33. Brownell I, Guevara E, Bai CB, Loomis CA, Joyner AL. Nerve-derived sonic hedgehog defines a niche for hair follicle stem cells capable of becoming epidermal stem cells. *Cell Stem Cell.* (2011) 8:552–65. doi: 10.1016/j.stem.2011.02.021
34. Vidal VP, Chaboissier MC, Lützkendorf S, Cotsarelis G, Mill P, Hui CC, et al. Sox9 is essential for outer root sheath differentiation and the formation of the hair stem cell compartment. *Curr Biol.* (2005) 15:1340–51. doi: 10.1016/j.cub.2005.06.064
35. Lee J, Rabbani CC, Gao H, Steinhart MR, Woodruff BM, Pflum ZE, et al. Hair-bearing human skin generated entirely from pluripotent stem cells. *Nature.* (2020) 582:399–404. doi: 10.1038/s41586-020-2352-3
36. Grose R, Fantl V, Werner S, Chioni AM, Jarosz M, Rudling R, et al. The role of fibroblast growth factor receptor 2b in skin homeostasis and cancer development. *EMBO J.* (2007) 26:1268–78. doi: 10.1038/sj.emboj.7601583
37. Rippa AL, Kalabusheva EP, Vorotelyak EA. Regeneration of dermis: scarring and cells involved. *Cells.* (2019) 8:607. doi: 10.3390/cells8060607
38. Botchkareva NV, Ahluwalia G, Shander D. Apoptosis in the hair follicle. *J Invest Dermatol.* (2006) 126:258–64. doi: 10.1038/sj.jid.5700007
39. Ding H, Cheng G, Leng J, Yang Y, Zhao X, Wang X, et al. Analysis of histological and microRNA profiles changes in rabbit skin development. *Sci Rep.* (2020) 10:454. doi: 10.1038/s41598-019-57327-5
40. Song LL, Cui Y, Yu SJ, Liu PG, He JF. TGF-β and HSP70 profiles during transformation of yak hair follicles from the anagen to catagen stage. *J Cell Physiol.* (2019) 234:15638–46. doi: 10.1002/jcp.28212
41. Tanimura S, Tadokoro Y, Inomata K, Binh NT, Nishie W, Yamazaki S, et al. Hair follicle stem cells provide a functional niche for melanocyte stem cells. *Cell Stem Cell.* (2011) 8:177–87. doi: 10.1016/j.stem.2010.11.029
42. Rendl M, Lewis L, Fuchs E. Molecular dissection of mesenchymal-epithelial interactions in the hair follicle. *PLoS Biol.* (2005) 3:e331. doi: 10.1371/journal.pbio.0030331
43. Rezza A, Sennett R, Tanguy M, Clavel C, Rendl M. PDGF signalling in the dermis and in dermal condensates is dispensable for hair follicle induction and formation. *Exp Dermatol.* (2015) 24:468–70. doi: 10.1111/exd.12672
44. Botchkarev VA, Kishimoto J. Molecular control of epithelial-mesenchymal interactions during hair follicle cycling. *J Investig Dermatol Symp Proc.* (2003) 8:46–55. doi: 10.1046/j.1523-1747.2003.12171.x
45. Wu XJ, Jing J, Lu ZF, Zheng M. Expression and localization of VEGFR-2 in hair follicles during induced hair growth in mice. *Arch Dermatol Res.* (2018) 310:591–8. doi: 10.1007/s00403-018-1843-7
46. Li W, Man XY, Li CM, Chen JQ, Zhou J, Cai SQ, et al. VEGF induces proliferation of human hair follicle dermal papilla cells through VEGFR-2-mediated activation of ERK. *Exp Cell Res.* (2012) 318:1633–40. doi: 10.1016/j.yexcr.2012.05.003
47. Xu HL, Chen PP, Wang LF, Tong MQ, Ou ZH, Zhao YZ, et al. Skin-permeable liposome improved stability and permeability of bFGF against skin of mice with deep second degree scald to promote hair follicle neogenesis through inhibition of scar formation. *Colloids Surf B Biointerfaces.* (2018) 172:573–85. doi: 10.1016/j.colsurfb.2018.09.006
48. Kowalczyk-Quintas C, Schneider P. Ectodysplasin A (EDA) - EDA receptor signalling and its pharmacological modulation. *Cytokine Growth Factor Rev.* (2014) 25:195–203. doi: 10.1016/j.cytogfr.2014.01.004
49. Gong L, Xiao J, Li X, Li Y, Gao X, Xu X. IL-36α promoted wound induced hair follicle neogenesis via hair follicle stem/progenitor cell proliferation. *Front Cell Dev Biol.* (2020) 8:627. doi: 10.3389/fcell.2020.00627
50. Chai M, Jiang M, Vergnes L, Fu X, de Barros SC, Doan NB, et al. Stimulation of Hair Growth by Small Molecules that Activate Autophagy. *Cell Rep.* (2019) 27:3413–21.e3. doi: 10.1016/j.celrep.2019.05.070
51. Jing J, Wu XJ, Li YL, Cai SQ, Zheng M, Lu ZF. Expression of decorin throughout the murine hair follicle cycle: hair cycle dependence and anagen phase prolongation. *Exp Dermatol.* (2014) 23:486–91. doi: 10.1111/exd.12441
52. Lei M, Schumacher LJ, Lai YC, Juan WT, Yeh CY, Wu P, et al. Self-organization process in newborn skin organoid formation inspires strategy to restore hair regeneration of adult cells. *Proc Natl Acad Sci U S A.* (2017) 114:E7101–10. doi: 10.1073/pnas.1700475114
53. Lee EY, Choi EJ, Kim JA, Hwang YL, Kim CD, Lee MH, et al. Malva verticillata seed extracts upregulate the Wnt pathway in human dermal papilla cells. *Int J Cosmet Sci.* (2016) 38:148–54. doi: 10.1111/ics.12268
54. Fan SM, Tsai CF, Yen CM, Lin MH, Wang WH, Chan CC, et al. Inducing hair follicle neogenesis with secreted proteins enriched in embryonic skin. *Biomaterials.* (2018) 167:121–31. doi: 10.1016/j.biomaterials.2018.03.003
55. Ariza de. Schellenberger A, Horland R, Rosowski M, Paus R, Lauster R, Lindner G. Cartilage oligomeric matrix protein (COMP) forms part of the connective tissue of normal human hair follicles. *Exp Dermatol.* (2011) 20:361–6. doi: 10.1111/j.1600-0625.2010.01217.x
56. Takeo M, Lee W, Ito M. Wound healing and skin regeneration. *Cold Spring Harb Perspect Med.* (2015) 5:a023267. doi: 10.1101/cshperspect.a023267
57. Monavarian M, Kader S, Moeinzadeh S, Jabbari E. Regenerative scar-free skin wound healing. *Tissue Eng Part B Rev.* (2019) 25:294–311. doi: 10.1089/ten.teb.2018.0350
58. Kim HS, Sun X, Lee JH, Kim HW, Fu X, Leong KW. Advanced drug delivery systems and artificial skin grafts for skin wound healing. *Adv Drug Deliv Rev.* (2019) 146:209–39. doi: 10.1016/j.addr.2018.12.014
59. Sellheyer K, Krahl D. PHLDA1 (TDAG51) is a follicular stem cell marker and differentiates between morphoeic basal cell carcinoma and desmoplastic trichoepithelioma. *Br J Dermatol.* (2011) 164:141–7. doi: 10.1111/j.1365-2133.2010.10045.x
60. Gay D, Kwon O, Zhang Z, Spata M, Plikus MV, Holler PD, et al. Fgf9 from dermal γδ T cells induces hair follicle neogenesis after wounding. *Nat Med.* (2013) 19:916–23. doi: 10.1038/nm.3181
61. Joost S, Jacob T, Sun X, Annusver K, La Manno G, Sur I, et al. Single-cell transcriptomics of traced epidermal and hair follicle stem cells reveals rapid adaptations during wound healing. *Cell Rep.* (2018) 25:585–97.e7. doi: 10.1016/j.celrep.2018.09.059
62. Taylor G, Lehrer MS, Jensen PJ, Sun TT, Lavker RM. Involvement of follicular stem cells in forming not only the follicle but also the epidermis. *Cell.* (2000) 102:451–61. doi: 10.1016/S0092-8674(00)00050-7
63. Sharov A, Tobin DJ, Sharova TY, Atoyan R, Botchkarev VA. Changes in different melanocyte populations during hair follicle involution (catagen). *J Invest Dermatol.* (2005) 125:1259–67. doi: 10.1111/j.0022-202X.2005.23959.x
64. Wang D, Zhang Z, O'Loughlin E, Wang L, Fan X, Lai EC, et al. MicroRNA-205 controls neonatal expansion of skin stem cells by modulating the PIK pathway. *Nat Cell Biol.* (2013) 15:1153–63. doi: 10.1038/ncb2827
65. Telerman SB, Rognoni E, Sequeira I, Pisco AO, Lichtenberger BM, Culley OJ, et al. Dermal blimp1 acts downstream of epidermal tgfβ and wnt/β-catenin to regulate hair follicle formation and growth. *J Invest Dermatol.* (2017) 137:2270–81 doi: 10.1016/j.jid.2017.06.015
66. Amoh Y, Hoffman RM. Hair follicle-associated-pluripotent (HAP) stem cells. *Cell Cycle.* (2017) 16:2169–75. doi: 10.1080/15384101.2017.1356513
67. Chou WC, Takeo M, Rabbani P, Hu H, Lee W, Chung YR, et al. Direct migration of follicular melanocyte stem cells to the epidermis after wounding or UVB irradiation is dependent on Mc1r signaling. *Nat Med.* (2013) 19:924–9. doi: 10.1038/nm.3194
68. Ji S, Zhu Z, Sun X, Fu X. Functional hair follicle regeneration: an updated review. *Signal Transduct Target Ther.* (2021) 6:66. doi: 10.1038/s41392-020-00441-y
69. Tsai SY, Clavel C, Kim S, Ang YS, Grisanti L, Lee DF, et al. Oct4 and klf4 reprogram dermal papilla cells into induced pluripotent stem cells. *Stem Cells.* (2010) 28:221–8. doi: 10.1002/stem.281
70. Arwert EN, Hoste E, Watt FM. Epithelial stem cells, wound healing and cancer. *Nat Rev Cancer.* (2012) 12:170–80. doi: 10.1038/nrc3217
71. Dong L, Hao H, Liu J, Ti D, Tong C, Hou Q, et al. A Conditioned medium of umbilical cord mesenchymal stem cells overexpressing Wnt7a promotes wound repair and regeneration of hair follicles in Mice. *Stem Cells Int.* (2017) 2017:3738071. doi: 10.1155/2017/3738071
72. Rabbani P, Takeo M, Chou W, Myung P, Bosenberg M, Chin L, et al. Coordinated activation of Wnt in epithelial and melanocyte stem cells initiates pigmented hair regeneration. *Cell.* (2011) 145:941–55. doi: 10.1016/j.cell.2011.05.004
73. Nishimura EK, Suzuki M, Igras V, Du J, Lonning S, Miyachi Y, et al. Key roles for transforming growth factor beta in melanocyte stem cell maintenance. *Cell Stem Cell.* (2010) 6:130–40. doi: 10.1016/j.stem.2009.12.010
74. Suen WJ, Li ST, Yang LT. Hes1 regulates anagen initiation and hair follicle regeneration through modulation of hedgehog signaling. *Stem Cells.* (2020) 38:301–14. doi: 10.1002/stem.3117

75. Goodarzi P, Falahzadeh K, Nematizadeh M, Farazandeh P, Payab M, Larijani B, et al. Tissue Engineered Skin Substitutes. *Adv Exp Med Biol.* (2018) 1107:143–88. doi: 10.1007/5584_2018_226
76. So K, McGrouther DA, Bush JA, Durani P, Taylor L, Skotny G, et al. Avotermin for scar improvement following scar revision surgery: a randomized, double-blind, within-patient, placebo-controlled, phase II clinical trial. *Plast Reconstr Surg.* (2011) 128:163–72. doi: 10.1097/PRS.0b013e318217429b
77. Cai B, Zheng Y, Yan J, Wang J, Liu X, Yin G. BMP2-mediated PTEN enhancement promotes differentiation of hair follicle stem cells by inducing autophagy. *Exp Cell Res.* (2019) 385:111647. doi: 10.1016/j.yexcr.2019.111647
78. Nissen NN, Polverini PJ, Koch AE, Volin MV, Gamelli RL, DiPietro LA. Vascular endothelial growth factor mediates angiogenic activity during the proliferative phase of wound healing. *Am J Pathol.* (1998) 152:1445–52.
79. Graça MFP, Miguel SP, Cabral CSD, Correia IJ. Hyaluronic acid-Based wound dressings: a review. *Carbohydr Polym.* (2020) 241:116364. doi: 10.1016/j.carbpol.2020.116364
80. Pallaske F, Pallaske A, Herklotz K, Boese-Landgraf J. The significance of collagen dressings in wound management: a review. *J Wound Care.* (2018) 27:692–702. doi: 10.12968/jowc.2018.27.10.692
81. Zhou L, Jing J, Wang H, Wu X, Lu Z. Decorin promotes proliferation and migration of ORS keratinocytes and maintains hair anagen in mice. *Exp Dermatol.* (2018) 27:1237–44. doi: 10.1111/exd.13770
82. Jiménez F, Garde C, Poblet E, Jimeno B, Ortiz J, Martínez ML, et al. A pilot clinical study of hair grafting in chronic leg ulcers. *Wound Repair Regen.* (2012) 20:806–14. doi: 10.1111/j.1524-475X.2012.00846.x
83. Zomer HD, Trentin AG. Skin wound healing in humans and mice: challenges in translational research. *J Dermatol Sci.* (2018) 90:3–12. doi: 10.1016/j.jdermsci.2017.12.009
84. Millar SE. Molecular mechanisms regulating hair follicle development. *J Invest Dermatol.* (2002) 118:216–25. doi: 10.1046/j.0022-202x.2001.01670.x
85. Zhang Y, Wang H, Toratani S, Sato JD, Kan M, McKeehan WL, et al. Growth inhibition by keratinocyte growth factor receptor of human salivary adenocarcinoma cells through induction of differentiation and apoptosis. *Proc Natl Acad Sci U S A.* (2001) 98:11336–40. doi: 10.1073/pnas.191377098
86. Jin C, McKeehan K, Guo W, Jauma S, Ittmann MM, Foster B, et al. Cooperation between ectopic FGFR1 and depression of FGFR2 in induction of prostatic intraepithelial neoplasia in the mouse prostate. *Cancer Res.* (2003) 63:8784–90. doi: 10.1158/0008-5472.Can-12-4213
87. Yasumoto H, Matsubara A, Mutaguchi K, Usui T, McKeehan WL. Restoration of fibroblast growth factor receptor2 suppresses growth and tumorigenicity of malignant human prostate carcinoma PC-3 cells. *Prostate.* (2004) 61:236–42. doi: 10.1002/pros.20093
88. Jameson J, Ugarte K, Chen N, Yachi P, Fuchs E, Boismenu R, et al. A role for skin gammadelta T cells in wound repair. *Science.* (2002) 296:747–9. doi: 10.1126/science.1069639
89. Sardella C, Winkler C, Quignodon L, Hardman JA, Toffoli B, Giordano Attianese GMP, et al. Delayed hair follicle morphogenesis and hair follicle dystrophy in a lipoatrophy mouse model of Pparg total deletion. *J Invest Dermatol.* (2018) 138:500–10. doi: 10.1016/j.jid.2017.09.024
90. Li S, Zhou J, Bu J, Ning K, Zhang L, Li J, et al. Ectodysplasin A protein promotes corneal epithelial cell proliferation. *J Biol Chem.* (2017) 292:13391–401. doi: 10.1074/jbc.M117.803809
91. Yuhki M, Yamada M, Kawano M, Iwasato T, Itohara S, Yoshida H, et al. BMPR1A signaling is necessary for hair follicle cycling and hair shaft differentiation in mice. *Development.* (2004) 131:1825–33. doi: 10.1242/dev.01079

Conflict of Interest: The authors declare that the research was conducted in the absence of any commercial or financial relationships that could be construed as a potential conflict of interest.

Publisher's Note: All claims expressed in this article are solely those of the authors and do not necessarily represent those of their affiliated organizations, or those of the publisher, the editors and the reviewers. Any product that may be evaluated in this article, or claim that may be made by its manufacturer, is not guaranteed or endorsed by the publisher.

frontiers | Frontiers in Medicine

ORIGINAL RESEARCH
published: 06 May 2022
doi: 10.3389/fmed.2022.896943

Identification of a Novel *MLPH* Missense Mutation in a Chinese Griscelli Syndrome 3 Patient

Qiaorong Huang[1†], *Yefeng Yuan*[2†], *Juanjuan Gong*[2,3,4,5], *Tianjiao Zhang*[1], *Zhan Qi*[2,3,4,5], *Xiumin Yang*[1], *Wei Li*[2,3,4,5*] *and Aihua Wei*[1*]

[1] Department of Dermatology, Beijing Tongren Hospital, Capital Medical University, Beijing, China, [2] Beijing Key Laboratory for Genetics of Birth Defects, Beijing Pediatric Research Institute, Beijing, China, [3] Rare Disease Center, National Center for Children's Health, Beijing, China, [4] MOE Key Laboratory of Major Diseases in Children, Beijing, China, [5] Beijing Children's Hospital, Capital Medical University, Beijing, China

Melanophilin (MLPH) functions as a linker between RAB27A and myosin Va (MYO5A) in regulating skin pigmentation during the melanosome transport process. The MYO5A-MLPH-RAB27A ternary protein complex is required for anchoring mature melanosomes in the peripheral actin filaments of melanocytes for subsequent transfer to adjacent keratinocytes. Griscelli syndrome type 3 (GS3) is caused by mutations in the *MLPH* gene. So far, only five variants of *MLPH* associated with GS3 have been reported. Here, we reported the first patient with GS3 in a Chinese population. The proband carried a novel homozygous missense mutation (c.73G>C; p.D25H), residing in the conserved Slp homology domain of MLPH, and presented with hypopigmentation of the hair, eyebrows, and eyelashes. Light microscopy revealed the presence of abnormal pigment clumping in his hair shaft. *In silico* tools predicted this *MLPH* variant to be likely pathogenic. Using immunoblotting and immunofluorescence analysis, we demonstrated that the MLPH (D25H) variant had an inhibitory effect on melanosome transport by exhibiting perinuclear melanosome aggregation in melanocytes, and greatly reduced its binding to RAB27A, although the protein level of MLPH in the patient was not changed. Our findings suggest that MLPH (D25H) is a pathogenic variant that expands the genetic spectrum of the *MLPH* gene.

Keywords: Griscelli syndrome, MLPH, melanosome, pathogenic variant, hypopigmentation

OPEN ACCESS

Edited by:
Xing-Hua Gao,
The First Affiliated Hospital of China Medical University, China

Reviewed by:
Norihiko Ohbayashi,
University of Tsukuba, Japan
Zhimiao Lin,
Peking University First Hospital, China

***Correspondence:**
Aihua Wei
weiaihua3000@163.com
Wei Li
liwei@bch.com.cn

[†]These authors have contributed equally to this work

Specialty section:
This article was submitted to Dermatology, a section of the journal Frontiers in Medicine

Received: *15 March 2022*
Accepted: *08 April 2022*
Published: *06 May 2022*

Citation:
Huang Q, Yuan Y, Gong J, Zhang T, Qi Z, Yang X, Li W and Wei A (2022) Identification of a Novel MLPH Missense Mutation in a Chinese Griscelli Syndrome 3 Patient. Front. Med. 9:896943. doi: 10.3389/fmed.2022.896943

INTRODUCTION

Melanosomes are intracellular lysosome-related organelles (LRO) in which melanin is synthesized, stored, and transported (1, 2). After maturation in the perinuclear region of melanocytes, melanosomes are transported to the cell periphery and dendritic tips by coordinating bi-directional transport on microtubules and anterograde transport on actin filaments (3, 4). Melanophilin (MLPH), myosin Va (MYO5A), and RAB27A form a tripartite complex involved in melanosome transport along with the microtubules and actin-network (5, 6). Of these, MLPH has a critical role in bridging RAB27A on the melanosomes and MYO5A on the actin filaments during melanosome transport (7). Mutations of any subunit of the complex, MYO5A, RAB27A, and MLPH cause the rare autosomal recessive inherited disease, Griscelli syndrome (GS) types 1∼3 (8–10).

All patients with GS1∼3 present relatively mild hypopigmentation in their hair and skin. GS3 (*MLPH* mutations) is restricted to a hypopigmentation disorder, while GS1 (*MYO5A* mutations) and GS2 (*RAB27A* mutations) additionally exhibit neurological dysfunctions or immunological defects. Patients with GS3 are very rare compared with GS1 and GS2 (11). To date, there are only five variants of *MLPH* associated with GS3 recorded in the Human Gene Mutation Database (8, 11–13) (HGMD, version 2021.10) or reported in the literature (14).

In this study, we identified a novel *MLPH* p.D25H mutation in a Chinese GS3 non-consanguineous family, and we provide evidence that this *MLPH* missense mutation leads to aberrant melanosome transport in melanocytes.

MATERIALS AND METHODS

Patient Information

A 32-year-old male patient from the Chinese Han population had unexplained pigmentary dilution of the hair, eyebrows, and eyelashes. He visited Beijing Tongren Hospital, Capital Medical University in June 2021 and was recruited for this study. Blood samples were obtained from the patient and his parents. This study was approved by the ethics committees of Beijing Tongren Hospital and Beijing Children's Hospital, Capital Medical University. Written informed consent was obtained in accordance with the declaration of Helsinki.

Genetic Analysis

Whole exome sequencing was performed on genomic DNA from the proband. The Agilent SureSelect Human All ExonV6 Kit (Agilent Technologies, Santa Clara, CA, USA) was used to target the exonic regions of the genome. The Illumina NovaSeq 6000 platform (Illumina Inc., San Diego, CA, USA) was used for genomic DNA sequencing by Novogene Bioinformatics Technology Co., Ltd (Beijing, China) to generate 150 bp paired-end reads with a minimum coverage of 20× for ∼95% of the genome (mean coverage of ∼100×). The DNA sequences were analyzed by in-house quality control software to remove low-quality reads and were then aligned to the reference human genome (hs37d5) using the Burrows-Wheeler Aligner (BWA) (15), and duplicate reads were marked using Sambamba tools (16). Single nucleotide variants (SNVs) and indels were called by GATK to generate a gVCF file. The sequence variants in the proband and his parental samples were confirmed by Sanger sequencing analysis.

Homology Analysis and Structural Modeling of MLPH

The human MLPH protein (NP_077006.1) sequence was aligned for analysis of the conservation of the mutated residue (p.D25H) with the sequences of the following homologous proteins: *Mus musculus* (NP_443748.2), *Felis catus* (NP_001073123.1), *Ovis aries* (NP_001139743.1), *Oryctolagus cuniculus* (NP_001284414.1), *Canis lupus familiaris* (NP_001096689.2), *Rattus norvegicus* (NP_001012135.1), and *Gallus* (NP_001108552.1). Conservation analysis and alignment visualization were performed by Clustal Omega (http://www.clustal.org/omega/) and Jalview software (17). The protein structure was drawn using the online tool Illustrator for Biological Sequences (IBS) (http://ibs.biocuckoo.org/). The domains of human MLPH protein referred to the structure of mouse Slac2-a/melanophilin protein (18).

Plasmid Construction

The full-length cDNA of human *MLPH* with C terminal GFPSpark tag was synthesized by Sino Biological Inc. The human entire coding region of *MLPH* was subcloned into the pEGFP-C2 vector with an EGFP-tag and the pCMV-tag2B vector with a Flag-tag. The human *MLPH* sequence encoding the first 146 amino acids, termed Slp homology domain (SHD) (19), was subcloned into the pCMV-tag3B vector with a Myc-tag. The full-length cDNA of human RAB27A was amplified from total RNA of the human melanoma cell line MNT-1 cells (ATCC, USA) by one-step RT-PCR and the digested PCR product was cloned into the pCMV-tag2B vector with a Flag-tag. To introduce the point mutations into the *MLPH* or *SHD*, we used site-directed mutagenesis primers and high-fidelity polymerase to amplify the entire plasmid by PCR. The primers used were as follows: 5′-GTCTTGGAAGTTGTTCAACGACATTTTGACC TCCGAAGGAAAG-3′ (D25H primer; sense); 5′-CTTTCC TTCGGAGGTCAAAATGTCGTTGAACAACTTCCAAGAC-3′ (D25H primer; antisense); 5′-CGAAGGAAAGAAGAGGAA TGGCTAGAGGCGTTGAAG-3′ (R35W primer; sense); and 5′-CTTCAACGCCTCTAGCCATTCCTCTTCTTTCCTTCG-3′ (R35W primer; antisense).

Cell Culture and Transfection

Briefly, MNT-1 cells (ATCC, USA) were cultured in minimal essential medium (MEM) supplemented with 20% fetal bovine serum (FBS, Invitrogen), 10% AIM-V medium (Gibco), sodium pyruvate, and non-essential amino acids at 37°C with 5% CO_2 (20). Human embryonic kidney 293 T (HEK293T) cells were cultured in DMEM (Gibco) with 10% FBS at 37°C with 5% CO_2. Subsequently, FLAG-MLPH or GFP-MLPH wild-type (WT) and MLPH mutant (p.D25H) expression plasmids were transfected into the cells using Lipofectamine 3000 (Invitrogen) in Opti-MEM (Gibco). After 6 h, the medium was changed to a fresh medium for further experiments.

Western Blotting

A total of 2 ml of blood was collected from each individual in sodium citrate blood collection tubes. Platelet-rich plasma was obtained by centrifugation at 150 g for 10 min at room temperature. Washed platelets were lysed in a lysis buffer (50 mM Tris pH 7.4, 150 mM NaCl, 0.1% sodium dodecyl-sulfate (SDS), 1% Triton X-100, and 1% sodium deoxycholate) with a protease inhibitor cocktail (Sigma-Aldrich, P8340) mixture, boiled with 5× loading buffer and then separated by 10% SDS polyacrylamide gel electrophoresis (SDS-PAGE) (21). Samples were then transferred to a polyvinylidene difluoride (PVDF) membrane (Millipore). The membranes were blocked with 5% milk in PBS (0.1% Tween) for 1 h. Primary antibodies, anti-MLPH (Proteintech, 10338-1-AP, 1:5,000), anti-MYO5A (Cell Signaling Technology, 34025, 1:1,000), anti-RAB27A (Santa

Cruz Biotechnology, sc-81914, 1:2,000), and anti-glyceraldehyde-3-phosphate dehydrogenase (anti-GAPDH) (Cell Signaling Technology, 5174T, 1:5,000), were incubated overnight at 4°C. After washing with PBS-T, membranes were incubated with a secondary antibody (goat anti-mouse IgG or goat anti-rabbit IgG, 1:5,000; Invitrogen) for 2 h at room temperature, then developed with the ECL substrate (Thermo Scientific).

Immunofluorescence Staining and Confocal Imaging

In brief, MNT-1 cells transfected with GFP-MLPH (WT) or GFP-MLPH (D25H) were grown for 24 h on coverslips. Cells were fixed with 4% paraformaldehyde for 10 min, washed with PBS, permeabilized in 0.1% Triton X-100/PBS for 10 min, and blocked in 1% bovine serum albumin (BSA)/PBS for 1 h. Coverslips were then incubated with mouse anti-TYRP1 (Covance, SIG-38150) diluted 1:500 in 1% BSA/PBS at 4°C overnight. Then, cells were washed and incubated for 2 h with a 1:500 dilution with donkey anti-mouse secondary antibody conjugated to ALEXA-594 (Invitrogen) at room temperature. After washes, cells were mounted in 4',6-diamidino-2-phenylindole (DAPI, ZSGB-BIO). Finally, confocal images were acquired using the Zeiss LSM 880 Confocal Microscope (German).

Co-immunoprecipitation (Co-iP) Assays

Transfected HEK293T cells with Flag-tagged pCMV-tag2B-RAB27A and Myc-tagged pCMV-tag3B-SHD (WT, D25H, or R35W) were harvested after 48 h, then were incubated with a lysis buffer (150 mM NaCl, 50 mM Tris pH 7.4, 1 mM EDTA, and 1% Triton-100) with a protease inhibitor cocktail for 30 min at 4°C. Lysates were centrifuged at 12,000× g for 10 min at 4°C and 10% of the whole-cell lysates were taken as inputs. The remaining lysates were incubated with pre-washed anti-FLAG M2-Agarose affinity gel (Sigma-Aldrich, FLAGIPT-1) at 4°C, overnight. The bead complexes were washed 5 times with a washing buffer (150 mM NaCl and 50 mM Tris pH 7.4), and the proteins were eluted in a 2× loading sample buffer and then subjected to 10% SDS-PAGE for western blotting according to the procedures in our previous study (21).

RESULTS

Clinical Findings

The proband was a male patient aged 32 years at the time of the examination. He had brownish and silvery-gray hair, dark gray eyebrows, and white eyelashes (**Figures 1A–C**). His hair shaft showed uneven melanin granules under light microscopy (**Figure 1D**), a typical feature observed in GS3 (22). Blood parameters, such as hemoglobin, white blood cell (WBC), and platelets were within normal ranges. The value of erythrocyte sedimentation rate (ESR) was 3 mm/h (normal range, 0∼15 mm/h). Specific immunoglobulin levels (IgG, IgM, and IgA) were normal. Complement 3 (C3) was 89.3 mg/dl (normal range, 90∼180 mg/dl) and C4 was normal. The ADP-induced platelet aggregation of 43.6% (normal range, 59.1∼98.3%) was lower than normal. Several coagulation tests, such as prothrombin time (PT) of 11.8 s (normal range, 10.5∼15 s), activated partial thromboplastin time (APTT) of 27.2 s (normal range, 22.7∼31.8 s), and thrombin time (TT) of 17.5 s (normal range, 14∼21 s), were within normal limits. Fibrinogen (FIB) of 1.89 g/L (normal range, 2∼4 g/L) was slightly lower than normal. Brain MRI was normal. Visual acuity was 20/20 in both eyes. The fundus photograph (**Supplementary Figure S1A**), the anterior segment picture (**Supplementary Figure S1B**), and the optical coherence tomography (OCT) (**Supplementary Figure S1C**) were normal.

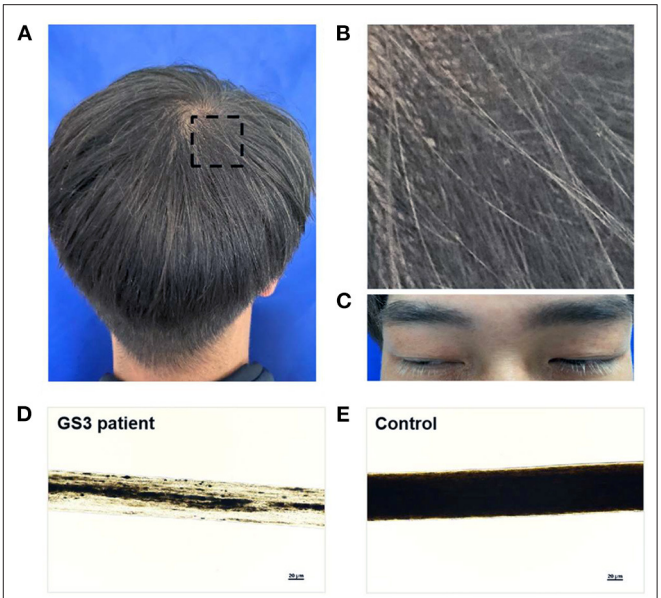

FIGURE 1 | Hair phenotypes of a patient with Griscelli syndrome type 3 (GS3). **(A,B)** A mixture of dark brown and silvery-gray hair in a 32-year-old man with GS3. The black rectangular frame is enlarged in **(B)**. **(C)** Dark gray eyebrows and white eyelashes of the patient. **(D,E)** Light microscopy images of the hair shafts, showing the irregular clumping of melanin in the patient's hair shaft **(D)**, and the even distribution of melanin in the hair shaft from a normal black hair individual **(E)**. The magnification of the objective lenses was ×20. Written informed consent was obtained from the patient for publication of the pictures **(A–C)**.

Identification of a Novel *MLPH* Mutation

Mutational screening for more than 200 hypopigmentation-related genes using next-generation sequencing (NGS) technologies identified a novel homozygous missense variant c.73G>C (p. Asp25His) (RefSeq NM_024101.7) of the *MLPH* gene in the proband (**Figure 2A**), which was verified by Sanger sequencing (**Figure 2B**). Meanwhile, Sanger sequencing revealed his parents who were not consanguineous as heterozygous carriers of this mutation (**Figure 2B**). Using *in silico* tools, such as PROVEAN, PolyPhen-2, and Mutation Taster, we evaluated the pathological effects of the c.73G>C mutation on the function of MLPH, and the allele frequency of the c.73G>C variant was not available in three common databases (**Table 1**), predicting it as likely pathogenic (23). Conservation analysis of the protein sequence in different species showed that the Asp25 residue is highly conserved (**Figure 2C**). Six *MLPH* mutations that caused

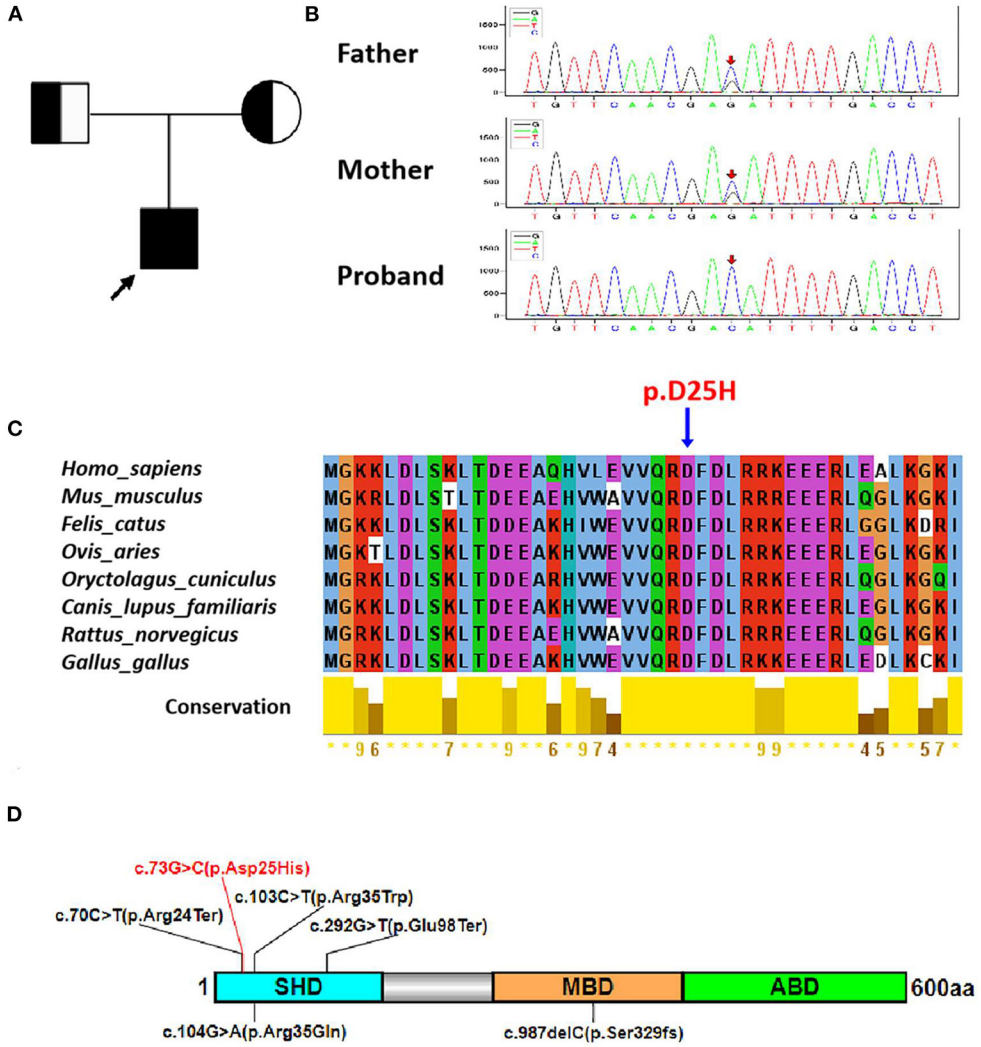

FIGURE 2 | The p.D25H variant in the patient with GS3. **(A)** A pedigree of the GS3 family. The black arrow indicates the proband. **(B)** Sanger sequencing analysis shows the homozygous c.73G>C mutation in proband, the heterozygous c.73G>C mutation in the parents of the patient. Red arrows show the mutational site. **(C)** Sequence alignment of MLPH protein in different species. The blue arrow indicates the mutational site. **(D)** Schematic representation of human MLPH protein structure. The novel missense mutation in this study and other reported mutations in MLPH are represented by red and black lines, respectively. SHD, Slp homology domain; MBD, MYO5A-binding domain; ABD, actin-binding domain.

GS3, including this newly reported allele, are mainly clustered on the SHD (**Figure 2D**) (8, 11–14), suggesting that this region appears to be a mutational hotspot region.

Expression and Localization of MLPH (D25H) Are Not Altered

To evaluate the impact of the D25H mutation on MLPH, the MLPH expression level in the platelets of the patient was determined by Western blotting. HEK293T cells were transfected with Flag-MLPH and our results showed both Flag and MLPH antibodies recognized the same specific band, which confirmed the specificity of the MLPH antibody (**Figure 3A**). As shown in **Figure 3B**, the protein levels of MLPH, MYO5A, and RAB27A were not altered in the patients with GS3 compared with an unaffected control. Next, we examined the localization pattern of the MLPH (D25H) protein in MNT-1 cells. We observed that both the WT and mutant MLPH proteins were associated primarily with punctate structures located throughout the cell body and peripheral dendrites (**Figures 4a,e**, **5a,d**), similar to the MLPH (WT) distribution described for melan-a melanocytes (5). Therefore, the D25H mutation did not interfere with the expression and localization of the MLPH protein.

SHD (D25H)-MLPH Reduced the Interaction With RAB27A

The RAB27A protein binds to the surface of the melanosome and participates in actin-dependent melanosome movement *via* direct interaction with its effector MLPH and indirect interaction

TABLE 1 | Effects of novel MLPH mutation predicted using *in silico* tools.

Chromosome 2 co-ordinates	cDNA alteration	Amino acid alteration	Mutation type	ExAC allele frequency	gnomAD allele frequency	1000 G Project	PROVEAN	PolyPhen-2	Mutation taster
238402142G>C	c.73G>C	p.D25H	Missense	N/A	N/A	N/A	Deleterious	Probably damaging	Disease causing

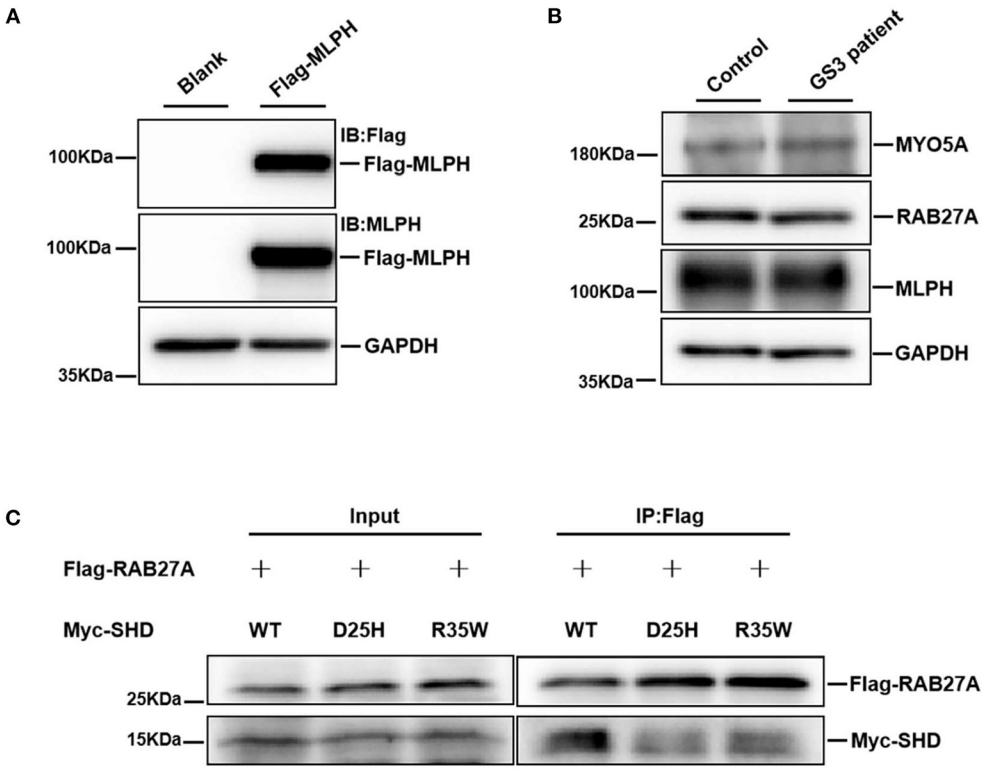

FIGURE 3 | The patient with GS3 displays normal expression of endogenous MLPH, MYO5A, and RAB27A, but the mutant MLPH (D25H) decreases its interaction with RAB27A. **(A)** HEK293T cells were transfected with the Flag-MLPH construct, and immunoblotted with indicated antibodies. Glyceraldehyde-3-phosphate dehydrogenase (GAPDH) serves as a loading control. The immunoblotting data show both Flag and MLPH antibody recognized the same specific band. **(B)** Western blotting analysis of protein extracts from peripheral platelets of a healthy control and the GS3 patient with indicated antibodies. There were no apparent differences in protein levels of MLPH, MYO5A, and RAB27A between control and patient. **(C)** Co-immunoprecipitation of Flag-RAB27A with Myc-SHD. SHD (R35W)-MLPH served as a positive control. Both SHD (D25H)-MLPH and SHD (R35W)-MLPH decreased the interaction with RAB27A. These experiments were repeated three independent times.

with MYO5A (24, 25). To further define whether the D25H substitution compromises the RAB27A-MLPH interaction, an SHD (D25H)-MLPH construct was used to express the D25H mutant. Flag-RAB27A and Myc-tagged SHD (WT), SHD (D25H), or SHD (R35W) were co-transfected into HEK293T cells, respectively. Cell lysates were immunoprecipitated with anti-Flag beads, followed by immunoblotting with anti-Flag and anti-Myc antibodies, respectively (**Figure 3C**). The results showed that the SHD (D25H)-MLPH variant reduced the binding to RAB27A protein, compared with the control SHD (WT)-MLPH (**Figure 3C**). As a positive control, the interaction between SHD (R35W)-MLPH and RAB27A was also decreased, as previously reported (8). These data suggest that the conserved D25 residue of MLPH plays role in the interaction with RAB27A.

MLPH (D25H) Induces Perinuclear Distribution of Melanosomes in Human Melanocytes

It was previously described that mutations in *MLPH* cause the clustered perinuclear distribution observed in leaden mice (26). The pathologic defect in a GS3 patient with the MLPH (R35W) substitution induced aggregation of melanosomes in the perinuclear area of the patient's melanocytes (27). To test whether MLPH (D25H) is disease-causing, light microscopy and immunofluorescence confocal microscopy

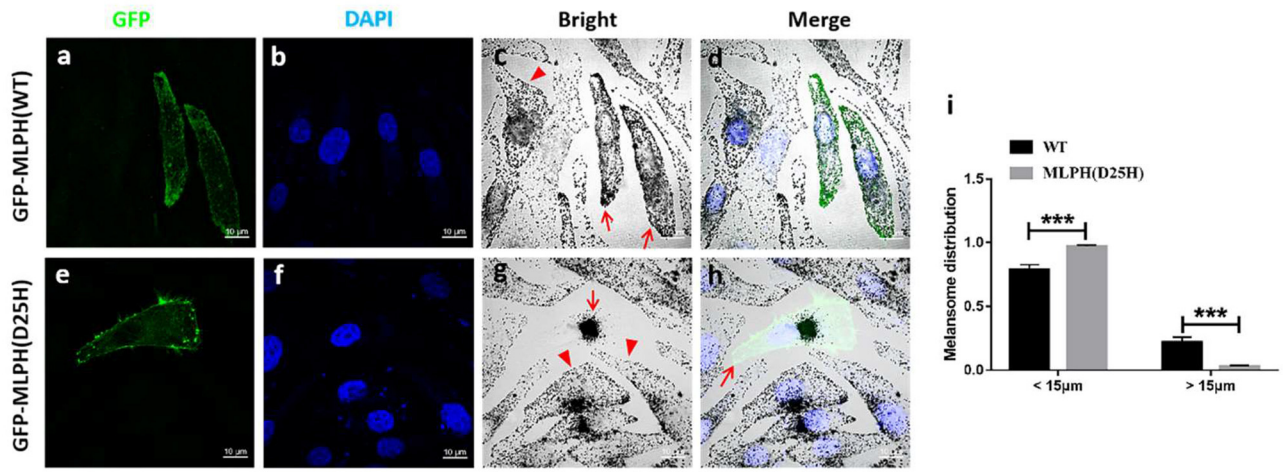

FIGURE 4 | The mutant MLPH (D25H) induces perinuclear melanosome accumulation in MNT1 cell by bright-field microscopy. **(a–h)** Images of transfected cells. Green fluorescence protein (GFP) [**(a,e),** green] represents the transfected cells. Blue staining represents DAPI-labeled nuclei **(b,f)**. Melanocytes transfected with GFP-MLPH (WT) show the presence of pigmented melanosomes in the cell peripheral [**(c,d)**, red arrows], while melanocytes transfected with GFP-MLPH (D25H) show a perinuclear aggregation of melanosomes [**(g)**, red arrow] and the absence of melanosomes in peripheral region [**(h)**, red arrow]. Cells failed to transfect with GFP-MLPH (WT) [**(c)**, red arrowhead] or GFP-MLPH (D25H) [**(g)**, red arrowheads] show a normal peripheral melanosome distribution. Bars: 10 μm. **(i)** Quantification of melanosome radial profile distribution. Melanosome distribution was quantified using Image J plugin radial profile. The radial melanosome intensity from each cell was quantified by drawing an equally-sized circle around its entire area. Percentage distribution of "perinuclear" melanosome (< 15 μm) and "peripheral" melanosome (> 15 μm) was calculated. In total, 11 cells in each group were analyzed. Quantified data were presented as mean ± standard error of the mean (SEM) using Student's *t*-test. Error bars indicate SEM (***$p < 0.001$).

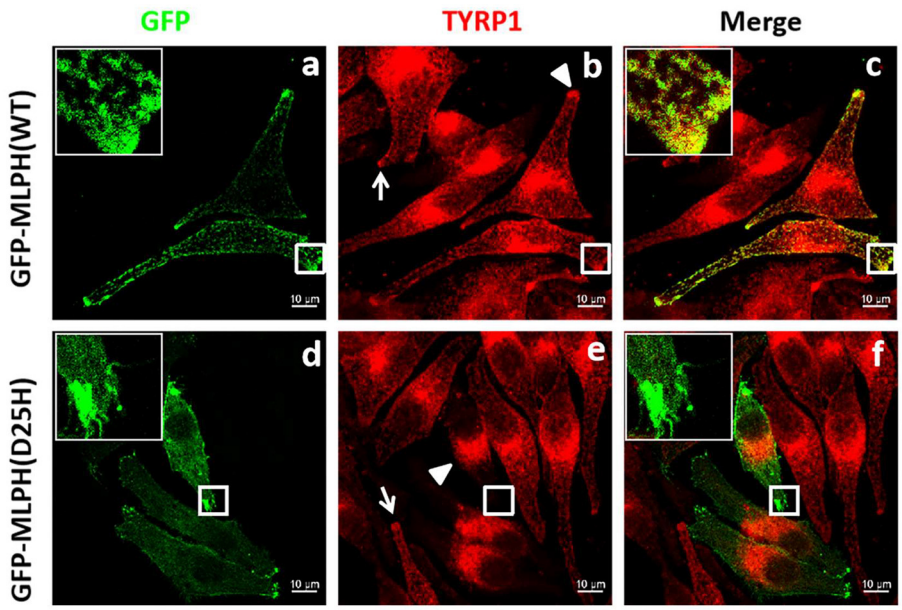

FIGURE 5 | Distribution of TYRP1 in melanocytes transfected with GFP-MLPH (WT) or GFP-MLPH (D25H). **(a–f)** MNT1 cells were transfected with GFP-MLPH (WT) or GFP-MLPH (D25H). Transfection with GFP-MLPH (WT) showed a peripheral distribution of TYRP1 [**(b)**, arrowhead], while transfection with GFP-MLPH (D25H) showed the typical clustering of TYRP1 in the perinuclear region [**(e)**, arrowhead] and lack of the TYRP1 in the cell periphery [**(e)**, rectangle]. GFP-MLPH (WT) colocalized with TYRP1 **(c)** in the cell periphery while GFP-MLPH (D25H) did not **(f)**. Bars: 10 μm.

were used to examine the distribution of melanosomes. Green fluorescence showed the plasmid was successfully transfected into the cells (**Figures 4a,e**, **5a,d**). Both melanocytes transfected with green fluorescence protein (GFP)-MLPH (WT) (**Figure 4c**, red arrows) and un-transfected cells from the same field of view (**Figure 4c**, red arrowhead) had a

normal distribution of melanosomes at the periphery of the cells. In contrast, melanocytes overexpressed GFP-MLPH (D25H) showed melanosome accumulation in the perinuclei (**Figure 4g**, red arrow) and a lack of melanosomes in the peripheral dendrites (**Figure 4h**, red arrow), while those adjacent un-transfected cells exhibited a normal melanosome distribution (**Figure 4g**, red arrowheads). Quantification of melanosome distribution showed that more melanosomes were clustered in the perinuclear region but less in the periphery (**Figure 4i**).

Next, we used laser scanning confocal microscopy to study the localization of the melanosome-specific protein TYRP1 (**Figures 5b,e**), which is involved in the biosynthesis of melanin and the maintenance of melanosome structures (28, 29). In melanocytes transfected with or without GFP-MLPH (WT) (**Figure 5b**), TYRP1 staining showed a punctate pattern in the cell periphery and dendrites (**Figure 5b**, white arrowhead and arrow), with a slight aggregation around the nuclei. MLPH colocalized with TYRP1 in the cell's periphery dendritic tip (**Figure 5c**). By comparison, melanocytes overexpressed GFP-MLPH (D25H) showed a perinuclear accumulation (**Figure 5e**, white arrowhead) and the dendrites were devoid of TYRP1 staining (**Figure 5e**, white rectangle). While un-transfected cells displayed a normal localization of TYRP1 (**Figure 5e**, arrow). However, there was almost no colocalization between the MLPH (D25H) and TYRP1 in the cell periphery (**Figure 5f**). Taken together, these results demonstrated that the D25H mutation resulted in perinuclear aggregation of melanosomes, suggesting the impeded movement of melanosomes toward the cell periphery, which underlies the pathological effects of the patient with GS3.

DISCUSSION

All members of the Slp-family proteins share an N-terminal SHD, including two conserved potential a-helical regions (SHD1 and SHD2) often separated by two zinc finger motifs (30). Within this region, SHD1 directly binds to the switch II region of the GTP-bound active form of RAB27A on the melanosome membrane (5, 31). Furthermore, RAB27A-GTP recruits MLPH to the melanosomes through its interaction with both SHD1 and SHD2 (32). Thus, the SHD domain is critical for the formation of the tripartite complex involved in melanosome transport. We here reported a new pathological missense variant c.73G > C (p.D25H) that is located in the SHD domain together with the other four reported variants (**Figure 2D**). Although the D25H variant did not alter the protein expression level and melanosomal localization, it resulted in the stuck of melanosomes in the perinuclear region of the melanocytes, leading to the clumps of pigment in the patient's hair shafts.

Slp homology domain 1 of melanophilin alone is both necessary and sufficient for high-affinity specific recognition of the GTP-bound form of RAB27A. By contrast, the zinc finger motifs and SHD2 seem to be important for the stabilization of the structure of the SHD or higher affinity RAB27A binding (31). The R35W/F/K mutation in the SHD1 domain prevents it from interacting with RAB27A (8), and R35W introduces melanosome aggregation in cultured melanocytes (27). Similarly, the D25H mutation is located in the SHD1 domain, leading to melanosome aggregation in transfected melanocytes. Furthermore, we confirmed the decreased interaction between SHD (D25H)-MLPH and RAB27A, similarly to SHD (R35W)-MLPH and RAB27A, suggesting that both D25H and R35W may have a similar mechanism in disrupting the MLPH-RAB27A interaction that blocks the melanosome transport to the cell periphery where the melanosome releases its melanin content. Our findings not only expand the mutational spectrum of MLPH but also emphasize the importance of the SHD1 domain in mediating melanosome transport.

DATA AVAILABILITY STATEMENT

The datasets presented in this article are not readily available because of ethical/privacy restrictions. Requests to access the datasets should be directed to the corresponding authors.

ETHICS STATEMENT

This study was approved by the Ethics Committees of Beijing Tongren Hospital and Beijing Children's Hospital, Capital Medical University. Written informed consent was obtained from the participant for the publication of any potentially identifiable data or images.

AUTHOR CONTRIBUTIONS

AW and WL designed the study and finalized the manuscript. QH and YY performed the experiments, analyzed the data, and wrote the manuscript. JG, TZ, ZQ, and XY provided technical support. All authors approved the submitted version of the manuscript.

FUNDING

This work was partially supported by grants from the Ministry of Science and Technology of China [2019YFA0802104 (WL)] and from the National Natural Science Foundation of China [(82173447 (AW), 31830054 (WL), and 31900496 (YY)].

SUPPLEMENTARY MATERIAL

The Supplementary Material for this article can be found online at: https://www.frontiersin.org/articles/10.3389/fmed.2022.896943/full#supplementary-material

REFERENCES

1. Le L, Sires-Campos J, Raposo G, Delevoye C, Marks MS. Melanosome biogenesis in the pigmentation of mammalian skin. *Integr Comp Biol.* (2021) 61:1517–45. doi: 10.1093/icb/icab078
2. Li W, Hao CJ, Hao ZH, Ma J, Wang QC, Yuan YF, et al. New insights into the pathogenesis of hermansky-pudlak syndrome. *Pigment Cell Melanoma Res.* (2022). doi: 10.1111/pcmr.13030
3. Hume AN, Seabra MC. Melanosomes on the move: a model to understand organelle dynamics. *Biochem Soc Trans.* (2011) 39:1191–6. doi: 10.1042/BST0391191
4. Fukuda M. Rab GTPases: Key players in melanosome biogenesis, transport, and transfer. *Pigment Cell Melanoma Res.* (2021) 34:222–35. doi: 10.1111/pcmr.12931
5. Strom M, Hume AN, Tarafder AK, Barkagianni E, Seabra MC, A. family of Rab27-binding proteins. Melanophilin links Rab27a and myosin Va function in melanosome transport. *J Biol Chem.* (2002) 277:25423–30. doi: 10.1074/jbc.M202574200
6. Fukuda M, Kuroda TS, Mikoshiba K. Slac2-a/melanophilin, the missing link between Rab27 and myosin Va: implications of a tripartite protein complex for melanosome transport. *J Biol Chem.* (2002) 277:12432–6. doi: 10.1074/jbc.C200005200
7. Nagashima K, Torii S, Yi Z, Igarashi M, Okamoto K, Takeuchi T, et al. Melanophilin directly links Rab27a and myosin Va through its distinct coiled-coil regions. *FEBS Lett.* (2002) 517:233–8. doi: 10.1016/S0014-5793(02)02634-0
8. Ménasché G, Ho CH, Sanal O, Feldmann J, Tezcan I, Ersoy F, et al. Griscelli syndrome restricted to hypopigmentation results from a melanophilin defect (GS3) or a MYO5A F-exon deletion (GS1). *J Clin Invest.* (2003) 112:450–6. doi: 10.1172/JCI200318264
9. Menasche G, Pastural E, Feldmann J, Certain S, Ersoy F, Dupuis S, et al. Mutations in RAB27A cause Griscelli syndrome associated with haemophagocytic syndrome. *Nat Genet.* (2000) 25:173–6. doi: 10.1038/76024
10. Pastural E, Barrat FJ, Dufourcq-Lagelouse R, Certain S, Sanal O, Jabado N, et al. Griscelli disease maps to chromosome 15q21 and is associated with mutations in the myosin-Va gene. *Nat Genet.* (1997) 16:289–92. doi: 10.1038/ng0797-289
11. Cagdas D, Ozgur TT, Asal GT, Tezcan I, Metin A, Lambert N, et al. Griscelli syndrome types 1 and 3: analysis of four new cases and long-term evaluation of previously diagnosed patients. *Eur J Pediatr.* (2012) 171:1527–31. doi: 10.1007/s00431-012-1765-x
12. Kelsen JR, Dawany N, Moran CJ, Petersen BS, Sarmady M, Sasson A, et al. Exome sequencing analysis reveals variants in primary immunodeficiency genes in patients with very early onset inflammatory bowel disease. *Gastroenterology.* (2015) 149:1415–24. doi: 10.1053/j.gastro.2015.07.006
13. Al-Mousa H, Abouelhoda M, Monies DM, Al-Tassan N, Al-Ghonaium A, Al-Saud B, et al. Unbiased targeted next-generation sequencing molecular approach for primary immunodeficiency diseases. *J Allergy Clin Immunol.* (2016) 137:1780–7. doi: 10.1016/j.jaci.2015.12.1310
14. Wasif N, Parveen A, Bashir H, Ashraf F, Ali E, Khan KR, et al. Novel homozygous nonsense variant in MLPH causing Griscelli syndrome type 3 in a consanguineous Pakistani family. *J Dermatol.* (2020) 47:e382–e3. doi: 10.1111/1346-8138.15565
15. Li H, Durbin R. Fast and accurate short read alignment with Burrows-Wheeler transform. *Bioinformatics.* (2009) 25:1754–60. doi: 10.1093/bioinformatics/btp324
16. Tarasov A, Vilella AJ, Cuppen E, Nijman IJ, Prins P. Sambamba: fast processing of NGS alignment formats. *Bioinformatics.* (2015) 31:2032–4. doi: 10.1093/bioinformatics/btv098
17. Waterhouse AM, Procter JB, Martin DM, Clamp M, Barton GJ. Jalview Version 2–a multiple sequence alignment editor and analysis workbench. *Bioinformatics.* (2009) 25:1189–91. doi: 10.1093/bioinformatics/btp033
18. Kuroda TS, Ariga H, Fukuda M. The actin-binding domain of Slac2-a/melanophilin is required for melanosome distribution in melanocytes. *Mol Cell Biol.* (2003) 23:5245–55. doi: 10.1128/MCB.23.15.5245-5255.2003
19. Kuroda TS, Fukuda M, Ariga H, Mikoshiba K. The Slp homology domain of synaptotagmin-like proteins 1-4 and Slac2 functions as a novel Rab27A binding domain. *J Biol Chem.* (2002) 277:9212–8. doi: 10.1074/jbc.M112414200
20. Patwardhan A, Bardin S, Miserey-Lenkei S, Larue L, Goud B, Raposo G, et al. Routing of the RAB6 secretory pathway towards the lysosome related organelle of melanocytes. *Nat Commun.* (2017) 8:15835. doi: 10.1038/ncomms15835
21. Yuan Y, Liu T, Huang X, Chen Y, Zhang W, Li T, et al. A zinc transporter, transmembrane protein 163, is critical for the biogenesis of platelet dense granules. *Blood.* (2021) 137:1804–17. doi: 10.1182/blood.2020007389
22. Ridaura-Sanz C, Duran-McKinster C, Ruiz-Maldonado R. Usefulness of the skin biopsy as a tool in the diagnosis of silvery hair syndrome. *Pediatr Dermatol.* (2018) 35:780–3. doi: 10.1111/pde.13624
23. Richards S, Aziz N, Bale S, Bick D, Das S, Gastier-Foster J, et al. Standards and guidelines for the interpretation of sequence variants: a joint consensus recommendation of the American College of Medical Genetics and Genomics and the Association for Molecular Pathology. *Genet Med.* (2015) 17:405–24. doi: 10.1038/gim.2015.30
24. Westbroek W, Lambert J, De Schepper S, Kleta R, Van Den Bossche K, Seabra MC, et al. Rab27b is up-regulated in human Griscelli syndrome type II melanocytes and linked to the actin cytoskeleton via exon F-Myosin Va transcripts. *Pigment Cell Res.* (2004) 17:498–505. doi: 10.1111/j.1600-0749.2004.00173.x
25. Hume AN, Collinson LM, Hopkins CR, Strom M, Barral DC, Bossi G, et al. The leaden gene product is required with Rab27a to recruit myosin Va to melanosomes in melanocytes. *Traffic.* (2002) 3:193–202. doi: 10.1034/j.1600-0854.2002.030305.x
26. Matesic LE, Yip R, Reuss AE, Swing DA, O'Sullivan TN, Fletcher CF, et al. Mutations in Mlph, encoding a member of the Rab effector family, cause the melanosome transport defects observed in leaden mice. *Proc Natl Acad Sci U S A.* (2001) 98:10238–43. doi: 10.1073/pnas.181336698
27. Westbroek W, Klar A, Cullinane AR, Ziegler SG, Hurvitz H, Ganem A, et al. Cellular and clinical report of new Griscelli syndrome type III cases. *Pigment Cell Melanoma Res.* (2012) 25:47–56. doi: 10.1111/j.1755-148X.2011.00901.x
28. Gautron A, Migault M, Bachelot L, Corre S, Galibert MD, Gilot D. Human TYRP1: Two functions for a single gene? *Pigment Cell Melanoma Res.* (2021) 34:836–52. doi: 10.1111/pcmr.12951
29. Ghanem G, Fabrice J. Tyrosinase related protein 1 (TYRP1/gp75) in human cutaneous melanoma. *Mol Oncol.* (2011) 5:150–5. doi: 10.1016/j.molonc.2011.01.006
30. Van Gele M, Dynoodt P, Lambert J. Griscelli syndrome: a model system to study vesicular trafficking. *Pigment Cell Melanoma Res.* (2009) 22:268–82. doi: 10.1111/j.1755-148X.2009.00558.x
31. Fukuda M. Synaptotagmin-like protein (Slp) homology domain 1 of Slac2-a/melanophilin is a critical determinant of GTP-dependent specific binding to Rab27A. *J Biol Chem.* (2002) 277:40118–24. doi: 10.1074/jbc.M205765200
32. Hume AN, Tarafder AK, Ramalho JS, Sviderskaya EV, Seabra MC, A. coiled-coil domain of melanophilin is essential for Myosin Va recruitment and melanosome transport in melanocytes. *Mol Biol Cell.* (2006) 17:4720–35. doi: 10.1091/mbc.e06-05-0457

Conflict of Interest: The authors declare that the research was conducted in the absence of any commercial or financial relationships that could be construed as a potential conflict of interest.

frontiers | Frontiers in Medicine

ORIGINAL RESEARCH
published: 24 May 2022
doi: 10.3389/fmed.2022.813917

Metformin Promotes Mechanical Stretch-Induced Skin Regeneration by Improving the Proliferative Activity of Skin-Derived Stem Cells

Shaoheng Xiong†, Wei Liu†, Yajuan Song, Jing Du, Tong Wang, Yu Zhang, Zhaosong Huang, Qiang He, Chen Dong, Zhou Yu and Xianjie Ma**

Department of Plastic Surgery, Xijing Hospital, Fourth Military Medical University, Xi'an, China

Background: Skin expansion by mechanical stretch is an essential and widely used treatment for tissue defects in plastic and reconstructive surgery; however, the regenerative capacity of mechanically stretched skin limits clinical treatment results. Here, we propose a strategy to enhance the regenerative ability of mechanically stretched skin by topical application of metformin.

Methods: We established a mechanically stretched scalp model in male rats (n = 20), followed by their random division into two groups: metformin-treated (n = 10) and control (n = 10) groups. We measured skin thickness, collagen volume fraction, cell proliferation, and angiogenesis to analyze the effects of topical metformin on mechanically stretched skin, and immunofluorescence staining was performed to determine the contents of epidermal stem cells and hair follicle bulge stem cells in mechanically stretched skin. Western blot was performed to detect the protein expression of skin-derived stem cell markers.

Results: Compared with the control group, metformin treatment was beneficial to mechanical stretch-induced skin regeneration by increasing the thicknesses of epidermis (57.27 ± 10.24 vs. 31.07 ± 9.06 μm, $p < 0.01$) and dermis (620.2 ± 86.17 vs. 402.1 ± 22.46 μm, $p < 0.01$), number of blood vessels (38.30 ± 6.90 vs. 17.00 ± 3.10, $p < 0.01$), dermal collagen volume fraction (60.48 ± 4.47% vs. 41.28 ± 4.14%, $p < 0.01$), and number of PCNA+, Aurora B+, and pH3+ cells. Additionally, we observed significant elevations in the number of proliferating hair follicle bulge stem cells [cytokeratin (CK)15+/proliferating cell nuclear antigen (PCNA)+] (193.40 ± 35.31 vs. 98.25 ± 23.47, $p < 0.01$) and epidermal stem cells (CK14+/PCNA+) (83.00 ± 2.38 vs. 36.38 ± 8.96, $p < 0.01$) in the metformin-treated group, and western blot results confirmed significant increases in CK14 and CK15 expression following metformin treatment.

Conclusion: Topical application of metformin enhanced the regenerative capacity of mechanically stretched skin, with the underlying mechanism possibly attributed to improvements in the proliferative activity of skin-derived stem cells.

Keywords: skin expansion, metformin, mechanical stretch, skin regeneration, hair follicle bulge stem cells, epidermal stem cells

OPEN ACCESS

Edited by:
Xing-Hua Gao,
The First Affiliated Hospital of China Medical University, China

Reviewed by:
Teng Su,
Duke University, United States
Özlem Su Küçük,
Bezmialem Vakif University, Turkey

****Correspondence:***
Zhou Yu
yz20080512@163.com
Xianjie Ma
majing@fmmu.edu.cn

† These authors have contributed equally to this work and share first authorship

Specialty section:
This article was submitted to Dermatology, a section of the journal Frontiers in Medicine

Received: *12 November 2021*
Accepted: *05 May 2022*
Published: *24 May 2022*

Citation:
Xiong S, Liu W, Song Y, Du J, Wang T, Zhang Y, Huang Z, He Q, Dong C, Yu Z and Ma X (2022) Metformin Promotes Mechanical Stretch-Induced Skin Regeneration by Improving the Proliferative Activity of Skin-Derived Stem Cells. Front. Med. 9:813917. doi: 10.3389/fmed.2022.813917

INTRODUCTION

Skin expansion is a viable method for mechanical stretch-induced skin regeneration (1). In the clinic, skin expansion is generally applied in skin-defect repair and organ reconstruction by plastic surgeons and represents a feasible way to achieve clinically complete skin regeneration *in vivo* by mechanical stretching. However, the regenerative capacity of mechanically stretched skin is limited (2). Thus, there is an immediate unmet need to explore novel approaches to promote skin regeneration for better clinical applications.

Multiple biological behaviors, including cell proliferation, dermal collagen synthesis, and angiogenesis, influence skin regeneration during the mechanical stretching process. Previous studies show that stem cell therapy using bone marrow-derived stem cells and/or adipose-derived stem cells promotes mechanically stretched skin regeneration (2–5). However, skin-derived stem cells, especially epidermal stem cells (ESCs) and hair follicle bulge stem cells (HFBSCs) (6), might also perform critical regenerative functions during skin expansion. Therefore, in this study, we mainly focused on the biological effects of ESCs and HFBSCs during mechanical stretching. Our previous work demonstrated that HFBSC transplantation enhanced skin regeneration during the mechanical stretch process by differentiation into epidermal cells, vascular endothelial cells, and the outer root sheath cells of hair follicles (7). However, the direct application of stem cells *in vitro* in clinical practice is difficult. Thus, identifying a pharmacotherapy capable of positively regulating these above biological behaviors and activating ESCs or HFBSCs might contribute to the regeneration of mechanically stretched skin.

Metformin is a first-line medication used to treat type 2 diabetes, as recommended by the American Diabetes Association (8). Growing evidence shows that topical application of metformin might favor tissue regeneration and wound repair, which partially correlates with promoting angiogenesis and activating HFBSCs (9, 10). Other studies suggest that metformin accelerates wound healing by increasing dermal collagen deposition and re-epithelialization (10–14). Coincidentally, the mechanical stretching process involves both cyclic damage and repair. These findings suggest that the topical application of metformin might represent an alternative option for improving mechanical stretch-induced skin regeneration.

In this study, we investigated the ability of metformin to promote regeneration of mechanically stretched skin. To test this hypothesis, we constructed a rat scalp-expansion model to observe the effects of metformin on mechanically stretched skin regeneration and focused on the changes in ESCs and HFBSCs.

MATERIALS AND METHODS

Animals and the Mechanical Stretch Model

All animal procedures were performed according to protocols approved by the Institutional Animal Care and Use Committee of the Fourth Military Medical University (approval no. IACUC-20120117). Male Sprague–Dawley rats (6-week old; 180–220 g) were purchased from the Animal Center of the Fourth Military Medical University (Xi'an, China). Twenty rats were used in total, with 10 in the metformin-treated group and 10 in the control group. Rats were housed in groups of five animals per cage and *ad libitum* access to food and water in a 12-/12-h light/dark cycle.

A mechanical stretch model was established, as described previously (15). Briefly, rats were placed in the prone position after being anesthetized (1.5% pentobarbital sodium; 40 mg/kg body weight), and the neck skin of each rat was then incised at ∼1.5 cm, followed by implantation of a customized round 1-mL silicone expander (Guangzhou Wanhe Plastic Materials Co., Ltd., Guangzhou, China) under the scalp after blunt dissection. Normal saline (1 mL) was injected every 2 days to a final injection volume of 10 mL (**Figure 1**). From the beginning of the expansion, rats were treated topically every other day with 300 mM metformin (Sigma-Aldrich, St. Louis, MO, United States) or vehicle (double-steamed water). The animals were subjected to sample collection on day 29 and immediately euthanized (**Figure 1B**).

Skin Microvascular Flow Analysis

Analysis of microvascular flow in mechanically stretched skin was performed, as described previously (7). Dermal microvascular blood-flow intensity was measured using laser Doppler flowmetry (moorFLPI Full-Field Laser Perfusion Imager 3.0; Moor Instruments Ltd., Axminster, United Kingdom). The mean value of 10 independent images from each rat was used to represent blood flow. After measuring and collecting blood-flow images of the mechanically stretched skin, data were analyzed using onboard software (MoorFLPI Image Review v.2.0; Moor Instruments Ltd., Axminster, United Kingdom).

Histologic Analysis

Tissue samples were fixed in 4% paraformaldehyde (Sigma-Aldrich, St. Louis, MO, United States) in phosphate-buffered saline (PBS) for 24 h and embedded in paraffin, after which 4-μm-thick sections were stained with hematoxylin and eosin (H&E; Servicebio, Wuhan, China), Picrosirius Red (Servicebio), and Masson's trichrome (Servicebio) for conventional morphological evaluation after deparaffinization and rehydration. For the measurement of epidermal and dermal thickness, five fields from each section were randomly selected for statistical analysis. Collagen fibers were observed using polarized light microscopy (Eclipse Ci; Nikon, Tokyo, Japan), with collagen I fibers stained red and newly synthesized fibers stained yellow to orange (16), whereas collagen III fibers appeared green. Collagen volume fraction (CVF) was used to assess the relative content of collagen in the dermis stained with Masson's trichrome.

Immunohistochemical and Immunofluorescence Staining

Tissue specimens embedded in paraffin were cut into 4-μm-thick sections and subjected to antigen retrieval at 96°C

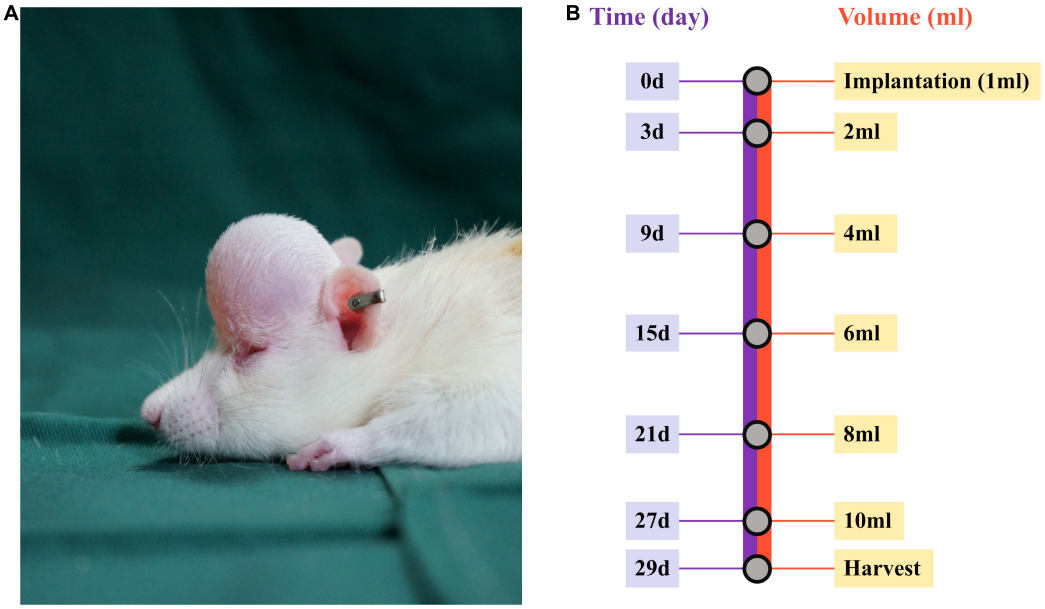

FIGURE 1 | Establishment of the mechanical stretch model and experimental design. **(A)** A round silicone expander was implanted under the rat scalp, and **(B)** 1 mL of normal saline was injected into the expander every other day up to a final injection on day 27. At 48 h after the final injection, the mechanically stretched skin was harvested for analysis.

for 20 min in citrate buffer (pH 6.0), followed by blocking for 1 h at room temperature with 5% goat serum in PBS. The following antibodies were used to investigate protein expression via IHC analysis: anti-Ki67 (1:500; Cell Signaling Technology, Danvers, MA, United States), anti-proliferating cell nuclear antigen (PCNA; 1:1000; Abcam, Cambridge, United Kingdom), anti-Aurora B (1:150; Abcam), anti-histone H3 (phospho S10; pH3; 1:600; Abcam), and anti-CD31 (1:2000; Cell Signaling Technology, Danvers, MA, United States) primary antibodies and a horseradish peroxidase-conjugated goat anti-rabbit secondary antibody (Jackson Laboratories, Bar Harbor, ME, United States). For immunofluorescence staining, the following primary antibodies were applied overnight at 4°C in a humidified chamber: mouse anti-rat PCNA (1:500; Abcam), rabbit anti-rat cytokeratin (CK)14 (1:200; Proteintech, Wuhan, China), and rabbit anti-rat CK15 (1:400; Proteintech). After washing in PBS, the sections were incubated with Alexa Fluor 488-conjugated goat anti-mouse IgG and IgM (H + L) secondary antibodies (1:1000; Invitrogen, Carlsbad, CA, United States) and an Alexa Fluor 568-conjugated goat anti-rabbit IgG (H + L) cross-adsorbed secondary antibody (1:1000; Invitrogen) for 1 h at room temperature in a humidified chamber. Nuclei were counterstained with 10 μg/mL 4′,6-diamidino-2-phenylindole (Invitrogen) for 15 min. Laser scanning confocal microscopy was performed using a confocal microscope (Nikon). Positive cell counting based on Ki67, PCNA, Aurora B, and pH3 was utilized to detect proliferating cells using ImageJ software (v.1.53k; NIH, Bethesda, MD, United States), and microvessel density (MVD) was determined by calculating the number of CD34+ blood vessels per field.

Transmission Electron Microscopy

Samples used for TEM were prepared, as described previously (17). The harvested skin sample was cut into small pieces (5 mm^3) and fixed in 2.5% glutaraldehyde (Sigma-Aldrich, St. Louis, MO, United States) in 0.1 M PBS for 24 h at 4°C. The samples were then post-fixed with 1% osmium tetroxide solution for 12 h, dehydrated with a descending ethanol series for 2 h, and embedded in epon resin. The area representative of the dermis was retained for ultrastructural analysis. Subsequently, 80-nm-thick ultrathin sections were cut and placed on copper grids for observation under a JEM-1400 transmission electron microscope (JEOL Ltd., Tokyo, Japan).

Western Blot Analysis

After homogenization, all skin tissues were lysed for 30 min with ice-cold radioimmunoprecipitation assay lysis buffer (CoWin Biosciences, Taizhou, China). Protein lysate (15 μg; concentration determined by a BCA assay) was subjected to sodium dodecyl sulfate polyacrylamide gel electrophoresis (SDS-PAGE; CoWin Biosciences, Taizhou, China) on a 6% gel for collagen I and collagen III; 10% gel for Aurora B, CK14, and CK15; 12% gel for PCNA, pH3, and glyceraldehyde 3-phosphate dehydrogenase (GAPDH) at 80 V for 1.5 h, and then transferred to polyvinylidene fluoride membranes (Merck, Darmstadt, Germany). The membranes were blocked with 5% bovine serum albumin in PBS at room temperature for 1.5 h, followed by incubation with primary antibodies against collagen I (1:1000; Cell Signaling Technology, Danvers, MA, United States), collagen III (1:1000; Cell Signaling Technology, Danvers, MA, United States), PCNA (1:1000; Abcam), Aurora B (1:1000;

Abcam), pH3 (1:200; Abcam), CK14 (1:1000; Proteintech), CK15 (1:2000; Proteintech), and GAPDH (1:20,000; Proteintech) at 4°C overnight. Quantitative analysis was performed on the immunoreactive bands using ImageJ software (v.1.53k; NIH, Bethesda, MD, United States).

Statistical Analysis

Data are expressed as the mean ± standard deviation. Student's *t*-test and a Mann–Whitney non-parametric test were performed to compare the data of unpaired samples using GraphPad Prism software (v.8.0; GraphPad Software, La Jolla, CA, United States). A $p < 0.05$ was considered significant.

RESULTS

Metformin Enhances Skin Thickening After Mechanical Stretching

Hematoxylin and eosin staining images showed an increased number of cell layers in the epidermis of the metformin-treated group, with the cells closely arranged in the epidermal stratum basale layer. Additionally, we observed numerous hair follicles in the dermis of mechanically stretched skin in the metformin-treated group. Moreover, statistical analysis confirmed that the thickness of mechanically stretched skin increased following metformin treatment (**Figures 2A,B**). Furthermore, mechanically stretched epidermis and dermis were thicker in the metformin-treated group relative to that in the control group [57.27 ± 10.24 vs. 31.07 ± 9.06 μm ($p < 0.01$) and 620.2 ± 86.17 vs. 402.1 ± 22.46 μm ($p < 0.01$), respectively] (**Figure 2B**).

Metformin Increases Dermal Collagen Deposition and Arrangement

Masson's trichrome staining to determine collagen deposition in the mechanically stretched dermis (**Figure 3A**) revealed that the metformin-treated group showed a higher CVF than the control group (60.48 ± 4.47% vs. 41.28 ± 4.14%, $p < 0.01$) (**Figure 3B**). Additionally, western blot results confirmed significant increases in collagen I and collagen III expression in the metformin-treated group (**Figures 3C,D**), and Picrosirius Red staining revealed more newly synthesized collagen in the metformin-treated group (**Figure 4A**). Furthermore, ultrastructural analysis showed more evenly arranged collagen fibrils without distortion in the metformin-treated group, whereas more broken and disorganized collagen fibrils were observed in the control group (**Figure 4B**).

Metformin Increases Cell Proliferation

The metformin-treated group showed significantly increased proportions of Ki67+ cells per field as compared with the control group (epidermis: 25.25 ± 1.71 vs. 76.00 ± 12.44, $p < 0.01$; dermis: 72.75 ± 4.03 vs. 143.00 ± 27.76, $p < 0.01$; **Supplementary Figures 1A,B**). Additionally, we respectively analyzed IHC staining of PCNA (**Figures 5A,B**), Aurora B (**Figures 5E,F**), and pH3 (**Figures 5I,J**) as markers for cell proliferation in different phases of the cell division cycle. We found more proliferating cells (PCNA+, Aurora B+, or pH3+) in the metformin-treated group than in the control group [epidermis: PCNA+ cells (50.25 ± 7.93 vs. 128.5 ± 16.60, $p < 0.01$), Aurora B+ cells (57.60 ± 5.94 vs. 103.9 ± 11.94, $p < 0.01$), and pH3+ cells (45.20 ± 6.87 vs. 107.00 ± 20.13, $p < 0.01$); dermis: PCNA+ cells (91.00 ± 23.08 vs. 273.3 ± 52.99, $p < 0.05$), Aurora B+ cells (54.75 ± 10.05 vs. 137.00 ± 16.70, $p < 0.01$), and pH3+ cells (228.50 ± 8.55 vs. 490.70 ± 68.49, $p < 0.01$); **Figures 5B,F,J**]. These proliferative cells were mainly located in the basal layer of the epidermis and the outer root sheath of hair follicles. Furthermore, western blot results confirmed that the protein level of PCNA (**Figures 5C,D**), Aurora B (**Figures 5G,H**), and pH3 (**Figures 5K,L**) were all markedly increased in the metformin-treated group.

Metformin Increases Blood Flow and the Number of Blood Vessels in the Skin

In vivo detection of microvascular blood flow showed improved blood flux in the metformin-treated group than in the control group (510.00 ± 73.59 vs. 322.40 ± 50.60, $p < 0.05$) (**Figures 6A,B**). Additionally, we identified an increased number of blood vessels in the mechanically stretched skin grafts (**Figure 6C**), with IHC staining of CD31 revealing more blood vessels per field in the metformin-treated group relative to the control group (38.30 ± 6.90 vs. 17.00 ± 3.10, $p < 0.01$) (**Figures 7A,B**).

Metformin Increases the Proliferative Capability of Skin-Derived Stem Cells

To determine the types of cells involved in skin regeneration, we performed double-immunofluorescence staining of PCNA and CK14 or CK15. The results showed that metformin treatment significantly increased the number of CK14+/PCNA+ cells in the stratum basale layer of the mechanically stretched epidermis (83.00 ± 2.38 vs. 36.38 ± 8.96, $p < 0.01$), with proliferating hair follicle outer-sheath cells (CK15+/PCNA+) also observed in the metformin-treated group (193.40 ± 35.31 vs. 98.25 ± 23.47, $p < 0.01$; **Figures 8A,B**). Moreover, western blot results confirmed the upregulated expression of CK14 and CK15 in the metformin-treated group, which was consistent with the results of double-immunofluorescence staining (**Figures 8C,D**).

DISCUSSION

Soft-tissue expansion by mechanical stretching represents an efficient surgical procedure for skin-defect repair and organ reconstruction; however, the skin-regenerative capacity is limited (2). Stem cell therapy represents an alternative method for enhancing the regeneration of mechanically stretched skin (2–5). In particular, ESCs and HFBSCs located *in situ* play a vital role in skin regeneration and repair. In this study, we found that metformin enhanced the regenerative capacity of mechanically stretched skin by thickening both the epidermis and dermis, increasing angiogenesis, and promoting cell proliferation in mechanically stretched skin, possibly as a result of the improved proliferative activity of ESCs and HFBSCs.

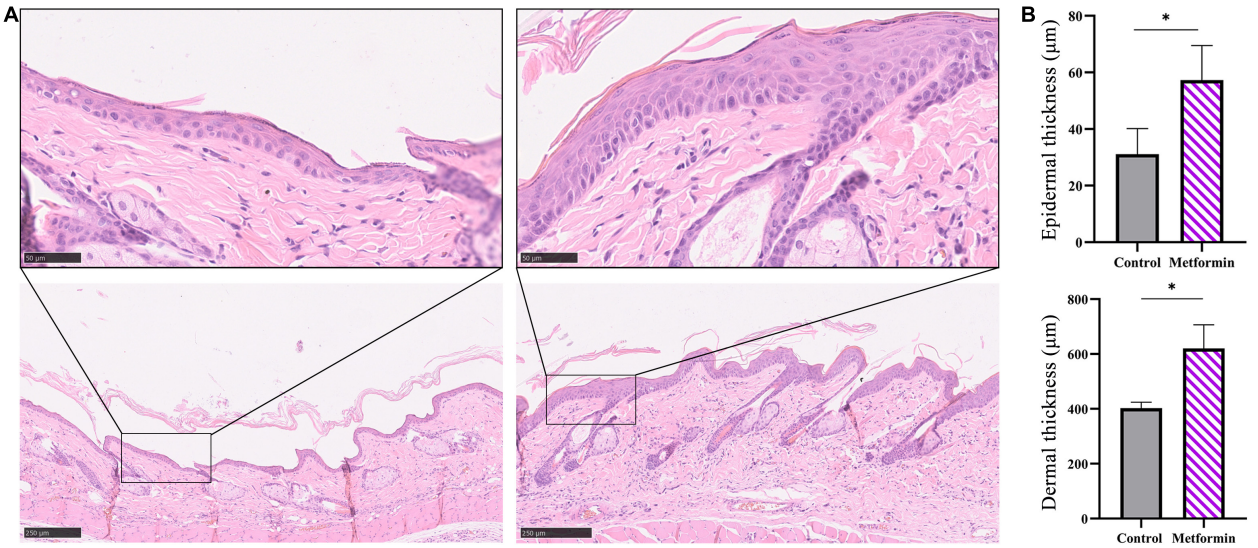

FIGURE 2 | Measurement of the thickness of mechanically stretched skin. **(A)** H&E staining of skin from the metformin-treated and control groups. Compared with the control group (top left), the metformin-treated group had more cell layers in the epidermis, with the cells closely arranged in the epidermal stratum basale layer (top right) and numerous hair follicles present in the metformin-treated group (bottom right). **(B)** Quantification of epidermal and dermal thickness. The epidermis and dermis in the metformin-treated group were significantly thicker than those in the control group. *$p < 0.05$.

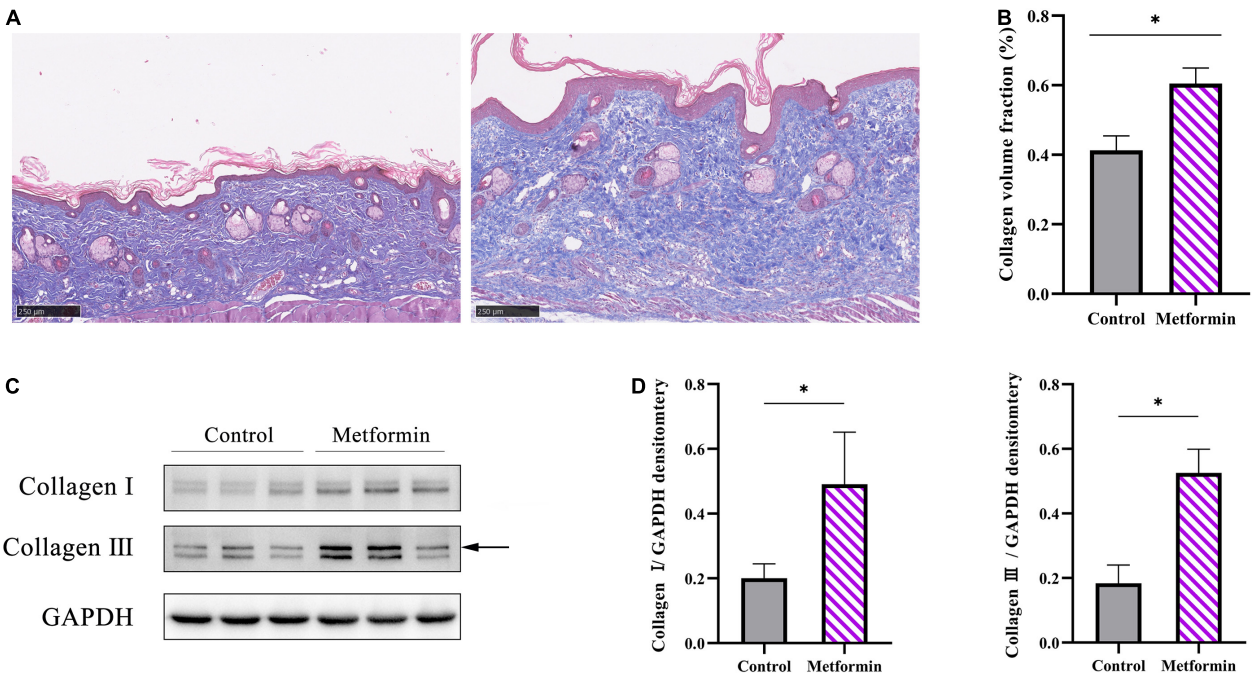

FIGURE 3 | Evaluation of collagen synthesis. **(A)** Masson's trichrome staining showed increased collagen deposition in the metformin-treated group, with **(B)** a significantly higher CVF than the control group. **(C)** Western blot analysis and **(D)** quantification of collagen I and collagen III expressions. *$p < 0.05$.

Angiogenesis and remodeling are important for the regeneration of mechanically stretched skin (18). In the present study, we observed significantly increased *in vivo* microvascular blood flow in mechanically stretched skin following metformin treatment. Moreover, metformin treatment improved the blood perfusion of the mechanically stretched skin, with subsequent histologic evaluation and quantitative assessment of CD31+ blood vessels confirming the improved angiogenesis in the metformin-treated group. Previous studies report that metformin promotes tissue repair directly or indirectly (14),

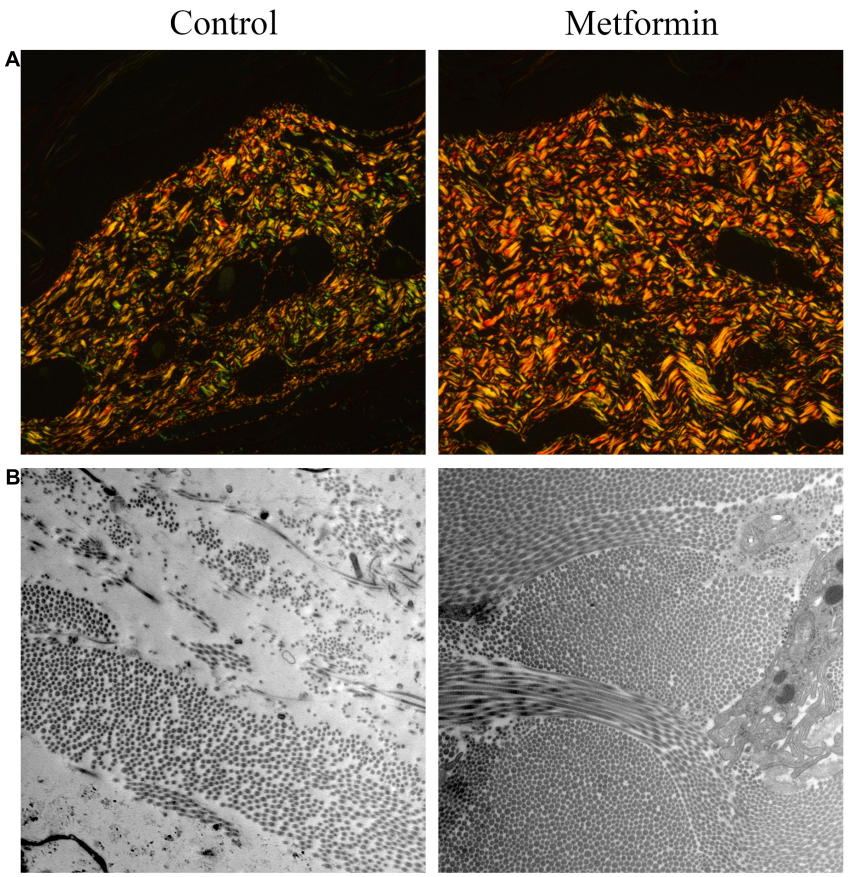

FIGURE 4 | Picrosirius Red staining ultrastructural analysis of dermal collagen fibrils. **(A)** Picrosirius Red images showed increased neocollagen development (yellow to orange) in the metformin-treated group. **(B)** TEM images revealed an improved arrangement of collagen fibrils in the metformin-treated group without a distorted ultrastructure, whereas collagen fibrils in the control group were broken and disorganized. Magnification: 15,000×.

mainly by improving the angiogenesis of wounds (10, 19, 20). Because mechanically stretched skin experiences similar stress and relaxation activities to that in injury- and repair-related mechanical stretching processes (18), the proangiogenic effect of metformin during wound healing is likely replicated in mechanically stretched skin. Previous reports demonstrated that metformin could promote angiogenesis both *in vitro* and *in vivo*. Local application of metformin significantly accelerated wound healing, which was attributed to the promotion of angiogenesis via stimulation of the AMP-activated protein kinase pathway (AMPK) (10). Additionally, metformin promoted angiogenesis and improved the survival of random pattern skin flaps by activating the AMPK–mammalian target of rapamycin–transcription factor EB signaling pathway (20). Moreover, low-dose metformin significantly enhanced the angiogenic differentiation of mesenchymal stem cells *in vivo* and *in vitro* and boosted mesenchymal stem cell-mediated promotion of HUVEC migration and tube formation by upregulating the expression of stem cell factor and vascular endothelial growth factor receptor 2 (21).

The synthesis and deposition of dermal collagen could be advantageous for skin regeneration during mechanical stretching. The present results showed that collagen deposition was significantly increased by metformin treatment and that the ultrastructure of collagen fibers was highly ordered according to TEM analysis. Moreover, we confirmed elevated levels of both collagen I and collagen III expression in the metformin-treated group. Additionally, the promotion of dermal angiogenesis can benefit collagen synthesis by increasing blood supply after treatment with metformin. A previous study reported that chronic topical administration of metformin (once daily for 14 days) accelerated wound healing by promoting collagen deposition (10).

Epidermal thickening is another important characteristic of regenerated mechanically stretched skin. In this study, we found that epidermal thickness was significantly increased in the metformin-treated group, which was mainly attributed to the increased proliferation of epidermal cells. We measured IHC staining to enumerate Ki67+ (cell cycle entry marker), PCNA+ (peak level reached around the late G1-phase and early S-phase of the cell cycle), Aurora B+ (peak level reached around mid-late M-phase of the cell cycle), and pH3+ (peak level reached in the late G2- and M-phase of the cell cycle) cells per field to evaluate cell proliferation in mechanically

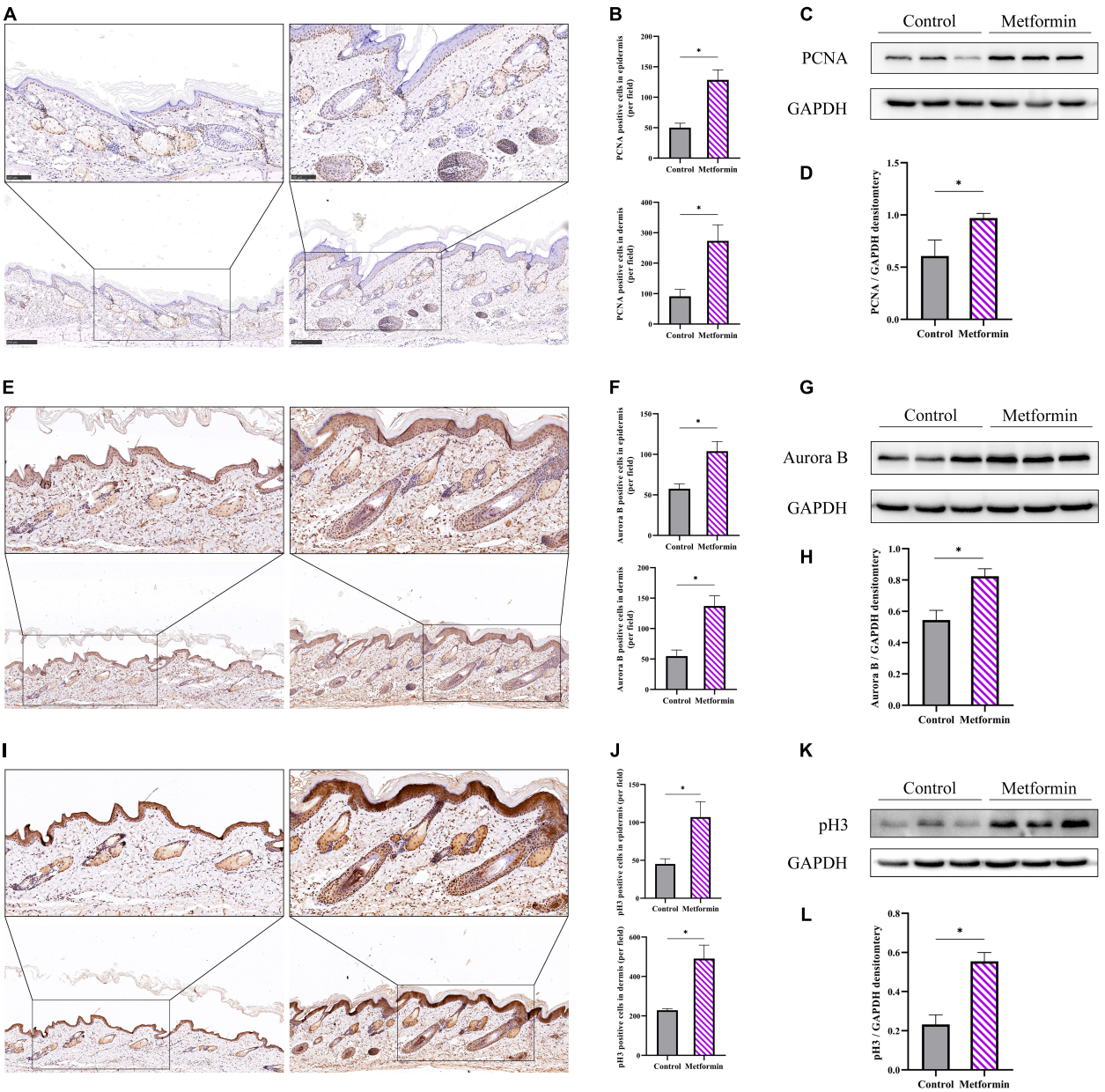

FIGURE 5 | Cell proliferation in the mechanically stretched skin. Immunohistochemistry (IHC) staining of PCNA **(A)**, Aurora B **(E)**, and pH3 **(I)** in mechanically stretched skin. Proliferative cells were mainly located in the basal layer of the epidermis and near the dermal hair follicles. More proliferating PCNA+ **(B)**, Aurora B+ **(F)**, and pH3+ **(J)** cells were present in both the epidermis and dermis of metformin-treated skin. Western blotting was used to detect the protein expression of PCNA **(C)**, Aurora B **(G)**, and pH3 **(K)**, and increased expression of PCNA **(D)**, Aurora B **(H)**, and pH3 **(L)** was observed in the metformin-treated group. $^*p < 0.05$.

stretched skin. The results showed that those positive cells were all increased in the metformin-treated group, and subsequent western blotting confirmed that the PCNA, Aurora B, and pH3 protein expression levels were also increased in the metformin-treated group compared to those in the control group. Moreover, IHC staining evaluation revealed that the proliferating cells were primarily located in the stratum basale layer, which probably comprises ESCs. To verify the source of proliferating cells in the stratum basale layer, we further used double-immunofluorescence staining of CK14+/PCNA+ to label ESCs. And the double-immunofluorescence staining showed that numerous CK14+/PCNA+ ESCs were present in the metformin-treated group, which would subsequently drive stronger proliferative activity in the epidermis. Further study confirmed that the expression of CK14 was significantly elevated in the metformin-treated group. Moreover, a recent study revealed that the proliferation and differentiation potential of CK14+ ESCs significantly contributed to the regeneration of

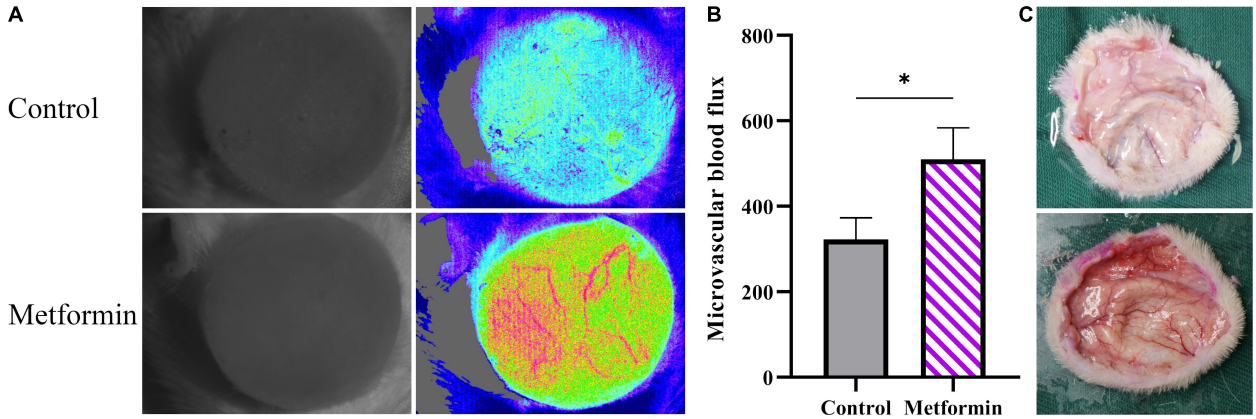

FIGURE 6 | Detection of microcirculatory blood flow. **(A)** Microcirculatory blood flows analysis of mechanically stretched skin from the metformin-treated and control groups. **(B)** The results showed significantly increased blood flow in the metformin-treated group and **(C)** a higher number of blood vessels observed in freshly isolated skin from the metformin-treated group relative to the control group. $^*p < 0.05$.

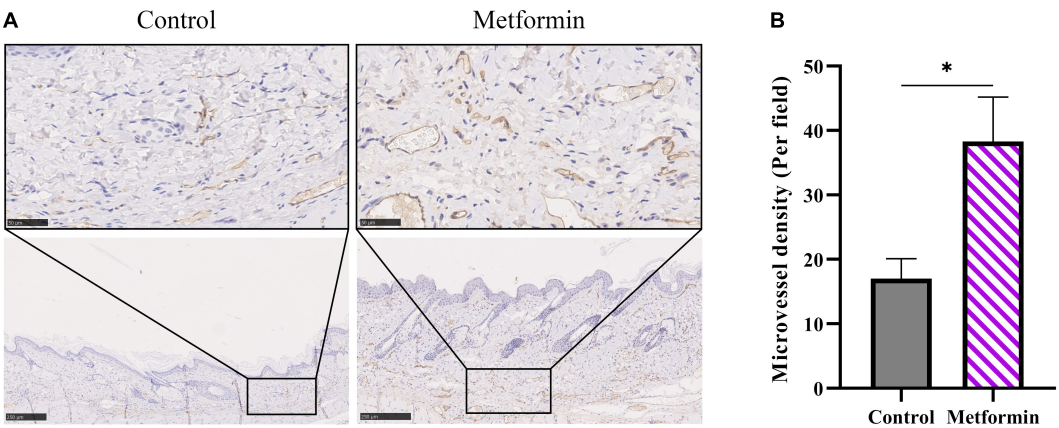

FIGURE 7 | IHC staining of CD31 in mechanically stretched skin. **(A)** IHC staining revealed more CD31+ vessels in mechanically stretched skin from the metformin-treated group relative to the control group. **(B)** Quantitative analysis of microvascular density. $^*p < 0.05$.

mechanically stretched skin (1). Additionally, others found that topical application of metformin benefited re-epithelialization during wound healing (10). These results indicate that metformin treatment might promote epidermal thickening by increasing ESC proliferation and differentiation.

Similarly, we analyzed dermal cell proliferation by IHC staining of PCNA, Aurora B, and pH3. Notably, we found that these positive cells (PCNA, Aurora B, and pH3) were significantly increased in the metformin-treated group compared with numbers in the control group, and most of these positive cells were located in the bulge region, whereas the outer-root sheath of hair follicles was thought to be the site of ESCs and HFBSCs. We next used double-immunofluorescence labeling of CK15+/PCNA+ HFBSCs to confirm the sources of these proliferating cells. We observed a significantly increasing number of CK15+/PCNA+ HFBSCs in mechanically stretched skin following metformin treatment. Further western blot analysis revealed increased CK15 expression in the metformin-treated group, indicating that more HFBSCs were present in metformin-treated mechanically stretched skin than in the control group. Our previous study showed that HFBSC transplantation promoted the regeneration of mechanically stretched skin via direct differentiation into epidermal cells, vascular endothelial cells, and the outer-root sheath cells of hair follicles (7). Therefore, we suggest that topical application of metformin might improve the regenerative capacity of mechanically stretched skin by activating local HFBSCs. Previous studies reported a higher number of hair follicles present at the wound edge following metformin treatment along with more rapid wound healing (10). Furthermore, previous studies showed that HFBSC activation is involved in skin regeneration and re-epithelialization during wound repair (22). These results suggest that metformin might benefit wound healing by activating HFBSCs present in hair follicles. Growing evidence suggests that metformin exerts pleiotropic effects to activate stem cells and promote functional rejuvenation (9, 23–28). Among these effects,

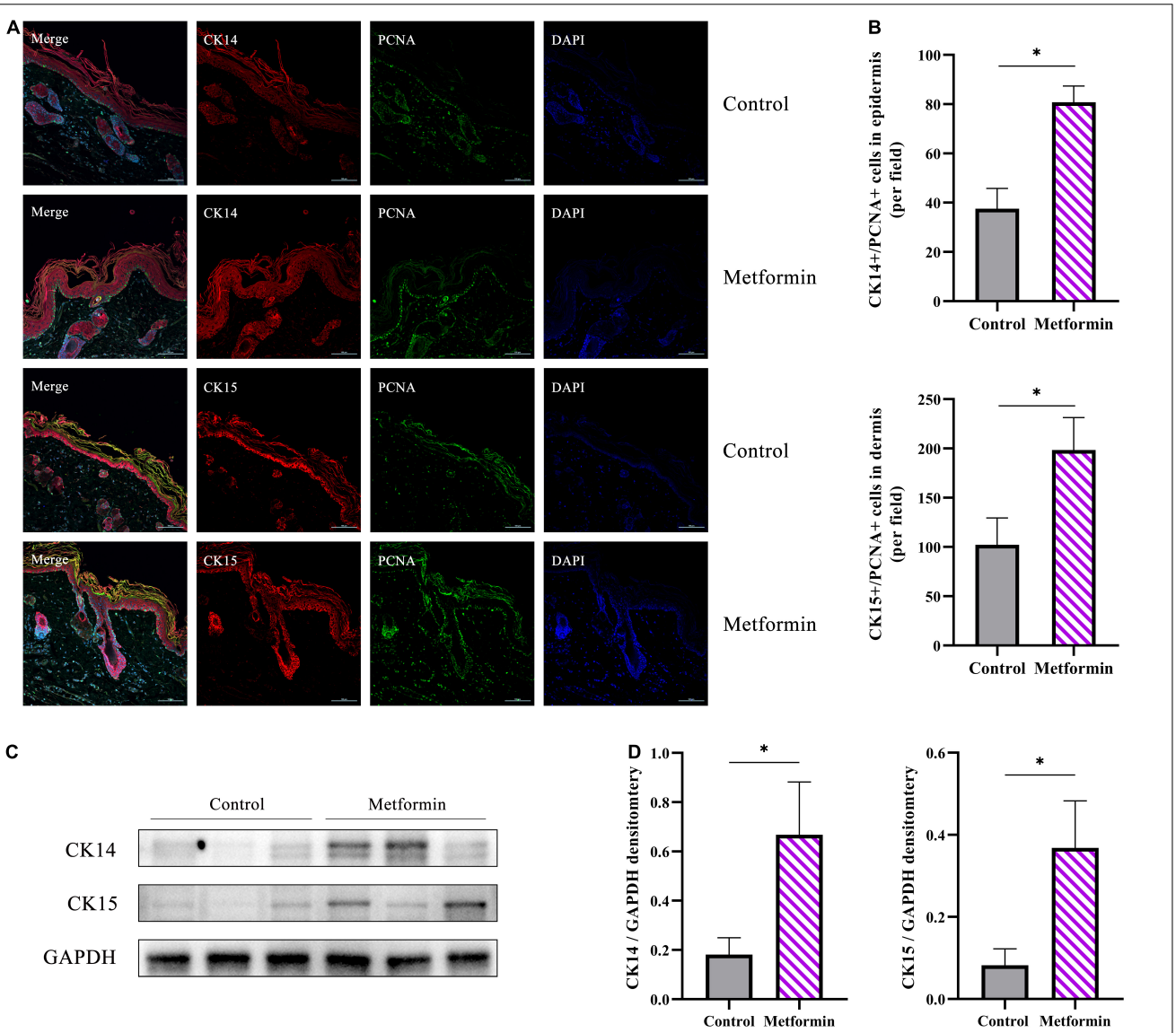

FIGURE 8 | Immunofluorescence staining of mechanically stretched skin. **(A)** Double-immunofluorescence staining of PCNA (green) and CK14 (red) or CK15 (red) revealed the proliferative status of epidermal stem cells (ESCs) and hair follicle bulge stem cells (HFBSCs). More CK14+/PCNA+ ESCs and CK15+/PCNA+ HFBSCs were identified in mechanically stretched skin from the metformin-treated group than in the control group. **(B)** Quantitative analysis revealed significantly increased numbers of CK14+/PCNA+ and CK15+/PCNA+ cells in skin samples from the metformin-treated group. **(C)** Western blot analysis and **(D)** quantification of CK14 and CK15 protein expression. The results showed that the protein levels of CK14 and CK15 were significantly increased in the metformin-treated group relative to those in the control group. $^*p < 0.05$.

topical application of metformin reactivated dormant HFBSCs, which subsequently contributed to initiating new anagen hair growth (9). Notably, a clinical randomized controlled trial comparing therapeutic efficacy between hair-follicle scalp grafts and non-hairy skin grafts demonstrated that transplanted skin with more hair follicles results in better wound healing (29). This evidence supports our finding that topical application of metformin further activated the proliferative capacity of HFBSCs.

Previous studies have demonstrated the effect of metformin on the hair follicle; however, there was no direct evidence that metformin promotes the proliferation of ESCs or HFBSCs. These mainly focused on evaluating hair growth and the number of hair follicles. In this study, we provided direct evidence that the topical application of metformin could promote the proliferation of ESCs and HFBSCs using IHC staining, double-immunofluorescence staining, and measurement of protein expression levels. In addition, previous work mainly focused on applying metformin to promote wound healing. Nevertheless, there currently is no evidence to confirm the effect of the topical application of metformin on mechanical stretch-induced skin regeneration. Skin expansion is an important means to clinically obtain complete skin regeneration induced by

mechanical stretching *in vivo*. Although previous studies have shown that stem cells could effectively promote expanded skin regeneration, alternative methods are required due to clinical ethical restrictions. This study found that HFBSCs activated by locally applied metformin might directly participate in the skin-regeneration process during mechanical stretching. These findings offer novel insights into improving mechanical stretch-induced skin regeneration by activating local HFBSCs.

However, this study has two limitations. First, the skin anatomy is not identical between rats and humans; therefore, species-specific differences in the observed therapeutic effects likely exist. Further clinical evidence in humans is needed to confirm these findings. Second, metformin's mechanisms associated with proliferative regulation of skin-derived stem cells, including HFBSCs and ESCs, are complex and require further investigation.

CONCLUSION

In summary, we found that topical application of metformin promoted the regenerative capacity of mechanically stretched skin, possibly attributed to enhanced collagen synthesis, angiogenesis, and skin-derived stem cell proliferation. These findings might provide a valuable alternative strategy for promoting mechanical stretch-induced skin regeneration.

DATA AVAILABILITY STATEMENT

The original contributions presented in the study are included in the article/**Supplementary Material**, further inquiries can be directed to the corresponding author/s.

ETHICS STATEMENT

The animal study was reviewed and approved by the Institutional Animal Care and Use Committee of the Fourth Military Medical University.

AUTHOR CONTRIBUTIONS

SX: designing the experiments, conducting the experiments, acquiring and analyzing the data, and writing the manuscript. WL: conducting the immunofluorescence staining and analyzing the data. YS, TW, YZ, and QH: conducting the animal experiments. JD and CD: conducting the western blot analysis. ZH: conducting the immunohistochemical staining. ZY: concept of the study, designing the experiments, and writing and editing the manuscript. XM: concept of the study, designing experiments, providing reagents, and writing and editing the manuscript. All authors contributed to the article and approved the submitted version.

FUNDING

This study was supported by grants from the National Natural Science Foundation of China (Nos. 82172229 and 81971851), Natural Science Foundation of Shaanxi Province (2022JM-600), and the Foundation of Xijing Hospital Grants (XJZT21CM33).

SUPPLEMENTARY MATERIAL

The Supplementary Material for this article can be found online at: https://www.frontiersin.org/articles/10.3389/fmed.2022.813917/full#supplementary-material

Supplementary Figure 1 | Cell proliferation in the mechanically stretched skin. **(A)** Immunohistochemistry (IHC) staining of Ki67 in mechanically stretched skin. Proliferative cells were mainly located in the basal layer of the epidermis and near the dermal hair follicles. **(B)** More proliferating Ki67+ cells were present in both the epidermis and dermis of the metformin-treated skin.

Supplementary Figure 2 | Raw data of **Figure 3C**.

Supplementary Figure 3 | Raw data of **Figure 5C**.

Supplementary Figure 4 | Raw data of **Figure 5G**.

Supplementary Figure 5 | Raw data of **Figure 5K**.

Supplementary Figure 6 | Raw data of **Figure 8C**.

REFERENCES

1. Aragona M, Sifrim A, Malfait M, Song Y, Van Herck J, Dekoninck S, et al. Mechanisms of stretch-mediated skin expansion at single-cell resolution. *Nature.* (2020) 584:268–73. doi: 10.1038/s41586-020-2555-7
2. Zhou SB, Zhang GY, Xie Y, Zan T, Gan YK, Yao CA, et al. Autologous stem cell transplantation promotes mechanical stretch induced skin regeneration: a randomized phase I/II clinical trial. *Ebiomedicine.* (2016) 13:356–64. doi: 10.1016/j.ebiom.2016.09.031
3. Li C, Zheng Y, Wang X, Xia W, Gao H, Li D, et al. Bone marrow-derived stem cells contribute skin regeneration in skin and soft tissue expansion. *J Cell Physiol.* (2011) 226:2834–40. doi: 10.1002/jcp.22634
4. Yang M, Li Q, Sheng L, Li H, Weng R, Zan T. Bone marrow-derived mesenchymal stem cells transplantation accelerates tissue expansion by promoting skin regeneration during expansion. *Ann Surg.* (2011) 253:202–9. doi: 10.1097/SLA.0b013e3181f9ba1ah
5. Tan PC, Chao PC, Cheng C, Chen CH, Huang RL, Zhou SB, et al. A randomized, controlled clinical trial of autologous stromal vascular fraction cells transplantation to promote mechanical stretch-induced skin regeneration. *Stem Cell Res Ther.* (2021) 12:243. doi: 10.1186/s13287-021-02318-5
6. Lisse TS, Sharma M, Vishlaghi N, Pullagura SR, Braun RE. GDNF promotes hair formation and cutaneous wound healing by targeting bulge stem cells. *NPJ Regen Med.* (2020) 5:13. doi: 10.1038/s41536-020-0098-z
7. Cheng X, Yu Z, Song Y, Zhang Y, Du J, Su Y, et al. Hair follicle bulge-derived stem cells promote tissue regeneration during skin expansion. *Biomed Pharmacother.* (2020) 132:110805. doi: 10.1016/j.biopha.2020.110805
8. American Diabetes Association. Pharmacologic approaches to glycemic treatment: standards of medical care in diabetes-2021. *Diabetes Care.* (2021) 44:S111–24. doi: 10.2337/dc21-S009
9. Chai M, Jiang M, Vergnes L, Fu X, de Barros SC, Doan NB, et al. Stimulation of hair growth by small molecules that activate autophagy. *Cell Rep.* (2019) 27:3413–21. doi: 10.1016/j.celrep.2019.05.070
10. Zhao P, Sui BD, Liu N, Lv YJ, Zheng CX, Lu YB, et al. Anti-aging pharmacology in cutaneous wound healing: effects of metformin, resveratrol, and rapamycin by local application. *Aging Cell.* (2017) 16:1083–93. doi: 10.1111/acel.12635

11. Chogan F, Mirmajidi T, Rezayan AH, Sharifi AM, Ghahary A, Nourmohammadi J, et al. Design, fabrication, and optimization of a dual function three-layer scaffold for controlled release of metformin hydrochloride to alleviate fibrosis and accelerate wound healing. *Acta Biomater.* (2020) 113:144–63. doi: 10.1016/j.actbio.2020.06.031
12. Yu JW, Deng YP, Han X, Ren GF, Cai J, Jiang GJ. Metformin improves the angiogenic functions of endothelial progenitor cells via activating AMPK/eNOS pathway in diabetic mice. *Cardiovasc Diabetol.* (2016) 15:88. doi: 10.1186/s12933-016-0408-3
13. Qing L, Fu J, Wu P, Zhou Z, Yu F, Tang J. Metformin induces the M2 macrophage polarization to accelerate the wound healing via regulating AMPK/mTOR/NLRP3 inflammasome singling pathway. *Am J Transl Res.* (2019) 11:655–68.
14. Miricescu D, Badoiu SC, Stanescu-Spinu II, Totan AR, Stefani C, Greabu M. Growth factors, reactive oxygen species, and metformin-promoters of the wound healing process in burns? *Int J Mol Sci.* (2021) 22:9512. doi: 10.3390/ijms22179512
15. Liu W, Xiong S, Zhang Y, Du J, Dong C, Yu Z, et al. Transcriptome profiling reveals important transcription factors and biological processes in skin regeneration mediated by mechanical stretch. *Front Genet.* (2021) 12:757350. doi: 10.3389/fgene.2021.757350
16. El-Domyati M, Abd-El-Raheem T, Abdel-Wahab H, Medhat W, Hosam W, El-Fakahany H, et al. Fractional versus ablative erbium: yttrium-aluminum-garnet laser resurfacing for facial rejuvenation: an objective evaluation. *J Am Acad Dermatol.* (2013) 68:103–12. doi: 10.1016/j.jaad.2012.09.014
17. Yu Z, Liu S, Cui J, Song Y, Wang T, Song B, et al. Early histological and ultrastructural changes in expanded murine scalp. *Ultrastruct Pathol.* (2020) 44:141–52. doi: 10.1080/01913123.2020.1720876
18. Ding J, Lei L, Liu S, Zhang Y, Yu Z, Su Y, et al. Macrophages are necessary for skin regeneration during tissue expansion. *J Transl Med.* (2019) 17:36. doi: 10.1186/s12967-019-1780-z
19. Takahashi N, Shibata R, Ouchi N, Sugimoto M, Murohara T, Komori K. Metformin stimulates ischemia-induced revascularization through an eNOS dependent pathway in the ischemic hindlimb mice model. *J Vasc Surg.* (2015) 61:489–96. doi: 10.1016/j.jvs.2013.09.061
20. Wu H, Ding J, Li S, Lin J, Jiang R, Lin C, et al. Metformin promotes the survival of random-pattern skin flaps by inducing autophagy via the AMPK-mTOR-TFEB signaling pathway. *Int J Biol Sci.* (2019) 15:325–40. doi: 10.7150/ijbs.29009
21. Lei T, Deng S, Chen P, Xiao Z, Cai S, Hang Z, et al. Metformin enhances the osteogenesis and angiogenesis of human umbilical cord mesenchymal stem cells for tissue regeneration engineering. *Int J Biochem Cell Biol.* (2021) 141:106086. doi: 10.1016/j.biocel.2021.106086
22. Joost S, Jacob T, Sun X, Annusver K, La Manno G, Sur I, et al. Single-cell transcriptomics of traced epidermal and hair follicle stem cells reveals rapid adaptations during wound healing. *Cell Rep.* (2018) 25:585–97. doi: 10.1016/j.celrep.2018.09.059
23. Neumann B, Baror R, Zhao C, Segel M, Dietmann S, Rawji KS, et al. Metformin restores CNS remyelination capacity by rejuvenating aged stem cells. *Cell Stem Cell.* (2019) 25:473–85. doi: 10.1016/j.stem.2019.08.015
24. Marycz K, Tomaszewski KA, Kornicka K, Henry BM, Wroński S, Tarasiuk J, et al. Metformin decreases reactive oxygen species, enhances osteogenic properties of adipose-derived multipotent mesenchymal stem cells in vitro, and increases bone density in vivo. *Oxid Med Cell Longev.* (2016) 2016:9785890. doi: 10.1155/2016/9785890
25. Fatt M, Hsu K, He L, Wondisford F, Miller FD, Kaplan DR, et al. Metformin acts on two different molecular pathways to enhance adult neural precursor proliferation/self-renewal and differentiation. *Stem Cell Rep.* (2015) 5:988–95. doi: 10.1016/j.stemcr.2015.10.014
26. Liao Z, Li S, Lu S, Liu H, Li G, Ma L, et al. Metformin facilitates mesenchymal stem cell-derived extracellular nanovesicles release and optimizes therapeutic efficacy in intervertebral disc degeneration. *Biomaterials.* (2021) 274:120850. doi: 10.1016/j.biomaterials.2021.120850
27. Jang SG, Lee J, Hong SM, Kwok SK, Cho ML, Park SH. Metformin enhances the immunomodulatory potential of adipose-derived mesenchymal stem cells through STAT1 in an animal model of lupus. *Rheumatology (Oxford).* (2020) 59:1426–38. doi: 10.1093/rheumatology/kez631
28. Fang J, Yang J, Wu X, Zhang G, Li T, Wang X, et al. Metformin alleviates human cellular aging by upregulating the endoplasmic reticulum glutathione peroxidase 7. *Aging Cell.* (2018) 17:e12765. doi: 10.1111/acel.12765
29. Martínez ML, Escario E, Poblet E, Sánchez D, Buchón FF, Izeta A, et al. Hair follicle-containing punch grafts accelerate chronic ulcer healing: a randomized controlled trial. *J Am Acad Dermatol.* (2016) 75:1007–14. doi: 10.1016/j.jaad.2016.02.1161

Conflict of Interest: The authors declare that the research was conducted in the absence of any commercial or financial relationships that could be construed as a potential conflict of interest.

Publisher's Note: All claims expressed in this article are solely those of the authors and do not necessarily represent those of their affiliated organizations, or those of the publisher, the editors and the reviewers. Any product that may be evaluated in this article, or claim that may be made by its manufacturer, is not guaranteed or endorsed by the publisher.

frontiers | Frontiers in Medicine

ORIGINAL RESEARCH
published: 24 May 2022
doi: 10.3389/fmed.2022.837332

Efficacy of Microneedling Combined With Local Application of Human Umbilical Cord-Derived Mesenchymal Stem Cells Conditioned Media in Skin Brightness and Rejuvenation: A Randomized Controlled Split-Face Study

Xuelei Liang[1†], Jiaying Li[2†], Yan Yan[1], Yongsheng Xu[1], Xiujuan Wang[1], Haixuan Wu[1], Yi Liu[1], Linfeng Li[1] and Fenglin Zhuo[1]*

[1] Department of Dermatology, Beijing Friendship Hospital, Capital Medical University, Beijing, China, [2] Department of Dermatology, Xuanwu Hospital, Capital Medical University, Beijing, China

OPEN ACCESS

Edited by:
Xing-Hua Gao,
The First Affiliated Hospital of China Medical University, China

Reviewed by:
Saritha Mohanan,
Indira Gandhi Medical College and Research Institute, India
Irina Khamaganova,
Pirogov Russian National Research Medical University, Russia

***Correspondence:**
Fenglin Zhuo
zflsunny@hotmail.com

† These authors have contributed equally to this work and share first authorship

Specialty section:
This article was submitted to Dermatology, a section of the journal Frontiers in Medicine

Received: 16 December 2021
Accepted: 14 April 2022
Published: 24 May 2022

Citation:
Liang X, Li J, Yan Y, Xu Y, Wang X, Wu H, Liu Y, Li L and Zhuo F (2022) Efficacy of Microneedling Combined With Local Application of Human Umbilical Cord-Derived Mesenchymal Stem Cells Conditioned Media in Skin Brightness and Rejuvenation: A Randomized Controlled Split-Face Study. Front. Med. 9:837332. doi: 10.3389/fmed.2022.837332

Background: Fighting skin aging signs is one of the major challenges of the 21st century, recently, mesenchymal stem cells (MSCs) and microneedling (MN) have been applied for anti-aging. This study aims to evaluate the efficacy of the combination of MN and human umbilical cord-derived mesenchymal stem cells conditioned media (hUC-MSCs-CM) in skin brightness and rejuvenation.

Methods: Thirty volunteers with facial skin aging were recruited for the randomized, controlled split-face study. The left and right sides of the face were randomly applied with saline *via* MN or hUC-MSCs-CM *via* MN. Five sessions were performed for each volunteer at 2-week intervals. Two dermatologists evaluated the clinical improvement, in terms of skin brightness and texture. A satisfaction score based on a self-evaluation questionnaire was recorded at 2 weeks after the last treatment. The objective evaluation was recorded before the first treatment, and at 2 weeks after the last treatment.

Results: Twenty-eight volunteers with a mean (SD) age of 41 (6.54) years old completed the trial. The investigator's assessment for skin brightness and texture, and the self-satisfaction score revealed statistically better effects in hUC-MSCs-CM -plus-MN group than in MN alone (MN saline) group. No severe side effects were reported during the whole study period. Compared to MN alone group, the objective assessment revealed significant improvements in skin brightness (reduced melanin index, ultraviolet spots,

and brown spots) and skin texture (reduced wrinkles and pores, and increased skin elasticity) in hUC-MSCs-CM-plus-MN group, while there were no obvious differences in skin hydration, *trans*-epidermal water loss, and the erythema index.

Conclusion: The combination of hUC-MSCs-CM and MN exhibite anti-aging efficacy, and this could be used for facial rejuvenation in the future.

Keywords: microneedling, human umbilical cord-derived mesenchymal stem cells, conditioned media, skin rejuvenation, skin brightness, efficacy

INTRODUCTION

Skin aging is subject to both intrinsic (chronological) and extrinsic (environmental) factors, resulting in poor appearance and loss of functional capacity. Rejuvenating skin by fighting aging signs, such as wrinkles, enlarged pores, reduced resilience and irregular pigmentation, is one of the major challenges of the 21st century (1). Skin aging not only affects physiological skin function, but also has impacts on a person's psychology and social life. As a result, several non-surgical treatments, such as oral treatments, ointments, dermabrasion, chemical peels, and laser therapy, have been developed over the past years, in order to counteract skin aging. However, these may be associated with prolonged recovery, dyspigmentation, and scarring.

Mesenchymal stem cells (MSCs) have the advantage of being easy to isolation, expansion, and multipotentiality, so they are popular in the field of skin rejuvenation therapy (2). These release several growth factors in autocrine and paracrine ways (3). There are various types of MSCs, including adipose-derived stem cells, bone marrow-derived stem cells (BMMSCs), and umbilical cord-derived mesenchymal stem cells. A recent study indicated that compared to BMMSCs-conditioned media, UC-MSCs-conditioned media (UC-MSCs-CM) can form premature adipocytes, collagen type 1 and collagen type 2 which have anti-aging effects (4).

Microneedling (MN) is a treatment widely applied for skin diseases and skin rejuvenation, due to its safety and efficacy. There are two main reasons for its medical use: (i) MN can accelerate the process of the skin's natural healing. It penetrates the epidermis and papillary dermis (5), creating pores, and thereby triggering the skin's repair mechanism (6). This can result in the short-term aggregation of inflammatory cells, fibroblasts proliferation, long-term remodeling, and the synthesis of collagen and elastin (5). (ii) MN can enhance the penetration of drugs (5). It is difficult for drugs to be absorbed through the skin due to the stratum corneum barrier (7). MN creates small transient holes that penetrate the stratum corneum barrier within a short period of time (8).

The present study aims to explore the synergistic effect of MN combined with hUC-MSCs-CM against aging skin. Non-invasive skin-measuring devices were used to objectively assess the changes in skin brightness and rejuvenation before and at 2 weeks after the final treatment.

MATERIALS AND METHODS

Subjects

A total of 30 volunteers with facial photo-aging (Fitzpatrick III 20, IV 10) were included for the present study. Two participants were withdrawn from the study due to job-related factors. The remaining 28 volunteers completed the study. These volunteers were within 35–60 years old, with a mean (SD) age of 41 (6.54) years old. The exclusion criteria included obvious inflammation, ulcer or effusion on the face, and previous skin rejuvenation treatment in the past 3 months.

Study Design

The present study was a randomized controlled split-face study. The Institutional Review Board of Beijing Friendship Hospital, Capital Medical University approved the study (Approval No. 2017-P2-086-01). All volunteers were thoroughly counseled on the potential risks and benefits before they signed the informed consent form, based on the 1975 Declaration of Helsinki. The registration number in http://www.chictr.org.cn is ChiCTR-INR-17013311.

Randomization and Allocation Concealment

MN plus hUC-MSCs-CM (Beijing Origife Health Care Co., Ltd., China) group and MN alone group (control) were randomly allocated to the left or right face side. Each participant was assigned a number, according to the random number table created by the computer software. If the number was odd, the left side was used as the test side. If the number was even, the right side was used as the test side. To ensure allocation concealment, the doctors in MN operation wore colorful glasses which are normally used to protect the eyes from Intense pulse Light treatment in our department. While each volunteer's eyes were covered with eight layers of sterile gauze before treatment.

Intervention

Prior to treatment, the faces of all participants were cleaned using facial cleanser (Nivea, Nivea Co., Ltd., Shanghai, China) and anesthetized with 5% compound lidocaine cream (Beijing Unisplendour Pharmaceutical Co., Ltd., China). For one side, 1.0 ml of saline or hUC-MSCs-CM was painted and the remaining 1.0 ml was added locally after dermaroller MN treatment, which was performed in eight rows, with a total of 192 needles, 0.5 mm in length (Suzhou Cynour Photoelectric

Technology Co., Ltd., China)., the same method was performed on the other side. The endpoint of treatment was the presence of uniform erythema over the face. Generally, 2 ml saline or hUC-MSCs-CM could be completely absorbed. The participants received five sessions of treatment at 2-week intervals for a total of 10 weeks. **Table 1** presents the densities of the main growth factors derived from hUC-MSCs-CM, which were measured using the Human ProcartaPlex Growth Factor Panel (11 plex) (Cat. No. EPX110-12170-901, Invitrogen, Thermo Fisher, United States).

Instrument Measurements

Prior to all measurements and assessments, the volunteers underwent an acclimatization period of 30 min under controlled standardized conditions (20°C, 40% humidity). Skin measurements were performed at baseline and 2 weeks after the 5th treatment. Cutometer® (MPA 580, Courage and Khazaka Electronic GmbH, Cologne, Germany) was used to test the hydration, transepidermal water loss (TEWL), elasticity, melanin index (MI), and erythema index. Photographs of both sides of the face, and the scores for skin spots, wrinkles, pores, ultraviolet spots, brown spots, and red spots were recorded by VISIA® skin analysis (Canfield Scientific, Inc., New York, NY, United States).

Self-Evaluation Questionnaire

At 2 weeks after the last treatment, the volunteers were instructed to evaluate their satisfaction with the efficacy, taking into account the adverse effects observed on both sides of the face, using the following scale: 0 = very dissatisfied, 1 = relatively dissatisfied, 2 = slightly dissatisfied, 3 = satisfied, 4 = relatively satisfied, and 5 = very satisfied.

Physician's Assessments

Two dermatologists, who were blinded to the study design and treatment, evaluated the clinical improvement, and compared it to the baseline. The assessment was based on the photographs taken by VISIA® skin analysis on both sides of the face at baseline and 2 weeks after the last treatment. The changes in skin brightness and rejuvenation were assessed, and the improvement was graded, as follows: 1 = 0–25% (no or minimal improvement), 2 = 26–50% (moderate improvement), 3 = 51–75% (marked improvement), and 4 = 76–100% (excellent improvement).

TABLE 1 | Analysis of multiple cytokines secreted from hUC-MSCs-CM.

Included growth factors	Concentration (pg/mL), Mean (SD)
BDNF	22.65 (3.21)
NGF beta	34.94 (5.79)
EGF	6983.63 (523.88)
FGF-2	296.32 (55.78)
HGF	880.11 (95.33)
LIF	11.03 (2.76)
PDGF-BB	35.21 (1.88)
PlGF	9.25 (1.37)
SCF	25.12 (2.19)
VEGF-A	930.93 (77.21)
VEGF-D	50.68 (10.76)

hUC-MSCs-CM: human umbilical cord-derived mesenchymal stem cells conditioned media; BDNF: Brain-derived neurotrophic factor; NGF beta: Nerve growth factor-beta; EGF: Epidermal growth factor; FGF-2: Fibroblast growth factor-2; HGF: Hepatocyte growth factor; LIF: Leukemia inhibitory factor; PDGF-BB: Platelet-derived growth factor-BB; PlGF: Placental growth factor; SCF: Stem cell factor; VEGF: Vascular endothelial growth factor.

Safety Assessment

Adverse reactions were recorded by questioning and examining the subjects during the follow-up visits.

Statistics

Statistical analysis was carried out by SPSS software 19.0 (IBM Corp., Armonk, NY, United States). Paired *t* test was used to compare the data of objective assessment between the test side and control side at every visit. The data of subjective evaluation was analyzed with the Wilcoxon signed-rank test. The measurements of both sides at baseline and the last visit were compared by paired *t* tests to see the effect of treatment. The statistically significant difference was set as $P < 0.05$.

RESULTS

Subjective Evaluation From Doctors and Participants

Self-Evaluation Questionnaire

A total of 28 volunteers completed the study. MN plus hUC-MSCs-CM side was more satisfied than MN alone side ($P < 0.05$, **Table 2**).

Clinical Assessment

The physician's global assessment of brightness and skin texture were greater improvements following hUC-MSCs-CM plus MN, compared to MN alone ($P < 0.05$, **Table 3**). The representative images revealed the larger improvement of pores and periocular wrinkles after MN plus hUC-MSCs-CM, compared to MN alone (**Figures 1**, **2**).

Objective Assessment

At baseline, there was no statistically significant difference for skin physiological parameters, skin brightness, and skin rejuvenation in the objective assessments between MN plus hUC-MSCs-CM group and MN alone group (**Table 4**).

Skin Physiological Parameters

Hydration and TEWL: The hydration content and TEWL are indicators for skin barrier function. There was no significant change in hydration content after treatment between MN plus hUC-MSCs-CM side [2.18 (5.80), $P = 0.06$] and MN alone side [2.07 (6.78), $P = 0.12$]. Furthermore, no significant change was found in the TEWL measurements between MN plus hUC-MSCs-CM side [1.96 (5.15), $P = 0.05$] and MN alone side [1.10 (3.79), $P = 0.13$], indicating that MN treatment did not damage the skin barrier.

TABLE 2 | Participant's overall satisfaction with the efficacy at 2 weeks after the last treatment.

(*n*)	Not satisfied	Slightly satisfied	Moderately satisfied	Satisfied	Very satisfied	*P*-value
MN alone	5	9	10	4	0	0.000*
MN plus hUC-MSCs-CM	0	5	9	9	5	

MN: microneedling; hUC-MSCs-CM: human umbilical cord-derived mesenchymal stem cells conditioned media.
Participant's overall satisfaction scores: ranging from 0, not satisfied, to 5, very satisfied.
**P < 0.05.*

TABLE 3 | Physician's global assessment at 2 weeks after the last treatment.

	No or minimal improvement	Moderate improvement	Marked improvement	Excellent improvement	*P*-value
Physician's global assessments for brightness (n)					0.001*
MN alone	5	18	5	0	
MN plus hUC-MSCs-CM	0	17	11	0	
Physician's global assessments for skin texture (n)					0.000*
MN alone	6	15	7	0	
MN plus hUC-MSCs-CM	2	13	7	6	

Physician's global assessments: grade 1: 0–25% = minimal or no improvement; grade 2: 26–50% = moderate improvement; grade 3: 51–75% = marked improvement; and grade 4: 75–100% = excellent improvement. MN: microneedling; hUC-MSCs-CM: human umbilical cord-derived mesenchymal stem cells conditioned media.
**P < 0.05.*

Skin Pigmentation (Skin Brightness)

Melanin Index

At 2 weeks after the last treatment, the MI decreased more in MN plus hUC-MSCs-CM group than in MN alone group [24.25 (15.55) vs. 12.36 (16.38), $P = 0.00$; **Figure 3A**], indicating the efficacy of hUC-MSCs-CM for skin lightening (**Figures 3A**, **1A,B**).

Ultraviolet Spots

Ultraviolet spots are associated with exposure to ultraviolet sun radiation. The ultraviolet spot score of the side treated with MN plus hUC-MSCs-CM decreased from 24.39 (7.11) to 14.47 (5.38), $P = 0.00$, while the score for the side treated with MN alone decreased from 23.08 (7.58) to 17.72 (6.18), $P = 0.00$. There was no significant difference in ultraviolet spot score between the two sides before first treatment, but a significant difference was observed at the last measurement ($P < 0.05$, **Figure 3B**), indicating that hUC-MSCs-CM was effective in decreasing ultraviolet spots.

Brown Spots

The formation of brown spots is related to dyspigmentation. Compared to baseline, either one side treated with MN plus hUC-MSCs-CM and MN presented with statistically significant changes in brown spot scores 2 weeks after the final treatment. The score for MN plus hUC-MSCs-CM side decreased from 40.21 (5.14) to 34.18 (6.32) ($P < 0.05$), while the score for MN alone side decreased from 39.71 (5.82) to 37.75 (5.63) ($P < 0.05$). At the last measurement, a significant change was observed between MN plus hUC-MSCs-CM side and MN alone side ($P = 0.00$, **Figure 3C**), indicating that MN plus hUC-MSCs-CM has a better effect in decreasing the brown scores.

Erythema Index

There was no significant difference in erythema index (EI) after treatment between MN plus hUC-MSCs-CM side ($P = 0.90$) and MN alone side ($P = 0.87$). The EI score for the sides treated with MN plus hUC-MSCs-CM increased from 336.69 (63.08) at baseline to 336.85 (60.06) at 2 weeks after the final treatment. Similarly, the EI score for the sides treated with MN alone increased from 336.68 (60.80) at baseline to 337.29 (57.05) at 2 weeks following the final treatment. This indicates that MN and hUC-MSCs-CM does not induce skin inflammation.

Red Spots

Spots in the side treated with MN plus hUC-MSCs-CM decreased from 29.30 (5.58) to 28.20 (4.92) ($P = 0.17$), while spots on the other side decreased from 29.17 (5.93) to 28.08 (5.38) ($P = 0.12$). There was no statistically significant difference in red spot scores at the last measurement ($P = 0.31$).

Skin Rejuvenation

Wrinkles

Compared to baseline, the wrinkle score for MN plus hUC-MSCs-CM side decreased to 5.06 (3.44) ($P = 0.00$), while the score for MN side decreased to 10.73 (10.63) ($P = 0.00$). At the final measurement, MN plus hUC-MSCs-CM side exhibited a more significant decrease in wrinkle measurements than in MN alone side [12.15 (10.26) vs. 7.46 (6.07), $P = 0.00$; **Figures 2**, **4A**].

Pores

Significant changes were observed for pores in both MN plus hUC-MSCs-CM group ($P = 0.00$) and MN alone group ($P = 0.00$). The pores' scores decreased from 23.55 (10.52) to 14.05 (6.11) in MN plus hUC-MSCs-CM group, while these decreased from

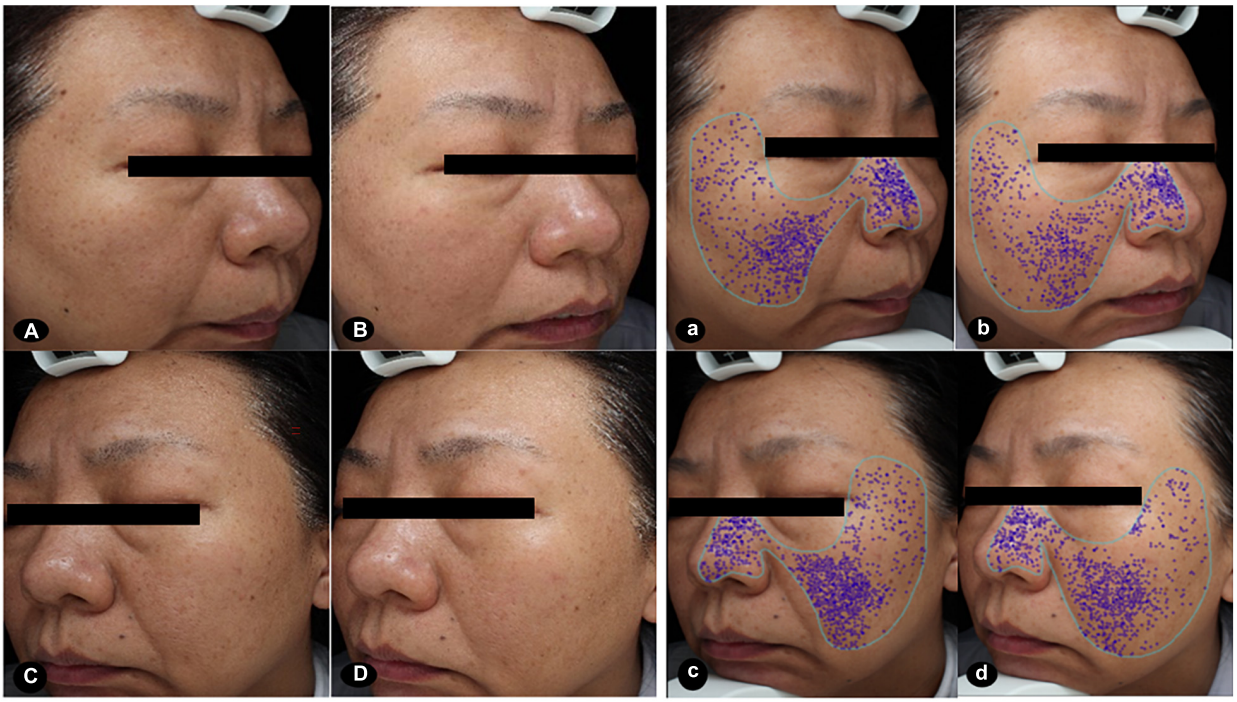

FIGURE 1 | Images at baseline and after the treatments. The clinical images presented greater improvements in brightness and size of pores after MN plus hUC-MSCs-CM [**(A,a)** baseline; **(B,b)** after treatment], compared to MN alone [**(C,c)** baseline; **(D,d)** after treatment]. The score of pores at the side of MN *via* hUC-MSCs-CM decreased from 20.29 to 13.32 after treatment. While the score of pores at another side of MN alone decreased from 22.64 to 17.71 after treatment. MN: microneedling; hUC-MSCs-CM: human umbilical cord-derived mesenchymal stem cells conditioned media.

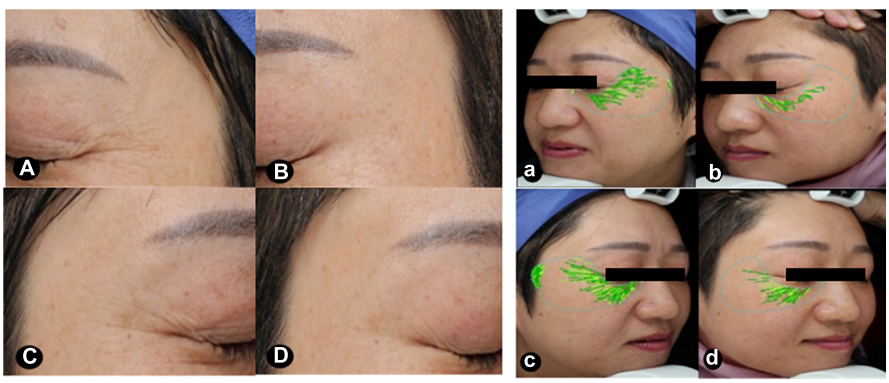

FIGURE 2 | Images focusing on the periorbital areas at baseline and after treatment. The periorbital wrinkles exhibited greater improvements after MN plus hUC-MSCs-CM [**(A,a)** baseline; **(B,b)** after treatment], compared to MN alone [**(C,c)**, baseline; **(D,d)** after treatment]. VISIA® skin analysis assessment for periorbital wrinkles: a = 29.53, b = 8.39, c = 32.37, d = 15.63. MN: microneedling; hUC-MSCs-CM: human umbilical cord-derived mesenchymal stem cells conditioned media.

24.40 (10.77) to 18.59 (7.70) in MN side. Furthermore, there was a significantly better effect after treatment in hUC-MSCs-CM side, compared to MN alone side ($P = 0.00$; **Figures 2**, **4B**), indicating that hUC-MSCs-CM can shrink the size of pores.

Elasticity

Compared to baseline, skin elasticity significantly improved in both groups ($P = 0.00$). At 2 weeks after the last treatment, there was a significantly higher increase in MN plus hUC-MSCs-CM group, compared to MN alone group ($P = 0.00$). Furthermore, the measurements of elasticity for MN alone group increased from 0.57 (0.06) to 0.65 (0.07), while the measurements for the other side increased from 0.56 (0.07) to 0.69 (0.05) (**Figure 4C**).

Side Effects

No severe side effects were reported during the whole study period. Two participants in MN plus hUC-MSCs-CM group reported dry skin and one reported erythema. Three patients

TABLE 4 | Objective assessment at baseline.

	MN alone	MN plus hUC-MSCs-CM	*P*-value
Skin physiological parameters			
Hydration	62.72 (7.96)	60.66 (7.96)	0.074
TEWL	20.88 (6.55)	20.31 (6.28)	0.130
Skin brightness			
Melanin Index	190.65 (40.12)	196.12 (40.91)	0.076
Ultraviolet Spots	23.08 (7.58)	24.39 (7.11)	0.067
Brown Spots	39.71 (5.82)	40.21 (5.14)	0.256
Erythema Index	336.68 (60.80)	336.69 (63.08)	0.999
Red Spots	29.17 (5.93)	29.30 (5.58)	0.754
Skin rejuvenation			
Wrinkles	18.18 (13.38)	17.21 (13.24)	0.227
Pores	24.40 (10.77)	23.55 (10.52)	0.295
Elasticity	0.57 (0.06)	0.56 (0.07)	0.067

MN: Microneedling; hUC-MSCs-CM: human umbilical cord-derived mesenchymal stem cells conditioned media; TEWL: Trans-epidermal water loss.

reported dry skin and two patients reported erythema in MN alone group, respectively.

DISCUSSION

A total of 28 volunteers with a mean (SD) age of 41 (6.54) years old completed the trial. The investigator's assessment of skin brightness and rejuvenation, and the self-satisfaction score revealed statistically better effects in MN plus hUC-MSCs-CM group, compared to MN alone group. No severe side effects were reported during the whole study period. The objective assessments revealed significantly more improvement in skin brightness (reduced MI, ultraviolet spots, and brown spots) and skin rejuvenation (reduced wrinkles and pores, and increased skin elasticity) in MN plus hUC-MSCs-CM group, compared to MN alone group, while there were no obvious differences in skin hydration, *trans*-epidermal water loss, and erythema index.

Microneedling stimulate the dermis, which increases new collagen and elastin, thereby rejuvenating the skin, improving wrinkles and increasing skin elasticity (9). Robati RM et al. compared MN to fractional Er:YAG laser in facial skin rejuvenation, and found a comparable efficacy. However, the slight "downtime" of MN makes it preferable for many patients (10). At present, MN is widely applied for various skin diseases, particularly in the skin-of-color population (i.e., Fitzpatrick skin types IV-VI) (11). Compared to laser treatments, MN is simple and inexpensive. Furthermore, the skin barrier disruption caused by MN resolves within 72 h (12). In the present study, the skin barrier signs, including skin hydration and TEWL, had no significant difference before and after treatment, in both MN plus hUC-MSCs-CM group and MN alone group. This finding indicates the safety of MN therapy.

The combination of MN with topical agents has successfully been used in the facial rejuvenation of aged skin (13). Most

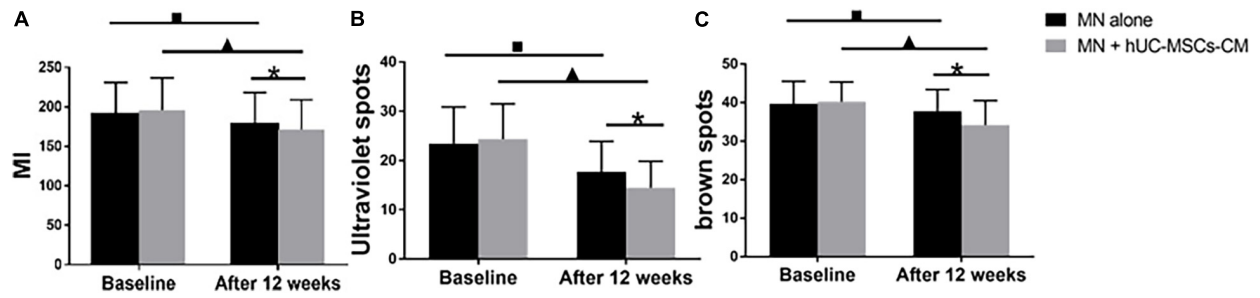

FIGURE 3 | Objective non-invasive skin pigmentation measurements. **(A)** Melanin index (MI); **(B)** Ultraviolet spots; **(C)** Brown spots. MN: microneedling; hUC-MSCs-CM: human umbilical cord-derived mesenchymal stem cells conditioned media. *$P < 0.05$, post-treatment comparison between MN alone and MN plus hUC-MSCs-CM; ▲$P < 0.05$, pre-treatment and post-treatment in MN plus hUC-MSCs-CM. ■$P < 0.05$, pre-treatment and post-treatment in MN alone.

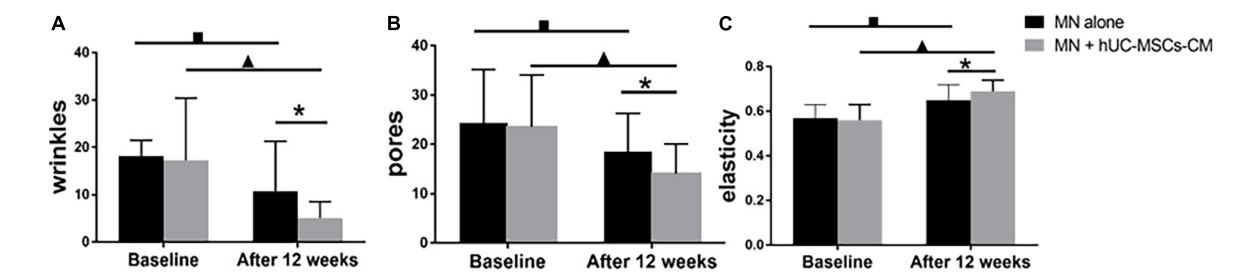

FIGURE 4 | Objective non-invasive skin texture measurements: **(A)** wrinkles; **(B)** pores; **(C)** elasticity. MN: microneedling; hUC-MSCs-CM: human umbilical cord-derived mesenchymal stem cells conditioned media. *$P < 0.05$, post-treatment comparison between MN alone and MN plus hUC-MSCs-CM; ▲$P < 0.05$, pre-treatment and post-treatment in MN plus hUC-MSCs-CM; ■$P < 0.05$, pre-treatment and post-treatment in MN alone.

recently, stem cell extracellular vesicles or cell therapies, such as adipose-derived stem cells, MSCs and BMMSCs, have been used for skin rejuvenation due to the ability to repair and regenerate tissues and organs in cosmetic and reconstructive surgeries (14, 15). The long-term safety and controllability of cell-based therapies remain controversial, making cell-derived extracellular vesicles (exosomes or conditioned medium) preferable for most therapeutic applications. The effect of conditioned media from BMMSC- or adipose-derived stem cells on skin rejuvenation has been demonstrated (16, 17). In the present study, the participant's satisfaction score and physician's global assessments score for facial rejuvenation were higher in MN plus hUC-MSCs-CM group, compared to MN alone group. These present results support another study, which reported that amniotic membrane stem cell-conditioned medium can rejuvenate the skin (24).

Skin brightness and texture are more correlated to skin rejuvenation. The less pigmented the skin is, the brighter it becomes. Objective pigmentation parameters, including the MI, ultraviolet spots, and brown spots, were explored in the present study. Compared to MN alone group, all three pigmentation parameters significantly decreased in combination group at 2 weeks after the final treatment. Compared to baseline, MN alone side presented with a significant decrease in MI. However, in a Korean study, the MI merely significantly decreased in subjects treated with MN combined with secretory factors of endothelial precursor cells derived from human embryonic stem cells (19). This difference may be attributed to the different length of microneedling (0.25 mm in the Korean study vs. 0.5 mm in this study). A previous study revealed that the single-session MN-treatment for melasma with a needle length of 0.5 mm resulted in significantly reduced melanin density, pendulous melanocytes, and a pathological basement membrane (20).

Except for pigmentation, the skin textures, such as wrinkles, pores and elasticity, tested by VISIA® skin analysis were also explored in the present study. Compared to baseline, wrinkles, pores, and elasticity improved in MN plus hUC-MSCs-CM group and MN alone, and the effect of the combined group was significantly better than that of MN alone group. These results can be attributed to the various growth factors of hUC-MSCs-CM, such as EGF, VEGF, PDGF-BB. For example, EGF stimulates epidermal cell proliferation (21). VEGF facilitates skin angiogenesis and increases blood vessel permeability to improve tissue nutrition. PDGF-BB is involved in fibroblast proliferation and regulates cell growth (22). According to the present findings, the changes in the skin micro-environment may lead to the greater improvement in wrinkles, pores and elasticity in combination group, compared to MN alone. A recent study concluded that the remodeling of dermal structures in skin biopsy pathology can be observed mainly on the combined side (23). Furthermore, the histometry of the epidermis revealed a significant increase in epidermal thickness on both the skin-needled and combined side (i.e., skin needling plus amniotic fluid mesenchymal stem cell derived conditioned media). This is consistent with the present results, in which the improvement in skin rejuvenation was greater in the combined side, compared to MN alone side.

In the present study, merely minor treatment-related side effects were observed. Two patients reported dry skin and one patient reported erythema in MN plus hUC-MSCs-CM group, while three patients reported dry skin and two patients reported erythema in MN alone group the dry skin was likely due to a temporary breakdown in skin barrier function caused by microneedling.

The small sample size and lack of pathological assessment were the main limitations of this study, despite the fact that great improvement was observed in the images taken by VISIA® test. However, the split—face study design presented the reliable comparison between the two groups with such a relatively small number of volunteers. In the future, a larger sample size will be considered and more objective evaluations will be applied. The repeatability and stability of hUC-MSCs-CM are always the focus when performing the project.

Up to now, only two randomized controlled trials and one control trial was published in the application of MN with and without MSCs-CM or extracts from media of MSCs in facial rejuvenation (**Table 5**), and these studies provide strong evidence for the effective treatment of facial aging by this method. The data from the three articles supported that combination therapy with MN *via* MSCs derivative improve significantly than MN alone.

In conclusion, MN combined with hUC-MSCs-CM is a safe and effective treatment modality for facial rejuvenation, and may potentially be used as a novel method for anti-aging.

TABLE 5 | Facial rejuvenation studies with MN plus with MSCs.

Reference	Sample size	Methods	Results
Wang et al. (24)	30 patients	One side: the protein extracts from medium of ADSCs + MN, the other side: ultrapure water + MN. once every 2 weeks, 6 times	Compared to ultrapure water + MN, the melanin index, skin brightness, gloss, skin roughness, elasticity and wrinkles improved significantly in the protein extracts from medium of ADSCs + MN at the 12th week
Prakoeswa et al. (18)	48 females	24 women: AMSC-CM + MN the other 24 women: NS + MN once every 2 weeks, 3 times	Compared to NS + MN group, mean change of wrinkles, pores, spot-polarized and spot-ultraviolet parameters improved significantly at 8 weeks in AMSC-CM + MN group. At weeks 8, there was no improvement in skin tone
El-Domyati et al. (23)	10 patients	Right side: MN + AF-MSC-CM, left side: MN once every 2 weeks, 5 times;	collagen fibers and elastic fibers remodeling was observed mainly on the right side at 1 month after the final treatment The epidermal thickness on both sides increased similarly

MN: microneedling; MSCs: mesenchymal stem cells; ADSCs: adipose-derived stem cells; AMSC-CM: amniotic membrane stem cell-conditioned media; NS: normal saline; AF-MSC-CM: amniotic fluid mesenchymal stem cell derived conditioned media.

DATA AVAILABILITY STATEMENT

The raw data supporting the conclusions of this article will be made available by the authors, without undue reservation.

ETHICS STATEMENT

The studies involving human participants were reviewed and approved by the Medical Ethics Committee of Beijing Friendship Hospital affiliated to Capital Medical University. The patients/participants provided their written informed consent to participate in this study. Written informed consent was obtained from the individual(s) for the publication of any potentially identifiable images or data included in this article.

AUTHOR CONTRIBUTIONS

All authors listed have made a substantial, direct, and intellectual contribution to the work, and approved it for publication.

FUNDING

This work was supported by Beijing Natural Science Foundation (No. 7222040).

REFERENCES

1. Boisma F, Serror K, Dobos G, Zuelgaray E, Bensussan A, Michel L. Skin aging: pathophysiology and innovative therapies. *Med Sci (Paris).* (2020) 36:1163–72. doi: 10.1051/medsci/2020232
2. Jo H, Brito S, Kwak BM, Park S, Lee MG, Bin BH. Applications of mesenchymal stem cells in skin regeneration and rejuvenation. *Int J Mol Sci.* (2021) 22:2410. doi: 10.3390/ijms22052410
3. Wang JV, Schoenberg E, Zaya R, Rohrer T, Zachary CB, Saedi N. The rise of stem cells in skin rejuvenation: a new frontier. *Clin Dermatol.* (2020) 38:494–6. doi: 10.1016/j.clindermatol.2020.04.003
4. Yang S, Huang S, Feng C, Fu X. Umbilical cord-derived mesenchymal stem cells: strategies, challenges, and potential for cutaneous regeneration. *Front Med.* (2012) 6:41–7. doi: 10.1007/s11684-012-0175-9
5. Yang D, Chen M, Sun Y, Jin Y, Lu C, Pan X, et al. Microneedle-mediated transdermal drug delivery for treating diverse skin diseases. *Acta Biomater.* (2021) 121:119–33. doi: 10.1016/j.actbio.2020.12.004
6. Soliman YS, Horowitz R, Hashim PW, Nia JK, Farberg AS, Goldenberg G. Update on acne scar treatment. *Cutis.* (2018) 102:21, 25, 47–8.
7. Choy YB, Prausnitz MR. The rule of five for non-oral routes of drug delivery: ophthalmic, inhalation and transdermal. *Pharm Res.* (2011) 28:943–8. doi: 10.1007/s11095-010-0292-6
8. Gupta J, Gill HS, Andrews SN, Prausnitz MR. Kinetics of skin resealing after insertion of microneedles in human subjects. *J Control Release.* (2011) 154:148–55. doi: 10.1016/j.jconrel.2011.05.021
9. Alessa D, Bloom JD. Microneedling options for skin rejuvenation, including non-temperature-controlled fractional microneedle radiofrequency treatments. *Facial Plast Surg Clin North Am.* (2020) 28:1–7. doi: 10.1016/j.fsc.2019.09.001
10. Robati RM, Hamedani B, Namazi N, Niknejad N, Gheisari M. Efficacy of microneedling versus fractional Er: YAG laser in facial rejuvenation. *J Cosmet Dermatol.* (2020) 19:1333–40. doi: 10.1111/jocd.13440
11. Cohen BE, Elbuluk N. Microneedling in skin of color: a review of uses and efficacy. *J Am Acad Dermatol.* (2016) 74:348–55. doi: 10.1016/j.jaad.2015.09.024
12. Han TY, Park KY, Ahn JY, Kim SW, Jung HJ, Kim BJ. Facial skin barrier function recovery after microneedle transdermal delivery treatment. *Dermatol Surg.* (2012) 38:1816–22. doi: 10.1111/j.1524-4725.2012.02550.x
13. Kim JH, Park HY, Jung M, Choi EH. Automicroneedle therapy system combined with topical tretinoin shows better regenerative effects compared with each individual treatment. *Clin Exp Dermatol.* (2013) 38:57–65. doi: 10.1111/j.1365-2230.2012.04405.x
14. Zarei F, Abbaszadeh A. Application of cell therapy for anti-aging facial skin. *Curr Stem Cell Res Ther.* (2019) 14:244–8. doi: 10.2174/1574888X13666181113113415
15. Suh A, Pham A, Cress MJ, Pincelli T, TerKonda SP, Bruce AJ, et al. Adipose-derived cellular and cell-derived regenerative therapies in dermatology and aesthetic rejuvenation. *Ageing Res Rev.* (2019) 54:100933. doi: 10.1016/j.arr.2019.100933
16. Kim SN, Lee CJ, Nam JH, Choi B, Chung E, Song SU. The effects of human bone marrow-derived mesenchymal stem cell conditioned media produced with fetal bovine serum or human platelet lysate on skin rejuvenation characteristics. *Int J Stem Cells.* (2021) 14:94–102. doi: 10.15283/ijsc20070
17. Li L, Ngo HTT, Hwang E, Wei X, Liu Y, Liu J, et al. Conditioned medium from human adipose-derived mesenchymal stem cell culture prevents UVB-induced skin aging in human keratinocytes and dermal fibroblasts. *Int J Mol Sci.* (2019) 21:49. doi: 10.3390/ijms21010049
18. Prakoeswa CRS, Pratiwi FD, Herwanto N, Citrashanty I, Indramaya DM, Murtiastutik D, et al. The effects of amniotic membrane stem cellconditioned medium on photoagi. *J Dermatolog Treat.* (2019) 30:478–82. doi: 10.1080/09546634.2018.1530438
19. Lee HJ, Lee EG, Kang S, Sung JH, Chung HM, Kim DH. Efficacy of microneedling plus human stem cell conditioned medium for skin rejuvenation: a randomized, controlled, blinded split-face study. *Ann Dermatol.* (2014) 26:584–91. doi: 10.5021/ad.2014.26.5.584
20. Cassiano DP, Espósito ACC, Hassun KM, Lima EVA, Bagatin E, Miot HA. Early clinical and histological changes induced by microneedling in facial melasma: a pilot study. *Indian J Dermatol Venereol Leprol.* (2019) 85:638–41. doi: 10.4103/ijdvl.IJDVL_44_19
21. Zhang XL, Zhang LT. Clinical study on the efficiency of rhEGFgel to skin function of facial hormone-dependent dermatitis. *Tian Jin Med J.* (2016) 44:629–31. doi: 10.11958/20150434
22. Fabi S, Sundaram H. The potential of topical and injectable growth factors and cytokines for skin rejuvenation. *Facial Plast Surg.* (2014) 30:157–71. doi: 10.1055/s-0034-1372423
23. El-Domyati M, Mofta NH, Nasif GA, Ameen SW, Ibrahim MR, Ragaie MH. Facial rejuvenation using stem cell conditioned media combined with skin needling: a split-face comparative study. *J Cosmet Dermatol.* (2020) 19:2404–10. doi: 10.1111/jocd.13594
24. Wang X, Shu X, Huo W, Zou L, Li L. Efficacy of protein extracts from medium of adipose-derived stem cells via microneedles on Asian skin. *J Cosmet Laser Ther.* (2018) 20:237–44. doi: 10.1080/14764172.2017.1400171

Conflict of Interest: The authors declare that the research was conducted in the absence of any commercial or financial relationships that could be construed as a potential conflict of interest.

Publisher's Note: All claims expressed in this article are solely those of the authors and do not necessarily represent those of their affiliated organizations, or those of the publisher, the editors and the reviewers. Any product that may be evaluated in this article, or claim that may be made by its manufacturer, is not guaranteed or endorsed by the publisher.

frontiers | Frontiers in Medicine

CASE REPORT
published: 25 May 2022
doi: 10.3389/fmed.2022.847382

Case Report: A Missense Mutation of *KIT* in Hyperpigmentation and Lentigines Unassociated With Systemic Disorders: Report of a Chinese Pedigree and a Literature Review

Lu Yang, Yuehua Liu and Tao Wang**

State Key Laboratory of Complex Severe and Rare Diseases, Department of Dermatology, Peking Union Medical College Hospital, Chinese Academy of Medical Sciences and Peking Union Medical College, National Clinical Research Center for Dermatologic and Immunologic Diseases, Beijing, China

OPEN ACCESS

Edited by:
Bing Song,
Cardiff University, United Kingdom

Reviewed by:
Seray Külcü Çakmak,
University of Health Sciences, Turkey
Philippe Lefrançois,
McGill University, Canada

***Correspondence:**
Yuehua Liu
yuehualiu63@163.com
Tao Wang
wangtaopumch@126.com

Specialty section:
This article was submitted to Dermatology, a section of the journal Frontiers in Medicine

Received: *02 January 2022*
Accepted: *26 April 2022*
Published: *25 May 2022*

Citation:
Yang L, Liu Y and Wang T (2022) Case Report: A Missense Mutation of KIT in Hyperpigmentation and Lentigines Unassociated With Systemic Disorders: Report of a Chinese Pedigree and a Literature Review. Front. Med. 9:847382. doi: 10.3389/fmed.2022.847382

Background: *KIT* is a proto-oncogene that is involved in the proliferation, survival, and regulation of melanocytes, mast cells, and the interstitial cells of Cajal. Mutations of *KIT* have been reported to be associated with hyperpigmentation and lentigines, mastocytosis, and gastrointestinal stromal tumors (GISTs). Some hotspot mutations of *KIT* have been reported to be associated with mastocytosis and GISTs, while the relationship between *KIT* mutations and hyperpigmentation and lentigines has not been fully elucidated.

Methods: In this study, we presented a three-generation Chinese pedigree with progressive hyperpigmentation and generalized lentigines inherited in an autosomal dominant pattern. High-throughput sequencing was performed to capture genetic variations in peripheral blood samples of the proband. Also, Sanger sequencing was performed to further verify the result. We also reviewed previous literature on *KIT* mutations with hyperpigmentation and lentigines.

Results: A missense mutation of the *KIT* gene was identified: c. 2485G > C, which was co-segregated in the proband and his insulted father. Germline *KIT* mutations presenting as generalized hyperpigmentation and lentigines without systemic disorders are rare, with only two reports of c. 2485G > C mutation associated with this phenotype in previous literature.

Conclusion: Our pedigree, together with those two reports, indicates a possible phenotype-genotype correlation of this germline *KIT* mutation, which might be helpful for genetic counseling, further functional segregation of KIT, and design of targeted therapy in the future.

Keywords: KIT, hyperpigmentation, generalized lentigines, missense mutation, hotspot

INTRODUCTION

Lentigines are usually a benign proliferation of epidermal melanocytes, which are commonly seen in sun-exposed areas. However, numerous or generalized lentigines might be an indicator of systemic disorders, including Peutz-Jeghers syndrome, Carney complex, LEOPARD syndrome, Dowling-Degos disease, *PTEN* hamartoma tumor syndrome, and familial progressive hyperpigmentation with or without hypopigmentation (1).

KIT (OMIM:164920) is a proto-oncogene, which encodes a type III receptor tyrosine kinase for stem cell factors. It plays an important role in the development and regulation of melanocytes, mast cells, germ cells, the interstitial cells of Cajal, and hematopoietic progenitor cells (2, 3). *KIT* mutations are reported to be associated with a variety of cutaneous disorders, including piebaldism, mastocytosis, hyperpigmentation, and lentigines (1, 4–8). They are also involved in malignancies including testicular germ cell tumor, acute myelogenous leukemia, gastrointestinal stromal tumor (GIST), and melanomas (2, 6, 9). Some hotspots of somatic and germline mutations of *KIT* have been found in GIST and mastocytosis, but not in hyperpigmentation and lentigines (2).

There are two reports of a missense mutation at the kinase activation loop of *KIT* (c. 2485G > C) that is associated with hyperpigmentation and lentigines without GIST or mastocytosis (1, 5). In this study, we reported a Chinese pedigree with progressive hyperpigmentation and generalized lentigines in which the same missense mutation of *KIT* was confirmed. We also reviewed the literature and discussed a possible phenotype-genotype correlation in this entity.

MATERIALS AND METHODS

Pedigree and Subjects

We studied a three-generation Chinese pedigree presented as hyperpigmentation and generalized lentigines. Peripheral blood specimens were collected for genetic analysis. Written informed consent was obtained from this patient and his parents for skin biopsy, mutation screening, and publication of their images or data included in this article. The study was approved by the Institutional Review Board.

Mutation Screening and Sequencing

The DNA library was constructed by hybridization capture from the genomic DNA extracted from the peripheral blood samples after fragmentation, splicing, amplification, and purification, and was detected by a high-throughput sequencing platform (mean sequencing depth, 130.19 ×). The original sequencing data were compared with the UCSC hg19 human reference genome sequence and further filtered out with synonymous variants or small non-frame shift InDel variants in repeat regions. The remaining data were analyzed according to the inheritance patterns and clinical phenotypes. Candidate

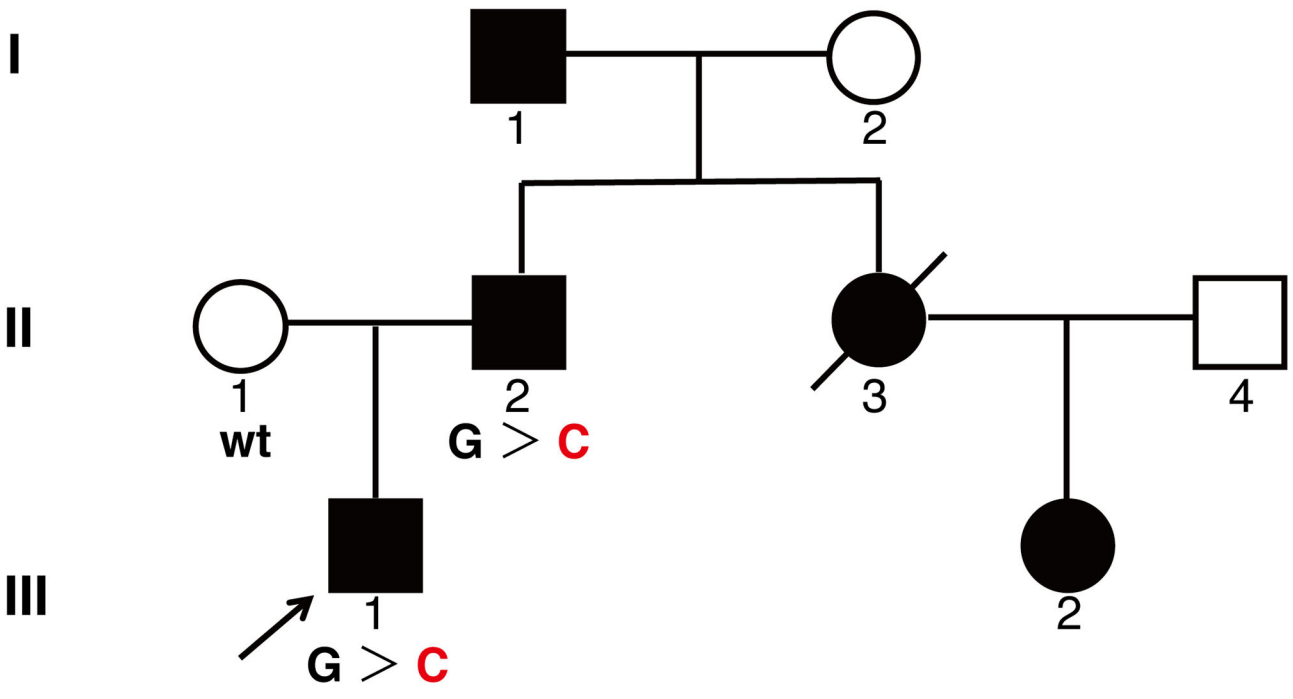

FIGURE 1 | A pedigree showing phenotypes of the family. Three family members were genotyped for *KIT* mutation. Affected men and women are indicated by filled squares and circles, respectively. A crossed symbol indicated a deceased individual due to urenia. An arrow head indicates the proband. wt, wild type; G > C, heterozygote of c.2485G > C.

variations were further verified by Sanger sequencing. The pathogenicity of genetic variation was classified according to ACMG guidelines (10).

RESULTS

A 26-year-old man came to our department complaining of progressive hyperpigmentation and generalized lentigines over his body for 18 years. The patient had a family history that his father, grandfather, aunt, and cousin had similar symptoms (**Figure 1**). He was otherwise healthy without abdominal pain or mass, dysphagia, and weight loss. The patient and his father underwent annual physical examination without abnormal routine blood and urine test, liver, and renal function test, and abdominal CT scans. His grandfather lived a healthy longevous life without any obvious systemic disorders. Physical examination revealed hyperpigmentation with a dark brown spot

FIGURE 2 | Clinical presentation of the proband showing hyperpigmentation and multiple lentigines on face, neck, back, and inguinal areas.

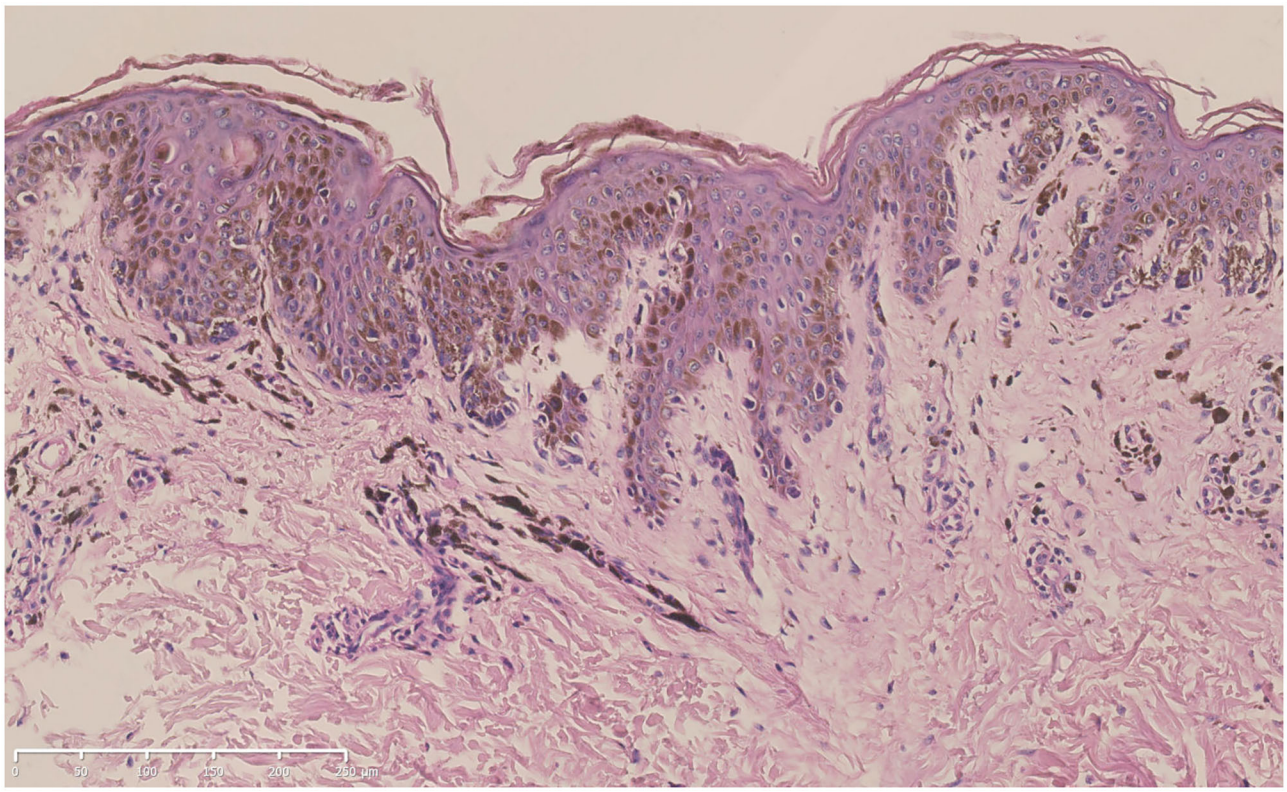

FIGURE 3 | Hematoxylin-eosin staining of the biopsy specimen from the proband (bar = 250 μm). Increased melanin production from the basal layer to the spinous layer of the epidermis, lentiginous hyperplasia of melanocytes along the basal layer, and melanophages in the superficial dermis could be seen.

and lentiginous-like lesions on his face, neck, vermillion of the lip, inguinal region, natal cleft, hands, and feet (**Figure 2**). Similar lesions were scattered on his trunk and extremities. The oral cavity was not involved. There was no tenderness or palpable mass of the abdomen.

A skin biopsy was taken from one of the lentigines after obtaining written informed consent. Histologic examination revealed increased melanin production from the basal layer to the spinous layer of the epidermis. Lentiginous hyperplasia of melanocytes along the basal layer and melanophages in the superficial dermis could be observed (**Figure 3**).

An inherited disorder was highly suspected. After obtaining informed consent, peripheral blood samples were obtained for further genetic analysis. High-throughput sequencing revealed c. 2485G > C mutation of *KIT* in the proband (III:1), which was a likely pathogenic mutation according to the ACMG standards and guidelines (10). Sanger sequencing was performed and verified the heterozygous c. 2485G > C mutation both in the proband (III:1) and his insulted father (II:2), while his mother did not carry the mutation.

DISCUSSION

KIT, located on human chromosome 4q12, encodes a type III receptor tyrosine kinase composed of an extracellular ligand-binding domain, a transmembrane domain, a juxta-membrane domain, and an intracellular kinase domain. Stimulation by stem cell factor leads to its dimerization, followed by activation of its intrinsic kinase activity and phosphorylation of specific tyrosine residues in the intracellular domain. These residues could act as a docking site to recruit downstream signaling molecules (2, 3). Although KIT is involved in lineage commitment and regulation of interstitial cells of Cajal, mast cells, and melanocytes, different *KIT* mutations may not induce the simultaneous deregulation of all three types of cells. Somatic D816V mutation of *KIT* in exon 17 is the most common mutation in mastocytosis, while genetic variations in exons 9 and 11 are most commonly seen in GISTs. These hotspot sites suggest a possible phenotype-genotype correlation in *KIT*, although the underlying mechanism is not clarified (2).

In contrast to mutations in mastocytosis and GISTs, mutations of *KIT* in melanomas have been found throughout the coding regions, with increased frequency in the juxta-membrane domain and tyrosine kinase domains (3). Somatic *KIT* mutations have been reported in both primary and metastatic melanomas, especially in triple-negative melanomas lacking *BRAF, NRAS, or NF* mutations, accounting for 6–20% of melanomas arising on mucosal, acral, and chronically sun-damaged sites (3, 9, 11)/ In a recent large retrospective study of a Chinese patient with melanoma, the frequency of *KIT* mutation was 9.4%, which was comparable with that of the Caucasian population. While a more enriched mutation hotspot region was observed in the

cohort, with *KIT* mutations most frequently found in exon 11 (72.3%) (12). However, the study was based in a single center. A large population-based study is needed to further draw the mutation landscape of *KIT* in the future. Until now, there have been 36 *KIT* mutations reported to be associated with melanomas. However, the oncogenicity of these mutations is not fully elucidated, with only 18 of them predicated to be oncogenic or likely oncogenic based on an *in vitro* experiment and some prediction modalities, probably acting through the regulation in MAPK/MEK, PI3K/AKT, and JAK/STAT pathways (3, 11).

Apart from somatic mutations of *KIT* in melanomas, germline *KIT* mutations are reported to be associated with other pigmented disorders, often accompanied by GIST or mastocytosis (1, 2, 4–7). However, two independent groups have recently revealed a new missense mutation of *KIT* in patients with hyperpigmentation and lentigines without systemic disorders. T. Takeichi et al. reported the c. 2485G > C mutation in exon 17 of *KIT* in a Japanese pedigree that manifested as progressive hyperpigmentation and lentigines unassociated with any other familiar systemic disease (5). Almost at the same time, Alain K. et al. revealed the same mutation in a 6-year-old girl who presented with atypical lentiginosis and hyperpigmentation without systemic disorders (1).

In this report, we examined a Chinese pedigree presented with progressive hyperpigmentation and generalized lentigines, carrying the same germline mutation of *KIT*, suggesting its role in the regulation of the proliferation and melanin production of melanocytes. This missense mutation would lead to an amino acid substitution from alanine to proline at position 829 (A829P) on the kinase activation loop of KIT, generating a unique sequence "Pro-Arg-Leu-Pro," which was postulated to serve as an Src homology 3 (SH3) domain-binding motif and activate the MAPK signaling cascade (2, 5). It has been reported that a secondary somatic A829P mutation of *KIT* was associated with acquired drug resistance during long-term treatment with imatinib mesylate in GISTs (13, 14). Similarly, *in vitro* study has shown that a secondary A829P mutation of *KIT* in the melanoma cell line would lead to the acquired resistance of both imatinib mesylate and sunitinib, while remaining responsive to dasatinib and nilotinib, with unknown mechanisms (9). These findings indicated that the A829P mutation of *KIT* might disturb the interaction interface of specific drugs with the kinase. Clinicians should keep in mind such differences when considering receptor tyrosine kinase inhibitors as a treatment option for patients with hyperpigmentation and lentigines carrying A829P mutation of *KIT*.

It is worth noting that, until now, all the reports of primary germline c. 2485G > C mutation of *KIT*, including our pedigree, have been presented as hyperpigmentation and lentigines without prominent systemic disorders. This indicates a possible phenotype and genotype correlation of this missense mutation, which would be an ideal model to study the proliferation, survival, and melanogenesis of melanocytes. However, considering the association of somatic A829P mutation of *KIT* with tumors, including GISTs and melanomas reported in previous literature, a close follow-up of the patients should be carried out for surveillance of possible atypical hyperplasia, melanomas, or other types of tumors in the future.

DATA AVAILABILITY STATEMENT

The datasets presented in this study can be found in online repositories. The names of the repository/repositories and accession number(s) can be found below: GenBank, Accession Number: OM304357.

ETHICS STATEMENT

Written informed consent was obtained from the patients for the publication of potentially identifiable data and images.

AUTHOR CONTRIBUTIONS

YL and TW contributed to conception and design of the study. TW collected clinical and histologic data. YL organised the data, constructed the figures, and wrote the first draft of the manuscript. All authors contributed to manuscript revision, read, and approved the submitted version.

REFERENCES

1. Tran AK, Pearce A, Lopez-Sanchez M, Perez-Jurado LA, Barnett C. Novel KIT mutation presenting as marked lentiginosis. *Pediatr Dermatol.* (2019) 36:922–5. doi: 10.1111/pde.13952
2. Ke H, Kazi JU, Zhao H, Sun J. Germline mutations of KIT in gastrointestinal stromal tumor (GIST) and mastocytosis. *Cell Biosci.* (2016) 6:55. doi: 10.1186/s13578-016-0120-8
3. Meng D, Carvajal RD. KIT as an Oncogenic driver in melanoma: an update on clinical development. *Am J Clin Dermatol.* (2019) 20:315–23. doi: 10.1007/s40257-018-0414-1
4. Shibusawa Y, Tamura A, Mochiki E, Kamisaka K, Kimura H, Ishikawa O. c-kit Mutation in generalized lentigines associated with gastrointestinal stromal tumor. *Dermatology.* (2004) 208:217–20. doi: 10.1159/000077302
5. Takeichi T, Sugiura K, Tanahashi K, Noda K, Kono M, Akiyama M. Autosomal dominant progressive hyperpigmentation and lentigines in a Japanese pedigree due to a missense mutation near the C-terminus of KIT. *Br J Dermatol.* (2018) 179:1210–1. doi: 10.1111/bjd.16895
6. Wali GN, Halliday D, Dua J, Ieremia E, McPherson T, Matin RN. Cutaneous hyperpigmentation and familial gastrointestinal stromal tumour associated with KIT mutation. *Clin Exp Dermatol.* (2019) 44:418–21. doi: 10.1111/ced.13757
7. Hasegawa M, Shimizu A, Ieta K, Shibusawa K, Ishikawa O, Ishida-Yamamoto A, et al. Generalized lentigines associated with familial gastrointestinal stromal tumors dramatically improved by imatinib treatment. *J Dermatol.* (2020) 47:e241–2. doi: 10.1111/1346-8138.15321
8. Jiang X, Lin Z, Wang H. Multiple lentigines and cutaneous hyperpigmentation caused by a KIT mutation. *Br J Dermatol.* (2020) 183:e148. doi: 10.1111/bjd.19295
9. Todd JR, Becker TM, Kefford RF, Rizos H. Secondary c-Kit mutations confer acquired resistance to RTK inhibitors in c-Kit mutant melanoma cells. *Pigment Cell Melanoma Res.* (2013) 26:518–26. doi: 10.1111/pcmr.12107

10. Richards S, Aziz N, Bale S, Bick D, Das S, Gastier-Foster J, et al. Standards and guidelines for the interpretation of sequence variants: a joint consensus recommendation of the American college of medical genetics and genomics and the association for molecular pathology. *Genet Med.* (2015) 17:405–24. doi: 10.1038/gim.2015.30
11. Delyon J, Lebbe C, Dumaz N. Targeted therapies in melanoma beyond BRAF: targeting NRAS-mutated and KIT-mutated melanoma. *Curr Opin Oncol.* (2020) 32:79–84. doi: 10.1097/CCO.0000000000000606
12. Ren M, Zhang J, Kong Y, Bai Q, Qi P, Zhang L, et al. BRAF, C-KIT, and NRAS mutations correlated with different clinicopathological features: an analysis of 691 melanoma patients from a single center. *Ann Transl Med.* (2022) 10:31. doi: 10.21037/atm-21-4235
13. Zhao J, Quan H, Xu Y, Kong X, Jin L, Lou L. Flumatinib, a selective inhibitor of BCR-ABL/PDGFR/KIT, effectively overcomes drug resistance of certain KIT mutants. *Cancer Sci.* (2014) 105:117–25. doi: 10.1111/cas.12320
14. Carvajal RD, Antonescu CR, Wolchok JD, Chapman PB, Roman RA, Teitcher J, et al. KIT as a therapeutic target in metastatic melanoma. *JAMA.* (2011) 305:2327–34. doi: 10.1001/jama.2011.746

Conflict of Interest: The authors declare that the research was conducted in the absence of any commercial or financial relationships that could be construed as a potential conflict of interest.

frontiers | Frontiers in Medicine

ORIGINAL RESEARCH
published: 27 May 2022
doi: 10.3389/fmed.2022.818543

The Efficacy and Psychoneuroimmunology Mechanism of Camouflage Combined With Psychotherapy in Vitiligo Treatment

Yuqian Chang†, Shaolong Zhang†, Weigang Zhang, Shuli Li and Chunying Li**

Department of Dermatology, Xijing Hospital, Fourth Military Medical University, Xi'an, China

Background and Objectives: The efficacy of camouflage combined with psychotherapy and the underlying mechanisms are poorly understood in vitiligo management. This study aimed to investigate the joint efficacy and further explore psycho-neuro-endocrine-immune-skin interactions.

Patients and Methods: In a prospective, non-randomized and concurrent controlled trial, patients were divided into two groups. Quality of life (QOL) was evaluated using the Chinese version of the Vitiligo Life Quality Index (VLQI-C). Serum levels of neuropeptides and cytokines were detected by enzyme-linked immunosorbent assay.

Results: A total of 149 patients were included for final evaluation. After treatment for 4 weeks, total and subcategory quality of life scores in the intervention group were much lower than in the control group. Serum levels of neuropeptide-Y (NPY) and melanin-concentrating hormone (MCH) significantly decreased, and serum level of adrenocorticotropic hormone (ACTH) increased in both active and stable patients of the intervention group, but not in the control group. In addition, the serum levels of interferon-γ (IFN-γ), CXC chemokine ligand 10 (CXCL10), and interleukin-1β (IL-1β) decreased in both the active and stable patients of the intervention group and only in the active patients of the control group.

Conclusions: The combination of camouflage and psychotherapy provided a clinically meaningful improvement in quality of life and ameliorated the outcome by likely modulating the psycho-neuro-endocrine-immuno-skin system during vitiligo management.

Clinical Trial Registration: www.clinicaltrials.gov/ct2/show/NCT03540966, identifier: NCT03540966.

Keywords: vitiligo, camouflage, psychotherapy, quality of life, psychoneuroimmunology

OPEN ACCESS

Edited by:
Xing-Hua Gao,
The First Affiliated Hospital of China Medical University, China

Reviewed by:
Manuel Valdebran Canales,
Medical University of South Carolina, United States
Tiechi Lei,
Renmin Hospital of Wuhan University, China

****Correspondence:***
Chunying Li
lichying@fmmu.edu.cn
Shuli Li
lishli@fmmu.edu.cn

† These authors have contributed equally to this work

Specialty section:
This article was submitted to Dermatology, a section of the journal Frontiers in Medicine

Received: *19 November 2021*
Accepted: *06 April 2022*
Published: *27 May 2022*

Citation:
Chang Y, Zhang S, Zhang W, Li S and Li C (2022) The Efficacy and Psychoneuroimmunology Mechanism of Camouflage Combined With Psychotherapy in Vitiligo Treatment. Front. Med. 9:818543. doi: 10.3389/fmed.2022.818543

INTRODUCTION

Vitiligo is a common autoimmune depigmentation of the skin with a preference for exposed sites (faces, hands, and feet) resulting in cosmetically disfiguring, psychologically disturbing and subsequently significant impairment of quality of life (QOL), posing a potent therapeutic demand for the treatment (1, 2). The

melanocyte destruction in vitiligo is multifactorial, involving psychological, physical, and environmental stressors, immune dysfunction, abnormal metabolism, and genetic predisposition (1, 3). Notably, psychological stress is related to the onset, progression, relapse, and remission of vitiligo by altering the levels of catecholamines, neuropeptides, cortisol, and cytokines (4–7). Recently, an innovative study demonstrated that stress activates the release of norepinephrine from sympathetic nerves, which in turn causes melanocyte stem cells to shift into pigment-producing cells, prematurely eliminate the reservoir from hair follicles, and then induce hair graying (8). These findings prompt us to investigate the importance of maintaining a positive psychological state in the selection of management modalities.

Current vitiligo therapeutic approaches are dependent on regulating immune dysfunction with immunomodulators, reducing accumulative oxidative stress in lesions with antioxidants, and activating melanocyte regeneration by narrowband ultraviolet B irradiation (NB-UVB) or transplanting healthy melanocytes (9–11). However, rates of halting progression and regimentation of these conventional options are only approximately 50%–60%, and these options inevitably lead to the absence of compliance of patients in vitiligo practice (12, 13). Notably, a series of studies has demonstrated that both camouflage and psychotherapy can effectively alleviate the patients' burden by improving quality of life (14, 15), and camouflage application has been an essential part of vitiligo management in some countries (16–18). However, camouflage treatment has always been considered a dispensable cosmetic option for many patients in China based on our clinical observations because of lack of corresponding psychological construct and clear mechanism statement when patients are recommended to apply masking agents.

Considering the knowledge gap, we designed this prospective, non-randomized, concurrent controlled intervention trial to evaluate efficacy improvements of camouflage combined with psychotherapy, and to explore further the possible mechanism of psychoneuroimmunology regulation by measuring change in neuropeptide and cytokine levels.

PATIENTS AND METHODS

Study Design, Patients, and Clinical Samples

This study was designed as a prospective, non-randomized concurrent controlled trial that was reviewed and approved by the ethics review board of Xijing Hospital (approval code: KY20182005-1) and registered on ClinicalTrials.gov.cn (NCT03540966). A total of 238 patients with non-segmental vitiligo were recruited between May 2018 and December 2019 in Xijing Hospital. The key inclusion criteria were as follows: aged 18 to 60 years (read and filled out the questionnaire independently), diagnosed with vitiligo according to the consensus on the diagnosis and treatment of vitiligo in China (19), with vitiliginous patches on exposed sites (face, neck, hands, or feet where vitiligo can be recognized). The exclusion criteria were as follows: treatment with topical calcineurin inhibitors or topical corticosteroids within 2 weeks or immunosuppressive or immunomodulating medicines within 4 weeks, experienced any camouflage products to cover white patches or psychological support for vitiligo, diagnosed with psychiatric and psycho-related illnesses, concomitant with other autoimmune skin disorders such as atopic dermatitis, psoriasis, and alopecia areata, with QOL-threatening conditions such as cancer and chronic or autoimmune diseases, in hormonal imbalance contexts (women during pregnancy or menopause), or any other condition that the investigator deemed unsuitable for entering the study. The participants were assigned into two groups on a voluntary basis. Patients in the intervention group were treated with conventional medical treatments plus a camouflage and psychotherapy program, which was specifically designed for this trial, while patients in the control group received conventional medical treatment alone. All the patients were offered a follow-up at the dermatology clinic in Xijing Hospital 4 weeks later. For quantification of serum levels of neuropeptides and cytokines associated with vitiligo pathogenesis, 5-mL peripheral blood samples were collected from 10 patients in the active phase and from 20 patients in the stable phase of each group at both baseline and after 4 weeks of treatment. The patients were matched for age and gender. Protocols for human samples were performed according to the principles of the Declaration of Helsinki, and written informed consent was obtained from all the participants before initializing the treatment. The detailed trial design is shown in **Figure 1**, and the recruitment detail is shown in **Figure 2**.

Camouflage and Psychotherapy Program and Procedures

The camouflage and psychotherapy program for this study was developed based on a literature review and experience summary by vitiligo experts ($n = 7$) in our dermatology department. All details were reviewed by the dermatologists and then validated in 9 patients with vitiligo. The program includes 4 dimensions: (1) one-to-one cognitive behavioral therapy for one session per week, (2) vitiligo popular science education and camouflage information provided as video tutorial, (3) camouflage skills training, and (4) answering of questions about vitiligo and camouflage *via* WeChat (communication software) during treatment. Through a series of procedures, the patients obtained psychological support, knowledge on vitiligo, and instructions for Capulin^{TM} (a commercial camouflage agent in China that mainly contains dihydroxyacetone, and the repigmentation mechanism involves polymerizing amino acids (histidine and tryptophan) of proteins and peptides in the stratum corneum, forming a special brown appearance within 8 h, characterized by good color-matching, 3–7-day longevity, simple application, and being waterproof and sweat-resistant). It should be noted that patients should use Capulin^{TM} 2 h before performing other topical management strategies to prevent interference with their respective effects. The camouflage and psychotherapy program and Capulin^{TM} are freely provided to all the participants in the intervention group.

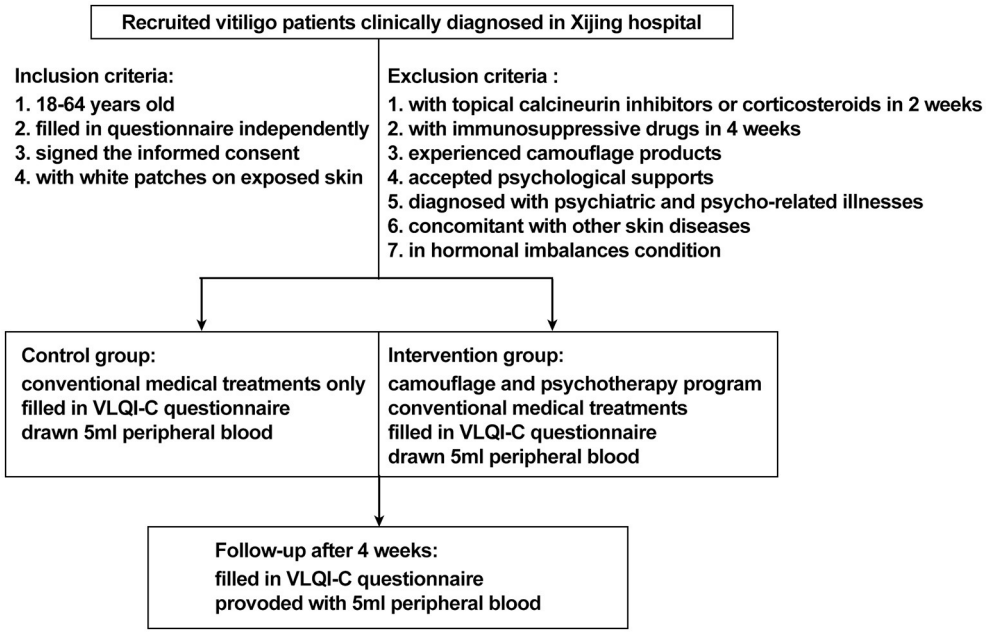

FIGURE 1 | Overview of trial design.

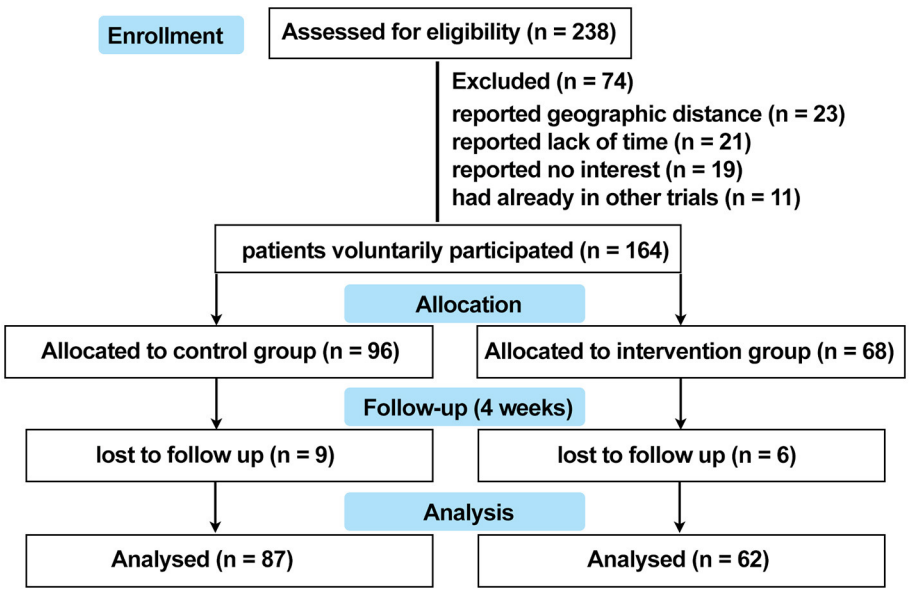

FIGURE 2 | Flow chart to show cohort recruitment.

Conventional Medical Treatment for Patients

The choice of treatment depends on how much skin is involved and where and how quickly the disease is progressing. Generally, mid-potency topical corticosteroids are applied to the affected skin twice daily, and topical calcineurin inhibitors tacrolimus and pimecrolimus are used in place of depigmented macules involving the face, genitals, or any areas at high risk of skin atrophy. For patients with widespread or extensive lesions, NB-UVB phototherapy (with increase of 0.1 J/cm^2 each time up to a maximum of 3 J/cm^2 based on the initial dose 0.2 J/cm^2; Phillips, Amsterdam, The Netherlands) was performed two to three times a week. For patients with minor lesions and those unable to go to an

outpatient clinic room, smaller portable or handheld NB-UVB therapy devices are recommended for home use according to user guide.

The VLQI-C Score Assessments

VLQI-C is a vitiligo-specific, cultural context-targeted QoL instrument for Chinese patients with vitiligo, and has been demonstrated to reflect the impact of vitiligo on patients' QoL with good internal consistency and temporal stability in another study (under review). The questionnaire contains 25 optional questions (Q1–Q25) that are further divided into 3 subscales named psychosomatic and social affects (PSAs, Q1–7, Q9, Q12, Q15–19, Q21–22, and Q24), self–perception (SP, Q8, Q10–11, and Q13–14), and disease management (DM, Q20, Q23), and 1 self-reported severity question (SRS: Q25) according to the results of exploratory factor analysis and contents of the items. Details of VLQI-C are provided in **Supplementary Table 1**. Each question is evaluated on a 4-point scale ranging from 1 (not at all) to 4 (very much), and total score ranges from 0 (best) to 100 (worst), where higher scores indicate worse quality of life. In this study, all the participants filled out the VLQI-C questionnaire by scanning the quick response code provided by their doctors and completed the questionnaire at both baseline and after 4 weeks treatment. Information on demographics, overall health, and vitiligo characteristics was also incorporated into the questionnaire.

Detection of Neuropeptides and Cytokines by ELISA

Samples of 5-mL peripheral blood were collected with a serum-separating tube, left undisturbed to clot for 20–30 min at room temperature, and centrifuged at 3,000 rpm for 10 mins; the resulting supernatant was aspirated with a fresh polypropylene tube stored at −80°C for follow-up unified testing. The concentration of neuropeptide-Y (NPY), melanin-concentrating hormone (MCH), adrenocorticotropic hormone (ACTH), interferon-γ (IFN-γ), CXC chemokine ligand 10 (CXCL10), and interleukin-1β (IL-1β) was determined as previously described (20) using enzyme-linked immunosorbent assay (ELISA) kits (Labscience Biotechnology and Cusabio Biotechnology Co., Ltd, Wuhan, China) according to the manufacturer's instructions. Resultant absorbance was measured with a spectrophotometric microplate reader (Thermo Fisher Scientific, United States).

Statistical Analysis

The IBM SPSS Statistics version 22.0 program was used for statistical analysis. Shapiro-Wilk test was conducted to test for normal distribution. For study population demographics, difference between the two groups was analyzed by Mann-Whitney U test. The association of each categorical variable with the study group was evaluated by Pearson's chi-squared test. Independent samples *t*-test was conducted to compare changes in VLQI-C scores between the two groups, and paired samples *t*-test was performed to compare changes in VLQI-C scores before and after treatment. Student's *t*-test is performed to compare the means between the two groups, and one-way ANOVA with Dunnett *post hoc* tests is conducted for groups of 3 or more. Two-tailed *P*-values were reported from all the *t*-tests.

RESULTS

Characteristics of the Study Population

As a result, the data from a total of 149 patients with vitiligo were enrolled into the database, with 62 patients in the intervention group and 87 patients in the control group. The detailed overview of recruitment is shown in **Figure 2**. Full demographic information and baseline clinical characteristics of patients from both groups are summarized in **Table 1**. There was no statistically significant relationship between the two groups in terms of age, gender, education level, income level, marital status, exposited location, duration, lesion area, and phase ($P > 0.05$).

Camouflage and Psychotherapy Program Markedly Improved the QOL of Patients With Vitiligo

According to the VLQI-C evaluation, the baseline scores in the intervention group were slightly higher but without statistical significance than the corresponding scores in the control group (total: 65.27 ± 13.77 vs. 61.99 ± 12.2; PSA, 42.45 ± 11.1 vs. 40.13 ± 9.04; SP, 14.68 ± 3.16 vs. 14.03 ± 3.12; DM, 5.19 ± 1.13 vs. 4.91 ± 1.20; SRS, 2.95 ± 0.76 vs. 2.92 ± 0.85) (**Table 2**), suggesting that patients with lower level of QOL were more willing to accept the camouflage and psychotherapy program.

The VLQI-C scores (total, 65.27 ± 13.77 vs. 55.97 ± 14.79; PSA, 42.45 ± 11.1 vs. 36.87 ± 11.98; SP, 14.68 ± 3.16 vs. 12.52 ± 2.78; DM, 5.19 ± 1.13 vs. 4.19 ± 1.34; SRS, 2.95 ±0.76 vs. 2.39 ±0.66) markedly decreased after 4 weeks of treatment in the intervention group, but there were no statistically significant differences (total, 61.99 ± 12.2 vs. 59.14 ± 10.35; PSA, 40.13 ± 9.04 vs. 38.51 ± 7.11; SP, 14.03 ± 3.12 vs. 13.23 ± 3.11; DM, 4.91 ± 1.2 vs. 4.66 ± 1.23; SRS, 2.92 ±0.85 vs. 2.75 ±0.81) in the control group (**Table 3**; **Figure 3**). These results indicated that the camouflage and psychotherapy program could improve the QOL of patients with vitiligo.

Camouflage and Psychotherapy Program Reduced NPY and MCH Levels and Upregulated the Level of ACTH in Patients With Vitiligo

Elevated level of NPY has been shown to be associated with vitiligo (21). We found that there was an obvious decrease in NPY serum level after 4 weeks of treatment in the intervention group; however, there was no significant change in the control group (**Table 4**; **Figure 4A**). MCH is the vital hypothalamic peptide that controls skin pigmentation (22). First, we identified a higher expression of MCH serum level in vitiligo cases as opposed to healthy controls (**Supplementary Figure 1**); subsequently, we observed a significant reduction of MCH level in the intervention group, whereas it was almost unchanged in the control group (**Table 4**; **Figure 4B**). Additionally, ACTH is involved in the response to biological stress, and its serum level is decreased in

TABLE 1 | Demographics and baseline clinical characteristics of the patients.

Variables		Groups				*P*
		Intervention		Control		
		Numbers/medium	Percentage/range	Numbers/medium	Percentage/range	
Age		27	18–55	28	18–55	0.63
Gender	Male	27	43.5%	39	44.8%	0.88
	Female	35	56.5%	48	55.2%	
Education level	Primary school	3	4.8%	10	11.5%	0.53
	Middle school	13	21. %	19	21.8%	
	High school	38	61.3%	47	54.0%	
	College or higher	8	12.9%	11	12.6%	
Income level	<3,000	19	30.6%	24	27.6%	0.81
	3,000–5,000	19	30.6%	24	27.6%	
	5,000–10,000	16	25.8%	29	33.3%	
	≥10,000	8	12.9%	10	11.5%	
Marital status	Married	23	37.1%	41	47.1%	0.22
	Single	39	62.9%	46	52.9%	
Exposed site	Face/neck	27	43.5%	38	43.7%	0.89
	Hands/feet	24	38.7%	36	41.4%	
	Face/neck & hands/feet	11	17.7%	13	14.9%	
Duration (month)	<12	16	25.8%	16	18.4%	0.71
	12–60	20	32.3%	33	37.9%	
	60–120	18	29.0%	25	28.7%	
	≥120	8	12.9%	13	14. 9%	
Depigmented macule area (face, neck, and hands) (BSA)	0–0.5	31	50.0%	36	41.4%	0.53
	0.5–1	25	40.3%	39	44.8%	
	≥1	6	9.7%	12	13.8%	
Phase	Stable	37	59.7%	57	65.5%	0.50
	Active	25	40.3%	30	34.5%	

vitiligo sufferers compared with healthy controls (4). The results of this study demonstrated that ACTH serum level increased under the intervention of camouflage and psychotherapy, but that there was no obvious change in the control group (**Table 4**; **Figure 4C**). Taken together, camouflage and psychotherapy promote the restoration of neuropeptide levels in patients with vitiligo.

Camouflage and Psychotherapy Program Had a Synergistic Effect With Routine Care in Vitiligo Treatment by Down-Regulating the Expression of IFN-Γ, CXCL10, and IL-1β

IFN-γ, CXCL10, and IL-1β have emerged as dependable serum markers and play a critical role in T-cell response in vitiligo (23–25). Our results showed that the serum levels of IFN-γ, CXCL10, and IL-1β were significantly reduced in both the active and stable patients after camouflage and psychotherapy combined with conventional treatment for 4 weeks. However, only the active patients experienced the reduction in inflammation factors, not the stable patients within 4 weeks of convention treatment in the control group (**Table 4**; **Figures 4D–F**). Together, the results indicated that the intervention of camouflage and psychotherapy program could modulate inflammatory reactions in the short term.

TABLE 2 | Baseline levels of total and subscales scores of patients with vitiligo in the intervention group and the control group.

Variables	Mean ± SD	95% CI	*P*
Total score of IG	65.27 ± 13.77	−0.94–7.52	0.127
Total score of CG	61.99 ± 12.20		
PSA score of IG	42.45 ± 11.10	−0.94–5.59	0.162
PSA score of CG	40.13 ± 9.04		
SP score of IG	14.68 ± 3.16	−0.39–1.67	0.219
SP score of CG	14.03 ± 3.12		
DM score of IG	5.19 ± 1.13	−0.10–0.67	0.144
DM score of CG	4.91 ± 1.20		
SRS score of IG	2.95 ± 0.76	−0.24–0.30	0.813
SRS score of CG	2.92 ± 0.85		

SD, standard deviation; CI, confidence interval; IG, intervention group; CG, control group; PSA, psychosomatic and social affect; SP, self perception; DM, disease management; SRS, self-reported severity.

TABLE 3 | Total and subscales scores evaluated before and after 4 weeks of treatment in the intervention group and the control group.

Variables	Intervention group			Control group		
	Mean ± SD	95% CI	*P*	Mean ± SD	95% CI	*P*
Total score of before	65.27 ± 13.77	3.68–14.94	0.002	61.99 ± 12.20	−0.33–6.04	0.079
Total score of after	55.97 ± 14.79			59.14 ± 10.35		
PSA score of before	42.45 ± 11.10	0.92–10.24	0.020	40.13 ± 9.04	−0.73–3.98	0.175
PSA score of after	36.87 ± 11.98			38.51 ± 7.11		
SP score of before	14.68 ± 3.16	1.17–3.15	<0.0001	14.03 ± 3.12	−0.07–1.68	0.071
SP score of after	12.52 ± 2.78			13.23 ± 3.11		
DM score of before	5.19 ± 1.13	0.58–1.42	<0.0001	4.91 ± 1.20	−0.07–0.58	0.128
DM score of after	4.19 ± 1.34			4.66 ± 1.23		
SRS score of before	2.95 ± 0.76	0.32–0.81	<0.0001	2.92 ± 0.85	−0.05–0.39	0.120
SRS score of after	2.39 ± 0.66			2.75 ± 0.81		

SD, standard deviation; CI, confidence interval; PSA, psychosomatic and social affect; SP, self perception; DM, disease management; SRS, self-reported severity.

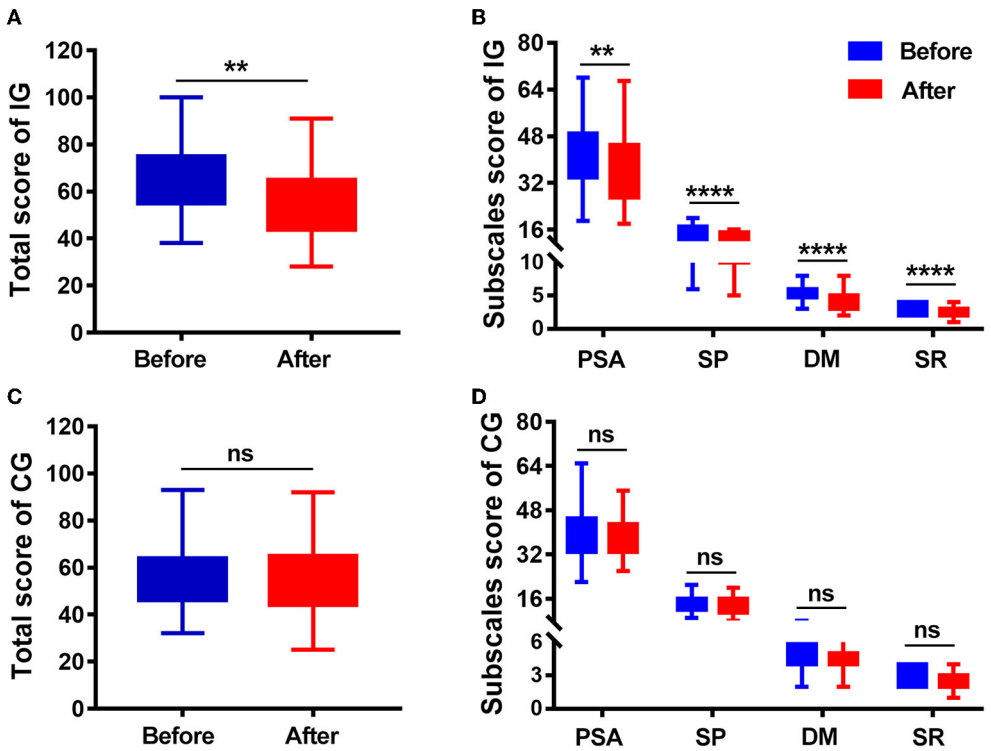

FIGURE 3 | Quality of life (QoL) score at baseline (before) and 4 weeks later (after). **(A)** Total VLQI-C scores before and after camouflage and psychotherapy in the IG. **(B)** PSA, SP, DM, and SRS scores before and after camouflage and psychotherapy in the IG. **(C)** Total VLQI-C scores before and after 4 weeks in the CG. **(D)** PSA, SP, DM, and SRS scores before and after camouflage and psychotherapy in the CG. IG, intervention group; CG, control group; PSA, psychosomatic and social affect; SP, self perception; DM, disease management; SRS, self-reported severity. $^{**}P < 0.01$, $^{****}P < 0.0001$, ns, nonsignificant.

DISCUSSION

This prospective, non-randomized, concurrent controlled study evaluated the efficacy of camouflage and psychotherapy intervention in patients with acrofacial vitiligo. Our study showed that patients with a relatively higher initial VLQI-C score preferred camouflage and psychotherapy and experienced significant reductions in VLQI-C scores within 4 weeks of treatment compared with those with routine care alone. Moreover, the significant changes in the NPY, MCH, ACTH, IFN-γ, CXCL10 and IL-1β serum levels induced by camouflage and psychotherapy in the patients with vitiligo indicated the mechanism of psycho-neuro-endocrine-immuno-skin interaction.

Lack of awareness and understanding of vitiligo in terms of etiology, pathogenesis, and treatment remains challenging

TABLE 4 | Serum levels of NPY, MCH, ACTH, IFN-γ, CXCL10, IL-1β in patients with vitiligo of active ($n = 10$) and stable ($n = 20$) phases in both the intervention and control groups.

Variables	Phase	Status	Intervention group		Control group	
			Mean ± SD	*P*	Mean ± SD	*P*
NPY (pg/mL)	Active	Before	431.29 ± 46.93	<0.0001	420.36 ± 40.34	0.079
		After	293.35 ± 43.10		396.28 ± 51.40	
	Stable	Before	351.75 ± 49.25	<0.0001	336.63 ± 48.91	0.087
		After	260.80 ± 39.87		321.26 ± 61.57	
MCH (pg/mL)	Active	Before	115.26 ± 19.31	<0.0001	111.73 ± 20.25	0.050
		After	61.81 ± 11.61		100.24 ± 10.42	
	Stable	Before	93.74 ± 13.05	<0.0001	90.41 ± 12.19	0.059
		After	53.74 ± 9.92		83.47 ± 13.17	
ACTH (pg/mL)	Active	Before	8.89 ± 1.74	<0.0001	9.31 ± 3.25	0.064
		After	21.20 ± 3.72		11.61 ± 3.58	
	Stable	Before	12.97 ± 3.95	<0.0001	12.59 ± 2.43	0.075
		After	22.65 ± 5.01		14.42 ± 4.12	
IFN-γ (pg/mL)	Active	Before	254.14 ± 45.90	0.010	268.89 ± 48.66	0.013
		After	208.75 ± 27.62		226.41 ± 31.94	
	Stable	Before	213.26 ± 29.32	0.011	196.84 ± 34.56	0.131
		After	193.52 ± 24.00		185.27 ± 30.66	
CXCL10 (pg/mL)	Active	Before	480.33 ± 46.03	0.001	470.63 ± 40.76	0.001
		After	369.78 ± 34.75		389.77 ± 51.41	
	Stable	Before	392.37 ± 36.58	0.001	396.14 ± 45.05	0.082
		After	341.93 ± 44.52		373.04 ± 40.32	
IL-1β (pg/mL)	Active	Before	7.88 ± 0.64	<0.0001	7.74 ± 1.12	0.004
		After	6.05 ± 0.68		6.55 ± 0.60	
	Stable	Before	6.87 ± 0.90	0.004	6.88 ± 0.88	0.158
		After	5.99 ± 0.89		6.64 ± 0.59	

NPY, neuropeptide-Y; MCH, melanin-concentrating hormone; ACTH adrenocorticotropic hormone; IFN-γ, interferon gamma; CXCL10, C-X-C motif chemokine ligand 10; IL-1β, interleukin 1; SD, standard deviation.

for Asian patients (26, 27). Several studies have demonstrated that increasing access for psychotherapy including mental health counseling and cognitive behavioral therapy could markedly improve the quality of life of patients with vitiligo (28, 29). It was reported that vitiligo patients with facial involvement and higher Dermatology Life Quality Index (DLQI, a general questionnaire for all skin diseases) scores benefited from camouflage in a Belgian study; 40 vitiligo cases with camouflage showed a significant reduction in their DLQI scores compared to non-camouflaged users in an Egyptian study; camouflage lessons and self-camouflage for 4 weeks are effective for Japanese patients with vitiligo; psychological therapy for a period of 8 weeks has a positive effect on the progression of patients with vitiligo in a UK study (14). Recently, an observer-blinded self-controlled study from China demonstrated that camouflage can make significant improvement in QOL by assessing scores on DLQI and Vitiligo Impact Scale-22 (VIS-22, based on Indian patients) (30). It is worth noting that, here, we used a reliable and validated vitiligo-specific QoL instrument in the Chinese context. Our trial demonstrated improvement in QOL with the combination of camouflage and psychotherapy instead of a single therapeutic effect.

Melanocytes are derived from neural crest stem cells, so they have an embryologic link to the nervous system (31). Melanin synthesis is affected by several neurotransmitters and cytokines, and vitiliginous melanocytes are prone to neuro-endocrinal changes (4, 32). Psycho-neuro-endocrine-immuno-skin system is the study of the interactions among psychology, neural, endocrine, immune and skin processes (33, 34). Few studies have explored changes in neuropeptides and inflammatory cytokines after camouflage and/or psychotherapy interventions in vitiligo treatment. Psychological stress exposure resulting from vitiligo can lead to endocrine perturbation by altered neuropeptides and cytokines (33). These factors can, in turn, influence melanin synthesis by interacting with melanocytes and immune cells *via* their receptors (35–37).

NPY, a 36 amino acid neuromodulator secreted by neurons, is believed to be involved in control of vitiligo development (7, 21, 38, 39). Several studies have shown that the NPY levels of lesions and plasma in patients with vitiligo are significantly higher than in healthy volunteers (7, 21, 38). Furthermore, *NPY*−399T/C (rs16147) and +1128T/C (rs16139) polymorphisms are correlated with vitiligo susceptibility and increase NPY transcription activity (39, 40). In this study, we found that camouflage combined with psychotherapy could considerably decrease serum NPY level. MCH, a hypothalamic neuropeptide, controls skin pigmentation and is an antagonist of alpha-melanocyte–stimulating hormone-induced skin darkening

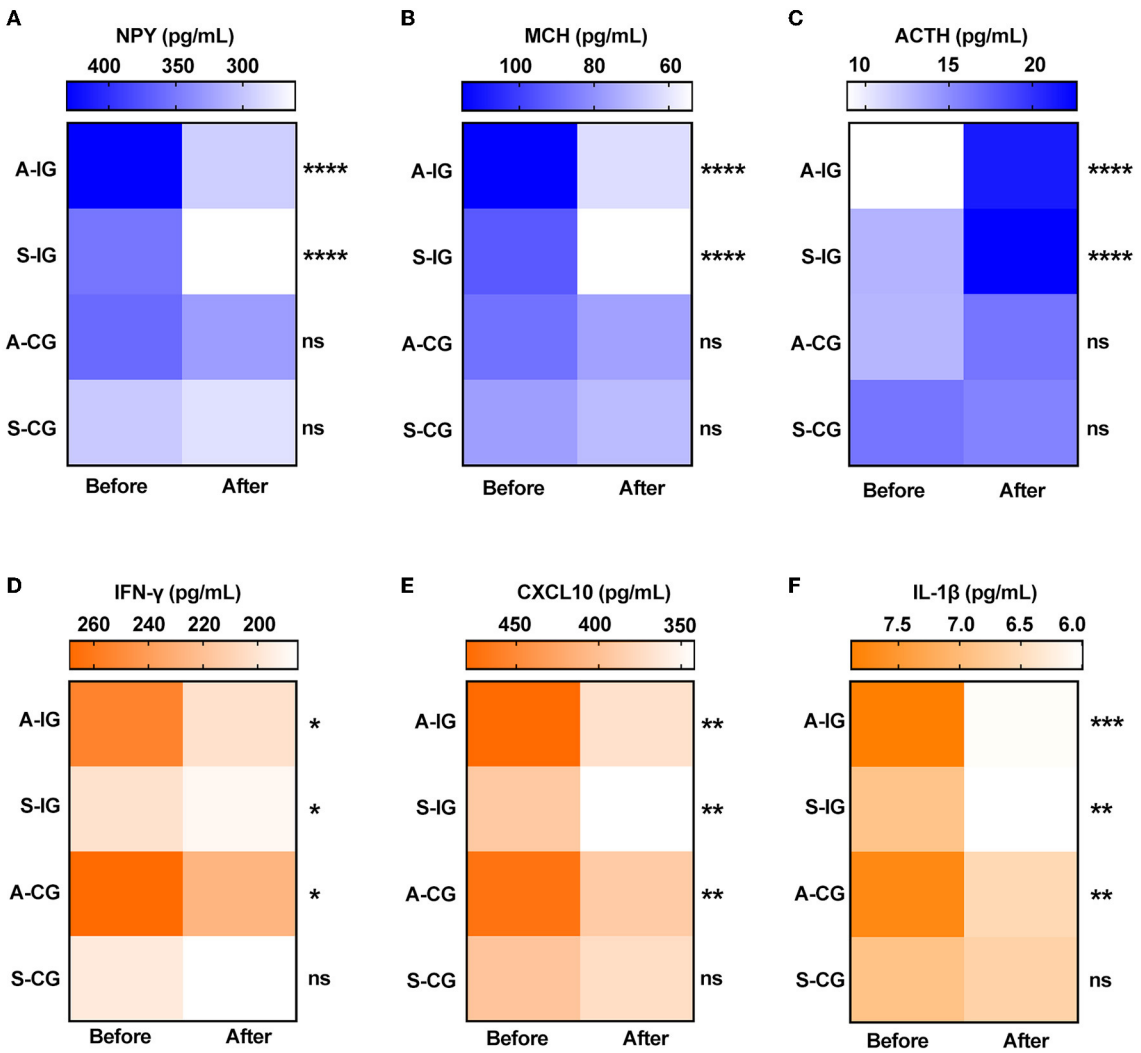

FIGURE 4 | Serum levels of neuropeptides and cytokines before and after 4 weeks in the two groups. **(A)** NPY, **(B)** MCH, **(C)** ACTH, **(D)** IFN-γ, **(E)** CXCL10, and **(F)** IL-1β. A-IG, active phase of intervention group; S-IG, stable phase of intervention group; A-CG, active phase of control group; S-IG, stable phase of control group. $^{*}P < 0.05$, $^{**}P < 0.01$, $^{***}P < 0.001$, $^{****}P < 0.0001$, ns, nonsignificant.

(41, 42). Notably, in the serum of patients with vitiligo, autoantibodies against MCH receptor 1 (MCH-R1) were found to block the activity of MCHR1 and the binding of MCH with MCHR1 in a competitive manner (43). MCH mRNA expression in both lesion and non-lesion areas are upregulated in patients with vitiligo compared to healthy control, and MCH stimulation in human melanocytes reduces melanogenic actions (44, 45). However, the level of circulating MCH remains unknown in vitiligo. In this study, we primarily revealed a higher level of serum MCH in patients with vitiligo and discovered a reduced MCH level associated with camouflage and psychotherapy. ACTH, a prominent polypeptide hormone, stimulates the adrenal cortex, producing glucocorticoids to cope with stress (32). ACTH can cause dispersion of melanin granules (46), and prolonged administration of ACTH can induce skin hyperpigmentation (47, 48). There is a lower serum level of ACTH in either active or stable patients with vitiligo compared to healthy controls, which might be caused by the negative feedback regulation of higher serum levels of cortisol in active patients with vitiligo (4, 49). Our results demonstrated that camouflage and psychotherapy intervention markedly increased the level of ACTH.

Autoreactive cytotoxic $CD8^+$ T cells specifically damage melanocytes and provoke the development and progression of vitiligo *via* presentation of IFN-γ and other cytotoxic effectors (50). Keratinocytes and fibroblasts stressed by IFN-γ can secrete chemokines CXCL9 and CXCL10, recruiting more $CD8^+$ T cells to skin lesions (51–53). In addition, psychiatric factors may increase the release of IFN-γ in skin disorders (54). Hence, in this study, we observed the changes in IFN-γ and CXCL10 and found that the serum level of both decreased more drastically when combined with camouflage and psychotherapy. *IL1B*−511C/T SNP upregulates IL-1β transcript levels and results in increased risk for vitiligo. Moreover, IL-1β can induce biosynthesis and

release of NPY; in turn, NPY can be involved in the humoral immune mechanism leading to a higher level of IL-1β in vitiligo (40, 55). In our previous study, we have demonstrated increased serum IL-1β levels in patients with vitiligo and correlated it with disease activity and severity, as well as a decrease after routine care (56). In this study, we found that IL-1β levels were reduced following camouflage combined with psychotherapy. These findings will help us understand the potential psycho-neuro-endocrine-immuno-skin system mechanism in management of vitiligo.

Some limitations were considered in the study. First, the number of patients was relatively small, as only 149 patients were willing to participate in the study. Second, the method for patient grouping was based on a voluntary basis instead of randomization of patients, because successful masking and allocation concealment are not possible because of the visibility of camouflage management. Future studies with larger samples might avoid selection bias through loss or withdrawal of randomized patients. Third, the study was limited to one region, and it would be difficult to conclude the results directly for people from the other regions and races. Last, long-term follow-up data are lacking, and we do not know if the benefit of psychotherapy in the intervention group was durable.

In conclusion, this study indicates that camouflage combined with psychotherapy may provide a valuable treatment modality that not only improves the quality of life but also enhances efficacy *via* psycho-neuro-endocrine-immuno-skin interactions in vitiligo management. Dermatologists should be aware of the importance of easing psychosocial burdens using cover products and psychological support during treatment of vitiligo.

DATA AVAILABILITY STATEMENT

The data presented in the current study are available from the corresponding author on reasonable request.

ETHICS STATEMENT

The studies involving human participants were reviewed and approved by Ethics Review Board of Xijing Hospital (Approval Code: KY20182005-1). The patients/participants provided their written informed consent to participate in this study. Written informed consent was obtained from the individual(s) for the publication of any potentially identifiable images or data included in this article.

AUTHOR CONTRIBUTIONS

YC, SZ, WZ, SL, and CL were involved in the conception and design of the study. YC and SZ participated in the acquisition, analysis, and interpretation of data. YC drafted the manuscript. All authors critically revised the article for important intellectual content, contributed to the article, and approved the submitted version.

FUNDING

The study was supported by National Natural Science Foundation of China (Grant Numbers: 12126606, 81803124, 81930087, and 81903207).

ACKNOWLEDGMENTS

We thank all the patients who participated in this study.

SUPPLEMENTARY MATERIAL

The Supplementary Material for this article can be found online at: https://www.frontiersin.org/articles/10.3389/fmed.2022.818543/full#supplementary-material

REFERENCES

1. Frisoli ML, Essien K, Harris JE. Vitiligo: mechanisms of pathogenesis and treatment. *Annu Rev Immunol.* (2020) 38:621–48. doi: 10.1146/annurev-immunol-100919-023531
2. Henning SW, Jaishankar D, Barse LW, Dellacecca ER, Lancki N, Webb K, et al. The relationship between stress and vitiligo: evaluating perceived stress and electronic medical record data. *PLoS One.* (2020) 15:e0227909. doi: 10.1371/journal.pone.0227909
3. Rodrigues M, Ezzedine K, Hamzavi I, Pandya AG, Harris JE, Vitiligo Working G. New discoveries in the pathogenesis and classification of vitiligo. *J Am Acad Dermatol.* (2017) 77:1–13. doi: 10.1016/j.jaad.2016.10.048
4. Kotb El-Sayed MI, Abd El-Ghany AA, Mohamed RR. Neural and endocrinal pathobiochemistry of vitiligo: comparative study for a hypothesized mechanism. *Front Endocrinol (Lausanne).* (2018) 9:197. doi: 10.3389/fendo.2018.00197
5. Ucuz I, Altunisik N, Sener S, Turkmen D, Kavuran NA, Marsak M, et al. Quality of life, emotion dysregulation, attention deficit and psychiatric comorbidity in children and adolescents with vitiligo. *Clin Exp Dermatol.* (2020) 16:22. doi: 10.1111/ced.14196
6. Chen CY, Wang WM, Chung CH, Tsao CH, Chien WC, Hung CT. Increased risk of psychiatric disorders in adult patients with vitiligo: a nationwide, population-based cohort study in Taiwan. *J Dermatol.* (2020) 47:470–5. doi: 10.1111/1346-8138.15290
7. Al'Abadie MS, Senior HJ, Bleehen SS, Gawkrodger DJ. Neuropeptide and neuronal marker studies in vitiligo. *Br J Dermatol.* (1994) 131:160–5. doi: 10.1111/j.1365-2133.1994.tb08486.x
8. Zhang B, Ma S, Rachmin I, He M, Baral P, Choi S, et al. Hyperactivation of sympathetic nerves drives depletion of melanocyte stem cells. *Nature.* (2020) 577:676–81. doi: 10.1038/s41586-020-1935-3
9. Abdel-Malek ZA, Jordan C, Ho T, Upadhyay PR, Fleischer A, Hamzavi I. The enigma and challenges of vitiligo pathophysiology and treatment. *Pigment Cell Melanoma Res.* (2020) 33:778–87. doi: 10.1111/pcmr.12878
10. Passeron T. Medical and Maintenance Treatments for Vitiligo. *Dermatol Clin.* (2017) 35:163–70. doi: 10.1016/j.det.2016.11.007
11. Mohammad TF, Al-Jamal M, Hamzavi IH, Harris JE, Leone G, Cabrera R, et al. The vitiligo working group recommendations for narrowband ultraviolet B light phototherapy treatment of vitiligo. *J Am Acad Dermatol.* (2017) 76:879–88. doi: 10.1016/j.jaad.2016.12.041
12. Rajatanavin N, Suwanachote S, Kulkollakarn S. Dihydroxyacetone: a safe camouflaging option in vitiligo. *Int J Dermatol.* (2008) 47:402–6. doi: 10.1111/j.1365-4632.2008.03356.x

13. Ongenae K, Van Geel N, De Schepper S, Vander Haeghen Y, Naeyaert JM. Management of vitiligo patients and attitude of dermatologists towards vitiligo. *Eur J Dermatol.* (2004) 14:177–81.
14. Papadopoulos L, Bor R, Legg C. Coping with the disfiguring effects of vitiligo: a preliminary investigation into the effects of cognitive-behavioural therapy. *Br J Med Psychol.* (1999) 71:385-96. doi: 10.1348/000711299160077
15. Tanioka M, Yamamoto Y, Kato M, Miyachi Y. Camouflage for patients with vitiligo vulgaris improved their quality of life. *J Cosmet Dermatol.* (2010) 9:72–5. doi: 10.1111/j.1473-2165.2010.00479.x
16. Hossain C, Porto DA, Hamzavi I, Lim HW. Camouflaging agents for vitiligo patients. *J Drugs Dermatol.* (2016) 15:3847.
17. Bassiouny D, Hegazy R, Esmat S, Gawdat HI, Ahmed Ezzat M, Tawfik HA, et al. Cosmetic camouflage as an adjuvant to vitiligo therapies: effect on quality of life. *J Cosmet Dermatol.* (2021) 20:159–65. doi: 10.1111/jocd.13459
18. Ongenae K, Dierckxsens L, Brochez L, van Geel N, Naeyaert JM. Quality of life and stigmatization profile in a cohort of vitiligo patients and effect of the use of camouflage. *Dermatology.* (2005) 210:279–85. doi: 10.1159/000084751
19. Lei T-C, Xu A-E, Gao T-W, He L, Gu H, Li M, et al. The Vitiligo Expert Group of the Dermatovenereology Professional Committee CSoIC, Western M. Consensus on the Diagnosis and Treatment of Vitiligo in China (2021 Revision)#. *Int J Dermatol Venereol.* (2021) 4:1. doi: 10.1097/JD9.0000000000000151
20. Chen X, Guo W, Chang Y, Chen J, Kang P, Yi X, et al. Oxidative stress-induced IL-15 trans-presentation in keratinocytes contributes to CD8(+) T cells activation via JAK-STAT pathway in vitiligo. *Free Radical Biol Med.* (2019) 139:80–91. doi: 10.1016/j.freeradbiomed.2019.05.011
21. Tu C, Zhao D, Lin X. Levels of neuropeptide-Y in the plasma and skin tissue fluids of patients with vitiligo. *J Dermatol Sci.* (2001) 27:178–82. doi: 10.1016/S0923-1811[01]00134-7
22. Kemp EH, Waterman EA, Hawes BE, O'Neill K, Gottumukkala RVSRK, Gawkrodger DJ, et al. The melanin-concentrating hormone receptor 1, a novel target of autoantibody responses in vitiligo. *J Clin Invest.* (2002) 109:923–30. doi: 10.1172/JCI0214643
23. Abdallah M, El-Mofty M, Anbar T, Rasheed H, Esmat S, Al-Tawdy A, et al. CXCL-10 and Interleukin-6 are reliable serum markers for vitiligo activity: A multicenter cross-sectional study. *Pigment Cell Melanoma Res.* (2018) 31:330–6. doi: 10.1111/pcmr.12667
24. Ala Y, Pasha MK, Rao RN, Komaravalli PL, Jahan P. Association of IFN-gamma: IL-10 cytokine ratio with nonsegmental vitiligo pathogenesis. *Autoimmune Dis.* (2015) 2015:423490. doi: 10.1155/2015/423490
25. Tomaszewska K, Kozlowska M, Kaszuba A, Lesiak A, Narbutt J, Zalewska-Janowska A. Increased serum levels of IFN-gamma, IL-1beta, and IL-6 in patients with alopecia areata and nonsegmental vitiligo. *Oxid Med Cell Longev.* (2020) 2020:5693572. doi: 10.1155/2020/5693572
26. Salman A, Kurt E, Topcuoglu V, Demircay Z. Social anxiety and quality of life in vitiligo and acne patients with facial involvement: a cross-sectional controlled study. *Am J Clin Dermatol.* (2016) 17:305–11. doi: 10.1007/s40257-016-0172-x
27. Bú EAD. Alexandre MESd, Scardua A, Araújo CRFd. Vitiligo as a psychosocial disease: apprehensions of patients imprinted by the white Interface—Comunicação, Saúde. *Educação.* (2017) 22:481–91. doi: 10.1590/1807-57622016.0925
28. Pun J, Randhawa A, Kumar A, Williams V. The impact of vitiligo on quality of life and psychosocial well-being in a nepalese population. *Dermatol Clin.* (2021) 39:117–27. doi: 10.1016/j.det.2020.08.011
29. Thompson AR, Clarke SA, Newell RJ, Gawkrodger DJ, Appearance Research C. Vitiligo linked to stigmatization in British South Asian women: a qualitative study of the experiences of living with vitiligo. *Br J Dermatol.* (2010) 163:481–6. doi: 10.1111/j.1365-2133.2010.09828.x
30. Li M, Wang F, Ding X, Xu Q, Du J. Evaluation of the potential interference of camouflage on the treatment of vitiligo: an observer-blinded self-controlled study. *Dermatol Ther.* (2020) 14:e14545. doi: 10.1111/dth.14545
31. Vandamme N, Berx G. From neural crest cells to melanocytes: cellular plasticity during development and beyond. *Cellul Mol Life Sci CMLS.* (2019) 76:1919–34. doi: 10.1007/s00018-019-03049-w
32. Rousseau K, Kauser S, Pritchard LE, Warhurst A, Oliver RL, Slominski A, et al. Proopiomelanocortin (POMC), the ACTH/melanocortin precursor, is secreted by human epidermal keratinocytes and melanocytes and stimulates melanogenesis. *FASEB J.* (2007) 21:1844–56. doi: 10.1096/fj.06-7398com
33. Pondeljak N, Lugovic-Mihic L. Stress-induced interaction of skin immune cells, hormones, and neurotransmitters. *Clin Ther.* (2020) 42:757–70. doi: 10.1016/j.clinthera.2020.03.008
34. Vidal Yucha SE, Tamamoto KA, Kaplan DL. The importance of the neuro-immuno-cutaneous system on human skin equivalent design. *Cell Prolif.* (2019) 52:e12677. doi: 10.1111/cpr.12677
35. Tausk F, Elenkov I, Moynihan J. Psychoneuroimmunology. *Dermatol Ther.* (2008) 21:22–31. doi: 10.1111/j.1529-8019.2008.00166.x
36. Honeyman JF. Psychoneuroimmunology and the Skin. *Acta Derm Venereol.* (2016) 96:38–46. doi: 10.2340/00015555-2376
37. Gieler U, Gieler T, Peters EMJ, Linder D. Skin and Psychosomatics—Psychodermatology today. *J Dtsch Dermatol Ges.* (2020) 18:1280–98. doi: 10.1111/ddg.14328
38. Liu PY, Bondesson L, Lontz W, Johansson O. The occurrence of cutaneous nerve endings and neuropeptides in vitiligo vulgaris: a case-control study. *#N/A.* (1996) 288:670–5. doi: 10.1007/BF02505276
39. Bakry O, Mariee A, Badr I, Tayel N, El Gendy S, NPY. Gene Polymorphism in Vitiligo: a case-control study in Egyptian Patients. *Indian J Dermatol.* (2020) 65:65–7. doi: 10.4103/ijd.IJD_104_18
40. Laddha NC, Dwivedi M, Mansuri MS, Singh M, Patel HH, Agarwal N, et al. Association of neuropeptide Y (NPY), interleukin-1B (IL1B) genetic variants and correlation of IL1B transcript levels with vitiligo susceptibility. *PLoS One.* (2014) 9:e107020. doi: 10.1371/journal.pone.0107020
41. Kawauchi H, Kawazoe I, Tsubokawa M, Kishida M, Baker BI. Characterization of melanin-concentrating hormone in chum salmon pituitaries. *Nature.* (1983) 305:321–3. doi: 10.1038/305321a0
42. Madelaine R, Ngo KJ, Skariah G, Mourrain P. Genetic deciphering of the antagonistic activities of the melanin-concentrating hormone and melanocortin pathways in skin pigmentation. *PLoS Genet.* (2020) 16:e1009244-e1009244. doi: 10.1371/journal.pgen.1009244
43. Gottumukkala RV, Gavalas NG, Akhtar S, Metcalfe RA, Gawkrodger DJ, et al. Function-blocking autoantibodies to the melanin-concentrating hormone receptor in vitiligo patients. *Lab Invest.* (2006) 86:781–9. doi: 10.1038/labinvest.3700438
44. Kemp EH, Weetman AP. Melanin-concentrating hormone and melanin-concentrating hormone receptors in mammalian skin physiopathology. *Peptides.* (2009) 30:2071–5. doi: 10.1016/j.peptides.2009.04.025
45. Hoogduijn MJ, Ancans J, Suzuki I, Estdale S, Thody AJ. Melanin-concentrating hormone and its receptor are expressed and functional in human skin. *Biochem Biophys Res Commun.* (2002) 296:698–701. doi: 10.1016/S0006-291X(02)00932-4
46. Shepherd RG, Howard KS, Bell PH, Cacciola AR, Child RG, Davies MC, et al. Studies with corticotropin. i isolation, purification and properties of β-corticotropin. *J Am Chem Soc.* (1956) 78:5051–9. doi: 10.1021/ja01600a065
47. Lerner AB, McGuire JS. Melanocyte-stimulating hormone and adrenocorticotrophic hormone. their relation to pigmentation. *New Engl J Med.* (1964) 270:539–46. doi: 10.1056/NEJM196403122701101
48. Slominski A, Pisarchik A, Tobin DJ, Mazurkiewicz JE, Wortsman J. Differential expression of a cutaneous corticotropin-releasing hormone system. *Endocrinology.* (2004) 145:941–50. doi: 10.1210/en.2003-0851
49. Pal SK, Ghosh KK, Panja RK, Banerjee PK. Adrenocortical function in vitiligo. *Clin Chim Acta.* (1981) 113:325–7. doi: 10.1016/0009-8981(81)90286-2
50. Plaza-Rojas L, Guevara-Patino JA. The role of the NKG2D in Vitiligo. *Front Immunol.* (2021) 12:624131. doi: 10.3389/fimmu.2021.624131
51. Zhang L, Chen S, Kang Y, Wang X, Yan F, Jiang M, et al. Association of clinical markers with disease progression in patients with vitiligo from China. *JAMA Dermatol.* (2020) 156:288–95. doi: 10.1001/jamadermatol.2019.4483
52. Rashighi M, Agarwal P, Richmond JM, Harris TH, Dresser K, Su MW, et al. CXCL10 is critical for the progression and maintenance of

depigmentation in a mouse model of vitiligo. *Sci Transl Med.* (2014) 6:223ra23. doi: 10.1126/scitranslmed.3007811
53. Xu Z, Chen D, Hu Y, Jiang K, Huang H, Du Y, et al. Anatomically distinct fibroblast subsets determine skin autoimmune patterns. *Nature.* (2021) 15:21. doi: 10.1038/s41586-021-04221-8
54. Urpe M, Buggiani G, Lotti T. Stress and psychoneuroimmunologic factors in dermatology. *Dermatol Clin.* (2005) 23:609–17. doi: 10.1016/j.det.2005.05.017
55. Rosmaninho-Salgado J, Araújo IM, Alvaro AR, Mendes AF, Ferreira L, et al. Regulation of catecholamine release and tyrosine hydroxylase in human adrenal chromaffin cells by interleukin-1beta: role of neuropeptide Y and nitric oxide. *J Neurochem.* (2009) 109:911–22. doi: 10.1111/j.1471-4159.2009.06023.x
56. Li S, Kang P, Zhang W, Jian Z, Zhang Q, Yi X, et al. Activated NLR family pyrin domain containing 3 (NLRP3) inflammasome in keratinocytes promotes cutaneous T-cell response in patients with vitiligo. *J Allergy Clin Immunol.* (2020) 145:632–45. doi: 10.1016/j.jaci.2019.10.036

Conflict of Interest: The authors declare that the research was conducted in the absence of any commercial or financial relationships that could be construed as a potential conflict of interest.

frontiers | Frontiers in Medicine

REVIEW
published: 09 June 2022
doi: 10.3389/fmed.2022.858824

The Therapeutic Role of ADSC-EVs in Skin Regeneration

Yixi Wang[1†], *Lihui Cheng*[2†], *Hanxing Zhao*[1], *Zhengyong Li*[1], *Junjie Chen*[1], *Ying Cen*[1] *and Zhenyu Zhang*[1*]

[1] *Department of Plastic and Burn Surgery, West China Hospital, Sichuan University, Chengdu, China,* [2] *Department of Central Sterile Supply, West China Hospital, Sichuan University, Chengdu, China*

Large skin defects caused by burns, unhealing chronic wounds, and trauma, are still an intractable problem for clinicians and researchers. Ideal skin regeneration includes several intricate and dynamic stages of wound repair and regeneration of skin physiological function. Adipose-derived stem cells (ADSCs), a type of mesenchymal stem cells (MSCs) with abundant resources and micro-invasive extraction protocols, have been reported to participate in each stage of promoting skin regeneration via paracrine effects. As essential products secreted by ADSCs, extracellular vesicles (EVs) derived from ADSCs (ADSC-EVs) inherit such therapeutic potential. However, ADSC-EVs showed much more clinical superiorities than parental cells. ADSC-EVs carry various mRNAs, non-coding RNAs, proteins, and lipids to regulate the activities of recipient cells and eventually accelerate skin regeneration. The beneficial role of ADSCs in wound repair has been widely accepted, while a deep comprehension of the mechanisms of ADSC-EVs in skin regeneration remains unclear. In this review, we provided a basic profile of ADSC-EVs. Moreover, we summarized the latest mechanisms of ADSC-EVs on skin regeneration from the aspects of inflammation, angiogenesis, cell proliferation, extracellular matrix (ECM) remodeling, autophagy, and oxidative stress. Hair follicle regeneration and skin barrier repair stimulated by ADSC-EVs were also reviewed. The challenges and prospects of ADSC-EVs-based therapies were discussed at the end of this review.

Keywords: skin regeneration, extracellular vesicles, adipose-derived stem cells, stem cells therapy, wound healing

OPEN ACCESS

Edited by:
Xing-Hua Gao,
The First Affiliated Hospital of China Medical University, China

Reviewed by:
Teng Su,
Duke University, United States
Marina Gomzikova,
Kazan Federal University, Russia

***Correspondence:**
Zhenyu Zhang
zhangzy.wch@foxmail.com

[†]These authors have contributed equally to this work and share first authorship

Specialty section:
This article was submitted to Dermatology, a section of the journal Frontiers in Medicine

Received: *20 January 2022*
Accepted: *20 May 2022*
Published: *09 June 2022*

Citation:
Wang Y, Cheng L, Zhao H, Li Z, Chen J, Cen Y and Zhang Z (2022) The Therapeutic Role of ADSC-EVs in Skin Regeneration. Front. Med. 9:858824. doi: 10.3389/fmed.2022.858824

INTRODUCTION

The skin, the largest organ of the human body, protects the body from exogenous irritation and pathogen invasion as the first barrier between organisms and the environment. Skin damage caused by diseases or trauma threatens the defensive function, leading to the suffering of patients and the burden of public health care (1, 2). Repair of skin, including both structural integrity and physiological function, is essential to maintain its protective property, which remains intractable for clinicians and researchers. Stem cells have been reported to possess considerable potential for skin regeneration through multiple mechanisms (3–5). Adipose-derived stem cells (ADSCs) are a promising type of mesenchymal stem cells (MSCs) for skin regeneration, with abundant resources among human tissue and minimally invasive extraction protocols. However, some severe complications impact the application of stem cells since they are large and sticky, such as elevation in pulmonary arterial pressure or even vascular embolism, along with potential oncogenesis and ethical issues (6, 7). Moreover, some properties of stem cells might impair the beneficial effect of stem cells. For example, restricted delivery of stem cells and uncertain differentiation

to proinflammatory or anti-inflammatory phenotype of stem cells in inflammatory conditions might lead to no benefit or even negative effect in the treatment of acute kidney injury after cardiac surgery (8).

Extracellular vesicles (EVs) are natural particles with a phospholipid bilayer membrane secreted by almost all types of cells during vital activities (9). Transferring proteins, nucleic acids, and lipids to recipient cells, EVs derived from stem cells have been deemed to be intercellular communicators and functional executors (10, 11). Compared to stem cells, EVs possess more advantages for clinical application. EVs are safer owing to their smaller size and non-tumorigenic. Because EVs show no immunogenicity and can be stored at −80°C, they are available once patients need, avoiding waiting for cell culture as autologous stem cells therapy (12). In recent years, considerable research efforts on EVs derived from ADSCs (ADSC-EVs) have indicated that ADSC-EVs have a positive impact on skin regeneration, similar to their parental cells. Moreover, ADSC-EVs manifested a superior impact on wound healing than EVs derived from other stem cells, which might be due to their robust angiogenic effect (13). ADSC-EVs might accelerate skin wound repair by participating in inflammation, angiogenesis, cell proliferation, and extracellular matrix (ECM) remodeling (14, 15), regulating cell apoptosis and autophagy (16, 17), and relieving oxidative stress in the wound microenvironment (18). The regeneration of skin appendages and recovery of physiological functions are also promoted by ADSC-EVs (19, 20), which is essential for ideal skin regeneration. Current documents have summarized the promoting effects of ADSC-EVs in skin regeneration, mostly focusing on mechanisms in wound healing but hardly with functional repair involved. In this review, the profile of ADSC-EVs, mechanisms in the promotion of skin regeneration, and potential for clinical applications are discussed (**Figure 1**). The existing challenges and prospects of ADSC-EVs in regenerative medicine are also discussed here. We hope this work replenishes current comprehension of how ADSC-EVs generate and work, and provides potential inspiration for future research on regenerative medicine.

EXTRACELLULAR VESICLE FROM ADIPOSE-DERIVED STEM CELLS

ADSCs are a subtype of MSCs isolated from adipose tissues with self-renewal and multiple differentiation properties. Through

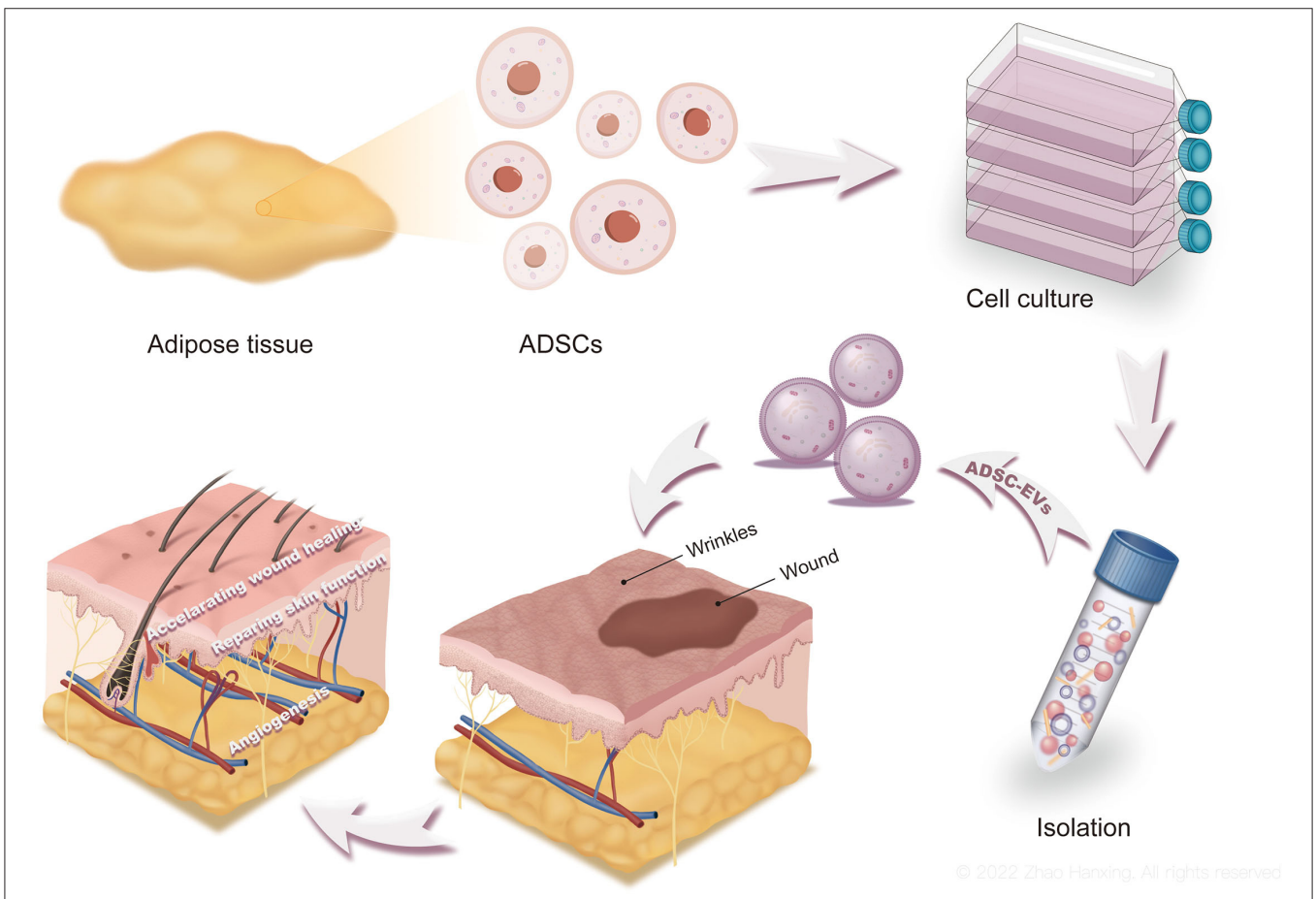

FIGURE 1 | The production, functions, and applications of ADSC-EVs. Culture medium of ADSCs was collected and processed to obtain ADSC-EVs. By accelerating wound healing and repairing skin function, ADSC-EVs promote skin regeneration. ADSC-EVs are promising for clinical applications as well.

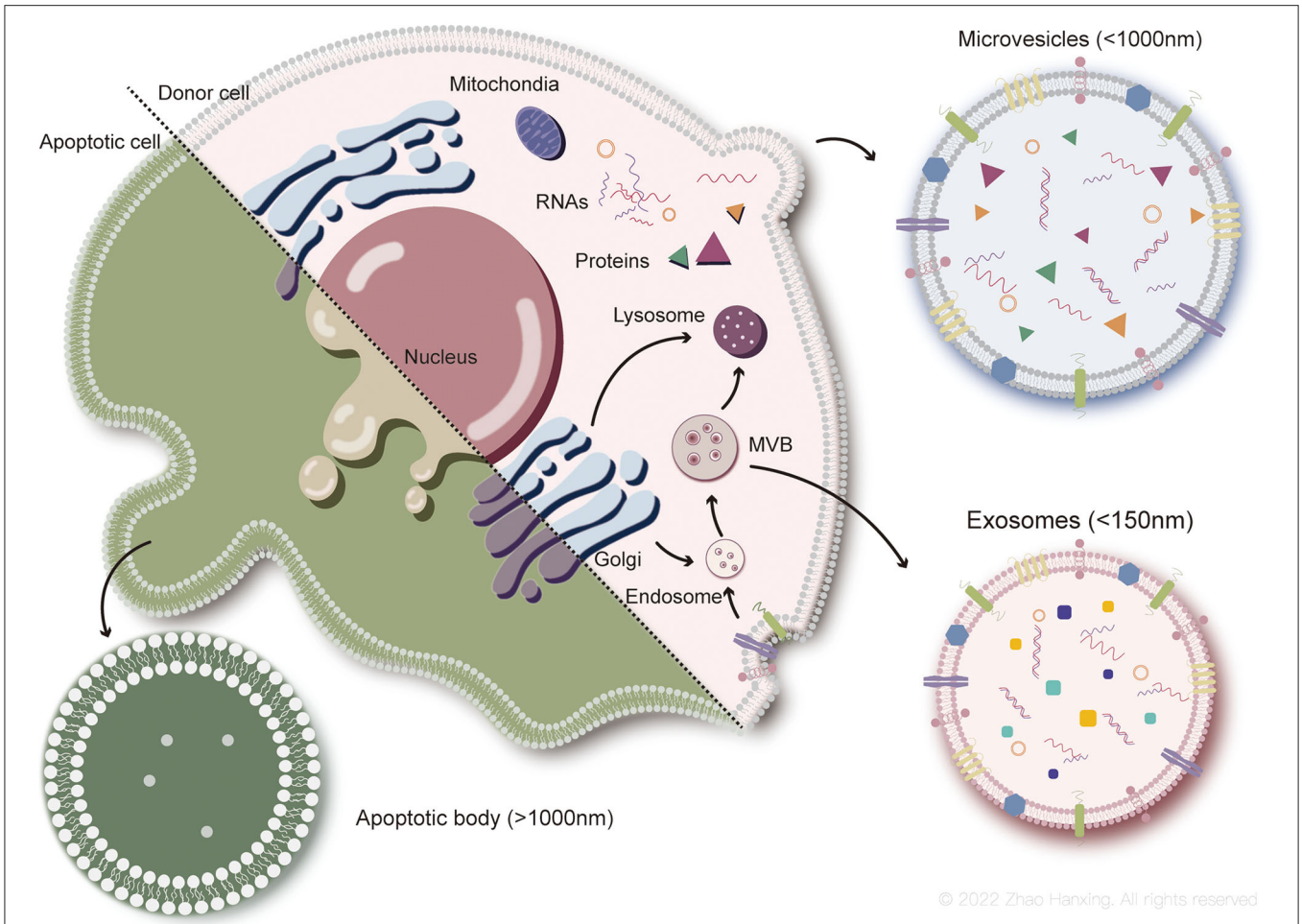

FIGURE 2 | Biogenesis of each subtype of EVs. Exosomes (<150 nm in size) originate from endosome. Microvesicles (up to 1,000 nm) generate from plasma membrane. Apoptotic bodies (more than 1,000 nm) are particles of apoptotic cells disassembly.

paracrine of a variety of cytokines, ADSCs are known as powerful therapeutics utilized in regenerative medicine (21, 22). In addition to direct secretion, ADSC-EVs have been reported to be functional executors of ADSCs (23). As products of ADSCs during biological activities, ADSC-EVs encapsulate cargoes, including DNA, RNA, proteins, and lipids produced by ADSCs, acting as intercellular communicators and biomolecule transporters (24).

Classification and Biogenesis of EVs

EVs are a generic term for particles with lipid bilayer membranes released by cells in natural activities and are divided into three main subtypes based on the current understanding of their biogenesis, size, and content: exosomes (<150 nm in size), microvesicles (up to 1,000 nm), and apoptotic bodies (more than 1,000 nm) (25–27). Exosomes and microvesicles seem to be generated by almost all types of viable cells (28) and are major subtypes of EVs studied in regenerative medicine to date. Apoptotic bodies, the relatively larger group in size, are products of cell apoptosis and encapsulate contents of cells disassembly. The biogenesis of the three main EV-subtypes is shown here (**Figure 2**).

The biogenesis of exosomes is a complex process. First, endocytosis of the plasma membrane forms the early sorting endosomes, carrying surface proteins and lipids. Early endosomes subsequently transform to late endosomes under interaction with the Golgi complex (28). Exosomes originate from the inward budding of the endosomal membrane as intraluminal vesicles (IVLs) during maturation of multivesicular endosomes (MVBs), which then enter lysosomes for degradation, or fuse with the plasma membrane to be released as exosomes (27). Exosomal membrane components are derived from plasma or the Golgi complex before the formation of IVLs in endosomes. The cargoes sorted into exosomes are heavily dependent on endosomal sorting mechanisms, which involve the endosomal sorting complex required for transport (ESCRT) proteins (29). ESCRT-independent mechanisms have also been demonstrated, including ceramide and its metabolites and tetraspanin family members (30–32).

Microvesicles released by healthy cells originate from the outward budding of the plasma membrane. Phospholipids on the plasma membrane rearrange with activation of scramblase by the inflow of Ca^{2+}, in which phosphatidylserine flips from the inner leaflet of the bilayer to the outer leaflet. Consequently, budding of the plasma membrane and degradation of the cytoskeleton occur, forming microvesicles (33). However, biogenesis of microvesicles can proceed without the rearrangement of phospholipids (34), indicating that other mechanisms may also be involved, such as the participation of cholesterol-rich lipid rafts (35).

Although the destinies differ between parental cells of apoptotic bodies and microvesicles, the formation of the two subtypes of EVs involves similar changes in the plasma membrane. Biogenesis of apoptotic bodies is described as three sequential well-coordinated steps with corresponding morphological changes: plasma membrane blebbing, thin membrane protrusion formation, and fragmentation (36). During blebbing, phosphatidylserine flips from the inner layer of the plasma membrane to the outer layer, which is induced by caspase-activated scramblase (37). Compared to the former two subtypes, cargoes of apoptotic bodies tend to include intact organelles, chromatin, and higher levels of histones (38). However, recent studies have also shown that some organelles might be enclosed by microvesicles (39). Information on cargoes in EVs needs to be enriched with further research.

Biomarkers of EVs include molecules involved in their biogenesis, such as transmembrane proteins anchored to the plasma membrane or endosomal membrane and cytosolic proteins (27). Non-EV proteins co-isolated with EVs are detected to assess the purity of EVs, such as apolipoproteins A1/2 and B, and albumin (26). According to the biogenesis of exosomes, their biomarkers are conventionally deemed to be ESCRT-associated proteins (Alix, TSG101, Syntenin, and HSC70), tetraspanin family proteins (CD9, CD63, and CD81), and major histocompatibility complex (MHC) class I and class II proteins. However, some of these proteins have also been demonstrated to be contained in other subtypes, such as flotillin-1, HSC70, and MHC class I and II proteins (40). Microvesicles derived from the plasma membrane mainly contain proteins present in the cytoplasm and plasma membrane, especially post-translational modified proteins (41). Apoptotic bodies contain high levels of apoptosis-associated proteins, such as cleaved caspase-3, C1q, and nuclear debris (42). Nevertheless, overlapping biomarkers exist among each group of EVs, making it imprecise for identification. In addition, isolation methods used in current studies, especially for microvesicles and apoptotic bodies, are mainly centrifugation based on the size and density of EVs, which leads to groups overlapping on the very edge of the size scale.

Exosomes and microvesicles transfer information and therapeutic molecules from viable cells to recipient cells (43), rendering them potential options for investigation in regenerative medicine. However, from the orthodox perspective, apoptotic bodies tend to be cell debris responsible for the clearance of dying cells (44). Moreover, cargoes distributed into apoptotic bodies vary in quantity and component (45, 46), along with a relatively large size scale, impeding the identification and mechanical exploration of apoptotic bodies. Hence, studies have paid more attention to the mechanisms and applications of the former two subtypes of EVs. In this review, our discussion of ADSC-EVs is mainly based on exosomes and microvesicles derived from ADSCs.

Isolation and Characterization of EVs

In the past few decades, researchers have isolated EVs by several common strategies (**Figure 3**). The traditional method is centrifugation, which is based on the density of different groups of EVs, allowing denser particles to sediment out first. Differential ultracentrifugation (DC) is the most frequently used method and is still the "gold standard" for the isolation of EVs (26). Density gradient centrifugation (DGC) is an improved ultracentrifugation method that produces EVs with higher purity, in which a prepared density gradient generally formed by sucrose or iodixanol is required. EVs pass through a gradient with increasing density from top to bottom in the DGC system, and then each subtype of EVs is separated into perspective layers with different densities. Common methods based on the size of EVs include ultrafiltration (UF) and size exclusion chromatography (SEC) (28). In UF, the target group of EVs passes through the filtration membrane with a certain molecular weight cut off (MWCO) while larger particles are retained. In SEC, EVs with different sizes pass through the column filled with porous polymer microspheres that allows smaller particles to penetrate. Routes in those pores take more time for smaller EVs to elute than larger EVs. Immunoaffinity capture (IC) technology relies on the binding between antigens on the surface of EVs and antibodies attached to the surface of tools, such as magnetic beads or plates. IC allows the isolation of EVs originating from a specific source with certain surface proteins. Polymer precipitation (PP), typically polyethylene glycol base, takes advantage of strong hydrophilicity to "grab" the water molecules in the solution, rendering EVs "dehydrated" to aggregate (41). Commercial isolation kits with various strategies described above have also been used in research. However, each method possesses its shortcomings. A large initial volume is required for DC and a long DC duration increases the risk of structural damage to EVs and protein contamination. DGC is associated with extra preparation and a low yield of EVs. When EVs pass through the filter membrane, the pores might be blocked, causing low yield, and the shear force leads to deformation and lysis of EVs. SEC and IC cannot process a large volume of solution. EVs isolated by PP tend to be contaminated by polymers and proteins (41). The isolation method, which is linked to the purity of EVs, is suggested to be chosen according to different research purposes (26).

With the boosted development of technology, novel strategies have been developed to isolate EVs efficiently. Microfluidic techniques allow the isolation of EVs considering their physical and biochemical properties simultaneously. Acoustic (47), electrical (48), and electromagnetic field forces (49) can be addressed inside microfluidic devices to isolate EVs, along with immuno-based (50) and asymmetric flow field flow-based (51) microfluidic techniques. While this technology is still developing, the efficiency, simplicity, and low initial volume of the sample

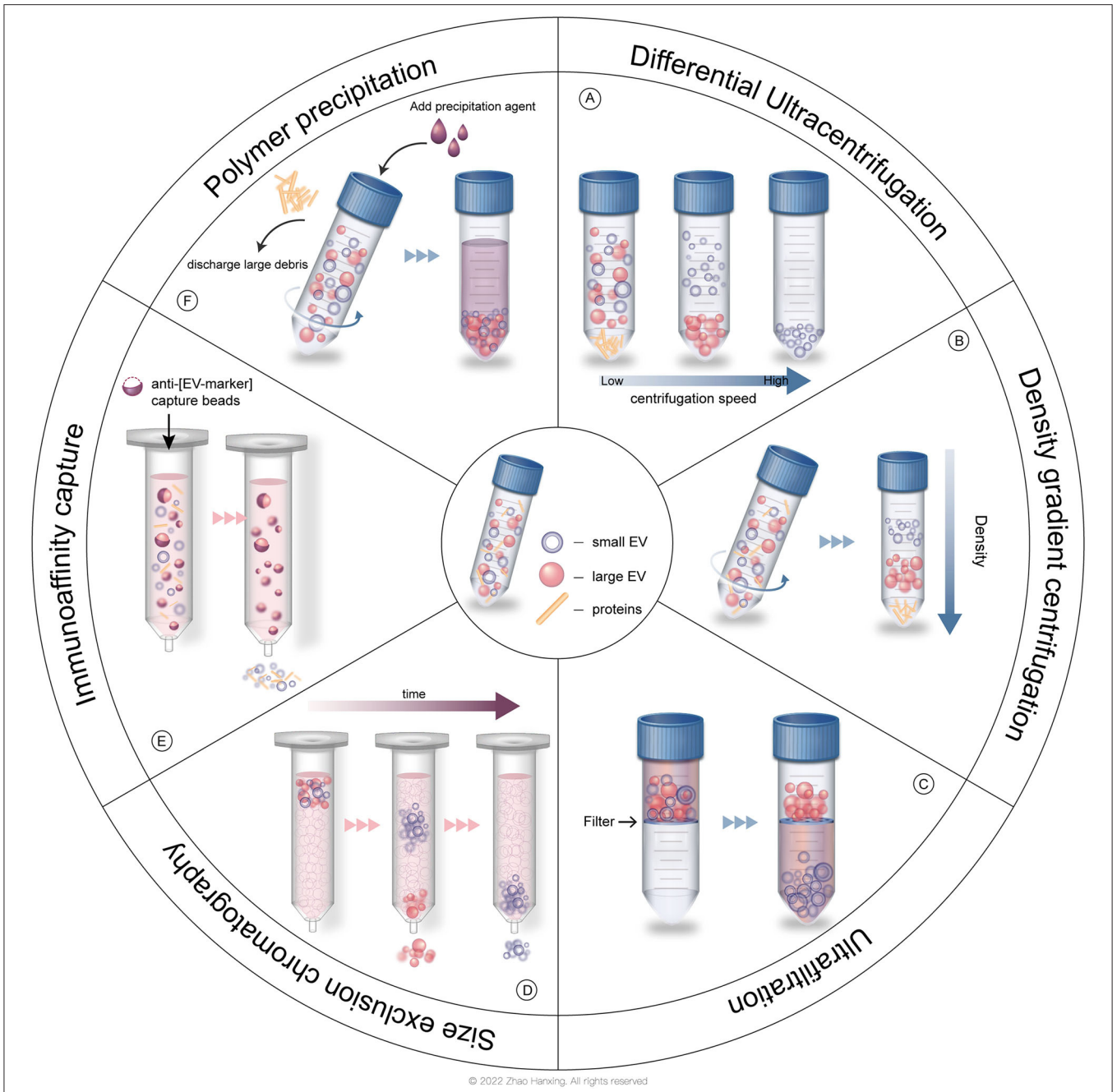

FIGURE 3 | Common isolation strategies of EVs. **(A)** Differential ultracentrifugation (DC). **(B)** Density gradient centrifugation (DGC). **(C)** Ultrafiltration (UF). **(D)** Size exclusion chromatography (SEC). **(E)** Immunoaffinity capture (IC). **(F)** Polymer precipitation (PP).

render it a promising method for future clinical application. Other methods of large-scale EV production include the use of bioreactor culture of parental cells, in which the characteristics of EVs need to be clarified with the culture condition in the bioreactor (52). Shear stress and cell extrusion can scale up EV-like vesicles production, while the purity of vesicles is relatively poor (53). Hydrostatic filtration dialysis and cytochalasin B induced vesicles have also been reported to improve EVs yield (54, 55). Immortalization of MSCs is also a potential strategy, along with increased safety concerns (56).

For the characterization of EVs, each subtype has been identified by some detection strategies based on their morphology, size, biomarkers of surface, and contents. The morphology of EVs is frequently observed by scanning electron microscopy and transmission electron microscopy (26). Electron cryo-microscopy and atomic force microscopy are

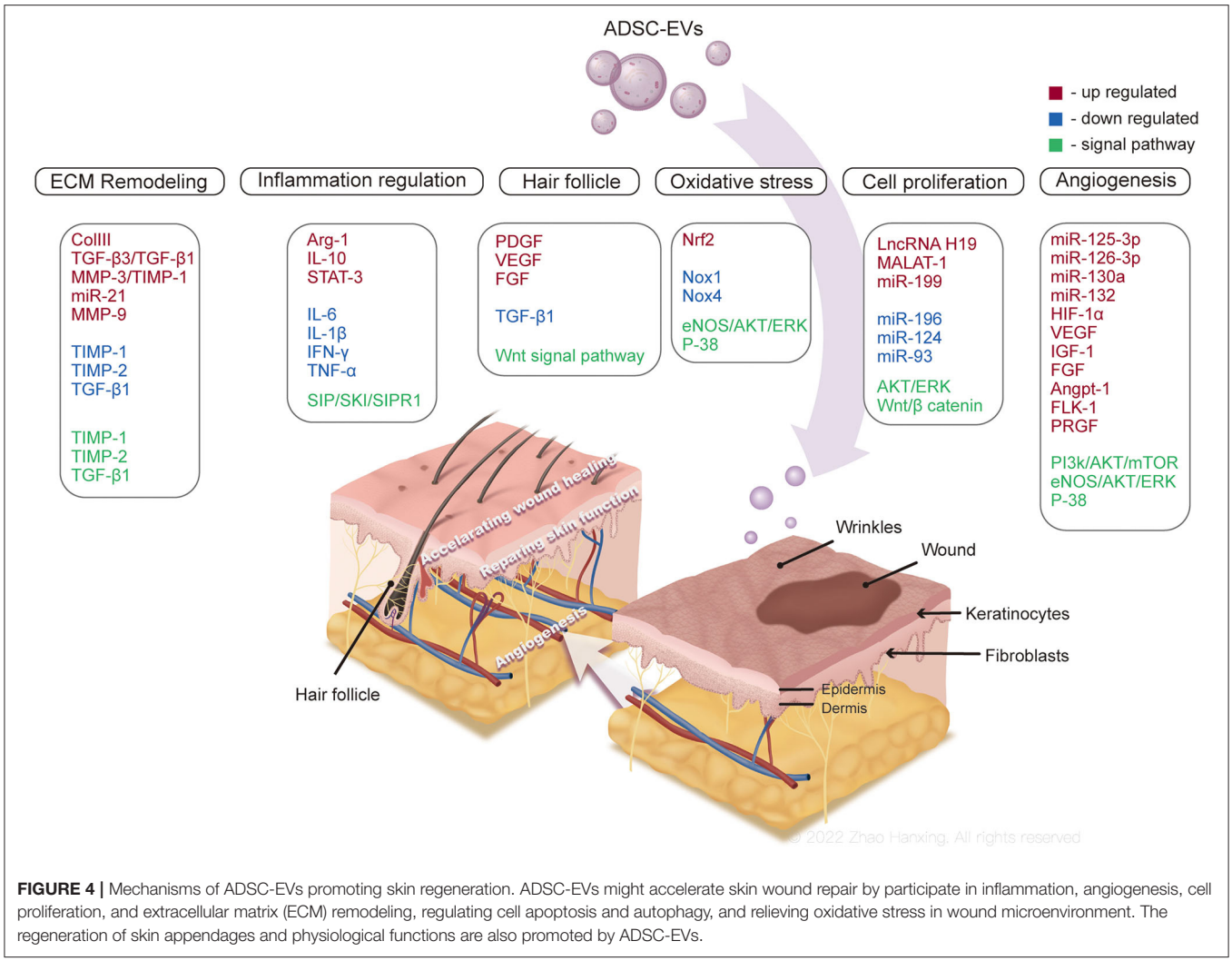

FIGURE 4 | Mechanisms of ADSC-EVs promoting skin regeneration. ADSC-EVs might accelerate skin wound repair by participate in inflammation, angiogenesis, cell proliferation, and extracellular matrix (ECM) remodeling, regulating cell apoptosis and autophagy, and relieving oxidative stress in wound microenvironment. The regeneration of skin appendages and physiological functions are also promoted by ADSC-EVs.

also used (28). The size distribution and concentration of EVs are usually detected by nanoparticle tracking analysis and dynamic light scattering, and tunable resistive pulse sensing (57). Some new technologies, such as light microscopic single EV analysis, have been utilized to analyze the properties of a single EV (58). Common biochemical analysis methods of EVs include western blotting, flow cytometry, and liquid chromatography and mass spectrometry. In recent years, new technologies for EVs analysis have emerged, including small particle flow cytometry, micronuclear magnetic resonance, and thermophoretic profiling (33).

MECHANISMS BY WHICH ADSC-EVs PLAY A THERAPEUTIC ROLE IN SKIN REGENERATION

Recent studies have demonstrated the beneficial role of ADSC-EVs in multiple tissue regeneration, such as skin (59), tendon (60), bone (61), and nerve tissue (62). ADSC-EVs exert a regenerative effect by delivering signals to cells with single or coordinated actions of biomolecules. Wound healing is one of the dominant components of skin regeneration and consists of several intricate and dynamic processes: hemostasis, inflammation, proliferation, and remodeling (63). ADSC-EVs participate in each process of wound healing, along with the regeneration of skin physiological functions to achieve ideal skin regeneration. The comprehensive abstract of current understandings of ADSC-EVs functioning in skin regeneration is shown in **Figure 4**.

Promote Wound Healing

Inflammation Regulation

In the process of ideal wound healing, the immune system is supposed to defend against the invasion of pathogens by a moderate inflammatory response. When immune homeostasis is compromised, excess and persistent inflammation contributes to impaired wound healing, such as in chronic diabetic wounds (64). ADSC-EVs improve the inflammatory microenvironment at wound sites by regulating the activities of immune cells, thereby accelerating wound repair.

ADSC-EVs can regulate the balance between CD4 T cell subsets (65) and inhibit the proliferation of T cells and the release of inflammatory factor IFN-γ (66). The engulfment of ADSC-EVs by macrophages and subsequent increased expression of Arg-1 and IL-10, soluble markers of anti-inflammatory phenotype macrophages (M2) (67), were observed in obese mice. Mechanically, ADSC-EVs induced transactivation of Arg-1 in macrophages by transferring signal transducer and activator of transcription 3 (68). Additionally, the polarization of M2 macrophages after treatment with ADSC-EVs was found to be associated with the S1P/SK1/S1PR1 signaling pathway, along with reduced expression of inflammatory cytokines IL-6, IL-1β, IFN-γ, and TNF-α (69).

The immunosuppressive activity of ADSC-EVs regulates inflammation in skin wounds, too. Interestingly, another study demonstrated that ADSC-EVs attenuated the polarization of inflammatory M1 macrophages, while hardly inducing M2 polarization (70). Although clarification of this controversy needs to be addressed in further investigation, both inhibited M1 polarization and increased M2 polarization led to improved inflammation. In addition, treatment of ADSC-EVs in ischemia-reperfusion skin flaps resulted in less infiltration of inflammatory cells and ameliorated apoptosis (71).

Current studies have demonstrated the effects of ADSC-EVs as mediators in the inflammatory response, in which the inhibition of inflammation dominates, promoting wound repair. However, it is noteworthy that a necessary inflammatory response also contributes to the protection of the wound microenvironment (72). In the early stage of using ADSC-EVs, they were indicated to cause inflammation, whereas exert pro-adipogenic function and promote collagen synthesis in the late stage (73). From this perspective, homeostasis of inflammation at wound sites needs to be considered in both research and application of ADSC-EVs, rather than absolute inhibition of inflammation.

Angiogenesis

Angiogenesis involves multiple cytokines and intricate signaling pathways, which are essential for the supply of oxygen and nutrients as skin wounds heal. ADSC-EVs have been documented to trigger angiogenesis by transferring contained proangiogenic mediators. Neovascularization of human umbilical vein endothelial cells (HUVECs) was promoted with the treatment of ADSC-EVs, which was more robust when miR-126-3p was overexpressed (74). Other microRNAs carried by ADSC-EVs were also reported to participate in angiogenesis, such as miR-126, miR-130a, and miR-132 (75). Additionally, miR-125a-3p from ADSC-EVs enhanced angiogenesis of HUVECs by activating the PI3K/AKT signaling pathway, targeting the PTEN gene (76). Another study indicated that ADSC-EVs also contributed to angiogenesis in the diabetes microenvironment by increasing HIF-1α and VEGF expression through the PI3K/AKT/mTOR signaling pathway (77). The angiogenic potential of ADSC-EVs might be enhanced in the specific microenvironment. Under hypoxia conditions, ADSC-EVs encapsulated more proangiogenic growth factors, including IGF-1, FGF, VEGF and their receptors (17), angiopoietin-1, and fetal liver kinase-1 (78), and demonstrated more prominent neovascularization and faster wound repair. With the stimulus of PDGF, secretion of ADSC-EVs increased, along with upregulated c-kit and SCF (79). The c-kit is a tyrosine kinase receptor that regulates the differentiation of progenitor cells to blood or vascular endothelial cells. C-kit ligand SCF is a kind of stem cell regulator that plays an important role in angiogenesis and recruitment of MSCs (80). EVs released by ADSCs overexpressing glyoxalase-1 (GLO-1) promoted capillary growth compared with normal ADEC-EVs under high-glucose conditions by upregulating the eNOS/AKT/ERK/P-38 signaling pathway, which regulates the proliferation and migration of HUVECs (17).

ADSC-EVs facilitate angiogenesis by providing cargos that participate in capillary growth or activate angiogenic signaling pathways, thereby promoting wound healing. However, newly formed capillaries are supposed to degrade to form an appropriate vascular density similar to normal skin at the late stage of wound healing without scarring (81). In wound repair, further experiments are necessary to figure out optimal administration time and quantity of ADSC-EVs, avoiding potential side effects, such as scar formation out of excessive angiogenesis caused by the overdose of ADSC-EVs.

Cell Proliferation

During the proliferative phase of wound healing, epithelialization occurs mainly by proliferating and migrating to the wound site of epithelial cells. Fibroblasts are activated to proliferate and produce ECM to repair the defect. ADSC-EVs can be engulfed by human skin fibroblasts (HSFs) and HaCaT keratinocytes, promoting subsequent proliferation and migration (74, 82) in a dose-dependent manner (83). After the uptake of ADSC-EVs, the cell cycle of HSF was stimulated to accelerate re-epithelialization (82, 83) by the activation of AKT and ERK signaling pathways (82). Intriguingly but predictably, the Wnt/β-catenin signaling pathway, which participates closely in cell growth and renewal, was also involved in the proliferative effect of ADSC-EVs (84, 85). Long non-coding RNA (lncRNA) H19 in ADSC-EVs combined with miR-19b and inhibited its expression, targeting SRY-related high-mobility-group box 9, thus promoting wound healing (84). ADSC-EVs promote the proliferation and migration of human dermal fibroblasts (HDFs) and HaCaT keratinocytes by lncRNA MALAT-1 targeting miR-124 (85). Additionally, boosted proliferation and migration of HDFs were induced by upregulated miR-199 and downregulated miR-93 contained in ADSC-EVs (86). Finally, ADSC-EVs-treated M2 macrophages contributed to the proliferation and self-renewal of ADSCs (68).

Extracellular Matrix Remodeling

The synthesis and remodeling of ECM affect the formation of hypertrophic scars and the time of wound healing. Scar, which is composed of ECM, mostly collagen I (87), provides temporary strength to injured skin and will be degraded by matrix metalloproteinases (MMPs) gradually in the wound healing process (88). ADSC-EVs have been demonstrated to regulate the process of ECM remodeling. With the treatment

of ADSC-EVs, deposition of collagen I and III with a well-organized histological structure increased at the wound site, along with the regeneration of skin appendages (89, 90). ADSC-EVs facilitated ECM remodeling during wound repair by upregulating the ratio of collagen III/I, TGF-β3/TGF-β1, and MMP-3/tissue inhibitors of MMP-1 (TIMP-1). The differentiation of fibroblasts to myofibroblasts that contribute to scarring was also inhibited by ADSC-EVs (91). Overexpressed miR-21 in ADSC-EVs promoted the expression of MMP-9 and MMP-3 and suppressed that of TIMP-1, TIMP-2 and TGF-β1 by activating the PI3K/AKT signaling pathway to restrain scar formation (92). Although persistent high MMPs levels indicated extra ECM degradation and poor prognosis in diabetic wounds (93), ADSC-EVs boosted the deposition of collagen, which is essential for ECM formation in skin wounds, exerting a positive effect on ECM remodeling (94). In the mouse model, ADSC-EVs were reported to increase the synthesis of collagen to accelerate wound repair, which was inhibited in the late stage to reduce scarring (83). However, with the treatment of ADSC-EVs, HSF produced less collagen I, collagen III, and α-SMA, which differed from other studies, although they all ameliorated scar formation (95). This controversial result might be because that HSF in this study was isolated from hypertrophic scar tissue, in which HSF remained persistently hyperactive (96) while other studies utilized cells from normal skin tissue.

Autophagy and Apoptosis Modulation

From the orthodox perspective, autophagy and apoptosis were merely considered to be essential parts during skin wound healing. However, some studies have documented that ADSC-EVs promote wound repair with autophagy and apoptosis involved in the microenvironment of the wound site. Overexpressed circular RNA mmu_circ_0000250 in ADSC-EVs suppressed the expression of miR-128-3p in endothelial progenitor cells (EPCs), hence activating autophagy of EPCs and attenuating apoptosis of skin tissue (16). Moderate autophagy has been demonstrated to augment angiogenesis by recovering the function of EPCs (97), thus promoting wound healing. ADSC-EVs also ameliorated apoptosis of skin cells under irritations, acting as a protective buffer in the wound microenvironment (17, 98). Interestingly, MSCs underwent remarkable apoptosis after transplantation *in vivo*, but they still exerted prominent therapeutic effects and prevented hypertrophic scar formation (99). ADSCs might participate in wound healing by secreting EVs in healthy conditions, but also transferring therapeutic information when they are dying. ADSC-EVs produced during apoptosis are potential functional parts, which need further investigations.

Oxidative Stress Relief

The generation of reactive oxygen species (ROS) in the processes of wound healing is required to defend against the invasion of pathogenic microbes and active cell survival signaling (100). Nevertheless, excessive ROS in the microenvironment of skin wounds causes oxidative damage and impaired wound healing. For example, in diabetic wounds, persistent high glucose level activates protein kinase C in smooth muscle and endothelial cells, increasing the activity of NDPH and the production of ROS, which leads to impairment of the viability of dermal fibroblasts and keratinocytes (64). After long-term exposure to high glucose, endothelial cells tend to reduce the secretion of vasoactive factor endothelial nitric oxide synthase (eNOS), resulting in restricted blood flow and difficult wound healing (101). ADSC-EVs have been investigated to exert protective effects in such an oxidative stress microenvironment, maintaining the biological activities of cells. ADSC-EVs relieved ROS damage in EPCs induced by high glucose via the reduced expression of oxidative stress-related proteins NOX1 and NOX4, which could be inhibited by the EV inhibitor GW4869 and enhanced by overexpression of nuclear factor erythroid 2-related factor 2 (102). When facing oxidative stress caused by hydrogen peroxide (H_2O_2), ADSC-EVs also maintained the viability and metabolic activity of keratinocytes and HSF (18), which might be attributed to lncRNA MALAT-1 contained in ADSC-EVs (85, 103). Additionally, EVs derived from ADSCs pretreated with H_2O_2 possessed a more prominent effect on oxidative stress relief and microvessel formation (71). Some studies have documented that pretreatment with H_2O_2 enables MSCs to produce higher levels of miR-21 to relieve cell death caused by oxidative stress (104, 105). Irritation seems to change the cargos of ADSC-EVs, thereby affecting their functions. GLO-1 is the rate-limiting enzyme in the glyoxalase system that plays an important role in the detoxification of advanced glycation end products (106, 107), accelerating the clearance of ROS in endothelial cells (108). After coculture with ADSC-EVs containing GLO-1, HUVECs accumulated less ROS and inflammatory cytokine IL-1β in a high glucose wound environment, with the involvement of the eNOS/AKT/ERK/P-38 signaling pathways (17).

Regeneration of Skin Physiological Function

The closure of skin wounds is not the end of perfect skin regeneration, in which the recovery of normal structure and physiological function are also important. The barrier function of the skin mainly relies on the external layer, the epidermis that lies openings of appendages (hair follicles, sweat glands, and sebaceous glands) and intercellular lipids (ceramides, filaggrin, and cholesterol) (109–111). Recent studies have demonstrated that ADSC-EVs function as positive regulators in recovering skin physiological function, at least partly.

Hair Follicle Regeneration

Hair deficiency is one of the major aesthetic complaints not only in patients with alopecia but also in those who have healed skin wounds without hair follicle regeneration. Moreover, skin with more hair follicles heals faster than that with less hair or without hair, which is due to the involvement of hair follicle stem cells in wound healing (112, 113). However, wound repair of adult mammals is likely to form scars without skin appendage regeneration (114). ADSC-EVs seemed to rescue hair regeneration in some way. In nude mice models, additional 50 μg/ml ADSC-EVs in experimental groups were grafted with dermal cells and epidermal cells to skin wounds, in which more hairs with

normal structure and mature hair follicles were observed, along with higher expression of PDGF and VEGF and lower TGF-β1 expression in skin tissue (20). Although morphological observation cannot provide a detailed explanation mechanically, PDGF and VEGF are deemed to be growth regulators of hair follicles in the anagen phase (115). In addition, the reduced expression of TGF-β1 might contribute to hair maintenance, since it participates in the catagen phase of hair development and affects hair follicle apoptosis-associated molecules (116, 117). ADSC-EVs themselves also contain cytokines that stimulate hair follicle growth, including VEGF and FGF (17, 118), and enable the activation of the Wnt signaling pathway essential to hair follicle induction (85, 98, 119, 120). Even so, more research in this field is required to decipher the specific molecular mechanism of hair follicle regeneration promoted by ADSC-EVs. Current studies are largely based on rodent models, however, the structure of the skin and mechanisms of wound healing in humans and rodents are different.

Skin Barrier Repair

The epidermal barrier of the skin is supplied by stratum corneum (SC), which consists of corneocytes and an intercellular lipid mixture of ceramides, free fatty acids, and cholesterol (111). Among lipids in SC, ceramides are the dominant content, with weight over 50% (121), the defect of which is a critical part of etiology in atopic dermatitis (AD). Recently, ADSC-EVs have been indicated to promote skin barrier repair in AD mouse models. With the injection of ADSC-EVs, impaired SC hydration induced by oxazolone was normalized. Meanwhile, the quantity of long-chain dihydroceramide, a precursor component during de novo synthesis of ceramides, was significantly increased (19, 122). Predictably, enhanced synthesis of sphingosine-1-phosphate (S1P), a metabolite of ceramides, was also observed in this study. S1P has been reported to inhibit ceramide-associated apoptosis and stimulate the viability and differentiation of keratinocytes (123, 124). As mentioned before, ADSC-EVs activated the S1P / SK1 / S1PR1 signaling pathway to promote M2 macrophages polarization, thus attenuating inflammation (69), which is in accordance with the reduced inflammatory cytokines, such as TNF-α and IFN-γ (19). The lipid regenerative function of ADSC-EVs might be partly due to their regulatory role in inflammation. The particular actions of contents in ADSC-EVs helping skin barrier repair remain elusive, but ADSC-EVs may be a potential cell-free therapeutic approach for regeneration of skin barrier function.

PRECLINICAL AND CLINICAL STUDIES OF ADSC-EVs FOR SKIN REGENERATION AND REPAIR AFTER INJURY

Wound Healing

After long-term exploration, researchers gradually found the advantages and appropriate drug delivery methods of ADSC-EVs in skin regeneration and repair. Initially, the application of human fibrocyte-derived EVs in wound models of diabetic mice showed that all wound healing was significantly enhanced (125). EVs derived from other MSCs were also found to play a critical role in promoting re-epithelialization, collagen synthesis and angiogenesis in skin wound healing (126, 127). Considering that it would be easier to obtain autologous ADSC when it is finally applied to human wound treatment because liposuction has been very common and mature, researchers mixed ADSC-EVs with fibroblasts and demonstrated that this synergistic effect was helpful to induce the enrichment of miRNAs related to promoting wound healing in fibroblasts (86). Earlier it was shown that direct IV administration of ADSC-EVs in a murine wound model was beneficial to ameliorate cutaneous repair by regulating ECM remodeling (91). Furthermore, local injection of ADSC-EVs into mouse full-thickness cutaneous wounds significantly increased re-epithelialization, collagen deposition, and neovascularization and induced accelerated wound closure (82). To explore the therapeutic potential of ADSC-EVs more accurately, BMSC-EVs and ADSC-EVs were applied, respectively to diabetic wounds, and the results demonstrated that ADSC-EVs possess the more potent pro-angiogenic activity and can promote the wound healing of diabetic ulcers (13). Considering the availability of adipose tissue and fewer ethical concerns of EVs, emerging skin regenerative studies tend to focus on ADSC-EVs to better transform to future clinical trials (128).

Since the regeneration and repair mechanism of swine skin is similar to that of humans, swine skin is more promising than rodent skin for studying skin wounds. The topical conditioned medium of ADSC therapy displayed increased angiogenesis and a diminished inflammatory response and improved the wound closure rates in the full-thickness dorsal wound models in pigs (129). However, such research reports are very scarce. We analyze the possible reasons from two aspects. On the one side, it is technically and economically more difficult to operate diabetic or burn wound models in large animals. On the other side, the application of EVs in large animals requires a larger dose of EVs, which is limited by current EV isolation methods. Researchers need to accelerate the maturation of methods producing large-scale EVs or find new delivery methods to improve local retention of EVs, which is more conducive to the research on EVs application in the future.

At the time of this review writing, only a few trials related to applying EVs to treat skin wounds can be searched on the web clinicaltrials.gov (accessed on Nov. 20, 2021). Unfortunately, no trial related to ADSC-EVs is included until now, however, the following summary of other EVs applied to skin wound repair has important reminder and reference values for the subsequent direct application of ADSC-EVs in this field. Autologous serum-derived EVs will be evaluated to determine whether they could play a positive role in cutaneous wound healing (NCT02565264) and venous ulcers not responsive to conventional treatments (NCT04652531). One trial will investigate the therapeutic potential of stem cell-conditioned medium as an additional growth factor in chronic skin ulcer healing (NCT04134676). Another trial that has completed patient recruitment aims to develop a safe and reasonable method of administering BMSC-EVs to burn wounds (NCT05078385). Although no EV product

had been approved by the FDA to date, it is firmly believed that more clinical studies will be included soon, and high-quality clinical trial results can energetically promote the final clinical application of EVs.

Skin Photoaging and Senescence

As the most commonly used stem cell therapeutics, the application of ADSCs in skin rejuvenation has been widely investigated. The paracrine effects of ADSCs, which are characterized by the release of cytokines in the form of EVs, are recognized as critical mechanisms in skin tissue repair and regeneration. Drawing support from their paracrine effects, ADSC-free derivatives, including ADSC-EVs and ADSC conditioned medium (ADSC-CM), have gained attention as novel therapeutics in ameliorating skin health (24, 130). As is universally acknowledged, human dermal fibroblasts (HDFs) work as essential objects in anti-wrinkle, wound healing, skin aging, and overall homeostasis studies. The ADSC-EVs and ADSC-CM acted as therapeutic agents in skin rejuvenation by improving proliferation, migration, and collagen synthesis in HDFs without adverse effects (131, 132). Because ADSC-CM could effectively downregulate the activation and transcription of UVB-related signaling pathways and upregulate antioxidant response agent expression, it was regarded to play a positive role in keeping HDFs away from UVB-induced photoaging damage (133). By decreasing ROS production and MMPs overexpression, which are directly linked to ECM proteins degradation, ADSC-EVs slowed wrinkle formation and skin photoaging (70, 134). Morphometric and morphological assessment of histological changes showed that ADSC-EVs could decrease UV-mediated epidermal thickening and prevent skin damage caused by UV photoaging (135). Because research on ADSC-EVs is still limited, the majority of studies on the therapeutic function of ADSC derivatives in skin rejuvenation focus on ADSC-CM. Despite slight differences in protein properties that exist between ADSC-EVs and ADSC-CM, these two main components in ADSC derivatives contain factors linked to ECM remodeling and immunoregulation, which are crucial for maintaining skin homeostasis and antiaging (136). Furthermore, the removal of EVs from ADSC-CM significantly weakened its positive effects on cell proliferation, migration, and scar prevention (137, 138). This demonstrates that EVs are crucial components in ADSC-CM and may possess an independent or synergistic role that is beneficial for anti-skin photoaging.

Skin Pigmentation After Trauma

In posttraumatic skin regeneration, the non-Caucasian race is more susceptible to pigmentation and/or scar formation. For such patients, anti-scar treatment while desalinating the pigment as far as possible will be conducive to the appearance of regenerated skin closer to normal. The increased expression of S1P induced by ADSC-EVs was negatively correlated with the production of melanin, which implies that ADSC-EVs have potential application value in skin-brightening (19). As shown in a prospective, double-blind, randomized, placebo-controlled study, a cosmetic formulation containing ADSC-EVs decreased skin melanin contents and reversed hyperpigmentation in human volunteers (139). Although the effect of ADSC-EVs on improving skin brightness becomes weak with time due to the limitation of transdermal delivery, the actuation duration of ADSC-EVs will be expected to be ameliorated with the continuous development of new drug delivery agents such as nano biomaterials. In the early stage of skin injury repair, the application of ADSC-EVs can promote scarless healing (83), but whether similar effects will appear in colored people and whether they could dilute pigmentation while reducing scarring need to be further studied.

Due to the different types of skin damage, the diversity of the involved skin layers also exists. Further research will be needed to locate which cells in the skin damage microenvironment are targets of ADSC-EVs. It is foreseeable that accurately applying EVs to selectively act on target cells in the epidermis or dermis will greatly contribute to further explaining the specific mechanism of EVs' regenerative function.

CHALLENGES AND PROSPECTS

ADSCs have been demonstrated to play a beneficial role in skin regeneration and rejuvenation due to their participation in multiple biological activities of skin cells. ADSC-EVs, the products, and the information disseminators of ADSCs, seem to inherit similar therapeutic effects from their parental cells but are safer and more convenient to use. ADSC-EVs may promote skin regeneration, including structural repair and functional recovery, by accelerating the canonical wound repair process and regulating the skin microenvironment. The regenerative effect of ADSC-EVs renders them a potential option for clinical application in wound treatment and skin cosmetology. With multiple signal recognition molecules anchoring to the natural lipid membrane, ADSC-EVs are underlying carriers delivering drugs *in vivo*. EVs have been modified to carry therapeutic molecules by multiple loading methods, such as transfection of parental cells for endogenous loading (16), electroporation (140), co-incubation (141), and freeze-thawing (142) for exogenous loading. Furthermore, the combination between ADSC-EVs and bioactive scaffolds is an effective strategy to improve the quick clearance of ADSC-EVs at the wound site. Meanwhile, hydrogel dressings containing ADSC-EVs can be modified to possess functions promoting wound repair, such as antibacterial (89) and antioxidation (18).

Nevertheless, as mentioned above, current comprehension of ADSC-EVs themselves and the mechanisms of their actions remain elusive, and challenges exist in their manufacture and application. With skin structure more similar to human skin, pigs and guinea pigs are preferred animal models for skin wound research than rodent models mostly used in current studies of ADSC-EVs in skin regeneration. More convincing evidence needs to be uncovered to clarify the current enigma existing in the mechanisms of ADSC-EVs. For example, regulation of ADSC-EVs on the proliferation and differentiation of fibroblasts, which is essential for wound repair but results in scar formation when overwhelming. From a current perspective, the effect of ADSC-EVs is strongly associated with their contents,

which are influenced by the physiological conditions of their parental cells (14, 143). Diverse isolation methods also lead to discrepancies in cargo (25). Quality control of ADSC-EVs is fundamental to probe the particular portion of ADSC-EVs functioning directly or mediately as key therapeutics in skin regeneration, thus further formulating instructive protocols to study or manufacture in the future. Likewise, a low yield of ADSC-EVs is also a crucial issue, which is attributed to the limited culture medium of ADSCs and repeated centrifugation processes in conventional isolation methods. Strategies for the production with large quantities and long-term storage of ADSC-EVs must be developed for clinical application. To date, research on ADSC-EVs has mainly remained at the laboratory level. To utilize the regenerative and therapeutic functions of ADSC-EVs, much more comprehensive information needs to be uncovered.

AUTHOR CONTRIBUTIONS

YW, LC, and ZZ: conceptualization. YW and ZZ: validation. YW, LC, HZ, ZL, and JC: investigation. YC and ZZ: resources. YW: original draft preparation. LC and ZZ: review and editing. HZ, YC, and JC: visualization. ZZ: supervision and project administration. ZZ and ZL: funding acquisition. All authors have read and agreed to the published version of the manuscript, accepted responsibility for the entire content of this manuscript, and approved its submission.

FUNDING

This work was supported by grants from the National Natural Science Foundation of China (No. 81871574), and Scientific Research Projects of Sichuan Health Commission (No. 19PJ097).

REFERENCES

1. Saeedi P, Petersohn I, Salpea P, Malanda B, Karuranga S, Unwin N, et al. Global and regional diabetes prevalence estimates for 2019 and projections for 2030 and 2045: results from the international diabetes federation diabetes atlas, 9(th) edition. *Diabetes Res Clin Pract.* (2019) 157:107843. doi: 10.1016/j.diabres.2019.107843
2. Walsh JW, Hoffstad OJ, Sullivan MO, Margolis DJ. Association of diabetic foot ulcer and death in a population-based cohort from the United Kingdom. *Diabet Med.* (2016) 33:1493–8. doi: 10.1111/dme.13054
3. Nourian Dehkordi A, Mirahmadi Babaheydari F, Chehelgerdi M, Raeisi Dehkordi S. Skin tissue engineering: wound healing based on stem-cell-based therapeutic strategies. *Stem Cell Res Ther.* (2019) 10:111. doi: 10.1186/s13287-019-1212-2
4. Welz PS. Clock regulation of skin regeneration in stem cell aging. *J Invest Dermatol*. (2021)141:1024–30. doi: 10.1016/j.jid.2020.10.009
5. Tompkins BA, DiFede DL, Khan A, Landin AM, Schulman IH, Pujol MV, et al. Allogeneic mesenchymal stem cells ameliorate aging frailty: a phase II randomized, double-blind, placebo-controlled clinical trial. *J Gerontol A Biol Sci Med Sci.* (2017) 72:1513–22. doi: 10.1093/gerona/glx137
6. Trounson A, McDonald C. Stem cell therapies in clinical trials: progress and challenges. *Cell Stem Cell.* (2015) 17:11–22. doi: 10.1016/j.stem.2015.06.007
7. Liu A, Zhang X, He H, Zhou L, Naito Y, Sugita S, et al. Therapeutic potential of mesenchymal stem/stromal cell-derived secretome and vesicles for lung injury and disease. *Expert Opin Biol Ther.* (2020) 20:125–40. doi: 10.1080/14712598.2020.1689954
8. Swaminathan M, Stafford-Smith M, Chertow GM, Warnock DG, Paragamian V, Brenner RM, et al. Allogeneic mesenchymal stem cells for treatment of AKI after cardiac surgery. *J Am Soc Nephrol.* (2018) 29:260–7. doi: 10.1681/ASN.2016101150
9. EL Andaloussi S, Mäger I, Breakefield XO, Wood MJ. Extracellular vesicles: biology and emerging therapeutic opportunities. *Nat Rev Drug Discov*. (2013) 12:347–57. doi: 10.1038/nrd3978
10. Keshtkar S, Azarpira N, Ghahremani MH. Mesenchymal stem cell-derived extracellular vesicles: novel frontiers in regenerative medicine. *Stem Cell Res Ther.* (2018) 9:63. doi: 10.1186/s13287-018-0791-7
11. Park JH, Hwang I, Hwang SH, Han H, Ha H. Human umbilical cord blood-derived mesenchymal stem cells prevent diabetic renal injury through paracrine action. *Diabetes Res Clin Pract.* (2012) 98:465–73. doi: 10.1016/j.diabres.2012.09.034
12. Jeyaram A, Jay SM. Preservation and storage stability of extracellular vesicles for therapeutic applications. *AAPS J.* (2017) 20:1. doi: 10.1208/s12248-017-0160-y
13. Pomatto M, Gai C, Negro F, Cedrino M, Grange C, Ceccotti E, et al. Differential therapeutic effect of extracellular vesicles derived by bone marrow and adipose mesenchymal stem cells on wound healing of diabetic ulcers and correlation to their cargoes. *Int J Mol Sci.* (2021) 22:3851. doi: 10.3390/ijms22083851
14. Casado-Díaz A, Quesada-Gómez JM, Dorado G. Extracellular vesicles derived from mesenchymal stem cells (MSC) in regenerative medicine: applications in skin wound healing. *Front Bioeng Biotechnol.* (2020) 8:146. doi: 10.3389/fbioe.2020.00146
15. Kim H, Lee JW, Han G, Kim K, Yang Y, Kim SH. extracellular vesicles as potential theranostic platforms for skin diseases and aging. *Pharmaceutics.* (2021) 13:760. doi: 10.3390/pharmaceutics13050760
16. Qu Y, Zhang Q, Cai X, Li F, Ma Z, Xu M, et al. Exosomes derived from miR-181-5p-modified adipose-derived mesenchymal stem cells prevent liver fibrosis via autophagy activation. *J Cell Mol Med.* (2017) 21:2491–502. doi: 10.1111/jcmm.13170
17. Zhang X, Jiang Y, Huang Q, Wu Z, Pu H, Xu Z, et al. Exosomes derived from adipose-derived stem cells overexpressing glyoxalase-1 protect endothelial cells and enhance angiogenesis in type 2 diabetic mice with limb ischemia. *Stem Cell Res Ther.* (2021) 12:403. doi: 10.1186/s13287-021-02475-7
18. Shiekh PA, Singh A, Kumar A. Exosome laden oxygen releasing antioxidant and antibacterial cryogel wound dressing OxOBand alleviate diabetic and infectious wound healing. *Biomaterials.* (2020) 249:120020. doi: 10.1016/j.biomaterials.2020.120020
19. Shin KO, Ha DH, Kim JO, Crumrine DA, Meyer JM, Wakefield JS, et al. Exosomes from human adipose tissue-derived mesenchymal stem cells promote epidermal barrier repair by inducing de novo synthesis of ceramides in atopic dermatitis. *Cells.* (2020) 9:680. doi: 10.3390/cells9030680
20. Wu J, Yang Q, Wu S, Yuan R, Zhao X, Li Y, et al. Adipose-derived stem cell exosomes promoted hair regeneration. *Tissue Eng Regen Med.* (2021) 18:685–91. doi: 10.1007/s13770-021-00347-y
21. Wolf DA, Beeson W, Rachel JD, Keller GS, Hanke CW, Waibel J, et al. Mesothelial stem cells and stromal vascular fraction for skin rejuvenation. *Facial Plast Surg Clin North Am.* (2018) 26:513–32. doi: 10.1016/j.fsc.2018.06.011
22. Zarei F, Abbaszadeh A. Stem cell and skin rejuvenation. *J Cosmet Laser Ther.* (2018) 20:193–7. doi: 10.1080/14764172.2017.1383615
23. Shukla L, Yuan Y, Shayan R, Greening DW, Karnezis T. Fat therapeutics: the clinical capacity of adipose-derived stem cells and exosomes for human disease and tissue regeneration. *Front Pharmacol.* (2020) 11:158. doi: 10.3389/fphar.2020.00158
24. Cai Y, Li J, Jia C, He Y, Deng C. Therapeutic applications of adipose cell-free derivatives: a review. *Stem Cell Res Ther.* (2020) 11:312. doi: 10.1186/s13287-020-01831-3
25. Gurunathan S, Kang MH, Jeyaraj M, Qasim M, Kim JH. Review of the isolation, characterization, biologial function, and multifarious therapeutic approaches of exosomes. *Cells*. (2019) 8:307. doi: 10.3390/cells8040307
26. Théry C, Witwer KW, Aikawa E, Alcaraz MJ, Anderson JD, Andriantsitohaina R, et al. Minimal information for studies of extracellular

vesicles 2018 (MISEV2018): a position statement of the international society for extracellular vesicles and update of the MISEV2014 guidelines. *J Extracell Vesicles.* (2018) 7:1535750. doi: 10.1080/20013078.2018.1535750
27. van Niel G, D'Angelo G, Raposo G. Shedding light on the cell biology of extracellular vesicles. *Nat Rev Mol Cell Biol.* (2018) 19:213–28. doi: 10.1038/nrm.2017.125
28. Wu P, Zhang B, Ocansey DKW, Xu W, Qian H. Extracellular vesicles: a bright star of nanomedicine. *Biomaterials.* (2021) 269:120467. doi: 10.1016/j.biomaterials.2020.120467
29. Colombo M, Moita C, van Niel G, Kowal J, Vigneron J, Benaroch P, et al. Analysis of ESCRT functions in exosome biogenesis, composition and secretion highlights the heterogeneity of extracellular vesicles. *J Cell Sci.* (2013) 126:5553–65. doi: 10.1242/jcs.128868
30. Kajimoto T, Okada T, Miya S, Zhang L, Nakamura S. Ongoing activation of sphingosine 1-phosphate receptors mediates maturation of exosomal multivesicular endosomes. *Nat Commun.* (2013) 4:2712. doi: 10.1038/ncomms3712
31. Trajkovic K, Hsu C, Chiantia S, Rajendran L, Wenzel D, Wieland F, et al. Ceramide triggers budding of exosome vesicles into multivesicular endosomes. *Science.* (2008) 319:1244–7. doi: 10.1126/science.1153124
32. Andreu Z, Yáñez-Mó M. Tetraspanins in extracellular vesicle formation and function. *Front Immunol.* (2014) 5:442. doi: 10.3389/fimmu.2014.00442
33. Shao H, Im H, Castro CM, Breakefield X, Weissleder R, Lee H. New technologies for analysis of extracellular vesicles. *Chem Rev.* (2018) 118:1917–50. doi: 10.1021/acs.chemrev.7b00534
34. Connor DE, Exner T, Ma DD, Joseph JE. The majority of circulating platelet-derived microparticles fail to bind annexin V, lack phospholipid-dependent procoagulant activity and demonstrate greater expression of glycoprotein Ib. *Thromb Haemost.* (2010) 103:1044–52. doi: 10.1160/TH09-09-0644
35. Del Conde I, Shrimpton CN, Thiagarajan P, López JA. Tissue-factor-bearing microvesicles arise from lipid rafts and fuse with activated platelets to initiate coagulation. *Blood.* (2005) 106:1604–11. doi: 10.1182/blood-2004-03-1095
36. Atkin-Smith GK, Poon IKH. Disassembly of the dying: mechanisms and functions. *Trends Cell Biol.* (2017) 27:151–62. doi: 10.1016/j.tcb.2016.08.011
37. Lemke G. How macrophages deal with death. *Nat Rev Immunol.* (2019) 19:539–49. doi: 10.1038/s41577-019-0167-y
38. Li M, Liao L, Tian W. Extracellular vesicles derived from apoptotic cells: an essential link between death and regeneration. *Front Cell Dev Biol.* (2020) 8:573511. doi: 10.3389/fcell.2020.573511
39. Gomzikova MO, James V, Rizvanov AA. Therapeutic application of mesenchymal stem cells derived extracellular vesicles for immunomodulation. *Front Immunol.* (2019) 10:2663. doi: 10.3389/fimmu.2019.02663
40. Kowal J, Arras G, Colombo M, Jouve M, Morath JP, Primdal-Bengtson B, et al. Proteomic comparison defines novel markers to characterize heterogeneous populations of extracellular vesicle subtypes. *Proc Natl Acad Sci U S A.* (2016) 113:E968–77. doi: 10.1073/pnas.1521230113
41. Doyle LM, Wang MZ. Overview of extracellular vesicles, their origin, composition, purpose, and methods for exosome isolation and analysis. *Cells.* (2019) 8:727. doi: 10.3390/cells8070727
42. Kakarla R, Hur J, Kim YJ, Kim J, Chwae YJ. Apoptotic cell-derived exosomes: messages from dying cells. *Exp Mol Med.* (2020) 52:1–6. doi: 10.1038/s12276-019-0362-8
43. Tkach M, Théry C. Communication by extracellular vesicles: where we are and where we need to go. *Cell.* (2016) 164:1226–32. doi: 10.1016/j.cell.2016.01.043
44. Caruso S, Poon IKH. Apoptotic cell-derived extracellular vesicles: more than just debris. *Front Immunol.* (2018) 9:1486. doi: 10.3389/fimmu.2018.01486
45. Atkin-Smith GK, Tixeira R, Paone S, Mathivanan S, Collins C, Liem M, et al. A novel mechanism of generating extracellular vesicles during apoptosis via a beads-on-a-string membrane structure. *Nat Commun.* (2015) 6:7439. doi: 10.1038/ncomms8439
46. Lleo A, Zhang W, McDonald WH, Seeley EH, Leung PS, Coppel RL, et al. Shotgun proteomics: identification of unique protein profiles of apoptotic bodies from biliary epithelial cells. *Hepatology.* (2014) 60:1314–23. doi: 10.1002/hep.27230
47. Lee K, Shao H, Weissleder R, Lee H. Acoustic purification of extracellular microvesicles. *ACS Nano.* (2015) 9:2321–7. doi: 10.1021/nn506538f
48. Ibsen SD, Wright J, Lewis JM, Kim S, Ko SY, Ong J, et al. Rapid isolation and detection of exosomes and associated biomarkers from plasma. *ACS Nano.* (2017) 11:6641–51. doi: 10.1021/acsnano.7b00549
49. Davies RT, Kim J, Jang SC, Choi EJ, Gho YS, Park J. Microfluidic filtration system to isolate extracellular vesicles from blood. *Lab Chip.* (2012) 12:5202–10. doi: 10.1039/c2lc41006k
50. Dorayappan KDP, Gardner ML, Hisey CL, Zingarelli RA, Smith BQ, Lightfoot MDS, et al. A microfluidic chip enables isolation of exosomes and establishment of their protein profiles and associated signaling pathways in ovarian cancer. *Cancer Res.* (2019) 79:3503–13. doi: 10.1158/0008-5472.CAN-18-3538
51. Zhang H, Lyden D. Asymmetric-flow field-flow fractionation technology for exomere and small extracellular vesicle separation and characterization. *Nat Protoc.* (2019) 14:1027–53. doi: 10.1038/s41596-019-0126-x
52. Patel DB, Luthers CR, Lerman MJ, Fisher JP, Jay SM. Enhanced extracellular vesicle production and ethanol-mediated vascularization bioactivity via a 3D-printed scaffold-perfusion bioreactor system. *Acta Biomater.* (2019) 95:236–44. doi: 10.1016/j.actbio.2018.11.024
53. Thone MN, Kwon YJ. Extracellular blebs: artificially-induced extracellular vesicles for facile production and clinical translation. *Methods.* (2020) 177:135–45. doi: 10.1016/j.ymeth.2019.11.007
54. Nair A, Bu J, Rawding PA, Do SC, Li H, Hong S. Cytochalasin B treatment and osmotic pressure enhance the production of extracellular vesicles (EVs) with improved drug loading capacity. *Nanomaterials.* (2021) 12:3. doi: 10.3390/nano12010003
55. Musante L, Tataruch-Weinert D, Kerjaschki D, Henry M, Meleady P, Holthofer H. Residual urinary extracellular vesicles in ultracentrifugation supernatants after hydrostatic filtration dialysis enrichment. *J Extracell Vesicles.* (2017) 6:1267896. doi: 10.1080/20013078.2016.1267896
56. Chen TS, Arslan F, Yin Y, Tan SS, Lai RC, Choo AB, et al. Enabling a robust scalable manufacturing process for therapeutic exosomes through oncogenic immortalization of human ESC-derived MSCs. *J Transl Med.* (2011) 9:47. doi: 10.1186/1479-5876-9-47
57. An Y, Lin S, Tan X, Zhu S, Nie F, Zhen Y, et al. Exosomes from adipose-derived stem cells and application to skin wound healing. *Cell Prolif.* (2021) 54:e12993. doi: 10.1111/cpr.12993
58. Lee K, Fraser K, Ghaddar B, Yang K, Kim E, Balaj L, et al. Multiplexed profiling of single extracellular vesicles. *ACS Nano.* (2018) 12:494–503. doi: 10.1021/acsnano.7b07060
59. Xiao S, Xiao C, Miao Y, Wang J, Chen R, Fan Z, et al. Human acellular amniotic membrane incorporating exosomes from adipose-derived mesenchymal stem cells promotes diabetic wound healing. *Stem Cell Res Ther.* (2021) 12:255. doi: 10.1186/s13287-021-02333-6
60. Liu H, Zhang M, Shi M, Zhang T, Lu W, Yang S, et al. Adipose-derived mesenchymal stromal cell-derived exosomes promote tendon healing by activating both SMAD1/5/9 and SMAD2/3. *Stem Cell Res Ther.* (2021) 12:338. doi: 10.1186/s13287-021-02410-w
61. Li Q, Yu H, Sun M, Yang P, Hu X, Ao Y, et al. The tissue origin effect of extracellular vesicles on cartilage and bone regeneration. *Acta Biomater.* (2021) 125:253–66. doi: 10.1016/j.actbio.2021.02.039
62. Rau CS, Kuo PJ, Wu SC, Huang LH, Lu TH, Wu YC, et al. Enhanced nerve regeneration by exosomes secreted by adipose-derived stem cells with or without FK506 stimulationInt. *J Mol Sci.* (2021) 22:8545. doi: 10.3390/ijms22168545
63. Rodrigues M, Kosaric N, Bonham CA, Gurtner GC. Wound healing: a cellular perspective. *Physiol Rev.* (2019) 99:665–706. doi: 10.1152/physrev.00067.2017
64. Moura J, Madureira P, Leal EC, Fonseca AC, Carvalho E. Immune aging in diabetes and its implications in wound healing. *Clin Immunol.* (2019) 200:43–54. doi: 10.1016/j.clim.2019.02.002
65. Bolandi Z, Mokhberian N, Eftekhary M, Sharifi K, Soudi S, Ghanbarian H, et al. Adipose derived mesenchymal stem cell exosomes loaded with miR-10a promote the differentiation of Th17 and Treg from naive CD4(+) T cell. *Life Sci.* (2020) 259:118218. doi: 10.1016/j.lfs.2020.118218
66. Blazquez R, Sanchez-Margallo FM, de la Rosa O, Dalemans W, Alvarez V, Tarazona R, et al. Immunomodulatory potential of human adipose mesenchymal stem cells derived exosomes on *in vitro* stimulated T cells. *Front Immunol.* (2014) 5:556. doi: 10.3389/fimmu.2014.00556

67. Fernandes TL, Gomoll AH, Lattermann C, Hernandez AJ, Bueno DF, Amano MT. Macrophage: a potential target on cartilage regeneration. *Front Immunol.* (2020) 11:111. doi: 10.3389/fimmu.2020.00111
68. Zhao H, Shang Q, Pan Z, Bai Y, Li Z, Zhang H, et al. Exosomes from adipose-derived stem cells attenuate adipose inflammation and obesity through polarizing M2 macrophages and beiging in white adipose tissue. *Diabetes.* (2018) 67:235–47. doi: 10.2337/db17-0356
69. Deng S, Zhou X, Ge Z, Song Y, Wang H, Liu X, et al. Exosomes from adipose-derived mesenchymal stem cells ameliorate cardiac damage after myocardial infarction by activating S1P/SK1/S1PR1 signaling and promoting macrophage M2 polarization. *Int J Biochem Cell Biol.* (2019) 114:105564. doi: 10.1016/j.biocel.2019.105564
70. Xu P, Xin Y, Zhang Z, Zou X, Xue K, Zhang H, et al. Extracellular vesicles from adipose-derived stem cells ameliorate ultraviolet B-induced skin photoaging by attenuating reactive oxygen species production and inflammation. *Stem Cell Res Ther.* (2020) 11:264. doi: 10.1186/s13287-020-01777-6
71. Bai Y, Han YD, Yan XL, Ren J, Zeng Q, Li XD, et al. Adipose mesenchymal stem cell-derived exosomes stimulated by hydrogen peroxide enhanced skin flap recovery in ischemia-reperfusion injury. *Biochem Biophys Res Commun.* (2018) 500:310–7. doi: 10.1016/j.bbrc.2018.04.065
72. Xia Y, Rao L, Yao H, Wang Z, Ning P, Chen X. Engineering macrophages for cancer immunotherapy and drug delivery. *Adv Mat.* (2020) 32:e2002054. doi: 10.1002/adma.202002054
73. Chen B, Cai J, Wei Y, Jiang Z, Desjardins HE, Adams AE, et al. Exosomes are comparable to source adipose stem cells in fat graft retention with up-regulating early inflammation and angiogenesis. *Plast Reconstr Surg.* (2019) 144:816e−27. doi: 10.1097/PRS.0000000000006175
74. Ma J, Zhang Z, Wang Y, Shen H. Investigation of miR-126-3p loaded on adipose stem cell-derived exosomes for wound healing of full-thickness skin defects. *Exp Dermatol.* (2021). doi: 10.1111/exd.14480
75. Zhu LL, Huang X, Yu W, Chen H, Chen Y, Dai YT. Transplantation of adipose tissue-derived stem cell-derived exosomes ameliorates erectile function in diabetic rats. *Andrologia.* (2018) 50:e12871. doi: 10.1111/and.12871
76. Pi L, Yang L, Fang BR, Meng XX, Qian L. Exosomal microRNA-125a-3p from human adipose-derived mesenchymal stem cells promotes angiogenesis of wound healing through inhibiting PTEN. *Mol Cell Biochem.* (2021). doi: 10.1007/s11010-021-04251-w
77. Liu W, Yuan Y, Liu D. Extracellular vesicles from adipose-derived stem cells promote diabetic wound healing via the PI3K-AKT-mTOR-HIF-1α signaling pathway. *Tissue Eng Regen Med.* (2021) 18:1035–44. doi: 10.1007/s13770-021-00383-8
78. Xue C, Shen Y, Li X, Li B, Zhao S, Gu J, et al. Exosomes derived from hypoxia-treated human adipose mesenchymal stem cells enhance angiogenesis through the PKA signaling pathway. *Stem Cells Dev.* (2018) 27:456–65. doi: 10.1089/scd.2017.0296
79. Lopatina T, Bruno S, Tetta C, Kalinina N, Porta M, Camussi G. Platelet-derived growth factor regulates the secretion of extracellular vesicles by adipose mesenchymal stem cells and enhances their angiogenic potential. *Cell Commun Signal.* (2014) 12:26. doi: 10.1186/1478-811X-12-26
80. Abu El-Asrar AM, Struyf S, Opdenakker G, Van Damme J, Geboes K. Expression of stem cell factor/c-kit signaling pathway components in diabetic fibrovascular epiretinal membranes. *Mol Vis.* (2010) 16:1098–107. doi: 10.1111/j.1755-3768.2010.2444.x
81. DiPietro LA. Angiogenesis and wound repair: when enough is enough. *J Leukoc Biol.* (2016) 100:979–84. doi: 10.1189/jlb.4MR0316-102R
82. Ren S, Chen J, Duscher D, Liu Y, Guo G, Kang Y, et al. Microvesicles from human adipose stem cells promote wound healing by optimizing cellular functions via AKT and ERK signaling pathways. *Stem Cell Res Ther.* (2019) 10:47. doi: 10.1186/s13287-019-1152-x
83. Hu L, Wang J, Zhou X, Xiong Z, Zhao J, Yu R, et al. Exosomes derived from human adipose mensenchymal stem cells accelerates cutaneous wound healing via optimizing the characteristics of fibroblasts. *Sci Rep.* (2016) 6:32993. doi: 10.1038/srep32993
84. Qian L, Pi L, Fang BR, Meng XX. Adipose mesenchymal stem cell-derived exosomes accelerate skin wound healing via the lncRNA H19/miR-19b/SOX9 axis. *Lab Invest.* (2021) 101:1254–66. doi: 10.1038/s41374-021-00611-8
85. He L, Zhu C, Jia J, Hao XY, Yu XY, Liu XY, et al. ADSC-Exos containing MALAT1 promotes wound healing by targeting miR-124 through activating Wnt/β-catenin pathway. *Biosci Rep.* (2020) 40:BSR20192549. doi: 10.1042/BSR20192549
86. Choi EW, Seo MK, Woo EY, Kim SH, Park EJ, Kim S. Exosomes from human adipose-derived stem cells promote proliferation and migration of skin fibroblasts. *Exp Dermatol.* (2018) 27:1170–2. doi: 10.1111/exd.13451
87. Verhaegen PD, van Zuijlen PP, Pennings NM, van Marle J, Niessen FB, van der Horst CM, et al. Differences in collagen architecture between keloid, hypertrophic scar, normotrophic scar, and normal skin: an objective histopathological analysis. *Wound Repair Regen.* (2009) 17:649–56. doi: 10.1111/j.1524-475X.2009.00533.x
88. Rohani MG, Parks WC. Matrix remodeling by MMPs during wound repair. *Matrix Biol.* (2015) 44–46:113–21. doi: 10.1016/j.matbio.2015.03.002
89. Wang C, Wang M, Xu T, Zhang X, Lin C, Gao W, et al. Engineering bioactive self-healing antibacterial exosomes hydrogel for promoting chronic diabetic wound healing and complete skin regeneration. *Theranostics.* (2019) 9:65–76. doi: 10.7150/thno.29766
90. Wang M, Wang C, Chen M, Xi Y, Cheng W, Mao C, et al. Efficient angiogenesis-based diabetic wound healing/skin reconstruction through bioactive antibacterial adhesive ultraviolet shielding nanodressing with exosome release. *ACS Nano.* (2019) 13:10279–93. doi: 10.1021/acsnano.9b03656
91. Wang L, Hu L, Zhou X, Xiong Z, Zhang C, Shehada HMA, et al. Exosomes secreted by human adipose mesenchymal stem cells promote scarless cutaneous repair by regulating extracellular matrix remodelling. *Sci Rep.* (2017) 7:13321. doi: 10.1038/s41598-017-12919-x
92. Yang C, Luo L, Bai X, Shen K, Liu K, Wang J, et al. Highly-expressed micoRNA-21 in adipose derived stem cell exosomes can enhance the migration and proliferation of the HaCaT cells by increasing the MMP-9 expression through the PI3K/AKT pathway. *Arch Biochem Biophys.* (2020) 681:108259. doi: 10.1016/j.abb.2020.108259
93. Jones JI, Nguyen TT, Peng Z, Chang M. Targeting MMP-9 in diabetic foot ulcers. *Pharmaceuticals.* (2019) 12:79. doi: 10.3390/ph12020079
94. Wang J, Yi Y, Zhu Y, Wang Z, Wu S, Zhang J, et al. Effects of adipose-derived stem cell released exosomes on wound healing in diabetic mice. *Chin J Reparative Reconstr Surg.* (2020) 34:124–31. doi: 10.7507/1002-1892.201903058
95. Li Y, Zhang J, Shi J, Liu K, Wang X, Jia Y, et al. Exosomes derived from human adipose mesenchymal stem cells attenuate hypertrophic scar fibrosis by miR-192-5p/IL-17RA/Smad axis. *Stem Cell Res Ther.* (2021) 12:221. doi: 10.1186/s13287-021-02290-0
96. Shao T, Tang W, Li Y, Gao D, Lv K, He P, et al. Research on function and mechanisms of a novel small molecule WG449E for hypertrophic scar. *J Eur Acad Dermatol Venereol.* (2020) 34:608–18. doi: 10.1111/jdv.16028
97. Dai X, Zeng J, Yan X, Lin Q, Wang K, Chen J, et al. Sitagliptin-mediated preservation of endothelial progenitor cell function via augmenting autophagy enhances ischaemic angiogenesis in diabetes. *J Cell Mol Med.* (2018) 22:89–100. doi: 10.1111/jcmm.13296
98. Ma T, Fu B, Yang X, Xiao Y, Pan M. Adipose mesenchymal stem cell-derived exosomes promote cell proliferation, migration, and inhibit cell apoptosis via Wnt/β-catenin signaling in cutaneous wound healing. *J Cell Biochem.* (2019) 120:10847–54. doi: 10.1002/jcb.28376
99. Liu S, Jiang L, Li H, Shi H, Luo H, Zhang Y, et al. Mesenchymal stem cells prevent hypertrophic scar formation via inflammatory regulation when undergoing apoptosis. *J Invest Dermatol.* (2014) 134:2648–57. doi: 10.1038/jid.2014.169
100. Cano Sanchez M, Lancel S, Boulanger E, Neviere R. Targeting oxidative stress and mitochondrial dysfunction in the treatment of impaired wound healing: a systematic review. *Antioxidants.* (2018) 7:98. doi: 10.3390/antiox7080098
101. Okonkwo UA, DiPietro LA. Diabetes and wound angiogenesis. *Int J Mol Sci.* (2017) 18:1419. doi: 10.3390/ijms18071419
102. Li X, Xie X, Lian W, Shi R, Han S, Zhang H, et al. Exosomes from adipose-derived stem cells overexpressing Nrf2 accelerate cutaneous wound healing by promoting vascularization in a diabetic foot ulcer

rat model. *Exp Mol Med.* (2018) 50:1–14. doi: 10.1038/s12276-018-0058-5
103. Cooper DR, Wang C, Patel R, Trujillo A, Patel NA, Prather J, et al. Human adipose-derived stem cell conditioned media and exosomes containing MALAT1 promote human dermal fibroblast migration and ischemic wound healing. *Adv Wound Care.* (2018) 7:299–308. doi: 10.1089/wound.2017.0775
104. Shi B, Wang Y, Zhao R, Long X, Deng W, Wang Z. Bone marrow mesenchymal stem cell-derived exosomal miR-21 protects C-kit+ cardiac stem cells from oxidative injury through the PTEN/PI3K/Akt axis. *PLoS One.* (2018) 13:e0191616. doi: 10.1371/journal.pone.0191616
105. Xiao J, Pan Y, Li XH, Yang XY, Feng YL, Tan HH, et al. Cardiac progenitor cell-derived exosomes prevent cardiomyocytes apoptosis through exosomal miR-21 by targeting PDCD4. *Cell Death Dis.* (2016) 7:e2277. doi: 10.1038/cddis.2016.181
106. Aragonès G, Rowan S, Francisco SG, Yang W, Weinberg J, Taylor A, et al. Glyoxalase system as a therapeutic target against diabetic retinopathy. *Antioxidants*. (2020) 9:1062. doi: 10.3390/antiox9111062
107. Morgenstern J, Campos Campos M, Nawroth P, Fleming T. The glyoxalase system-new insights into an ancient metabolism. *Antioxidants*. (2020) 9:939. doi: 10.3390/antiox9100939
108. Sachdeva R, Schlotterer A, Schumacher D, Matka C, Mathar I, Dietrich N, et al. TRPC proteins contribute to development of diabetic retinopathy and regulate glyoxalase 1 activity and methylglyoxal accumulation. *Mol Metab.* (2018) 9:156–67. doi: 10.1016/j.molmet.2018.01.003
109. Jia Y, Gan Y, He C, Chen Z, Zhou C. The mechanism of skin lipids influencing skin status. *J Dermatol Sci.* (2018) 89:112–9. doi: 10.1016/j.jdermsci.2017.11.006
110. Arda O, Göksügür N, Tüzün Y. Basic histological structure and functions of facial skin. *Clin Dermatol.* (2014) 32:3–13. doi: 10.1016/j.clindermatol.2013.05.021
111. Egawa G, Kabashima K. Multifactorial skin barrier deficiency and atopic dermatitis: Essential topics to prevent the atopic march. *J Allergy Clin Immunol*. (2016) 138:350–8.e1. doi: 10.1016/j.jaci.2016.06.002
112. Nuutila K. Hair follicle transplantation for wound repair. *Adv Wound Care.* (2021) 10:153–63. doi: 10.1089/wound.2019.1139
113. Joost S, Jacob T, Sun X, Annusver K, La Manno G, Sur I, et al. Single-cell transcriptomics of traced epidermal and hair follicle stem cells reveals rapid adaptations during wound healing. *Cell Rep*. (2018) 25:585–97.e7. doi: 10.1016/j.celrep.2018.09.059
114. Takeo M, Lee W, Ito M. Wound healing and skin regeneration. *Cold Spring Harb Perspect Med.* (2015) 5:a023267. doi: 10.1101/cshperspect.a023267
115. Tomita Y, Akiyama M, Shimizu H. PDGF isoforms induce and maintain anagen phase of murine hair follicles. *J Dermatol Sci.* (2006) 43:105–15. doi: 10.1016/j.jdermsci.2006.03.012
116. Boisvert WA, Yu M, Choi Y, Jeong GH, Zhang YL, Cho S, et al. Hair growth-promoting effect of Geranium sibiricum extract in human dermal papilla cells and C57BL/6 mice. *BMC Complement Altern Med.* (2017) 17:109. doi: 10.1186/s12906-017-1624-4
117. Zhu HL, Gao YH, Yang JQ Li JB, Gao J. Serenoa repens extracts promote hair regeneration and repair of hair loss mouse models by activating TGF-β and mitochondrial signaling pathway. *Eur Rev Med Pharmacol Sci.* (2018) 22:4000–8. doi: 10.26355/eurrev_201806_15285
118. Harshuk-Shabso S, Dressler H, Niehrs C, Aamar E, Enshell-Seijffers D. Fgf and Wnt signaling interaction in the mesenchymal niche regulates the murine hair cycle clock. *Nat Commun.* (2020) 11:5114. doi: 10.1038/s41467-020-18643-x
119. Gentile P, Garcovich S. Advances in regenerative stem cell therapy in androgenic alopecia and hair loss: wnt pathway, growth-factor, and mesenchymal stem cell signaling impact analysis on cell growth and hair follicle development. *Cells*. (2019) 8:466. doi: 10.3390/cells8050466
120. Rishikaysh P, Dev K, Diaz D, Qureshi WM, Filip S, Mokry J. Signaling involved in hair follicle morphogenesis and development. *Int J Mol Sci.* (2014) 15:1647–70. doi: 10.3390/ijms15011647
121. Boiten W, Absalah S, Vreeken R, Bouwstra J, van Smeden J. Quantitative analysis of ceramides using a novel lipidomics approach with three dimensional response modelling. *Biochim Biophys Acta.* (2016) 1861:1652–61. doi: 10.1016/j.bbalip.2016.07.004
122. Di Nardo A, Wertz P, Giannetti A, Seidenari S. Ceramide and cholesterol composition of the skin of patients with atopic dermatitis. *Acta Derm Venereol.* (1998) 78:27–30. doi: 10.1080/00015559850135788
123. Gomez-Larrauri A, Presa N, Dominguez-Herrera A, Ouro A, Trueba M, Gomez-Muñoz A. Role of bioactive sphingolipids in physiology and pathology. *Essays Biochem.* (2020) 64:579–89. doi: 10.1042/EBC20190091
124. Borodzicz S, Rudnicka L, Mirowska-Guzel D, Cudnoch-Jedrzejewska A. The role of epidermal sphingolipids in dermatologic diseases. *Lipids Health Dis.* (2016) 15:13. doi: 10.1186/s12944-016-0178-7
125. Geiger A, Walker A, Nissen E. Human fibrocyte-derived exosomes accelerate wound healing in genetically diabetic mice. *Biochem Biophys Res Commun.* (2015) 467:303–9. doi: 10.1016/j.bbrc.2015.09.166
126. Zhang J, Guan J, Niu X, Hu G, Guo S, Li Q, et al. Exosomes released from human induced pluripotent stem cells-derived MSCs facilitate cutaneous wound healing by promoting collagen synthesis and angiogenesis. *J Transl Med.* (2015) 13:49. doi: 10.1186/s12967-015-0417-0
127. Zhang B, Wang M, Gong A, Zhang X, Wu X, Zhu Y, et al. HucMSC-exosome mediated-wnt4 signaling is required for cutaneous wound healing. *Stem Cells.* (2015) 33:2158–68. doi: 10.1002/stem.1771
128. Bray ER, Oropallo AR, Grande DA, Kirsner RS, Badiavas EV. Extracellular vesicles as therapeutic tools for the treatment of chronic wounds. *Pharmaceutics*. (2021) 13:1543. doi: 10.3390/pharmaceutics13101543
129. Irons RF, Cahill KW, Rattigan DA, Marcotte JH, Fromer MW, Chang S, et al. Acceleration of diabetic wound healing with adipose-derived stem cells, endothelial-differentiated stem cells, and topical conditioned medium therapy in a swine model. *J Vasc Surg.* (2018) 68:115s−25. doi: 10.1016/j.jvs.2018.01.065
130. Basu J, Ludlow JW. Exosomes for repair, regeneration and rejuvenation. *Expert Opin Biol Ther.* (2016) 16:489–506. doi: 10.1517/14712598.2016.1131976
131. Xiong M, Zhang Q, Hu W, Zhao C, Lv W, Yi Y, et al. Exosomes from adipose-derived stem cells: the emerging roles and applications in tissue regeneration of plastic and cosmetic surgery. *Front Cell Dev Biol.* (2020) 8:574223. doi: 10.3389/fcell.2020.574223
132. Ha DH, Kim SD, Lee J, Kwon HH, Park GH, Yang SH, et al. Toxicological evaluation of exosomes derived from human adipose tissue-derived mesenchymal stem/stromal cells. *Regul Toxicol Pharmacol.* (2020) 115:104686. doi: 10.1016/j.yrtph.2020.104686
133. Li L, Ngo HTT, Hwang E, Wei X, Liu Y, Liu J, et al. Conditioned medium from human adipose-derived mesenchymal stem cell culture prevents UVB-induced skin aging in human keratinocytes and dermal fibroblasts. *Int J Mol Sci*. (2019) 21:49. doi: 10.3390/ijms21010049
134. Choi JS, Cho WL, Choi YJ, Kim JD, Park HA, Kim SY, et al. Functional recovery in photo-damaged human dermal fibroblasts by human adipose-derived stem cell extracellular vesicles. *J Extracell Vesicles.* (2019) 8:1565885. doi: 10.1080/20013078.2019.1565885
135. Syromiatnikova V, Idrisova K, Masgutova G, Gomzikova M, Kabwe E, Bek J, et al. Analyzing the effectiveness of adipose tissue stem cell and microvesicle therapy in premature skin aging caused by chronic exposure to ultraviolet radiation. *Bionanoscience.* (2020) 10:991–7. doi: 10.1007/s12668-020-00793-3
136. Niada S, Giannasi C, Magagnotti C, Andolfo A, Brini AT. Proteomic analysis of extracellular vesicles and conditioned medium from human adipose-derived stem/stromal cells and dermal fibroblasts. *J Proteomics.* (2021) 232:104069. doi: 10.1016/j.jprot.2020.104069
137. Zhu YZ, Hu X, Zhang J, Wang ZH, Wu S, Yi YY. Extracellular vesicles derived from human adipose-derived stem cell prevent the formation of hypertrophic scar in a rabbit model. *Ann Plast Surg.* (2020) 84:602–7. doi: 10.1097/SAP.0000000000002357
138. Lu Z, Chen Y, Dunstan C, Roohani-Esfahani S, Zreiqat H. Priming adipose stem cells with tumor necrosis factor-alpha preconditioning potentiates their exosome efficacy for bone regeneration. *Tissue Eng Part A*. (2017) 23:1212–20. doi: 10.1089/ten.tea.2016.0548

139. Cho BS, Lee J, Won Y, Duncan DI, Jin RC, Lee J, et al. Skin brightening efficacy of exosomes derived from human adipose tissue-derived stem/stromal cells: a prospective, split-face, randomized placebo-controlled study. *Cosmetics.* (2020) 7:12. doi: 10.3390/cosmetics7040090
140. Alvarez-Erviti L, Seow Y, Yin H, Betts C, Lakhal S, Wood MJ. Delivery of siRNA to the mouse brain by systemic injection of targeted exosomes. *Nat Biotechnol.* (2011) 29:341–5. doi: 10.1038/nbt.1807
141. Zhuang X, Xiang X, Grizzle W, Sun D, Zhang S, Axtell RC, et al. Treatment of brain inflammatory diseases by delivering exosome encapsulated anti-inflammatory drugs from the nasal region to the brain. *Mol Ther.* (2011) 19:1769–79. doi: 10.1038/mt.2011.164
142. Haney MJ, Klyachko NL, Zhao Y, Gupta R, Plotnikova EG, He Z, et al. Exosomes as drug delivery vehicles for Parkinson's disease therapy. *J Control Release.* (2015) 207:18–30. doi: 10.1016/j.jconrel.2015.03.033
143. Wang J, Wu H, Peng Y, Zhao Y, Qin Y, Zhang Y, et al. Hypoxia adipose stem cell-derived exosomes promote high-quality healing of diabetic wound involves activation of PI3K/Akt pathways. *J Nanobiotechnology.* (2021) 19:202. doi: 10.1186/s12951-021-00942-0

Conflict of Interest: The authors declare that the research was conducted in the absence of any commercial or financial relationships that could be construed as a potential conflict of interest.

frontiers | Frontiers in Medicine

ORIGINAL RESEARCH
published: 13 June 2022
doi: 10.3389/fmed.2022.812653

Solamargine Alleviated UVB-Induced Inflammation and Melanogenesis in Human Keratinocytes and Melanocytes *via* the p38 MAPK Signaling Pathway, a Promising Agent for Post-inflammatory Hyperpigmentation

*Juemin Zhao[1†], Yanjun Dan[1†], Ziqi Liu[1†], Qianqian Wang[1], Min Jiang[1], Chengfeng Zhang[1], Hamm-Ming Sheu[2], Chrang-Shi Lin[3,4] and Leihong Xiang[1]**

[1] Department of Dermatology, Huashan Hospital, Fudan University, Shanghai, China, [2] Kao Chao-Hsing Dermatologic Clinic, Kaohsiung City, Taiwan, [3] Department of Dermatology and Family Medicine, National Yang-Ming Chiao-Tung University, Taipei City, Taiwan, [4] Dr. Lin Skin Clinic, Taipei City, Taiwan

Post-inflammatory hyperpigmentation (PIH) is a common acquired pigmentary disorder occurring after skin inflammation or injury. Ultraviolet B irradiation could exaggerate PIH clinically due to its effect on promoting cutaneous inflammation and melanogenesis in keratinocytes and melanocytes, respectively. Solamargine (SM), a steroidal alkaloid glycoside extracted from *Solanum undatum*, significantly inhibits Ultraviolet B (UVB)-induced pro-inflammatory cytokines IL-1α, IL-1β, IL-8, and IFN-γ, as well as paracrine melanogenic factors ET-1, α-MSH, and bFGF in human keratinocytes. Additionally, SM significantly attenuated UVB-induced melanin synthesis in human epidermal melanocytes through down-regulation of tyrosinase activity and expression of MITF, TRP-1, TRP-2, and tyrosinase. SM exerted an anti-inflammatory effect in UVB-irradiated keratinocytes through the p38 MAPK/Nrf2/HO-1 signaling pathway. With its anti-inflammatory and whitening effect, SM may improve PIH through paracrine regulations of keratinocytes and direct action on melanocytes, making it a promising agent for PIH.

Keywords: post-inflammatory hyperpigmentation (PIH), SM (solamargine), p38, MAPK, Nrf2, HO-1, inflammation, melanogenesis

OPEN ACCESS

Edited by:
Hongxiang Chen,
Huazhong University of Science and Technology, China

Reviewed by:
Emi Dika,
University of Bologna, Italy
Zhouwei Wu,
Shanghai General Hospital, China
Zhe Jian,
Fourth Military Medical University, China

***Correspondence:**
Leihong Xiang
flora_xiang@vip.163.com

† These authors have contributed equally to this work and share first authorship

Specialty section:
This article was submitted to Dermatology, a section of the journal Frontiers in Medicine

Received: *10 November 2021*
Accepted: *24 May 2022*
Published: *13 June 2022*

Citation:
Zhao J, Dan Y, Liu Z, Wang Q, Jiang M, Zhang C, Sheu H-M, Lin C-S and Xiang L (2022) Solamargine Alleviated UVB-Induced Inflammation and Melanogenesis in Human Keratinocytes and Melanocytes via the p38 MAPK Signaling Pathway, a Promising Agent for Post-inflammatory Hyperpigmentation. Front. Med. 9:812653. doi: 10.3389/fmed.2022.812653

INTRODUCTION

Post-inflammatory hyperpigmentation (PIH) is an acquired hypermelanosis of the epidermis or dermis following cutaneous inflammation or injury. Although clinicians observed pigmentary change in all skin types, it more frequently affects individuals with Fitzpatrick skin types (FST) IV-VI due to the increased reactivity of melanocytes within the skin (1, 2). The treatment of PIH remains intractable. Except for a few anti-inflammatory agents, current therapies mainly target the pigmentary phase, which is primarily unsatisfactory. Current treatments demonstrate inconsistent

efficacies and different disadvantages: (1) depigmentation agents (e.g., hydroquinone, azelaic acid, tretinoin, and 4-hydroxyanisole) which are prone to irritant reactions and hypopigmentation in clinical use (3); (2) retinoids (e.g., retinoic acid, adapalene, tazarotene, etc.) which could cause irritant dermatitis such as redness, desquamation, and pruritus (4); (3) glucocorticoids (e.g., betamethasone, desonide, hydrocortisone butyrate, etc.) which could lead to adverse reactions such as skin thinning, atrophy, and capillary dilation with long-term use, even cause hyperpigmentation in some cases (3); (4) chemical peeling (e.g., glycolic acid, salicylic acid, trichloroacetic acid, etc.) which may cause burning and irritating during operation, thus increasing the risk of hyperpigmentation (5, 6); (5) laser therapy (e.g., intense pulsed light and 532, 694, and 1064 nm Q-switched lasers) which are expensive and may exaggerate hyperpigmentation (7–9). In addition to the adverse effects of the above treatments, improper timing of interventions may induce new inflammatory stimuli to result in aggravation of hyperpigmentation. It is of great interest for clinicians to provide targeted anti-inflammatory or whitening therapy depending on the stage of PIH. As our team previously reported, inflammatory and pigmentary phases were overlapped rather than isolated, so drugs with both anti-inflammatory and anti-pigmentary effects are ideal options for treating PIH (10). Plant extracts such as arbutin, licorice extract, soybean extract, and green tea polyphenols (11) have become popular choices in PIH patients due to their mild effects and high tolerance. New natural extracts with more potent anti-inflammatory and whitening effects are still of great clinical interest.

Solamargine (SM), a steroidal alkaloid glycoside extracted from *Solanum undatum*, has been proven to have anti-inflammatory, antioxidant and anti-tumor effects. Studies have shown that SM can exert anti-tumor effects (**Figure 1A**) by up-regulating the expression of TNF-α1 and TNF-α2 and activating caspase-3 to cause tumor cells apoptosis (12, 13); it can exert potent anti-inflammatory effects by inhibiting the NF-κB/p65 pathway and inhibiting the expression of COX-2 (14, 15). In addition, SM can exert some antioxidant effects by reducing ROS release and down-regulating the activity of i-NOS (16). SR-T100 solution, a novel water-soluble product whose active ingredient is SM at a concentration of 5.53 mg/ml (purity >99%), is currently used in Taiwan, China, for the treatment of solar keratosis, condyloma acuminata and viral warts with particular efficacy (17–22).

Since inflammation and oxidative stress contributed to PIH, and SM has anti-inflammatory and antioxidant effects, we speculate whether it could have therapeutic effects on PIH through the dual effects of anti-inflammation and anti-pigmentation. Current laboratory studies of SM have focused on the antitumor effects against tumor cells, and few studies reported the effects on keratinocytes and melanocytes. We examined the effects of SM in the UVB-induced PIH model on pro-inflammatory cytokines and melanogenic factors in keratinocytes and melanin synthesis in melanocytes after UVB irradiation and further investigated possible signaling pathways. We hope that studies on this novel compound's biological functions and mechanisms could provide a basis for screening future novel drugs and lay the theoretical foundation for clinical translation.

MATERIALS AND METHODS

Cell Culture and Ultraviolet B Irradiation

Human keratinocyte cells and Human Epidermal Melanocyte (HEM) cells were cultured at 37°C in a humidified CO_2 incubator (95% air, 5% CO_2) in Dulbecco's modified Eagle's medium (Gibco, United States) supplemented with 10% fetal bovine serum and 1% penicillin-streptomycin. After washing twice with phosphate-buffered saline (PBS), cells were irradiated with a thin cover of PBS, using handheld NB-UVB light (wavelength of 311 nm, SH1B, Sigma, Shanghai, China). The dose rate was 12 mW/cm2, and the test dose ladder was 100, 200, 300, 400, and 500 mJ/cm^2, with radiation times corresponding to 8, 17, 25, 33, and 42 s, respectively. Non-irradiated cells were covered with foil to prevent exposure. After UVB irradiation, PBS was removed and cells were incubated in fresh medium with or without SM for an additional 24 or 48 h before further experiments.

Assessment of Viability

Human keratinocyte cells and HEM cells (2×10^3 per well) were collected and seeded in triplicate 96-well plates in 100 μl of growth medium. Different seeding densities were optimized at the beginning of the experiments. 24 h after irradiation or SM treatment, Cell Count Kit-8 assay (Dojindo Laboratories, Kumamoto, Japan) was used to assess the cell viability of the HaCaT cells and HEM cells according to the manufacturer's instructions. Next, the absorbance of each well was measured at an absorbance of 475 nm with the Spectra Max 384 PLUS microplate reader (Molecular Devices, Sunnyvale, CA, United States).

Melanin Content Assay

HEM cells were seeded in a 60 mm culture dish at a density of 5×10^5 cells per well. 24 h after UVB irradiation or SM treatment, HEM cells were dissolved in 500 μL of 1 m NaOH with 10% DMSO for 1 h at 80°C and the relative melanin content was measured at an absorbance of 405 nm with the Spectra Max 384 PLUS microplate reader (Molecular Devices, Sunnyvale, CA, United States).

Tyrosinase Activity Assay

HEM cells were seeded in a 60 mm culture dish at a density of 5×10^5 cells per well. 24 h after UVB irradiation or SM treatment, HEM cells were washed with PBS and then were solubilized with 1% Triton X-100 at room temperature for 15 min. The lysates were centrifuged at 12,000 rpm for 10 min to obtain a supernatant. After quantification, 100 μl of lysis buffer was transferred into the 96-well plate with 100 μl of 1 mM L-DOPA added to each well. After incubation at 37°C for 1 h, absorbance was measured at 490 nm with the Spectra Max 384 PLUS microplate reader (Molecular Devices, Sunnyvale, CA, United States).

Reverse-Transcription PCR

Total RNA was prepared from the treated cells using Trizol (Life Technologies, Rockville, MD, United States). The quality and quantity of isolated RNA samples were assessed by measuring the 260/280 nm absorption ratio of RNA. Extracted RNA was used to generate cDNA using PrimeScript RT Master Mix Kit (Takara, Japan). The cDNA was applied as a template for quantitative RT-PCR, which was carried out in a Real-Time PCR 7500 System (Applied Biosystems, Invitrogen) with SYBR Premix Extaq (Takara, Japan) in a 40-cycle PCR. The denaturing, annealing and extension conditions of each PCR cycle were 95°C for 30 s, 95°C for 5 s, and 60°C for 34 s, respectively. The primers used were as follows: *IL-1α*, 5′-GAGGGAGTCATTTCATTGGCG-3′, 5′ ATGCAGCCTTCATGGAGTGG -3′, *IL-1β*, 5′- CTGAGCT CGCCAGTGAAATG -3′, 5′- TGTCCATGGCCACAACAACT -3′, *IL-8*, 5′- CAGTGCATAAAGACATACTCCAAACC -3′, 5′- TGGTCCACTCTCAATCACTCTCA -3′, *IFN-γ*, 5′- GAATGT CCAACGCAAAGCAA -3′, 5′- GCTGCTGGCGACCGTT -3′, *MITF*, 5′- TGGTTTGGGCTTGTTGTTTGT -3′, 5′- CTGC ACCCGGGAATCG -3′, *TYR*, 5′- GCTTGTGAGCTTGCT GTGTC -3′, 5′- GGTCAGGCTTTTTGGCCCTA -3′, *TRP-1*, 5′- AAGCTTTTCTTGCTGGCGTG -3′, 5′- CTCCCA AGCACATCTACGCA -3′, *TRP-2*, 5′- TTCATCTGCTCATATCT GGTTTCTG -3′, 5′- CAGACAAGCCACGCCCTAGA -3′, *ET-1*, 5′- CCCTCCAGAGAGCGTTATGTG -3′, 5′- CCCGAAGGT CTGTCACCAA -3′, *α-MSH*, 5′- CCCCTGGTGACGCTGTTC -3′, 5′- CCCTCACTCGCCCTTCTTG -3′, *bFGF*, 5′- TGGATA GTGTGAGAGAATTAGGCTGTA -3′, 5′- TTTTGTAGTGGT GTGAATGCTGAA -3′, *GAPDH*, 5′-GCACCGTCAA GGCTGAGAAC-3′, 5′-ATGGTGGTGAAGACGCCAGT-3′. The relative expression levels were calculated with ΔΔCt method. The mRNA levels of each target gene were normalized to the levels of GAPDH.

Western Blot Analysis

Human keratinocyte cells and HEM cells incubated under the indicated conditions were lysed, and total protein was extracted from HEM cells by the RIPA buffer, separated by 10% SDS-PAGE, and electro- transferred onto a polyvinylidene difluoride membrane (Millipore, Billerica, MA, United States). After blocking non-specific antibody binding by incubating the membrane in Tris-buffered saline containing 0.1% Tween-20 and 5% non-fat dried milk for 2 h at room temperature, the membranes were incubated at 4°C overnight with the following primary antibodies: from Abcam (Cambridge, MA, United States): anti-MITF (ab59232; 1:1000), anti-TYR (ab61294; 1:1000), anti-TRP-1 (ab83774; 1:500), TRP-2 (ab221144; 1:500), Nrf-2 (ab62352; 1:1000), HO-1 (ab52947; 1:2000), and from Cell Signaling Technology (Boston, MA, United States): p-p38 (ab178867; 1:1000), p38 (ab182453; 1:1000) and from Proteintech (Rosemont, United States):α-Tubulin (ab7291;1:10000). p38 inhibitor (SB203580) was purchased at Selleck and arbutin was purchased at Sigma. Afterward, the membranes were incubated with the appropriate horseradish peroxidase (HRP)-conjugated secondary antibody for 1 h at room temperature. Immunoreactive bands were detected by the Enhanced Chemiluminescence substrate (Pierce, Rockford, IL, United States) and visualized on the LAS-3000 Luminescence Image Analyzer (Fujifilm, Tokyo, Japan). Densitometric analysis was performed using the ImageJ software program.

ELISA Assay

The culture supernatants of the treated HaCaT cells were collected 48 h after irradiation and IL-1α, IL-1β, IL-8, IFN-γ, ET-1, α-MSH, bFGF level was detected using ELISA Kits from Abcam (Cambridge, MA, United States) following the manufacturer's instructions. Quantitative data analysis was performed using Raybio Q Analyzer software (RayBiotech, Inc.).

Statistical Analysis

Data are expressed as mean ± S.D. The differences among the three groups were analyzed using one-way analysis of variance (ANOVA) followed by the least square difference (LSD) *post-hoc* test. $P < 0.05$ was considered statistically significant. Statistical tests were performed using SPSS software (version 21.0, Chicago, IL, United States). Graphical representations of the data were performed by GraphPad Prism (GraphPad Software Inc, San Diego, CA, United States).

RESULTS

Ultraviolet B-Induced Inflammation and Hyperpigmentation in Keratinocytes and Melanocytes as an *in vitro* Model for Post-inflammatory Hyperpigmentation

According to previous studies, the doses of NB-UVB treatment of human keratinocytes and melanocytes generally vary from 30 to 300 mJ/cm^2 (23–25). This study used 100, 200, 300, and 500 mJ/cm^2 UVB to irradiate HaCaT cells and HEM cells, respectively. The cell morphology was observed by phase-contrast microscopy 24 h after irradiation, and the cell viability was measured by CCK-8. The results showed that with increasing irradiation dosage, cell density decreased, morphology was irregular, and cell proliferation viability was inhibited correspondingly.

After irradiating HaCaT cells and HEM cells at a dose of 300 mJ/cm^2 UVB, the cell density decreased, the morphology was less regular, and the cell proliferation viability was significantly decreased (**Figure 1B**). The melanin content increased significantly after irradiating HEM cells using 250 mJ/cm^2 UVB (**Figure 1C**). Therefore, 250 mJ/cm^2 was chosen to establish the PIH model as the irradiation dose.

The Effect of Solamargine on Cell Viability of Human Keratinocyte Cells and HEM Cells

Previous literature has shown that SM intervenes in tumor cell lines and normal cell lines with different IC50 values for different cells, with safe doses within 10 μg/ml (26).

The results showed that SM at 0.1 μg/ml had a mild pro-proliferative effect on HaCaT cells and HEM cells, and SM at

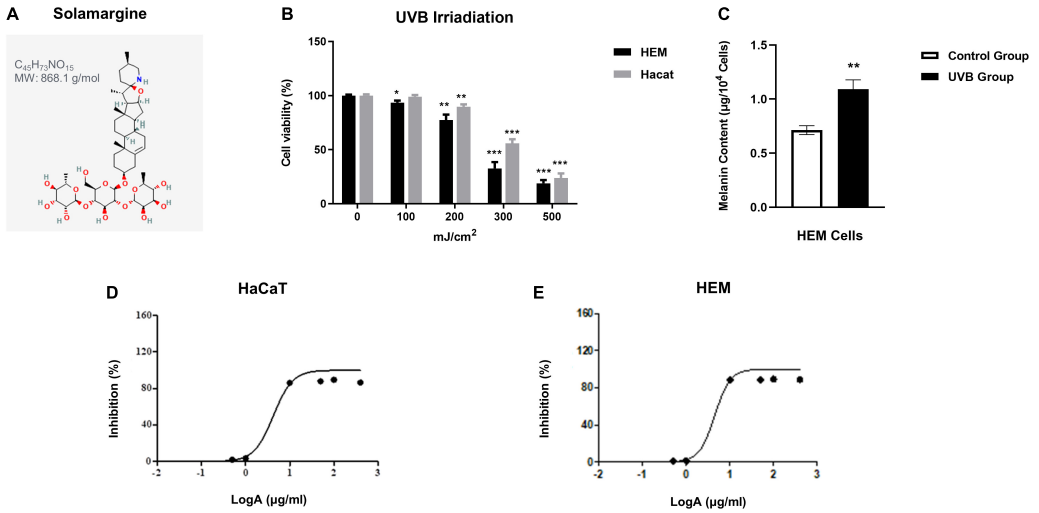

FIGURE 1 | Cell viability and melanin content of HaCaT and HEM cells after NB-UVB irradiation. The inhibition rate of HaCaT cells and HEM cells of different concentrations of SM. **(A)** The chemical structure of SM modified from https://pubchem.ncbi.nlm.nih.gov/compound/Solamargine. **(B)** Cell viability of HaCaT cells and HEM cells was detected by CCK-8 24 h after irradiation of NB-UVB with different fluences (100, 200, 300, and 500 mJ/cm^2). Cell viability is presented as a eprcentage of control. **(C)** Melanin content of HEM cells after irradiation of NB-UVB with 250 mJ/cm^2 Melanin content is percentage as a percentage of control. **(D,E)** The IC50 value for HaCaT cells was 4.252 μg/ml and for HEM cells was 4.472 μg/ml. $^*P < 0.05$, $^{**}P < 0.01$, and $^{***}P < 0.001$.

10 μg/ml and above had a strong inhibitory effect on both cells (**Table 1**). The IC50 value for HaCaT cells was 4.252 μg/ml and for HEM cells was 4.472 μg/ml. The log curves for different concentrations of SM are shown in **Figures 1D,E**. This study selected 1 and 2 μg/ml of SM as the intervention concentrations for HaCaT cells and HEM cells, respectively.

Solamargine Attenuated UVB-Induced Secretion of Pro-Inflammatory Cytokines (IL-1α, IL-1β, IL-8, IFN-γ) and Melanogenic Factors (ET-1, α-MSH, bFGF) in Human Keratinocyte Cells

To evaluate the anti-inflammatory and anti-pigmentation ability of SM in UVB-irradiated HaCaT cells, we detected mRNA and protein expression of pro-inflammatory cytokines (IL-1α, IL-1β, IL-8, IFN-γ) and paracrine melanogenic factors (ET-1, α-MSH, bFGF) in HaCaT cells.

TABLE 1 | Cell viability of HaCaT cells and HEM cells at different concentrations of SM.

SM concentration (μg/ml)	HaCaT cell inhibition rate (%)	HEM cell inhibition rate (%)
0	0 ± 1.01	0 ± 0.84
0.1	−2.91 ± 0.88	−2.79 ± 0.89
0.5	1.91 ± 1.93	1.22 ± 0.95
1	3.54 ± 1.20	1.21 ± 1.27
10	86.08 ± 1.09	88.34 ± 0.35
50	87.90 ± 0.50	88.21 ± 0.10
100	89.48 ± 0.33	89.36 ± 0.19
400	86.41 ± 4.33	88.88 ± 016

The results showed that the mRNA and protein expression of IL-1α, IL-1β, IL-8, and IFN-γ were significantly increased after UVB irradiation of HaCaT cells. SM at 1 and 2 μg/ml significantly inhibited the mRNA expression of IL-1α, IL-8, and IFN-γ in HaCaT cells after UVB irradiation. Upon treatment of 1 and 2 μg/ml SM, the mRNA and protein levels of IL-1α, IL-1β, IL-8, and IFN-γ significantly reduced compared to UVB irradiation alone, the anti-inflammatory effect of which is comparable to 150 μg/ml dexamethasone (**Figures 2A–D**).

In addition to pro-inflammatory cytokines, previous studies reported that certain paracrine factors secreted by keratinocytes, including ET-1, α-MSH, and bFGF (27, 28), could bind directly to corresponding receptors on melanocytes and promote melanogenesis upon inflammatory stimulation and UVB irradiation. The mRNA expression of the ET-1, α-MSH, and bFGF were all significantly increased after UVB irradiation of HaCaT cells (**Figures 2I–K**). There were also significantly higher protein concentrations in the cell supernatant of ET-1, α-MSH, and bFGF after UVB irradiation (**Figures 2L–N**). Similarly, at both mRNA and protein levels, 2 μg/ml SM significantly inhibited UVB-induced secretion of ET-1, α-MSH, and bFGF in HaCaT cells (**Figures 2E–H**). 150 μg/ml Arbutin was chosen to be a positive control. These results indicated SM prevented both pro-inflammatory and pro-melanogenic effects in UVB-irradiated HaCaT cells, making it a promising therapeutic alternative for the inflammatory phase of PIH.

Solamargine Inhibited UVB-Induced Melanogenesis in Human Epidermal Melanocyte Cells

Melanin contents are closely related to melanosome maturation. Microphthalmia-associated transcription factor (MITF) is the

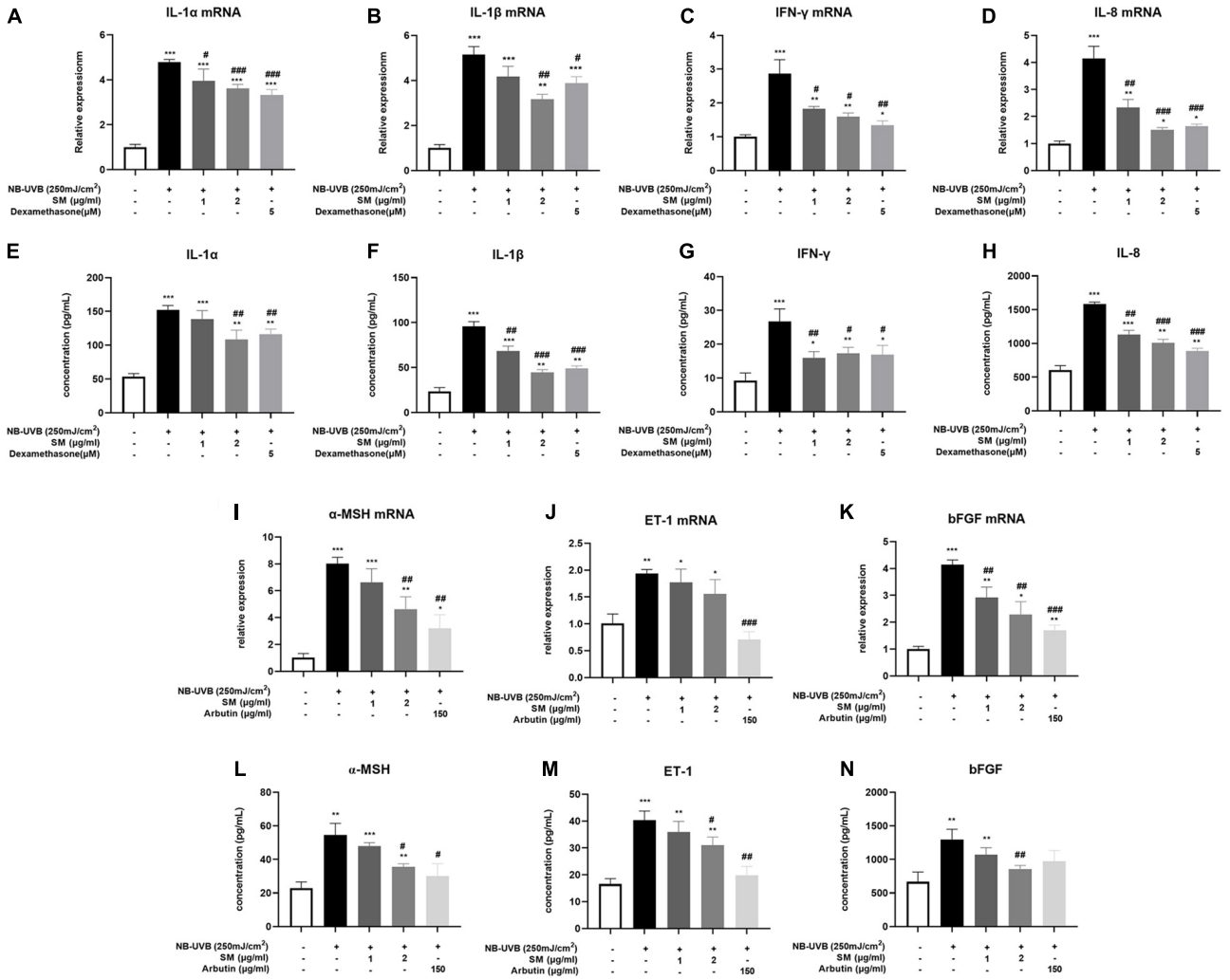

FIGURE 2 | Solamargine (SM) attenuated UVB-induced secretion of pro-inflammatory cytokines and melanogenic factors in HaCaT cells. Real-time PCR (24 h after incubation with SM) and ELISA assay (48 h after incubation with SM) demonstrated SM attenuated UVB-induced secretion of pro-inflammatory cytokines, IL-1α **(A,E)**, IL-1β **(B,F)**, IL-8 **(C,G)**, and IFN-γ **(D,H)** in HaCaT cells. Treatment with SM after UVB irradiation significantly decreased the mRNA and protein levels of IL-1α, IL-1β, IL-8, and IFN-γ. The anti-inflammatory effect of SM is comparable to 150 μg/ml dexamethasone. Real-time PCR and ELISA assay demonstrated SM attenuated UVB-induced secretion of melanogenic factors, ET-1 **(I,L)**, α-MSH **(J,M)**, and bFGF **(K,N)** in HaCaT cells. Treatment with SM after UVB irradiation significantly decreased the mRNA and protein levels of ET-1, α-MSH, and bFGF. The anti-melanogenic effect of SM is comparable to 150 μg/ml Arbutin. The data were represented as mean ± SD from three independent experiments. $^{*}P < 0.05$, $^{**}P < 0.01$, $^{***}P < 0.001$ (vs. non-treated group); $^{\#}P < 0.05$, $^{\#\#}P < 0.01$; $^{\#\#\#}P < 0.001$ (vs. NB-UVB irradiated group).

central transcriptional factor governing the expression of melanogenic enzymes such as tyrosinase-related protein (TRP)-1, TRP-2 and tyrosinase (TYR) (29). To evaluate the role of SM in melanogenesis, we examined the melanin contents, tyrosinase activity, and the expression of several critical melanogenic factors, such as MITF, TRP-1, TRP-2, and TYR on both mRNA and protein levels. HEM cells were irradiated with 250 mJ/cm^2 UVB and incubated with 1 μg/ml, 2 μg/ml of SM and 150 μg/ml of arbutin (a classical whitening component as a positive control) for 24 h. The results showed a significant increase in melanin contents (**Figure 3A**) and tyrosinase activity (**Figure 3B**) in the UVB group compared to the negative control group, and a slight decrease in melanin content in the UVB + 1 μg/ml SM group compared to the UVB group, but the difference was not statistically significant. Melanin contents and tyrosinase activity in the UVB + 2 μg/ml group and UVB + arbutin group decreased significantly compared to the UVB irradiated group.

Microphthalmia-associated transcription factor, TRP-1, TRP-2, and TYR mRNA and protein levels were significantly increased after UVB irradiation in HEM cells. SM at 2 μg/ml significantly inhibited the mRNA expression of TYR, MITF, and TRP-2 in HEM cells after UVB irradiation and to some extent on TRP-1 mRNA expression, but there were no statistically significant differences (**Figures 3D–G**). At the protein level, SM at 2 μg/ml significantly inhibited the expression of TYR, MITF, TRP-1, and TRP-2 proteins in HEM cells after UVB

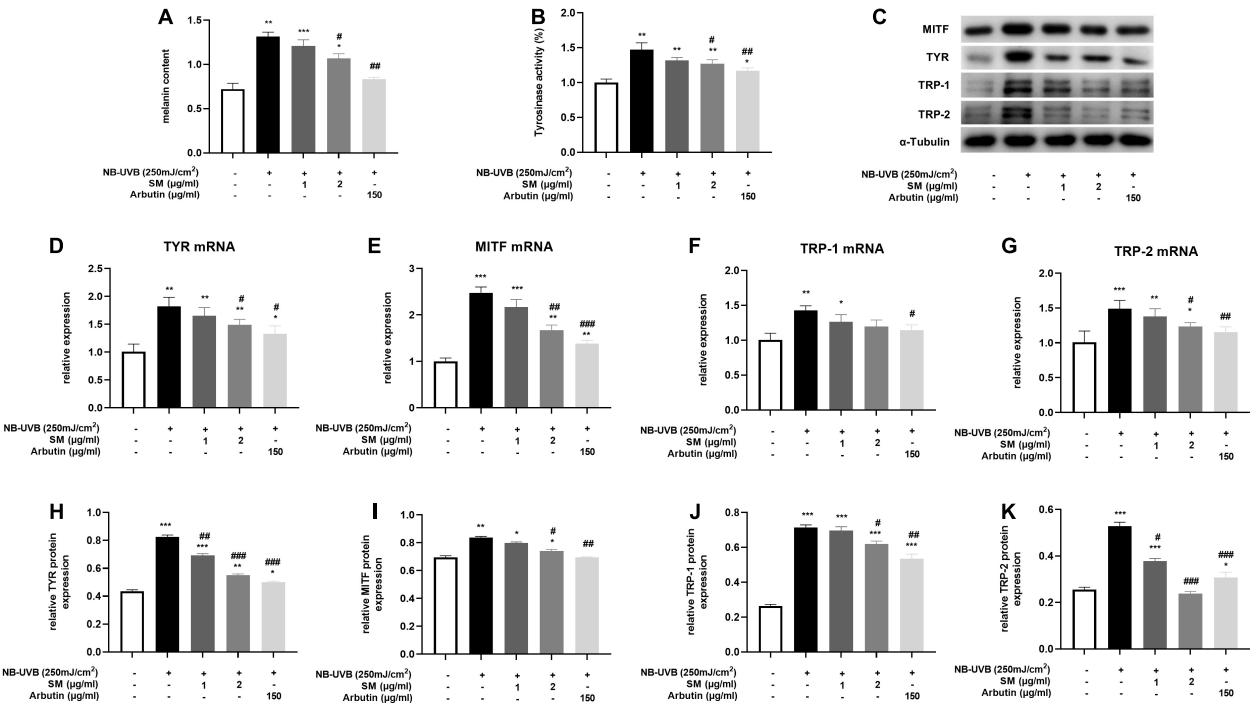

FIGURE 3 | Solamargine (SM) Inhibited UVB-induced melanogenesis in HEM cells. **(A)** Melanin content of HEM cells 48 h after the UVB irradiation with SM or arbutin treatment. **(B)** Tyrosinase activity of HEMs 24 h after the UVB irradiation with SM or arbutin treatment. Tyrosinase activity is presented as a percentage of control. Real-time PCR (24 h after incubation with SM) and Western Blot (48 h after incubation with SM) demonstrated SM attenuated UVB-induced secretion of melanogenic factors, TYR **(C)** Western blot assay of MITF, TYR,TRP-1 and TRP-2 after UVB exposure with/without SM or arbutin treatment. **(D,H)**, MITF **(E,I)**, TRP-1 **(F,J)**, and TRP-2 **(G,K)** in HEM cells. Treatment with SM after UVB irradiation significantly decreased the mRNA and protein levels of TYR, MITF, TRP-1, and TRP-2. The anti-melanogenesis effect of SM is comparable to 150 μg/ml Arbutin. The data represent the mean ± S.D. from three independent experiments. $^{*}P < 0.05$, $^{**}P < 0.01$, $^{***}P < 0.001$ (vs. non-treated group); $^{\#}P < 0.05$, $^{\#\#}P < 0.01$, $^{\#\#\#}P < 0.001$ (vs. NB-UVB irradiated group).

irradiation (**Figures 3C,H–K**). These results indicated that 2 μg/ml of SM could significantly inhibit the expression of critical regulatory molecules of melanin synthesis in HEM cells after UVB irradiation, comparable to 150 μ g/ml arbutin.

The Effect of Solamargine Exerted Through p38 MAPK/Nrf2/HO-1 Pathway in Human Keratinocyte Cells

The MAPK signaling pathway is an ancient classical signaling pathway closely related to inflammatory response, and p38 MAPK/Nrf2/HO-1 pathway is also involved in mediating the oxidative stress response. After UVB irradiation of HaCaT cells, compared with the negative control group, Nrf-2, HO-1 protein expression was significantly decreased, and p-p38/p38 expression was significantly increased. The expression of Nrf-2 and HO-1 proteins in HaCaT cells was significantly higher and p-p38/p38 expression was significantly lower in the UVB + SM group compared with the UVB group, indicating SM induced the activation of the Nrf-2/HO-1 pathway to attenuate oxidative stress and inflammation possibly through inhibiting p38 phosphorylation. The expression of Nrf-2 and HO-1 proteins in HaCaT cells was significantly decreased, and p-p38/p38 expression was significantly increased in the UVB + SM + p38 inhibitor (SB203580) group compared with the UVB + SM group (**Figures 4A–D**), indicating SM could activate the p38 MAPK/Nrf2/HO-1 signaling pathway in HaCaT cells after UVB irradiation. SB203580 is a p38 inhibitor acting primarily to block the catalytic activity of p38 MAPK by the inhibition of the activation of MAPKAP K2, a specific physiological substrate of p38 MAPK. SB203580 specifically inhibits the activity of p38 MAPK but not its activation by upstream MAPKK (30).

To verify that SM down-regulates the expression of pro-inflammatory cytokines through the p38 MAPK/Nrf2/HO-1 signaling pathway in HaCaT cells, we compared the UVB + SM + p38 inhibitor (SB203580) group with the UVB + SM group. The results showed that after the addition of the p38 inhibitor, IL-1α, IL-1β, IL-8, and IFN-γ in the cell supernatant were significantly increased as shown in **Figures 4E–H**, suggesting that SM inhibited the expression of pro-inflammatory cytokines through the p38 MAPK/Nrf2/HO-1 signaling pathway in HaCaT cells thereby exerting an anti-inflammatory effect.

DISCUSSION

Solamargine (SM), a novel natural extract from *Solanum undatum*, was previously reported as a mild anti-tumor agent for precancerous cutaneous lesions like solar keratosis. Previous

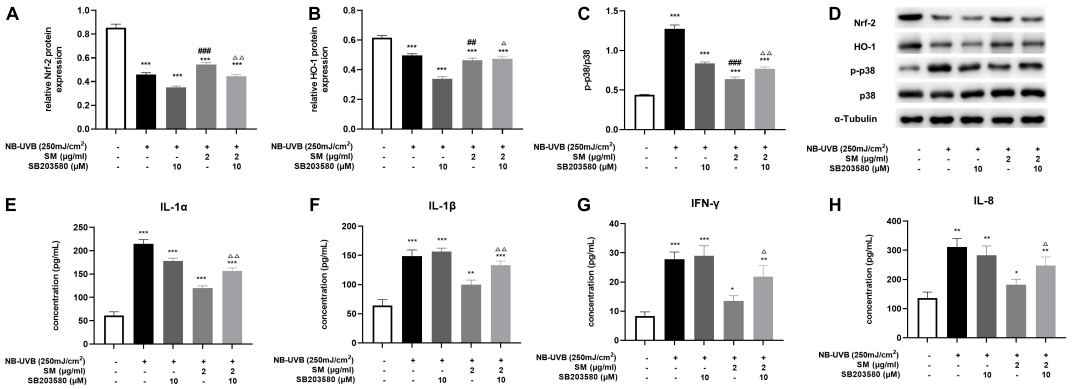

FIGURE 4 | Solamargine (SM) exerting anti-inflammatory effect *via* the activation of p38 MAPK/Nrf2/HO-1 signaling pathways in HaCaT cells. After UVB irradiation of HaCaT cells, the protein level of Nrf-2 **(A)** and HO-1 **(B)** was significantly decreased, and p-p38/p38 **(C)** expression was significantly increased. This effect can be reversed by SM. The expression of Nrf-2 and HO-1 proteins in HaCaT cells was significantly decreased and p-p38/p38 expression was significantly increased in the UVB + SM + p38 inhibitor (SB203580) group compared with the UVB + SM group. After the addition of the p38 inhibitor, IL-1α **(D)** Western blot assay of Nrf-2, HO-1, p-p38 and p38 after UVB exposure with/without SM or SB203580 treatment. **(E)**, IL-1β **(F)**, IL-8 **(G)**, and IFN-γ **(H)** in the cell supernatant were significantly increased. The data represent the mean ± S.D. from three independent experiments. $^{*}P < 0.05$, $^{**}P < 0.01$, $^{***}P < 0.001$ (vs. non-treated group); $^{\Delta}P < 0.05$, $^{\Delta\Delta}P < 0.01$ (vs. NB-UVB irradiated group); $^{\#\#}P < 0.01$, $^{\#\#\#}P < 0.001$ (vs. NB-UVB irradiated and SM treated group).

researchers revealed anti-inflammatory and anti-oxidant activity of SM in skin tumor cell lines, which led to our interest in its possible therapeutic effect on PIH. This study further examined its bioactivity in human keratinocytes and melanocytes and found SM could alleviate UVB-induced inflammation and melanogenesis, making it a promising choice for PIH.

The pathogenesis of PIH relied on the activation of the epidermal pigmentary unit by primary inflammation. The indirect paracrine effect from keratinocytes and other cell types played a major role in accelerating melanin synthesis and promoting melanosome transfer. Different from previous studies on melanocytes, we focused on keratinocytes, which build up the microenvironment of melanocytes, and chose UVB irradiation as the trigger of PIH. Results showed that 2 μg/ml of SM could significantly reduce the mRNA and protein expression of inflammatory cytokines IL-1α, IL-1β, IL-8, and IFN-γ in HaCaT cells upon UVB irradiation, which was consistent with the results of classical anti-inflammatory drug dexamethasone. Besides, we also checked the changes in paracrine melanogenic factors ET-1, α-MSH, and bFGF excreted by keratinocytes upon UVB-irradiation and found similar alleviating effects of SM comparable to classical whitening ingredient arbutin. These results indicated potent anti-inflammatory effects and inhibitory effects on the paracrine melanogenic pathway, making it a possible candidate for PIH therapy from the keratinocyte's side.

The MAPK signaling pathway is an ancient classical pathway that plays cell division, proliferation, migration, survival, apoptosis, and differentiation. MAP kinase family members, especially p38 and JNK, played crucial regulatory roles in the inflammation processes. Recently, p38 MAPK/Nrf2/HO-1 signaling pathway has become very popular as a protective pathway in response to oxidative stress (31, 32). Studies found that Asteraceae plant Dioscorea (33) alleviated inflammatory cytokines IL-1β and TNF-α *via* the p38 MAPK/Nrf2/HO-1 pathway. Another natural extract Shikonin (34) also exerted anti-inflammatory and antioxidant effects through p38 MAPK/Nrf2/HO-1 pathway by reduction of TNF-α, IL-6, IL-1β, and IFN-γ as well as activation of SOD and GSH.

Our results indicated SM could also inhibit UVB-induced p38 phosphorylation in keratinocytes. Moreover, SM inhibition of UVB-induced cytokines: IL-1α, IL-1β, IL-8, and IFN-γ was reversed by p38 MAPK inhibitor SB203580. Previous studies have proved SM exerted anti-inflammatory effects by inhibiting the NF-κB/p65 pathway and expression of COX-2 (14). Our research added that SM could also downregulate inflammatory cytokines like IL-1α, IL-1β, IL-8, and IFN-γ by inhibiting the p38 MAPK pathway. Oxidative stress is a major contributive factor in UVB-induced cutaneous inflammation. Our study found that the expression of Nrf-2 and HO-1 was significantly decreased upon UVB irradiation. Meanwhile, SM treatment significantly upregulated the expression of Nrf-2 and HO-1, consistent with its previously reported antioxidant effect, where SM reduced ROS release and downregulated the activity of i-NOS (16). Similarly, SM upregulation of Nrf-2 and HO-1 was reversed by p38 MAPK inhibitor SB203580, indicating SM might exert anti-oxidant activity through the p38 MAPK/Nrf2/HO-1 signaling pathway. Future studies on the change of ROS level in UVB-irradiated keratinocytes and melanocytes upon SM treatment could further confirm SM's antioxidant activity.

After examination of SM's anti-inflammatory activity and its molecular basis in keratinocytes, we then evaluated whether SM could directly interfere with melanin synthesis in UVB-irradiated melanocytes. We found that 2 μg/ml SM could significantly decrease UVB-induced melanin production in HEM cells comparable to arbutin. More specifically, SM inhibited UVB-induced upregulation of key players in melanogenesis in HEM cells: TYR, TRP-1/2, and MITF, and downregulated UVB-induced tyrosinase activation. These results indicated SM could effectively alleviate UVB-induced hyperpigmentation by

suppressing the expression and activity of critical modulators in melanin synthesis in melanocytes. Korean scholars found that purple grape root extract birchic acid inhibited melanin synthesis by modulating MEK/ERK and PI3K/Akt pathways to suppress CREB, MITF, and TRP-1/2 expression in B16F10 melanoma cells (27). Centipede extract Jineol inhibited MITF and TYR through p38 and ERK pathways and downstream TRP-1/2 mRNA and protein expression to inhibit melanin synthesis (28). Whether SM inhibited melanogenesis in HEM through the same pathway is of great interest and would be a promising direction for future SM research. Notably, we used NB-UVB lamp (311 nm) rather than broad-band UVB (290–320 nm) as the irradiation source in our study and found 250 mJ/cm^2 as the appropriate dose for melanocyte pigmentation study. Future researches might adjust the dose according to different light sources and cell lines.

Our study explored the bioactivity of SM in keratinocytes and melanocytes, and examined its anti-inflammatory effect and anti-melanogenic effect of both paracrine way and direct inhibition of melanin synthesis, making it a promising agent targeting both inflammation and hyperpigmentation for early intervention for PIH. Besides, we found SM exerted anti-inflammatory activity *via* the p38 MAPK/Nrf2/HO-1 signaling pathway, which replenished the existing molecular mechanism of SM. Further investigation of SM bioactivity could be conducted through a co-culture trans well assay or 3D skin model to provide a more direct and accurate examination of the paracrine effect and interaction between keratinocytes and melanocytes.

CONCLUSION

Our study characterized the anti-inflammatory and anti-melanogenic effects of SM on UVB-irradiated keratinocytes and melanocytes model comparable to dexamethasone and arbutin, respectively. SM alleviated UVB-induced inflammation in keratinocytes *via* p38 MAPK/Nrf2/HO-1 pathway and inhibited UVB-induced melanin synthesis through downregulation of critical modulators of melanogenesis. In conclusion, SM could become a promising therapeutic agent for PIH targeting both inflammatory and pigmentary phases. Future clinical investigations could further elucidate its efficacy and safety in PIH.

DATA AVAILABILITY STATEMENT

The raw data supporting the conclusions of this article will be made available by the authors, without undue reservation.

AUTHOR CONTRIBUTIONS

LX: conceptualization and funding acquisition. JZ: methodology. ZL: formal analysis and investigation. YD: writing – original draft preparation. QW, MJ, and CZ: writing – review and editing. H-MS and C-SL: resources. LX, H-MS, and C-SL: supervision. All authors contributed to the article and approved the submitted version.

REFERENCES

1. Kaufman BP, Aman T, Alexis AF. Postinflammatory hyperpigmentation: epidemiology, clinical presentation, pathogenesis and treatment. *Am J Clin Dermatol.* (2018) 19:489–503. doi: 10.1007/s40257-017-0333-6
2. Zhai H, Dika E, Goldovsky M, Maibach HI. Tape-stripping method in man: comparison of evaporimetric methods. *Skin Res Technol.* (2007) 13:207–10. doi: 10.1111/j.1600-0846.2007.00218.x
3. Picardo M, Carrera M. New and experimental treatments of cloasma and other hypermelanoses. *Dermatol Clin.* (2007) 25:353–62. doi: 10.1016/j.det.2007.04.012
4. Stratigos A, Katsambas A. Optimal management of recalcitrant disorders of hyperpigmentation in dark-skinned patients. *Am J Clin Dermatol.* (2004) 5:161–8. doi: 10.2165/00128071-200405030-00004
5. Ahn HH, Kim IH. Whitening effect of salicylic acid peels in Asian patients. *Dermatol Surg.* (2006) 32:372–5. doi: 10.1111/j.1524-4725.2006.32075.x
6. Burns R, Prevost-Blank P, Lawry M, Lawry T, Faria D, Fivenson D. Glycolic acid peels for postinflammatory hyperpigmentation in black patients. A comparative study. *Dermatologic.* (1997) 23:171–4. doi: 10.1111/j.1524-4725.1997.tb00014.x
7. Dierickx C, Goldman M, Fitzpatrick R. Laser treatment of erythematous/hypertrophic and pigmented scars in 26 patients. *Plast Reconstr Surg.* (1995) 95:84–90.
8. Taylor C, Anderson R. Ineffective treatment of refractory melasma and postinflammatory hyperpigmentation by Q-switched ruby laser. *J Dermatol Surg Oncol.* (1994) 20:592–7. doi: 10.1111/j.1524-4725.1994.tb00152.x
9. Fitzpatrick R, Goldman M, Ruiz-Esparza J. Laser treatment of benign pigmented epidermal lesions using a 300 nsecond pulse and 510 nm wavelength. *J Dermatol Surg Oncol.* (1993) 19:341–7. doi: 10.1111/j.1524-4725.1993.tb00355.x
10. Liu Z, Jiang M, Zhao J, Wang Q, Zhang C, Gao M, et al. Efficacy of a wound-dressing biomaterial on prevention of postinflammatory hyperpigmentation after suction blister epidermal grafting in stable vitiligo patients: a controlled assessor-blinded clinical study with in vitro bioactivity investigation. *Arch Dermatol Res.* (2020) 312:635–45. doi: 10.1007/s00403-020-02049-2
11. Davis E, Callender V. Postinflammatory hyperpigmentation: a review of the epidemiology, clinical features, and treatment options in skin of color. *J Clin Aesthet Dermatol.* (2010) 3:20–31.
12. Yu S, Sheu HM, Lee CH. *Solanum incanum* extract (SR-T100) induces melanoma cell apoptosis and inhibits established lung metastasis. *Oncotarget.* (2017) 8: 103509–17. doi: 10.18632/oncotarget.21508
13. Wu C, Liang C, Shiu L, Chang L, Lin T, Lan C, et al. *Solanum incanum* extract (SR-T100) induces human cutaneous squamous cell carcinoma apoptosis through modulating tumor necrosis factor receptor signaling pathway. *J Dermatol Sci.* (2011) 63:83–92. doi: 10.1016/j.jdermsci.2011.04.003
14. Chen Y, Tang Q, Wu J, Zheng F, Yang L, Hann S. Inactivation of PI3-K/Akt and reduction of SP1 and p65 expression increase the effect of solamargine on suppressing EP4 expression in human lung cancer cells. *J Exp Clin Cancer Res.* (2015) 34:154. doi: 10.1186/s13046-015-0272-0
15. Xing X, Dan Y, Xu Z, Xiang L. Implications of oxidative stress in the pathogenesis and treatment of hyperpigmentation disorders. *Oxid Med Cell Longev.* (2022) 2022:7881717. doi: 10.1155/2022/7881717
16. Atanu FO, Ebiloma UG, Ajayi EI. A review of the pharmacological aspects of *Solanum nigrum* Linn. *Biotechnol Mol Biol Rev.* (2011) 6:001–7
17. Yang CC, Wu CH, Wong TW, Lai FJ, Wei KC, Lin TK, et al. Effects of *Solanum undatum* extract (SR-T100) on photocarcinogenesis and photoaging of actinic keratosis. *J Dermatol.* (2021) 48:344–52. doi: 10.1111/1346-8138.15703
18. Tomita Y, Maeda K, Tagami H. Melanocyte-stimulating properties of arachidonic acid metabolites: possible role in postinflammatory pigmentation. *Pigment Cell Res.* (2010) 5:357–61. doi: 10.1111/j.1600-0749.1992.tb00562.x

19. Ortonne JP. Retinoic acid and pigment cells: a review of in-vitro and in-vivo studies. *Br J Dermatol.* (1992) 127:43–7. doi: 10.1111/j.1365-2133.1992.tb16987.x
20. Son J., Kim M, Jou I, Park KC, Kang HY. IFN-γ inhibits basal and α-MSH-induced melanogenesis. *Pigment Cell Melanoma Res.* (2014) 27:201–8.
21. Swope VB, Abdel-Malek Z, Kassem LM, Nordlund JJ. Interleukins 1 alpha and 6 and tumor necrosis Factor-alpha are paracrine inhibitors of human melanocyte proliferation and melanogenesis. *J Invest Dermatol.* (1991) 96:180. doi: 10.1111/1523-1747.ep12460991
22. Kitamura R, Tsukamoto K, Harada K, Shimizu A, Shimada S, Kobayashi T, et al. Mechanisms underlying the dysfunction of melanocytes in vitiligo epidermis: role of SCF/KIT protein interactions and the downstream effector, MITF-M. *J Pathol.* (2004) 202:463–75. doi: 10.1002/path.1538
23. Hwang E, Lin P, Ngo HTT, Gao W, Wang YS, Yu HS, et al. Icariin and icaritin recover UVB-induced photoaging by stimulating Nrf2/ARE and reducing AP-1 and NF-kappaB signaling pathways: a comparative study on UVB-irradiated human keratinocytes. *Photochem Photobiol Sci.* (2018) 17:1396–408.
24. Choi E, Yi YS, Lee J, Park SH, Kim S, Hossain MA, et al. Anti-apoptotic and anti-inflammatory activities of edible fresh water algae *Prasiola japonica* in UVB-irradiated skin keratinocytes. *Am J Chin Med.* (2019) 47:1853–68. doi: 10.1142/S0192415X19500940
25. Xu F, Hou B, Wang Y, Meng F, Zhuang C, Pan Q, et al. Combination of PDTC and GBE could better alleviate the damage to HaCaT cells caused by UVB. *Biomed Environ Sci.* (2019) 32:779–82. doi: 10.3967/bes2019.097
26. Kalalinia F, Karimi-Sani I. Anticancer properties of solamargine: a systematic review. *Phytother Res.* (2017) 31:858–70. doi: 10.1002/ptr.5809
27. Serre C, Busuttil V, Botto JM. Intrinsic and extrinsic regulation of human skin melanogenesis and pigmentation. *Int J Cosmet Sci.* (2018) 40:328–47. doi: 10.1111/ics.12466
28. Yuan XH, Jin ZH. Paracrine regulation of melanogenesis. *Br J Dermatol.* (2018) 178:632–9. doi: 10.1111/bjd.15651
29. Vachtenheim J, Borovanský J. "Transcription physiology" of pigment formation in melanocytes: central role of MITF. *Exp Dermatol.* (2010) 19:617–27.
30. Kumar S, Jiang MS, Adams JL, Lee JC. Pyridinylimidazole compound SB 203580 inhibits the activity but not the activation of p38 mitogen-activated protein kinase. *Biochem Biophys Res Commun.* (1999) 263:825–31. doi: 10.1006/bbrc.1999.1454
31. Gao J, Yu Z, Jing S, Jiang W, Liu C, Yu C, Sun J, et al. Protective effect of Anwulignan against D-galactose-induced hepatic injury through activating p38 MAPK-Nrf2-HO-1 pathway in mice. *Clin Interv Aging.* (2018) 13:1859–69
32. Sulaiman I, Tan K, Mohtarrudin N, Lim J, Stanslas J. Andrographolide prevented toluene diisocyanate-induced occupational asthma and aberrant airway E-cadherin distribution via p38 MAPK-dependent Nrf2 induction. *Pulm Pharmacol Ther.* (2018) 53:39–51.
33. Chan CK, Tan TH, Andy SN, Alfarizal K, Bey-Hing G, Abdul KH. Anti-neuroinflammatory Activity of *Elephantopus scaber* L. via activation of Nrf2/HO-1 signaling and inhibition of p38 MAPK pathway in LPS-induced microglia BV-2 Cells. *Front Pharmacol.* (2017) 8:397. doi: 10.3389/fphar.2017.00397
34. Tian Y, Li Z, Shen B, Wu L, Han L, Zhang Q, et al. The protective effects of Shikonin on lipopolysaccharide/D-galactosamine-induced acute liver injury via inhibiting MAPK and NF-κB and activating Nrf2/HO-1 signaling pathways. *RSC Adv.* (2017) 7:34846–56.

Conflict of Interest: The authors declare that the research was conducted in the absence of any commercial or financial relationships that could be construed as a potential conflict of interest.

Publisher's Note: All claims expressed in this article are solely those of the authors and do not necessarily represent those of their affiliated organizations, or those of the publisher, the editors and the reviewers. Any product that may be evaluated in this article, or claim that may be made by its manufacturer, is not guaranteed or endorsed by the publisher.

Advantages of publishing in Frontiers

OPEN ACCESS
Articles are free to read for greatest visibility and readership

FAST PUBLICATION
Around 90 days from submission to decision

HIGH QUALITY PEER-REVIEW
Rigorous, collaborative, and constructive peer-review

TRANSPARENT PEER-REVIEW
Editors and reviewers acknowledged by name on published articles

Frontiers
Avenue du Tribunal-Fédéral 34
1005 Lausanne | Switzerland

Visit us: www.frontiersin.org
Contact us: frontiersin.org/about/contact

REPRODUCIBILITY OF RESEARCH
Support open data and methods to enhance research reproducibility

DIGITAL PUBLISHING
Articles designed for optimal readership across devices

FOLLOW US
@frontiersin

IMPACT METRICS
Advanced article metrics track visibility across digital media

EXTENSIVE PROMOTION
Marketing and promotion of impactful research

LOOP RESEARCH NETWORK
Our network increases your article's readership